climatechange in Australia




technical report 2007

technical report 2007

climatechange in Australia

Climate change in Australia.

Bibliography.
ISBN 9781921232930 (pbk.).

1. Climatic changes – Australia. 2. Australia – Climate.
I. CSIRO. II. Australia. Bureau of Meteorology.

551.6594

Acknowledgements

Chapter 2:
Authors: Wenju Cai, David Jones, Katherine Harle, Tim Cowan, Scott Power, Ian Smith, Julie Arblaster and Debbie Abbs
Contributors: David Etheridge, Ming Feng, Kevin Hennessy, John Hunter, Craig Macaulay, Jo Brown, Suppiah Ramasamy, Brad Murphy, Bertrand Timbal, Susan Wijffels

Chapter 3:
Authors: Bertrand Timbal and Neville Nicholls
Contributors: Wenju Cai, Kevin Hennessy and Pandora Hope

Chapter 4:
Authors: Kevin Hennessy and Rob Colman
Contributors: Ian Watterson and Roger Jones

Chapter 5:
Authors: Ian Watterson, Penny Whetton, Aurel Moise, Bertrand Timbal, Scott Power, Julie Arblaster and Kathy McInnes

5.1 Ian Watterson, Penny Whetton, Aurel Moise, Bertrand Timbal, Scott Power and Julie Arblaster
Contributors: Janice Bathols, Kevin Hennessy, Jim Ricketts and Roger Jones

5.2 Ian Watterson, Penny Whetton, Aurel Moise, Bertrand Timbal, Scott Power and Julie Arblaster
Contributors: Janice Bathols, Kevin Hennessy and Dewi Kirono

5.3 Author: Kevin Hennessy
Contributors: Janice Bathols, Dewi Kirono and Julian O'Grady

5.4 Author: Kevin Hennessy
Contributor: Freddie Mpelasoka

5.5 Author: Kathy McInnes
Contributor: Ian Macadam

5.6 Authors: Kevin Hennessy
Contributors: Chris Lucas and Graham Mills

5.7 Authors: Kathy McInnes and Siobhan O'Farrell
Contributor: Bernadette Sloyan

5.8 Author: Kathy McInnes
Contributors: Alistair Hobday, Richard Matear and Bernadette Sloyan

5.9 Authors: Debbie Abbs, Bertrand Timbal, Tony Rafter and Kevin Walsh

5.10 Authors: Scott Power, Julie Arblaster, Pandora Hope and Aurel Moise
Contributors: Ian Smith, Suppiah Ramasamy and Adam Morgan

Chapter 6:
Author: Benjamin Preston
Contributors: Roger Jones and Kevin Hennessy

Project Coordinator:
Paul Holper

Editorial:
Karen Pearce, Paul Holper, Mandy Hopkins, Willem Bouma, Penny Whetton, Kevin Hennessy and Scott Power

Design and layout:
Lea Crosswell

We gratefully acknowledge the invaluable assistance from Steve Crimp, CSIRO; David Karoly, University of Melbourne; and Graeme Pearman, Monash University.

We acknowledge the modelling groups, the Program for Climate Model Diagnosis and Intercomparison and the WCRP's Working Group on Coupled Modelling for their roles in making available the WCRP CMIP3 multi-model dataset. Support of this dataset is provided by the Office of Science, US Department of Energy.

Contents

Executive summary

Climate Change in Australia is based on international climate change research including conclusions from the Fourth Assessment Report of the Intergovernmental Panel on Climate Change (IPCC), and builds on a large body of climate research that has been undertaken for the Australian region in recent years. This includes research completed within the Australian Climate Change Science Program by CSIRO and the Australian Bureau of Meteorology in partnership with the Australian Greenhouse Office.

The purpose of this report is to provide an up-to-date assessment of observed climate change over Australia, the likely causes, and projections of future changes to Australia's climate. It also provides information on how to apply the projections in impact studies and in risk assessments. The two main strategies for managing climate risk are mitigation (net reductions in greenhouse gas emissions) to slow climate change and adaptation to climate impacts that are unavoidable.

A number of major advances have been made since the last report on climate change projections in Australia (CSIRO 2001) including:

- a much larger number of climate and ocean variables are projected (21 and 6 respectively)
- a much larger number (23) of climate models are used
- the provision of probabilistic information on some of the projections, including the probability of exceeding the 10th, 50th and 90th percentiles
- greater emphasis on projections from models that are better able to simulate observed Australian climate
- a detailed assessment of observed changes in Australian climate and likely causes; and
- information on risk assessment, to provide guidance for using climate projections in impact studies.

Past climate change

Temperature and rainfall

Australian average temperatures have increased by 0.9ºC since 1950, with significant regional variations. The frequency of hot nights has increased and the frequency of cold nights has declined.

Rainfall trends from 1900 to 1949 were generally rather weak and spatially incoherent. Rainfall trends since 1950 are both large and spatially coherent. The east coast, Victoria, and south-west Australia have all experienced substantial rainfall declines since 1950. Across New South Wales and Queensland these rainfall trends partly reflect a very wet period around the 1950s, and recent years that have been unusually dry. In stark contrast, north-west Australia has experienced an increase in rainfall over this period.

Trends in extreme daily rainfall vary across Australia. From 1950 to 2005, there have been increases in north-western and central Australia and over the western tablelands of New South Wales, but decreases in the south-east, south-west and central east coast. Trends in most extreme rainfall events are rising faster than trends in the mean.

Since the start of the 20th century, the period with the lowest rainfall was from the 1930s to the early 1940s. However recent droughts have been hotter, with both the maximum and minimum temperatures higher than in the earlier dry periods.

Maximum winter snow depth at Spencers Creek in the Snowy Mountains has decreased slightly since 1962, and the snow depth in spring has declined strongly (by about 40%).

Tropical cyclones and hail

Large changes have occurred in our ability to detect tropical cyclones since the advent of regular radar observations in the 1950s and with the development of meteorological satellite-based detection techniques in the 1970s and 1980s. Our ability to detect significant trends in the intensity of tropical cyclones in the Australian region is limited because of changes to techniques, and particularly the use of less accurate methods in the past.

There are no comprehensive studies of changes in hail occurrence in Australia, but one study for the Sydney region showed a 30% decline in the number of hailstorms affecting Sydney from 1989-2002 compared with 1953-1988. However, the most severe hail storm affecting Sydney occurred in April 1999, causing Australia's largest insurance loss ($1.7 billion) due to a natural disaster.

Oceans

Global sea levels rose by approximately 17 cm during the twentieth century. The average rate between 1950 and 2000 was 1.8 ± 0.3 mm per year, but for the period when satellite data are available (i.e. from 1993), the rate increased to 3 mm per year. Since 1990, the observed rate of global sea level rise corresponds to the upper limit of IPCC projections. For the period 1950 to 2000, sea level rose at all of the Australian coastal sites monitored, with substantial variability in trends from location to location. Over the period 1920 to 2000 the estimated average relative sea level rise around Australia was 1.2 mm per year.

Substantial warming has occurred in the three oceans surrounding Australia. Warming has been large off the south-east coast of Australia and in the Indian Ocean. The tropical Pacific Ocean has warmed over recent decades. Long term observations off Maria Island near Tasmania reveal a warming trend far greater than the global average, and this may be due to changes in the East Australian Current.

Southern Ocean temperatures have warmed since the 1950s to a depth of 1000 m in some locations. The warming is associated with a 50 km southward migration of the Antarctic Circumpolar Current. Seawater near the bottom of the ocean off Antarctica has rapidly become less salty and less dense. This freshening may be the signature of increased melt from Antarctic glaciers.

El Niño – Southern Oscillation and the Southern Annular Mode

Instrumental and palaeo-climate records show large variations in the frequency and intensity of the El Niño – Southern Oscillation (ENSO), and the impact of ENSO on Australia has varied from decade to decade. This variability has been accompanied by a downward trend in the Southern Oscillation Index (SOI, an index used to track ENSO) since 1876, consistent with a weakening of the Walker Circulation. While there has been an increase in the frequency of El Niño events in recent years, there is no consensus amongst current climate models that global warming should cause an increase. The increase might therefore reflect naturally occurring variability.

The relationship between the SOI and Australian temperature and rainfall has changed. For example, all-Australia rainfall and temperature since the mid 1970s have been higher for any given value of the SOI than they were previously.

Mid-latitude westerly winds appear to have decreased, with a corresponding increase in wind speed in the polar latitudes in most seasons from 1979 to the late 1990s. There has been a 20% reduction in the strength of the subtropical jet over Australia and an associated reduction in the likelihood of low pressure systems developing over south-west Western Australia since the early 1970s. This is linked to winter rainfall declines along the southern coastal regions of Australia and a poleward shift of storm tracks in winter.

Palaeo-records

Pollen records of past vegetation in eastern Australia indicate precipitation was generally higher than present between 9,000 and 3,500 years ago. This is consistent with a regional climatic shift, possibly related to the movement of the subtropical anti-cyclone belt, the westerlies and/or the monsoon. Evidence from lakes in Victoria suggests that conditions between about 1800 to 1840 were wetter than present, after which the dry conditions of the recent instrumental period became established. There is less information relating to past temperature variations.

The tropical cyclone palaeo-record from the past 5,000 years for Cairns and the Great Barrier Reef suggests that the historical record may greatly underestimate the frequency of the most severe tropical cyclones likely to strike the region.

Evidence from Tasmanian tree rings indicates significant shifts in the intensity of climate variability over the last 3,000 years, with a recent shift occurring around 1900.

Causes of past climate change

Climate can change as a result of both natural and anthropogenic factors. Detection and attribution studies attempt to tease out the anthropogenic component of this variability.

Temperature

Australian surface temperatures have risen significantly over the past century. Warming since the middle of the 20th century is likely to be mostly due to anthropogenic increases in greenhouse gases.

Rainfall

The rainfall decrease in south-western Australia since the mid-1970s is likely to be at least partly due to anthropogenic increases in greenhouse gases. It is not yet possible to attribute the post-1950 rainfall decreases in eastern Australia and rainfall increases in north-western Australia to human activities.

Drought

Recent Australian droughts have been accompanied by higher surface temperatures due to anthropogenic warming. This may have exacerbated the impact of drought in regions where warming increases water demand and surface water loss.

Snow

The decline in snow cover observed in recent decades is probably due to anthropogenic warming.

Extremes

There has been an increase in the frequency of warm days and warm nights and a decrease in the frequency of cool days and cool nights. It is likely that these changes are mostly due to anthropogenic warming.

Oceans

Rapid warming in the Tasman Sea is likely to have been partly driven by Antarctic ozone depletion.

Global climate change projections

Scenarios of greenhouse gas emissions, concentrations and radiative forcing

The greenhouse gas and aerosol emissions described here are those due to human activities, such as energy generation, transport, agriculture, land clearing, industrial processes and waste. The IPCC (SRES) emission scenarios used in this report combine a variety of assumptions about demographic, economic and technological factors likely to influence future emissions. They allow projected carbon dioxide, methane, nitrous oxide and sulfate aerosol emissions to be determined. Carbon cycle models are used to convert emissions into atmospheric concentrations, allowing for uptake of emissions by the land and ocean, climate feedbacks, and transport and chemical reactions in the atmosphere. The projected greenhouse gas concentrations are converted to a radiative forcing of the climate system, where positive forcing warms the Earth, and negative forcing cools the Earth. Changes in radiative forcing are used as input to climate models.

Using global climate models to estimate future climate change

Climate models are the best available tools we have for projecting climate. A climate model is a mathematical representation of the Earth's climate system based on well-established laws of physics, such as conservation of mass, energy and momentum. As our understanding of the underlying processes that govern the climate system improves, so too does our ability to represent the processes in climate models.

While projections of global and regional climate change contain uncertainties, global climate models continue to improve in their ability to represent current global and regional patterns of temperature, precipitation and other variables. Simulation of major patterns of climatic variability particularly relevant to Australia (e.g. ENSO, the Southern Annular Mode and the Madden-Julian Oscillation) has improved as well, increasing our confidence in the models.

A new set of experiments from 23 models from research groups around the world is now available and has been used in the generation of the climate projections for Australia. The models in this database represent the current state-of-the-art in climate modelling, with more sophisticated representations of physical and dynamical processes, and finer spatial resolution than in the past.

Each of the 23 models was given a skill score based on its ability to simulate the average (1961-1990) patterns of Australian temperature, rainfall and mean sea level pressure. These skill scores were used to weight regional climate projections based on the assumption that models with higher skill scores are likely to give more reliable projections of future climate.

Probability distributions were developed to represent the models' varying global warming projections for each year and emission scenario. These global warming probability distributions were essential for the creation probabilistic regional climate change projections.

Regional climate change projections

For annual and seasonal mean changes to temperature, precipitation, humidity, solar radiation, wind speed, potential evaporation and sea surface temperature, projections are provided in a probabilistic form. The other climate variables could not be treated similarly due either to the necessary data being unavailable, our assessment that the assumptions underlying the probabilistic approach may not be applicable (particularly relevant for some aspects of extremes), or that understanding of the topic was such that a qualitative assessment was all that was warranted.

Projections for 2030 demonstrate different patterns of regional change between climate models but little variation due to the different emission scenarios. This is because near-term changes in climate are strongly affected by greenhouse gases that have already been emitted. Climate changes centred on 2050 and 2070 are more dependent on the greenhouse gas emissions scenario, so variations due to emission scenarios are more significant. In each case, the best estimate is the median or 50th percentile, while the range of uncertainty is the difference between the 10th and 90th percentile.

Temperature

Projected warming by 2030

The best estimate of annual warming over Australia by 2030 relative to the climate of 1990 is approximately 1.0ºC, with warmings of around 0.7-0.9ºC in coastal areas and 1-1.2ºC inland. Mean warming in winter is a little less than in the other seasons, as low as 0.5ºC in the far south. The range of uncertainty is about 0.6ºC to 1.5ºC in each season for most of Australia. These warmings are based on the A1B emission scenario, but allowing for emission scenario uncertainty expands the range only slightly - warming is still at least 0.4ºC in all regions and can be as large as 1.8ºC in some inland regions. Natural variability in decadal temperatures is small relative to these projected warmings.

Projected warming for 2050 and 2070

Later in the century the warming is more dependent upon the assumed emission scenario. By 2050, annual warming over Australia ranges from around 0.8 to 1.8ºC (best estimate 1.2ºC) for the B1 (low emissions) scenario and 1.5 to 2.8ºC (best estimate 2.2ºC) for the A1FI (high emissions) scenario. By 2070, the annual warming ranges from around 1.0 to 2.5ºC (best estimate 1.8ºC) for the B1 scenario to 2.2 to 5.0ºC (best estimate 3.4ºC) for the A1FI scenario. Regional variation follows the pattern seen for 2030, with less warming in the south and north-east and more inland. In 2070, the risk of a warming above 4ºC in 2070 exceeds 30% over inland Australia under the A1FI scenario, whereas under the B1 scenario the warming is likely to be less than 2.0ºC except in the north-west.

Local variations to projected warming

Projected warming may vary significantly from that given by the global climate models in mountainous areas and near the coast. This has been demonstrated through the application of fine-resolution spatial downscaling techniques.

Extreme temperatures

Projected changes in maximum and minimum temperature indicate an increase in the diurnal temperature range in the south and a decrease in the north. This is associated with a projected strong increase in frequency of hot days and warm nights and a moderate decrease in frost. For the Murray-Darling Basin, a simulated increase in the day-to-day variability of minimum temperature reduced the impact of the mean warming on simulated frost frequency.

Precipitation

Projected precipitation change for 2030

Best estimates of annual precipitation indicate little change in the far north and decreases of 2% to 5% elsewhere. Decreases of around 5% prevail in winter and spring, particularly in the south-west where they reach 10%. In summer and autumn decreases are smaller and there are slight increases in the east.

The range of precipitation change in 2030 allowing for model-to-model differences is large. Annually averaged, the range is around -10% to +5% in northern areas and -10% to little change in southern areas. Decreases in rainfall are thus more consistently indicated for southern areas compared to northern areas. Winter and spring changes range from decreases of around 10% to little change in southern areas of the south-east of the continent, decreases of 15% to little change in the south-west, and decreases of around 15% to possible increases of 5% in eastern areas. In summer and autumn, the range is typically -15% to +10%. Decadal-scale natural variability in precipitation is comparable in magnitude to these projected changes and may therefore mask, or significantly enhance, the greenhouse-forced changes.

Projected change for 2050 and 2070

Later in the century, the projected precipitation changes are larger and vary more according to emission scenario.

By 2050 under the B1 (low emissions) scenario, the range of annual precipitation change is -15% to +7.5% in central, eastern and northern areas, with a best estimate of little change in the far north grading southwards to a decrease of 5%. The range of change in southern areas is from -15% to little change, with a best estimate of approximately -5%. Under the A1FI (high emissions) scenario, changes in precipitation are larger. The range of annual precipitation change is -20% to +10% in central, eastern and northern areas, with a best estimate of little change in the far north grading to around -7.5% decrease elsewhere. The range of change in southern areas is from a 20% decrease to little change, with a best estimate of around -7.5%. Seasonal changes follow the pattern seen for 2030, but are larger under A1FI in 2050. The projected decreases in the south-west in winter and spring are up to 30%.

In 2070, precipitation changes under the B1 scenario are comparable to those for 2050 under the A1FI scenario. Those under the A1FI scenario in 2070 are substantially larger. The range of annual precipitation change is -30% to +20% in central, eastern and northern areas, with a best estimate of little change in the far north grading to around -10% in the south. The range of change in southern areas is from -30% to +5%, with a best estimate of around -10%. Seasonal changes may be larger, with the projected decreases in the south-west of up to 40%.

Local variations to projected change

As for temperature, statistical downscaling studies have shown that projected precipitation change can vary significantly at fine spatial scales, particularly in coastal and mountainous areas.

Daily precipitation intensity, frequency of dry days and extreme precipitation

Models show an increase in daily precipitation intensity but also in the number of dry days. Extreme daily precipitation tends to increase in many areas but not in the south in winter and spring when there is a strong decrease in mean precipitation.

Snow

Snow cover, average season lengths and peak snow depths are projected to decrease in Australian alpine regions, and there is a tendency for the time of maximum snow depth to occur earlier in the season.

Solar radiation, relative humidity and potential evaporation

Solar radiation

Projections of solar radiation generally show little change although a tendency for increases in southern areas of Australia is evident, particularly in winter and spring. The projected range of change is typically -1% to +2% in 2030. The magnitude of changes is larger in 2050 and 2070, particularly under higher emission scenarios.

Relative humidity

Small decreases in relative humidity are projected over most of Australia. The range of change in annual humidity by 2030 is around -2% to +0.5% with a best estimate of around a 1% decline. The projected changes are larger for 2050 and 2070, particularly under the higher emission scenarios.

Potential evapotranspiration

Annual potential evapotranspiration is projected to increase over Australia. Largest increases are in the north and east, where the change by 2030 ranges from little change to a 6% increase, with best estimate of around a 2% increase. By 2070, the B1 scenario gives increases of 0% to 6% (best estimate around 3%) in the south and west and 2% to 8% (best estimate around 6%) in the north and east, while the A1FI emissions scenario gives increases of 2% to 10% (best estimate of around 6%) in the south and west and 6% to 16% (best estimate around 10%) in the north and east.

Drought

Drought occurrence is projected to increase over most of Australia, but particularly in south-western Australia.

Wind

Average wind speed projections

There is a tendency for increased wind speed in most coastal areas in 2030 (range of -2.5% to +7.5% with best estimates of +2% to +5%) except for the band around latitude 30°S in winter and 40°S in summer where there are decreases (-7.5% to +2.0%, with best estimates of -2% to -5%).

Later in the century, changes of wind strength can be larger, depending on the emission scenario. Under the A1FI scenario in 2070, best estimate increases of more than 15% apply in some regions, whereas under the B1 scenario increases are less than 10% everywhere.

Extreme wind speed projections

In winter, changes to extreme wind speed are likely to be similar to the changes to seasonal mean wind speed. However, there is little relationship between summer mean and extreme wind speed changes. Extreme winds in summer are likely to be governed more by small scale systems (including tropical cyclones). On the other hand, winter extreme wind events are more likely to be governed by larger scale systems (e.g. trade winds, mid-latitude cyclones).

Fire weather

A substantial increase in fire weather risk is likely at most sites in south-eastern Australia. Such a risk may exist elsewhere in Australia, but this has yet to be examined.

Sea level rise

Mean sea level rise

Global sea level rise is projected by the IPCC to be 18-59 cm by 2100, with a possible additional contribution from ice sheets of 10 to 20 cm. However, further ice sheet contributions, that cannot be quantified at this time, may substantially increase the upper limit of sea level rise.

Sea level extremes

Storm surges occurring in conditions of higher mean sea levels will enable inundation and damaging waves to penetrate further inland, increasing flooding, erosion and the subsequent impacts on built infrastructure and natural ecosystems. Changes to wind speed will also affect storm surge height.

Storm surge studies for portions of the Victorian and Queensland coasts demonstrate the potential for significant increases in inundation due to higher mean sea level and more intense weather systems.

Marine projections

Sea surface temperature

By 2030 the best estimate of sea surface temperature rise is 0.6-0.9ºC in the southern Tasman Sea and off the north-west shelf of Western Australia and 0.3-0.6ºC elsewhere. Allowing for model-to-model variations, the ranges are 0.4-1.4ºC in the southern Tasman Sea and 0.4-1.0ºC off the north-west coast.

Beyond the first few decades of the 21st century, the magnitude of the sea surface temperature change will become increasingly dependent on the emission scenario. Under the B1 scenario in 2070, the sea surface temperature best estimate increase is 0.6 to 1.0ºC along the south coast of Australia while elsewhere it is 1.2 to 1.5ºC. Under the A1FI emission scenario, the regions of highest warming are about 1.0ºC higher than those for the B1 scenario.

Ocean acidification

Increases in ocean acidity are expected in the Australian region with the largest increases in the high- to mid-latitudes. Under-saturation of aragonite could occur by the middle of the century in the higher latitudes, affecting the capacity for shell and endoskeleton creation by marine organisms.

East Australian Current

The East Australian Current is likely to strengthen throughout the 21st century, which will result in warmer waters extending further southward.

Severe weather

Tropical cyclones

Similar to studies for other basins, Australian region studies indicate a likely increase in the proportion of the tropical cyclones in the more intense categories, but a possible decrease in the total number of cyclones.

Severe thunderstorms

Conditions will become less suitable for the occurrence of tornadoes in southern Australia in the cool season (May to October). There is an indication that hail risk may increase over the south-east coast of Australia.

ENSO, the Southern Annular Mode and storm tracks

ENSO's impact on Australia under global warming

In south-eastern Australia, models analysed indicate that El Niño events will tend to become drier and La Niña events will tend to become wetter, even if Pacific Ocean variability linked to ENSO does not increase.

The Southern Annular Mode

All climate models exhibit a trend in the Southern Annular Mode towards its positive phase (weaker westerly winds over southern Australia, stronger westerly winds at higher latitudes) when driven with increasing greenhouse gas concentrations.

Storm tracks

A decrease in the occurrence of winter low pressure systems over south-west Western Australia is likely during the 21st century.

Application of climate projections in impact and risk assessments

Risk management is an iterative process, where scoping and risk identification usually takes place before more detailed assessments are carried out. Care must be exercised when using the projections in any risk assessment, particularly when selecting climate variables, determining temporal and/or spatial resolution, and dealing with uncertainty.

Detailed risk assessments generally require purpose-built climate projections, including time series, or probabilistic representations of future climate. Various tools have been developed which represent different methods for enhancing the delivery of climate information to stakeholders both for education and for risk assessment and management. Nevertheless, significant challenges remain for communicating climate risk in ways that can be effectively used in risk management.

Chapter 1 Introduction

This report is provided for researchers, public and private policy developers and the community at large to assess their respective exposure, risk and opportunities that may flow from regional climate change due to global warming. There is still much that we do not know, but this report provides the most up-to-date assessment of observed Australian climate changes and causes, and projections for 2030 to 2070. It supersedes earlier projections (CSIRO 2001) and builds on a greatly improved global scientific knowledge on this issue.

'Climate change' is defined by the IPCC as a change in the state of the climate that can be identified by changes in the mean (and/or the variability), and that persists for an extended period, typically decades or longer.

Since 1988 the scientific findings on atmospheric change and the potential for human induced changes in the Earth's climate have been reviewed and summarised by the Intergovernmental Panel on Climate Change (IPCC). Four major reports were issued (IPCC 1990; IPCC 1996; IPCC 2001 and IPCC 2007a). The Fourth Assessment Report on the physical science basis of climate change (IPCC 2007a) stated the following amongst its key conclusions:

- Global atmospheric concentrations of carbon dioxide, methane and nitrous oxide have increased markedly as a result of human activities since 1750 and now far exceed pre-industrial values determined from ice cores spanning many thousands of years.
- Warming of the climate system is unequivocal as is now evident from observations of increases in global average air temperatures, widespread melting of snow and ice, and rises in global average sea level.
- At continental, regional, and ocean-basin scales, numerous long-term changes in climate have been observed.
- Palaeo-climate information supports the interpretation that the warmth of the last half century is unusual in at least the previous 1300 years.
- Most of the observed increase in globally averaged temperatures since the mid-20th century is very likely due to the observed increase in anthropogenic greenhouse gas concentrations ... Discernible human influences now extend to other aspects of climate, including ocean warming, continental average temperatures, temperature extremes and wind patterns.
- For the next two decades a warming of about 0.2ºC per decade is projected for a range of SRES emission scenarios.
- Continued greenhouse gas emissions at or above current rates would cause further warming and induce many changes in the global climate system during the 21st century that would very likely be larger than those observed during the 20th century.
- There is now higher confidence in projected patterns of warming and other regional-scale features, including changes in wind patterns, precipitation, and some aspects of extremes and of ice.

In summary, the message is that global warming is real, humans are *very likely* to be causing it, and that it is *very likely* that there will changes in the global climate system in the centuries to come larger than those seen in the recent past. Future changes have the potential to have a major impact on human and natural systems throughout the world including Australia.

This report follows IPCC in its use of terms indicating likelihood. This is as follows: Virtually certain > 99% probability of occurrence, extremely likely > 95%, very likely > 90%, likely > 66%, more likely than not > 50%, unlikely < 33%, very unlikely < 10%, and extremely unlikely < 5%.

Each major IPCC report has produced global projections of climate change due to scenarios of greenhouse gas and aerosol emissions that become widely used until the time of the next IPCC report. As the science has improved, so have the breadth and detail of these projections. Projections of regional climate change for Australia have followed the major IPCC reports, providing regional detail consistent with the global projections produced by the IPCC (CSIRO 1992, 1996, 2001).

Climate Change in Australia is the latest such assessment. It is based upon international climate change research including the latest IPCC (2007a) conclusions. Moreover, it builds on a large body of climate research that has been undertaken for the Australian region in recent years. This includes research completed within the Australian Climate Change Science Program by CSIRO and the Australian Bureau of Meteorology in partnership with the Australian Greenhouse Office.

The purpose of this report is to provide an up-to-date assessment of observed climate change over Australia (Chapter 2), the likely causes (Chapter 3), global climate change projections (Chapter 4), regional projections for Australia (Chapter 5) and guidance on using projections in risk assessments (Chapter 6).

A number of major advances have been made over the previous statements about Australian climate change making this technical report the most comprehensive to date. Advances include:

- A detailed assessment of observed changes in Australian climate and likely causes, absent from previous statements.
- Projections are given for 23 climate variables and six ocean variables based on up to 23 climate models and up to six greenhouse gas and aerosol emission scenarios.
- For some climate variables, results are based on weighting of models according to their ability to simulate features of the present (1961–1990) Australian climate.
- For some climate variables, probability distributions have been assigned, allowing the presentation of median changes, 10th to 90th percentile ranges of uncertainty, and the probability of exceeding selected thresholds.
- A chapter on risk assessment, which provides guidance material for using climate projections in impact studies.

This technical report provides details of the national assessment and how it was developed, including references to the underpinning research. The report is aimed at researchers and informed experts. Supplementary material is available on the *Climate Change in Australia* website www.climatechangeinaustralia.gov.au.

Report context

Although our understanding of climate change has improved markedly over the past several decades and continues to improve, the issue is still beset by uncertainty. The sources of uncertainty are many and diverse but can be grouped into:

- socio-economic uncertainties associated with the current and future activities of humans
- scientific uncertainties associated with our understanding of how the Earth's major biophysical systems behave
- fundamental uncertainties associated with the behaviour of complex systems.

This report mostly deals with scientific uncertainties associated with projecting future climate change but also needs to consider socio-economic and complex systems uncertainties. Because of the substantial and complex uncertainties surrounding climate change, new concepts and specific uses of terminology have been developed for its management. Traditionally, characterisations of future climate have been described as scenarios, but as the types and uses of such characterisations grow, the terminology has become more detailed (Box 1; Carter *et al.* 2007).

This report describes characterisations of future climate that range from artificial experiments through to probabilistic futures. They are intended to provide a general overview of plausible climate change over Australia for general information, and are suitable for scoping exercises such as the identification of potential climate risks. For more applied purposes, further work will be needed to prepare climate change information that is fit for the purpose intended. Chapter 6 provides a general overview of how this may be achieved but it is also an area of active research that will continually be updated.

Box 1.1: Definitions of future characterisations

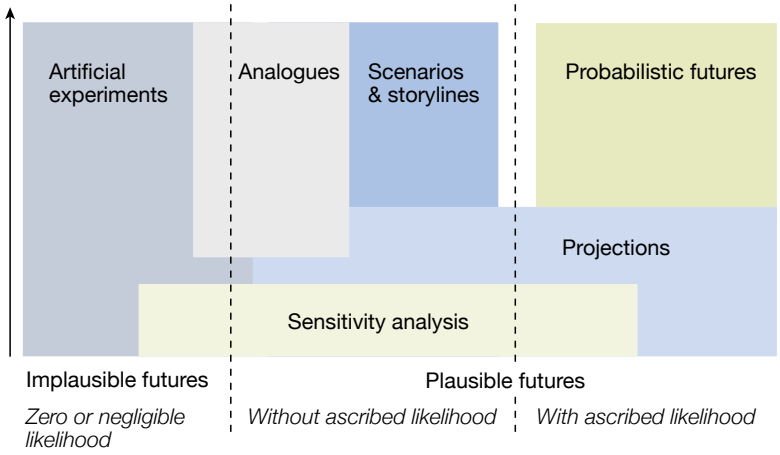

Figure 1.1: Characterisations of the future

Definitions have been developed by the IPCC for terminology relating to the use of climate information (Carter *et al*. 2007).

Comprehensiveness indicates the degree to which a characterisation of the future captures the various aspects of the socio-economic/biophysical system it aims to represent. Secondarily, it indicates the detail with which any single element is characterised.

Plausibility is a subjective measure of whether a characterisation of the future is possible. Implausible futures are assumed to have zero or negligible likelihood. Plausible futures can be further distinguished by whether a specific likelihood is ascribed or not.

An artificial experiment is a characterisation of the future constructed without regard to plausibility (and hence often implausible) that follows a coherent logic in order to study a process or communicate an insight.

Artificial experiments range in comprehensiveness from simple thought experiments to detailed integrated modelling studies.

Sensitivity analyses employ characterisations that involve arbitrary or graduated adjustments of one or several variables relative to a reference case. These adjustments may be plausible (e.g. changes are of a realistic magnitude) or implausible (e.g. interactions between the adjusted variables are ignored), but the main aim is to explore model sensitivity to inputs, and possibly uncertainty in outputs.

Analogues are based on recorded conditions that are considered to adequately represent future conditions in a study region. These records can be of past conditions (temporal analogues) or from another region (spatial analogues). Analogues are plausible in that they reflect a real situation, but may be implausible because no two places or periods of time are identical in all respects.

A *scenario* is a coherent, internally consistent, and plausible description of a possible future state of the world (IPCC 1994; IPCC 2000). Scenarios are not predictions or forecasts (which indicate outcomes considered most likely), but are alternative images without ascribed likelihoods of how the future might unfold. They may be qualitative, quantitative, or both. A *climate scenario* is a description of a plausible future climate.

Storylines are qualitative, internally consistent narratives of how the future may evolve. They describe the principal trends in socio-political-economic drivers of change and the relationships between these drivers. Storylines may be stand-alone, but more often underpin quantitative projections of future change that, together with the storyline, constitute a scenario.

A *projection* is generally regarded as any description of the future and the pathway leading to it but is defined by Carter *et al*. (2007) as a model-derived estimate of future conditions related to one element of an integrated system (e.g. an emission, a climate, or an economic growth projection). Projections may be probabilistic, while scenarios do not ascribe likelihoods.

Probabilistic futures. Futures with ascribed likelihoods are probabilistic. The degree to which the future is characterised in probabilistic terms can vary widely. For example, conditional probabilistic futures are subject to specific and stated assumptions about how underlying assumptions are to be represented. Assigned probabilities may also be imprecise or qualitative.

Chapter 2 Past climate change

Observational data reveal significant climate change in and surrounding Australia over the last century. Selected and quality-controlled surface observations from mostly rural sites are used, ensuring that the observed variability and trends reflect those occurring in the broader atmosphere and are generally not due to local factors. Changes in the ocean environment are less abrupt due primarily to the large heat content of the ocean. Further, there have been far less long-term oceanic observations. Therefore determination of ocean climate changes uses indirect evidence in addition to direct observations. To put recent changes in a historical perspective, palaeo-records that go back far beyond the instrumental record are also provided.

2.1 Surface temperature

Australia's annual mean surface air temperature has increased since 1910 (the time when reliable records in many parts of Australia became available) by about 0.9ºC. The first half of last century shows very little overall trend in temperatures, with higher temperatures tending to coincide with major drought years such as 1914-15 and 1938, while wetter periods, such as the 1950s, showed lower temperatures (Figure 2.1). From 1910 to 1950 annual mean Australian temperatures went down slightly, driven largely by increasing rainfall and lower daytime temperatures across eastern Australia. Since 1950, a warming trend of 0.16ºC per decade occurred. This rate is nearly double the observed trend over the century as a whole (0.09ºC per decade) and is comparable with the global trend since 1970. The year 2005 holds the record as Australia's warmest year since 1910 with a national average temperature of 22.9ºC, 1.1ºC above the 1961 to 1990 average, and 2.2ºC warmer than the coldest recorded year observed in 1917.

The spatial variation in the trends since 1910 is depicted in Figure 2.2. Trends have not been uniform across the country, ranging between 0.05-0.15ºC per decade. Largest changes occurred in parts of central Australia, with small pockets of lesser warming in various locations. Spatial variation in temperature trends since 1950 are also evident (Figure 2.2). Maximum warming (exceeding 0.3ºC per decade) occurred in central-eastern Australia and minimum warming/slight cooling over north-west Australia.

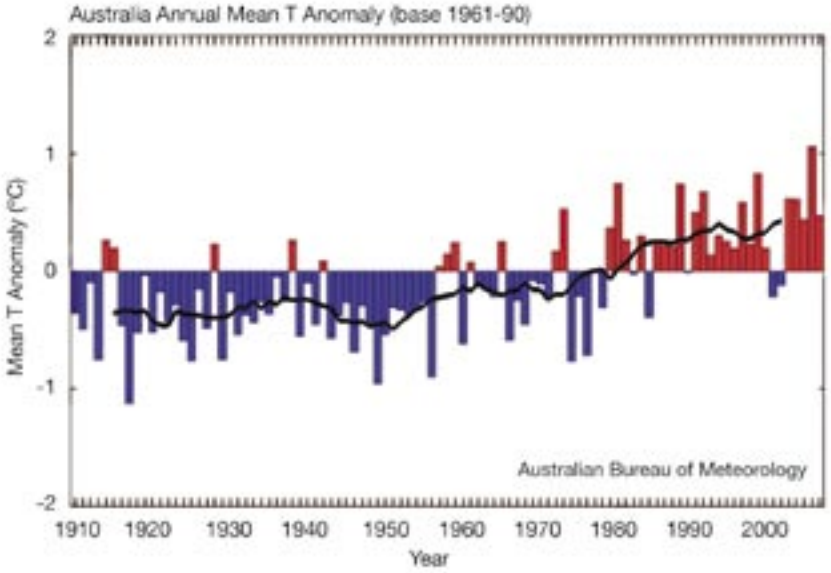

Figure 2.1: Annual mean Australian temperatures taken as anomalies from the 30-year 1961 to 1990 average. The black line is an 11-year running mean.

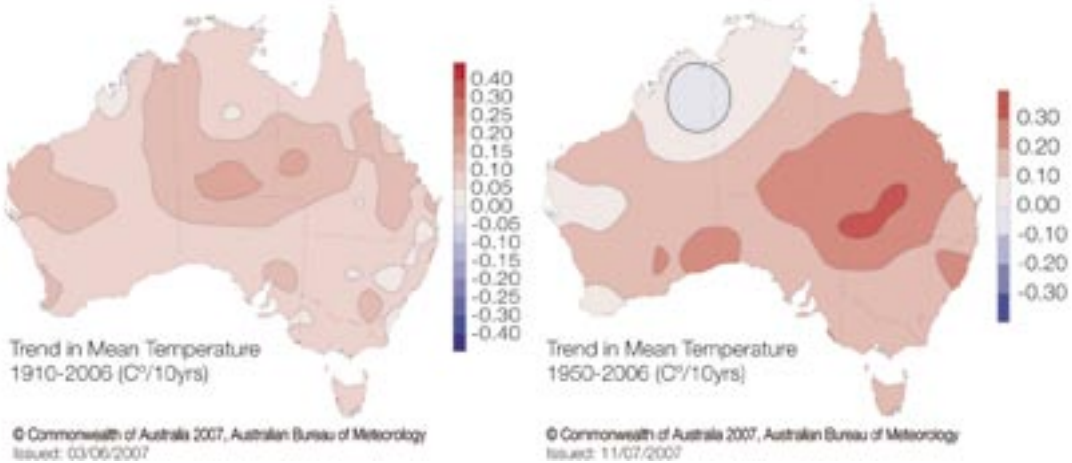

Figure 2.2: Linear trends in annual mean Australian temperatures since 1910 (left) and 1950 (right). Units are ºC per decade.

Accompanying the general warming since 1950 have been changes in the frequency of extremely high and low temperatures across Australia (Figure 2.3). From 1957, the Australian-average shows an increase in hot days, an increase in hot nights, a decrease in cold days and a decrease in cold nights (Nicholls and Collins 2006). The increase in the number of hot days was overlaid on considerable interannual variability largely linked to the swings from wet to dry years. For example, the severe drought year of 2002 was accompanied by a large number of hot days while the wet years from 1999 through 2001 saw relatively few hot days.

2.2 Precipitation, drought, pan evaporation, wind and stream flow

2.2.1 Precipitation

Similar to temperature trends, rainfall trends show a marked contrast between the first half of the last century and the period since 1950. Rainfall trends from 1900 to 1949 were generally rather weak and spatially incoherent. It is unclear whether the lack of substantial trends reflects the weak influence of global warming over this period or if it is simply a product of sampling only 50 years. In contrast, the rainfall trends across Australia since 1950 are both large and spatially coherent (Figure 2.4). North-west Australia has seen an increase in annual rainfall over this period, amounting to more than 30 mm per decade across the north-west third of Australia and exceeding 50 mm per decade on parts of the north-west coast. In marked contrast, eastern and south-western Australia have become drier since 1950, with largest drying along the east coast exceeding 50 mm per decade. Across New South Wales and Queensland these trends partly reflect a very wet period around the 1950s, though recent years have been unusually dry. In the south-west of Western Australia the rainfall decline reflects an apparent step-change to lower rainfall in the 1970s, exacerbated by very low rainfall in recent years.

Across Victoria, the trends reflect a combination of a very wet 1950s and an extremely dry last decade. The last decade takes the form of a step-change similar to that which occurred around Perth in the 1970s, with many parts of southern and central Victoria having experienced their driest 10-year period on record.

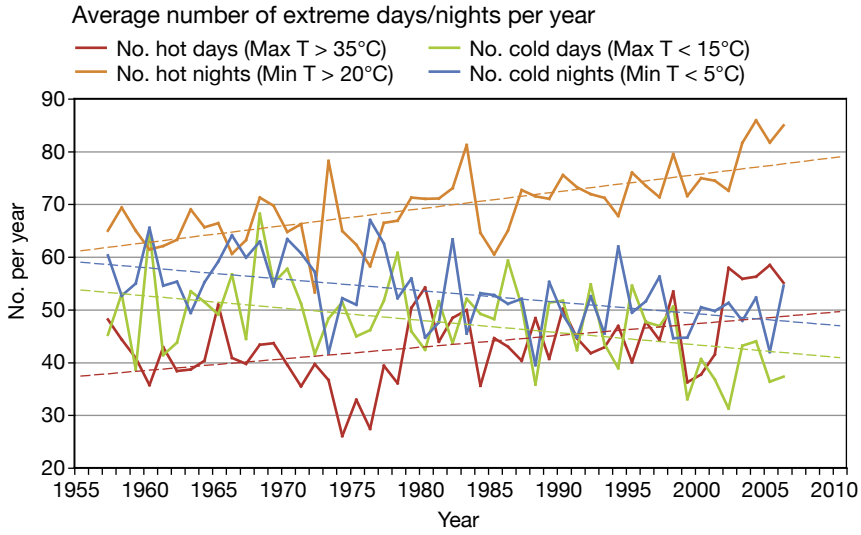

Figure 2.3: Time series of the annual average number of hot days (>35ºC), cold days (<15ºC), hot nights (>20ºC) and cold nights (<5ºC) in Australia. Dotted lines represent linear trends. (Courtesy of National Climate Centre, Bureau of Meteorology.)

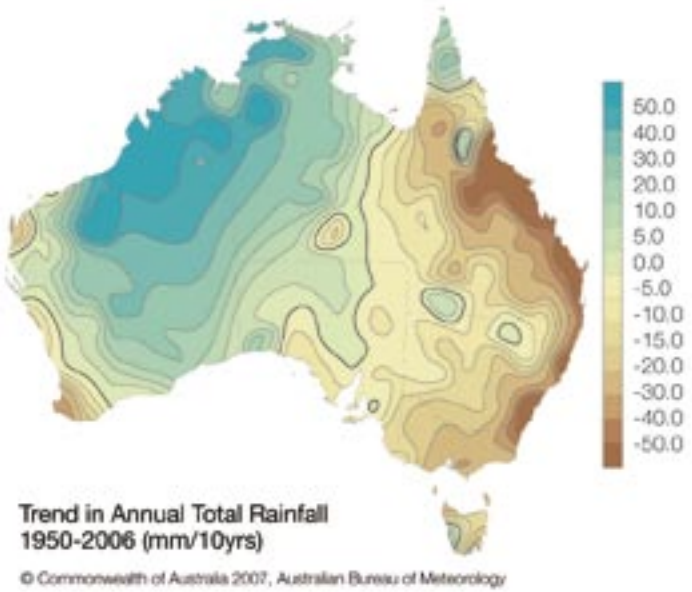

Figure 2.4: Trend in annual mean Australian rainfall since 1950. Units are mm per decade.

The last 5 to 10 years mark one of the most severe droughts in Australia's history (Trewin 2006). Figure 2.5 shows the rainfall deciles for March 2002 to December 2006. (A decile is a proportion of a set of data that has been ranked and divided into ten groups, where each group contains an equal number of data items.) This period starts with the onset of the 2002 El Niño event. Over this period very low rainfall was experienced across eastern Australia, with record low rainfall in key catchment areas of the Murray and Darling Rivers and water catchments for Sydney, Canberra and Melbourne.

Australian rainfall shows considerable variability from year-to-year, partly in association with the El Niño – Southern Oscillation (ENSO). Notably dry years such as 1902, 1972, 1982 and 2002 all coincide with major El Niño events, while the very wet years such as 1973, 1974, 1999 and 2000 coincide with La Niña events. Exceptions to this strong ENSO-linked interannual variability are extended periods of above or below average rainfall, such as the Federation Drought, which extended from the mid 1890s through to 1902; the lowest rainfall decade on record during most of the 1940s (in most of the south-east of Australia – Murphy and Timbal 2007); and the very wet period during the early 1970s.

An extreme rain event is defined as an event where the total rain recorded within a period of consecutive days exceeds a nominated threshold value. Annual rainfall variations are primarily caused by variations in intensity of extreme events. Trends in nine daily rainfall indices were examined from January 1910 to August 2005 using an updated high-quality rainfall dataset from the Australian Bureau of Meteorology (Gallant *et al*. 2007).

Extreme daily rainfall was defined by the 95th and 99th percentiles for six regions in the east and south-west of Australia. In the eastern central region, from 1910-2005, there have been significant increases in spring and annual rain days and extreme rainfall intensity (95th percentile), but significant decreases in spring and annual rain per rain day and the proportion of rainfall from extreme events. During spring, the New South Wales Tablelands showed a decrease in rain per rain day from 1910-1930 and increases from 1970-2005, most likely due to heavy-rain events. In south-west Western Australia, annual total rainfall has significantly decreased by 21 mm per decade since 1910, and by almost 24 mm per decade since 1950, accompanied by decreases in rain days and extreme rainfall indices. In the eastern coastal region, since 1950, there has been a significant decrease of almost 55 mm per decade in annual total rainfall, along with decreases in rain days and extreme rain, particularly in summer and winter. In the south-east, a significant decrease in annual total rainfall of 20 mm per decade since 1950 stems mainly from decreases during autumn. Generally, the direction of changes in extreme rainfall is consistent with changes in the mean. Trends in the extremes are often greater than the trend in the mean (Alexander *et al*. 2007).

2.2.2 Drought

In Australia, direct relationships between drought and global warming have been inferred through the extreme nature of high temperatures and heatwaves accompanying recent droughts, i.e. droughts are becoming hotter (Nicholls 2004). Since the start of the 20th century, the period of lowest rainfall across Australia was from the 1930s to the early 1940s. However, in the more recent droughts both the maximum and minimum temperatures have been higher (e.g. 2002 drought), as has potential evaporation.

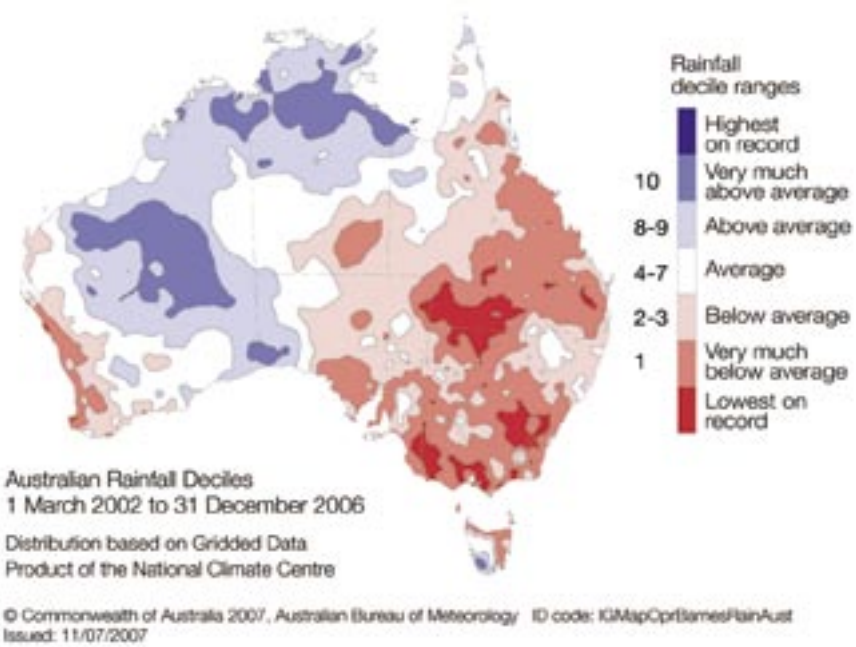

Figure 2.5: Rainfall deciles for the drought which commenced in March 2002.

2.2.3 Pan evaporation

Pan evaporation averaged over 60 high quality sites from 1970-2005 showed large interannual variability, with a small but insignificant decreasing trend of 2.5 mm per yr^2 (Jovanovic *et al*. 2007). This 36-year linear trend averaged over the whole of Australia masks the fact that evaporation has changed very little in the south, with increases in recent years. Pan evaporation is often regarded as a surrogate estimate of potential evaporation (the amount of evaporation that would occur if unlimited water were available), but whether this is the case remains to be tested. It is also unclear as to how pan evaporation relates to actual evapotranspiration as the latter is strongly constrained by the amount of water available and so the relevance of pan evaporation in a changing climate regime may be small (Murphy and Timbal 2007). Further analysis of the pan evaporation data suggests that many of the observed changes can be linked to local wind effects caused by changes in the local environments around observation stations (Rayner 2007) or other changes in observational sites (Jovanovic *et al*. 2007).

2.2.4 Wind

Trends in wind speed are an important aspect of climate change, but they are difficult to determine directly. Records of wind speed at any given station are highly sensitive to changes in the local environment (e.g. construction of buildings, removal of trees), as well as to systematic changes arising from altered instrument types. Considerably more work is needed to produce a dataset useful for determining trends in wind speed across Australia, especially extreme winds. However, it is known that mid-latitude westerly winds appear to have decreased, due to changes in the Southern Annular Mode (see section 2.5.2), with a corresponding increase in wind speed in the polar latitudes in most seasons from 1979 to the late 1990s, manifesting as a poleward displacement of the jet streams and storm tracks (Simmonds *et al*. 2002; Cai and Cowan 2007). There has been a 20% reduction in the strength of the subtropical jet over Australia and an associated reduction in the likelihood of synoptic disturbances developing over south-west Western Australia since the early 1970s (Frederiksen and Frederiksen 2005).

2.2.5 Changes in stream flow

One of the major impacts of the rainfall decline in southern and eastern Australia has been a reduction in surface water available for storage. The time series of May to April inflows to the south-west Western Australia Integrated Water Supply System is shown in Figure 2.6. The average annual inflow over the period 1911 to 1974 was 338 gigalitres (GL) which is almost twice the average of 177 GL per year over the period 1975 to 1996. Average inflow over the eight years from 1997 to 2005 was even less, at 114 GL per year, or close to a third of the 1911 to 1974 average. Further, for every 1% of rainfall decrease, the percentage reduction in inflow is far greater, and this factor grows as the drying condition persists. This nonlinear relationship is illustrated in Figure 2.7, which shows that the ratio between inflow reduction and rainfall decrease grows with time as the dry conditions persist.

The reduction in inflow to dams is also observed in Victoria (Figure 2.8). Victoria has experienced a 20% rainfall decrease since the mid-1990s, translating into an inflow reduction of about 40%.

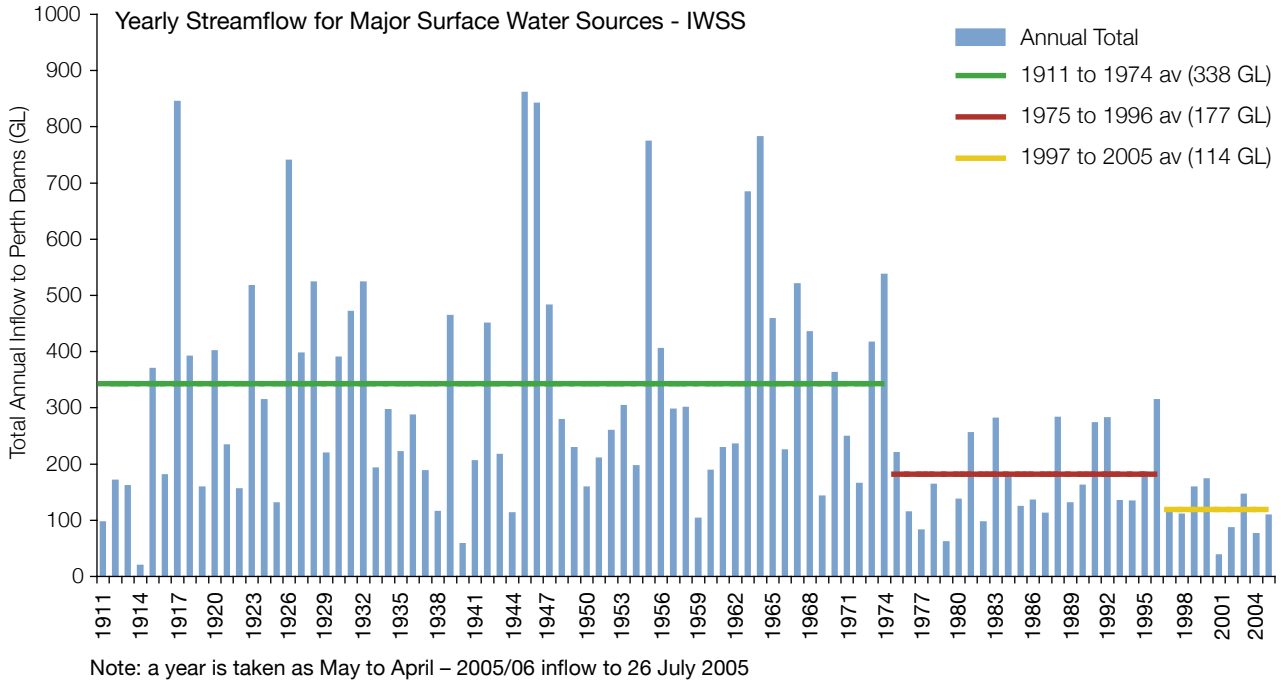

Figure 2.6: Yearly streamflow into Perth's dams. Values represent totals for May-April. Averages for 1911-1974, 1975-1996 and 1997-2005 are shown. (Courtesy of the Western Australia Water Corporation.)

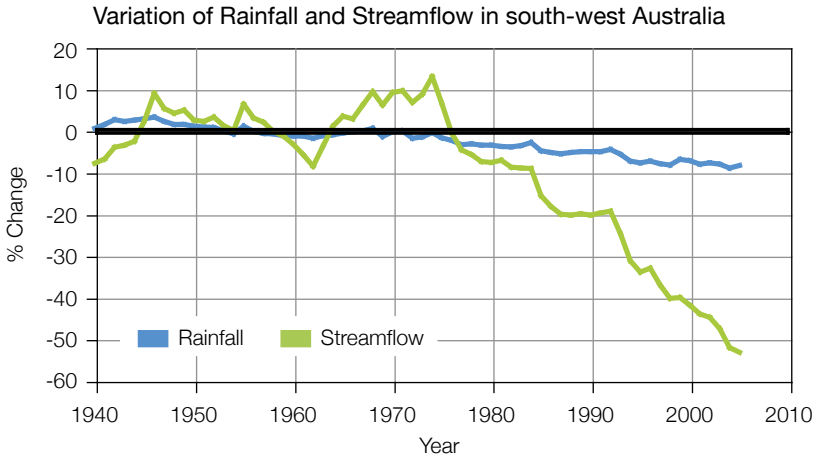

Figure 2.7: Yearly streamflow into Perth's dams. Values represent changes in percentage of mean for May-April. The plot demonstrates the non-linear relationship between rainfall decrease and streamflow reduction. (Data courtesy of the Western Australia Water Corporation and the Bureau of Meteorology's National Climate Centre).

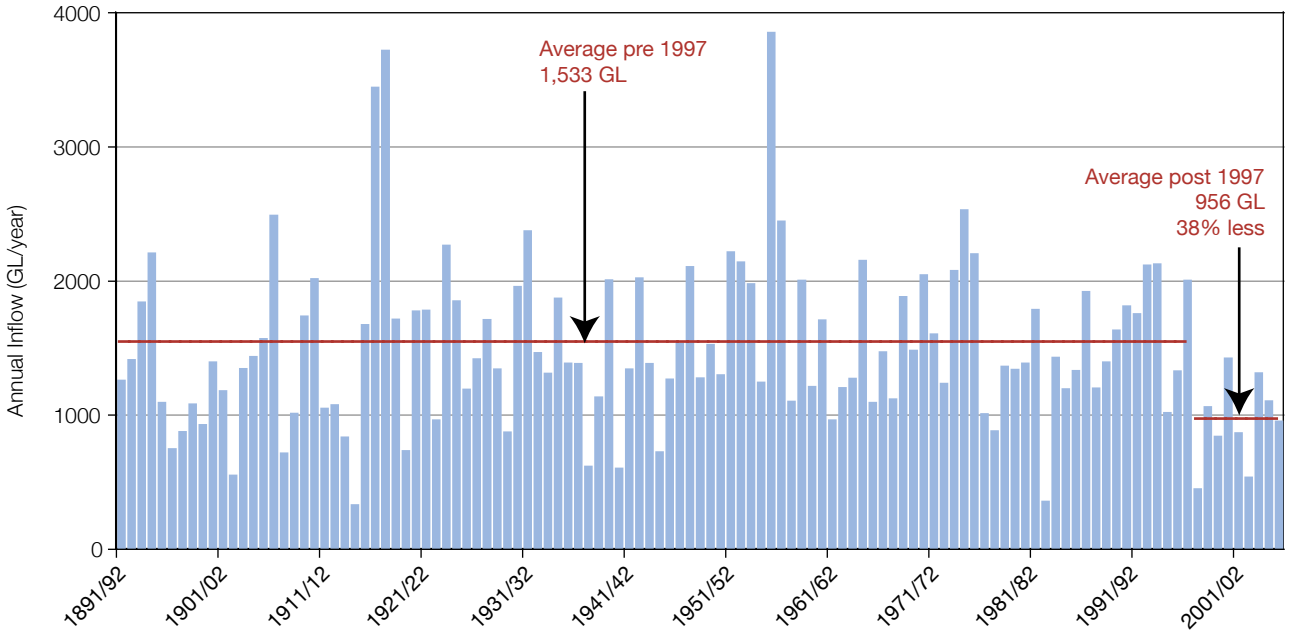

Figure 2.8: Yearly streamflow into Eildon dam in central Victoria. Values represent annual totals. Averages for 1992-1997 and 1997-2006 are shown. (Courtesy of Rae Moran, Victorian Department of Sustainability and Environment.)

2.3 Changes in tropical cyclones, east coast lows, thunderstorms, hail and snow

2.3.1 Tropical cyclones

There has been concern that globally the relative frequency of very strong tropical cyclones may be increasing (Emanuel 2005; Webster *et al*. 2005; Hoyos *et al*. 2006; Curry 2006), although these findings have generated significant controversy with the scientific community due to concerns with the quality of the historical tropical cyclone data on which these studies relied (McBride *et al*. 2006). The IPCC (2007a) summary states: *"There is observational evidence for an increase in intense tropical cyclone activity in the North Atlantic since about 1970, correlated with increases of tropical sea surface temperatures. There are also suggestions of increased intense tropical cyclone activity in some other regions where concerns over data quality are greater. Multi-decadal variability and the quality of the tropical cyclone records prior to routine satellite observations in about 1970 complicate the detection of long-term trends in tropical cyclone activity. There is no clear trend in the annual numbers of tropical cyclones."* Recent papers (Klotzbach 2006; Kossin *et al*. 2007) confirm the upward trend in tropical cyclone intensity for the North Atlantic but are unable to corroborate the presence of upward trends in intensity over the past two decades in other basins. Analysis of the existing Australian tropical cyclone database indicates substantial increases in detected tropical cyclone numbers with the advent of weather radar in the late 1950s, although there have been apparent decreases in east Australian numbers since the 1970s, largely due to increasing numbers of El Niños (Nicholls *et al*. 1998).

A review of the West Australian tropical cyclone database for 1968-2001 uncovered an artificial bias caused by underestimating tropical cyclone intensities (Harper and Callaghan 2006). After the removal of inconsistencies and biases, a smaller upward trend still remains in the dataset, with the proportion of tropical cyclones that were severe (i.e. 'category 3 or 4' cyclones) being larger (41%) during 1989-1998 than during the earlier period 1974-1988 (29%).

2.3.2 East coast lows

Low pressure systems influencing eastern Australia ('east coast lows') have strong winds and high rainfall, such as the one that flooded the Hunter Valley in June 2007. A consistent dataset of east coast lows based on station rainfall and surface winds from January 1958 to September 1992 showed significant correlations between the occurrence of east coast lows, the Southern Oscillation Index and the latitudinal

position of the subtropical high pressure belt (Hopkins and Holland 1997). There is a strong tendency for east coast lows to occur after El Niño years and in particular when an El Niño is followed by a La Niña. Hopkins and Holland (1997) found a long-term annual trend towards increased numbers of east coast lows over the period of their study, with almost a doubling of the frequency over the 30 years up to the early 1990s. However, there is a great deal of both interannual and decadal variability in the frequency of east coast lows. For example, after the late 1990s there was a decline in frequency up to 2006, while June 2007 saw a near-record monthly total of 5 east coast lows (P. Wiles, personal communication).

2.3.3 Cool-season tornadoes, hail and thunderstorms

About half of all tornadoes in Australia occur during May to October. These 'cool season tornadoes' are mostly observed in the southern part of the continent, especially Western Australia and South Australia (Hanstrum *et al*. 2002). Small-scale phenomena such as tornadoes are very difficult to monitor over a long period and it is therefore difficult to identify possible changes in frequency or intensity. Kounkou *et al*. (2007) estimated tornado risk during 1958 to 2002 by examining larger scale changes in the atmosphere linked to tornado incidence (Mills 2004). It was not possible to ascertain whether the risk of cool-season tornadoes has increased during the 1958 to 2000 period, despite a marked positive trend, due to an increase of the apparent risk since the introduction of satellite data in 1979.

The largest insured loss from a natural hazard in Australian history was $1.7 billion due to the April 1999 hailstorm in Sydney (Schuster *et al*. 2005; Insurance Council of Australia 2007). It is therefore important that observed and projected trends in hailstorm frequency and hailstorm intensity are documented and understood.

Schuster *et al*. (2005) report a decline of about 30% in the number of hailstorms affecting Sydney in the period 1989-2002 compared with 1953-1988. However, the intensity of hailstorms also needs to be considered when assessing the damage potential of hailstorm, and unfortunately there does not appear to be a published work on observed trends in intensity.

Thunderstorms are most frequent over northern Australia, with a secondary maximum in south-east Queensland and over central and eastern New South Wales, extending into north-eastern Victoria. The most severe thunderstorms are found along the eastern coastline, particularly in late spring and summer. ENSO does not appear to have a strong influence of thunderstorm activity, though thunderstorms were less frequent over south-eastern Australia (in Sydney, Adelaide and Canberra) during the strong El Niño year of 1982 and in Perth during the 1994 El Niño. There does not appear to be any evidence of a widespread trend in thunderstorm activity. See Kuleshov *et al*. (2002) for further details.

2.3.4 Snow

Maximum winter snow depth (Nicholls 2005) at Spencers Creek in the Snowy Mountains of south-eastern Australia has decreased slightly since 1962, and the snow depth in spring has declined strongly (by about 40%). Data from four alpine sites from 1957-2002 indicated a weak decline in maximum snow depths at three sites (Spencers Creek, Three Mile Dam and Deep Creek) and a moderate decline in mid-late season snow depths (August-September) at the same three sites (Hennessy *et al*. 2003).

2.4 Oceans

2.4.1 Sea level

Sea level rise is the result of thermal expansion of ocean water in response to global warming and increases in ocean mass from the melting of glaciers, with smaller contributions from the polar ice sheets. Global sea levels have risen by about 17 cm during the 20th century (Church and White 2006) and there has been a significant increase in the rate of sea level rise during the 20th century. The average rate between 1950 and 2000 was 1.8 ± 0.3 mm per year, and for the period when satellite data are available (i.e. from 1993), the rate was over 3 mm per year (Church and White 2006).

Since 1990, the observed rate of global sea level rise corresponds to the upper limit of the 2001 IPCC projections started from the base year of 1990 (Rahmstorf *et al*. 2007). While a longer record is needed to ascertain the importance of naturally occurring decadal variability (e.g. from violent volcanic eruptions (Church *et al*. 2005), this comparison of observed and modelled sea level raises concern that one or more of the model contributions to sea level rise may be underestimated.

Regional sea level reflects both the global mean rise, modulated by local effects of changing ocean currents, and patterns of atmospheric pressure. Knowledge of these combined influences on regional sea level will allow a more rational basis for the regional projection of such levels, their extremes and their likely impacts. For the period 1950 to 2000, sea level rose at all of the Australian coastal sites considered, with substantial variability in trends from location to location (Figure 2.9 (a); Church *et al*. 2006) and in sea level values from year-to-year. Over the period 1920 to 2000 the estimated average relative sea level rise around Australia was 1.2 mm per year.

Maps of trends in sea level over the region since the early 1990s are depicted in Figure 2.9 (b). These trends are based on data from the Australian Baseline Sea Level Monitoring Array (established in the early 1990s to provide a more accurate, robust national monitoring system for sea level) and the South Pacific Sea Level and Climate Monitoring Project. Figure 2.9 (a) and (b) are consistent in the sense that trends from the early 1990s (to the end of June 2007) are all positive with considerable variability from station to station. Note that Figure 2.9 (a) indicates that year-to-year variability is very important in determining trends over periods as short as the period for which the array in Figure 2.9 (b) has been operating, and that the trends since the early 1990s can differ considerably from trends over longer periods.

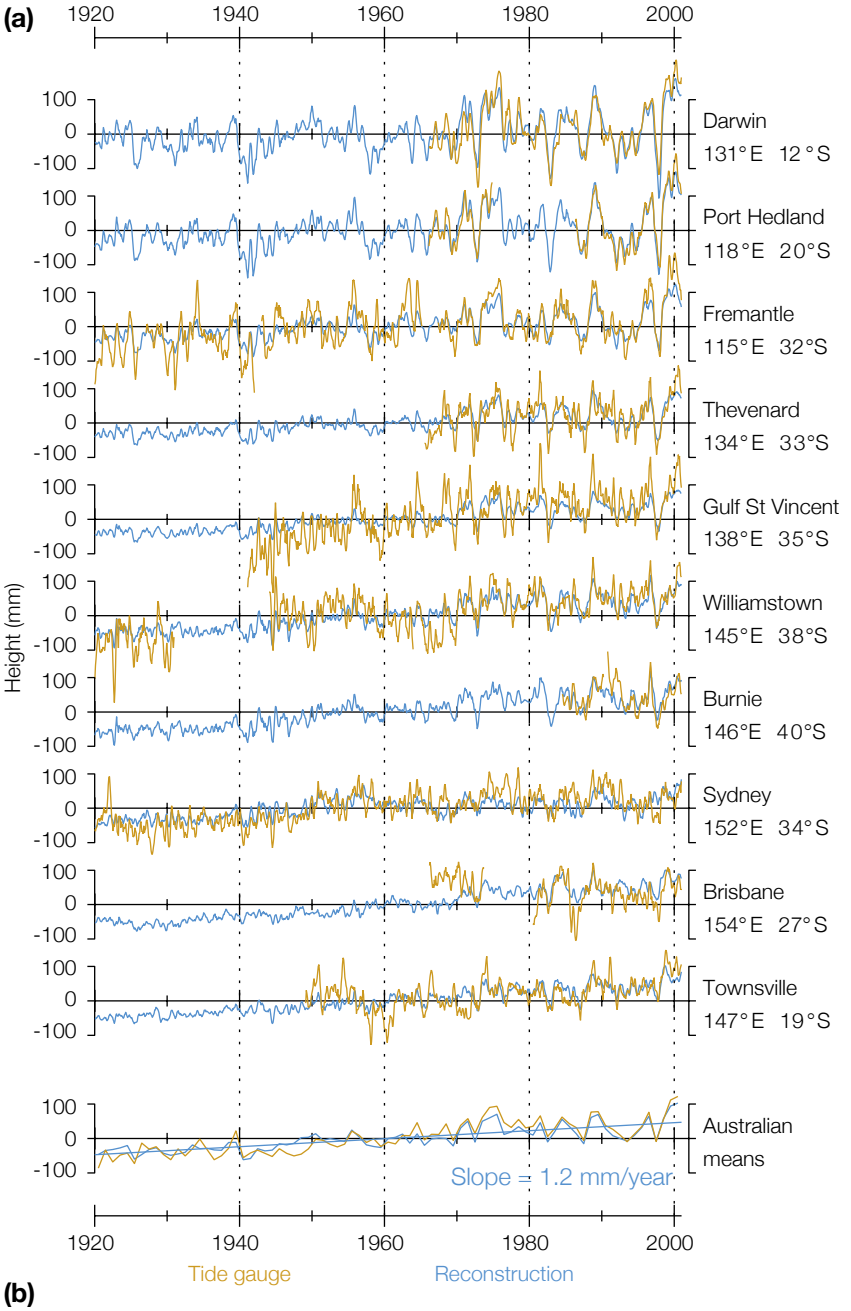

Figure 2.9: (a) Observed (with coastal tide gauges) and reconstructed sea levels (see Church *et al*. 2006 for further details) for the period 1920 to 2000 in the Australian region. The observed tide-gauge records are monthly average values. The Gulf St Vincent site is a composite record from three sites and is affected by local land motion. (Courtesy of J. Church, CSIRO). **(b)** The map shows observed rates of relative mean sea level rise (mm per year, with the vertical motion of the gauge with respect to the land excluded) from the early 1990s to June 2007 only, i.e. for a much shorter period than is depicted in **(a)**. Data used in **(b)** are from the Australian Baseline Sea Level Monitoring Array (white figures) and the South Pacific Sea Level and Climate Monitoring Project (yellow figures). Trends due to atmospheric pressure changes are retained in both **(a)** and **(b)**. Instruments that will enable the removal of the influence of additional vertical land movements on the records are currently being installed. (Courtesy of W. Mitchell, National Tidal Centre, Bureau of Meteorology)

2.4.2 Sea surface temperature

Substantial warming has occurred in the three oceans surrounding Australia. In the Pacific, an El Niño-like pattern features prominently in the warming trend with a stronger warming in the eastern Pacific (Figure 2.10). It is not clear whether the pattern is related to greenhouse gas induced global warming, or is caused by the fact that since the mid-1970s, natural variability has resulted in there having been more El Niño years than La Niña years. A feature of the south Pacific, near the east coast of Australia, is a large warming, thought to be associated with the changing East Australian Current. In the Indian Ocean, substantial warming in the tropical and southern subtropical zones contributes to a basin-wide warming rate that is fastest of all oceans. The warming along the West Australian coast is greater than that offshore. Further, the Indian Ocean sector of the sub-Antarctic zone shows the strongest warming of the Southern Ocean. While the gross patterns in Figure 2.10 are reproduced in different datasets, many of the details differ from similar analyses using other surface datasets, and so must be treated with care.

2.4.3 Ocean currents

The Leeuwin Current off Western Australia brings warm water from the tropics and increases the sea surface temperature compared to water offshore. Since the 1960s, sea surface temperatures in the Leeuwin Current have risen by about 0.6ºC, less than that offshore but closer to the rise of global average sea surface temperature. The current is stronger during a La Niña year and weaker during an El Niño year (Feng *et al*. 2003). Since the mid-1970s, there have been more El Niño than La Niña events (see section 2.5), so that the Leeuwin Current is weaker, and its sea surface temperature increase is damped by a shallow thermocline (Feng *et al*. 2004).

The East Australian Current is the largest ocean current closest to the eastern coastline of Australia and brings warmer water from the tropics. There is indirect evidence suggesting that there has been a significant change of the current. Long-term observations off Maria Island (148º16´E, 42º36´S) near Tasmania reveal a warming trend far greater than the global average, and recent studies suggest that to a large extent this is due to an intensifying East Australian Current. Summer surface wind changes induced by ozone depletion have generated a strengthening flow of the East Australian Current passing through the Tasman Sea (Cai 2006; Figure 2.11). This transports more warm water southwards and contributes to the large warming rate.

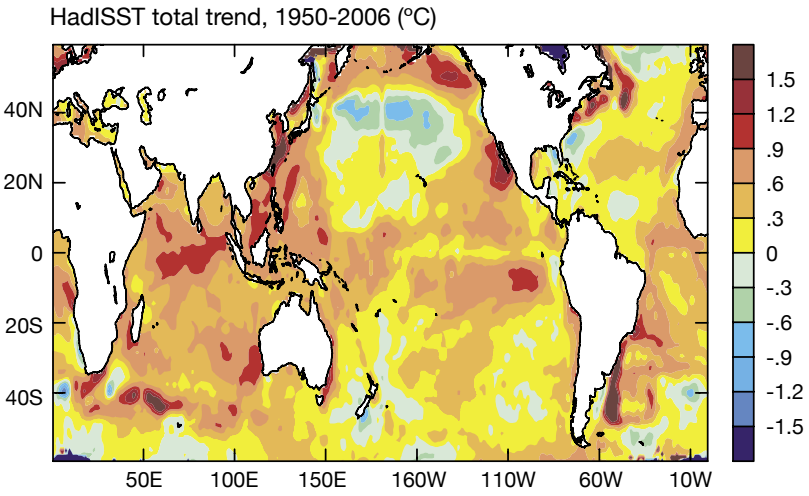

Figure 2.10: Pattern of linear warming rate (ºC/50 years) for the period 1950-2006 using updated observed sea surface temperature data (method of Rayner *et al*. 1996).

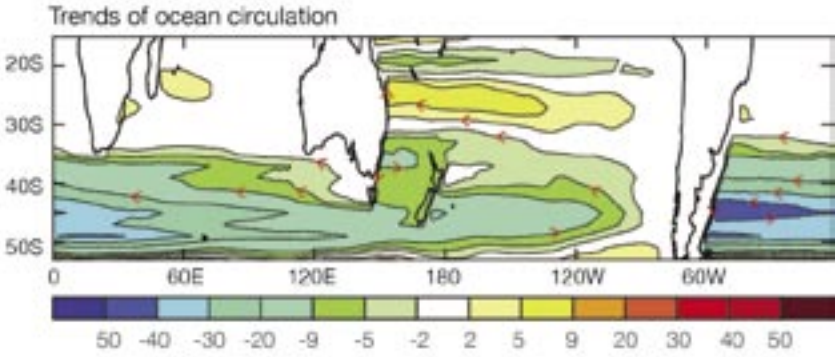

Figure 2.11: Linear trend in the transport stream-function (units are in Sverdrups where, 1 Sv = 106 m^3 s^{-1}) calculated using Godfrey's Island Rule model (Godfrey 1989). The model was forced by the linear trend-fitted surface wind stress (Kalnay *et al*. 1996) averaged over the summer months (December to May) from 1978-2002. The trends depicted include an intensification of both the East Australia Current and the Antarctic Circumpolar Current. The ocean flow directions induced by the wind-stress changes are indicated with arrows. See Cai (2006) for further details.

2.5 El Niño – Southern Oscillation and the Southern Annular Mode

2.5.1 El Niño – Southern Oscillation

The El Niño – Southern Oscillation (ENSO) is strongly related to major Australian anomalies in rainfall, temperature and tropical cyclones. There has been a small downward trend in the annual Southern Oscillation Index (SOI) since 1876 (Figure 2.12), at least partially associated with an increase in the frequency of El Niño events.

Instrumental and palaeo-climate records show large variations in the frequency and intensity of ENSO over time. (e.g. Allan *et al*. 1996; Power *et al*. 1999; Van Oldenborgh and Burgers 2005; Tudhope *et al*. 2001; McGregor and Gagan 2004; Shulmeister and Lees 1995). The impact of ENSO on Australia also varied from decade to decade (Power *et al*. 1999; 2006). The tropical Pacific Ocean (strongly linked to ENSO) has warmed over recent decades (Figure 2.13 and section 2.4.2).

The relationship between the SOI and both Australian temperature and rainfall has changed (Nicholls *et al*. 1996; Power *et al*. 1998a; Power *et al*. 2006). This is illustrated in Figure 2.14. Temperatures after 1973 were higher for any given value of the SOI than they were previously (Figure 2.14(a)). Rainfall since 1973 has also been higher for any given value of the SOI than it was previously (Figure 2.14(b)). Smith (2004) showed that the recent rainfall increases have been dominated by increases in the north and north-west of the continent during the summer half of the year.

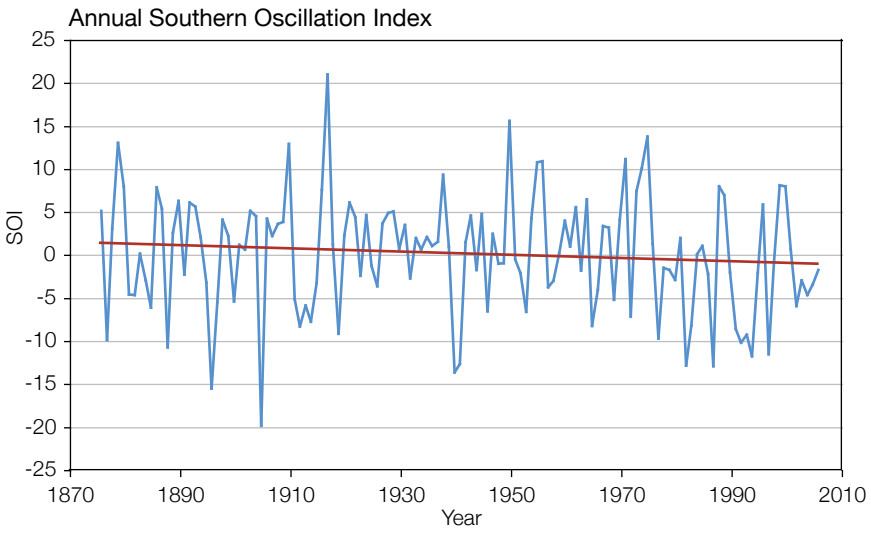

Figure 2.12: Variation of annual average Southern Oscillation Index, using data from Australia's National Climate Centre within the Bureau of Meteorology. Note the weak downward trend.

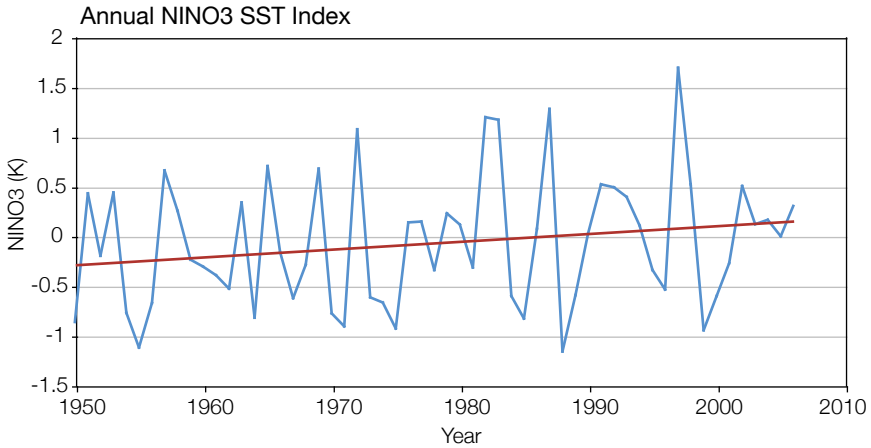

Figure 2.13: Annual sea surface temperature averaged over the Nino3 region in the tropical eastern Pacific Ocean (210-270°E and 5°S-5°N).

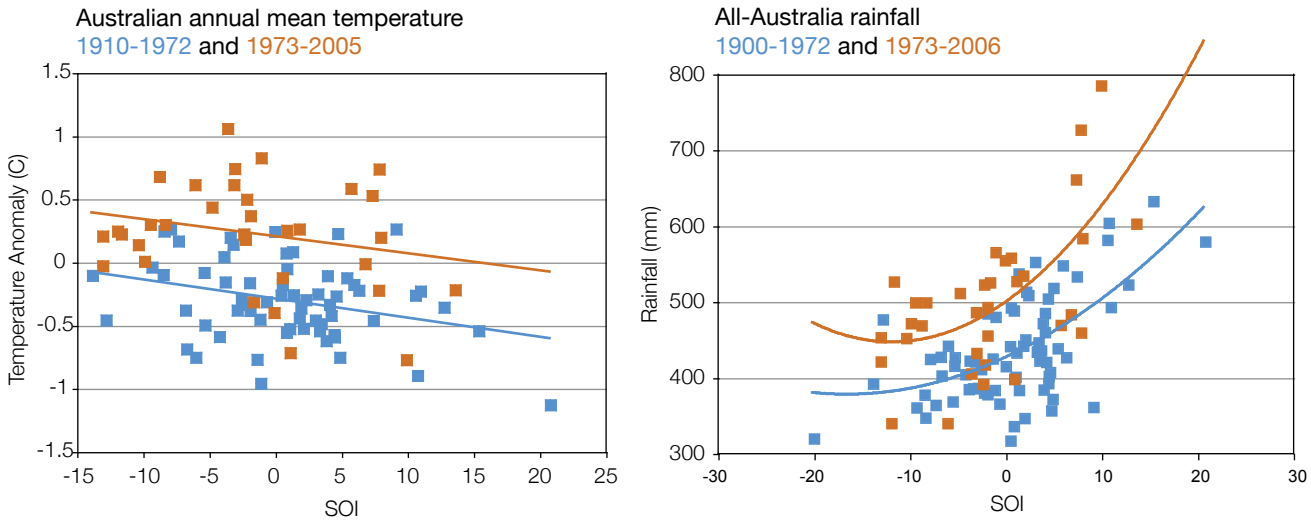

Figure 2.14 (a) Scatter plot showing the relationship between Australian temperature and the Southern Oscillation Index (SOI) for the two periods 1910-1972 and 1973-2005 (b) Scatter plot showing the relationship between Australian rainfall and the SOI for the two periods 1900-1972 and 1973-2004. The plots illustrate how the inter-relationships between Australian climate and the SOI have changed in recent decades.

2.5.2 The Southern Annular Mode

The Southern Annular Mode (SAM) can be characterised as a flip-flop in pressure between the high and mid-latitudes of the Southern Hemisphere (Rogers and van Loon 1982; Kidson 1988; Hartmann and Lo 1998; Karoly 1990; Thompson and Wallace 2000; Thompson and Solomon 2002). By convention, when the SAM is in its positive phase, anomalously low pressure occurs over Antarctica and anomalously high pressure over the mid-latitudes (40-55°S). During the positive phase of SAM, the circumpolar westerlies increase in strength and the circumpolar vortex contracts. These changes are associated with a poleward shift of the mid-latitude storm tracks (Yin 2005; Bengtsson *et al*. 2006). Although the SAM has largest influence on the surface climate of latitudes further south than Australia, it has been linked to changes in Australian climate (Hendon *et al*. 2007; Meneghini *et al*. 2007; Cai and Cowan 2006).

The positive phase of the SAM is associated with significant winter rainfall deficiencies in the southern regions of Australia and significant rainfall increases in the Murray-Darling Basin in summer (Hendon *et al*. 2007). Approximately 15% of the weekly spring/summer rainfall variance over south-eastern Australia is related to the SAM (Hendon *et al*. 2007). This is a similar magnitude to that explained by ENSO.

In recent decades, the SAM has increasingly spent more time in its positive phase, with statistically significant positive trends in the summer and autumn seasons and no significant changes in winter and spring (Thompson and Wallace 2000; Marshall 2003).

The potential for storm formation over southern Australia has decreased over the last 40 years. In the south-west of the continent, the reduction of wintertime rainfall in the region is associated with both a reduction in the intensity of cyclogenesis and a decrease in the number of some rain-bearing synoptic systems, and a southward deflection of some storms (Hope *et al*. 2006; Frederiksen and Frederiksen 2006; see also Lim and Simmonds 2007).

2.6 Palaeo-records

In order to help place climatic changes observed over the past century into perspective it is useful to know how Australia's climate varied before the instrumental period began. This can be achieved through the use of palaeo-records (i.e. proxy records derived from landscape features and biological, chemical and isotopic material stored in sediments, ice sheets, tree rings, cave deposits and corals). Palaeo-records increase our understanding of what climate variations can occur naturally and thus assist in our interpretation of current climate trends. The majority of palaeo-information is from the southern, eastern and northern regions of Australia. Arid areas are not well represented in the records.

2.6.1 Precipitation

Pollen records of past vegetation in eastern Australia indicate precipitation was generally higher than present between 9,000 and 3,500 years ago. Highest levels appear to have occurred between 9,000 and 6,000 years ago in Tasmania, between 7,500 and 4,000 years ago in southern mainland Australia and from 5,000 to 3,700 years ago in northern Australia (Shulmeister *et al*. 2004). This suggests a regional climatic shift, possibly related to the movement of the subtropical anti-cyclone belt, the westerlies and/or the monsoon.

From around 4,000 years ago onwards, palaeo-records indicate an increase in the seasonality of precipitation in the Australian region (Shulmeister and Lees 1995). Evidence from lakes in Victoria suggest that conditions between about 2,000 years ago to AD 1840 were wetter than present, after which the dry conditions of the recent instrumental period became established (Jones *et al*. 1998).

2.6.2 Temperature

Palaeo-evidence for temperatures in the Australian region is less widespread than for precipitation and is often debated. What is available indicates that here have been moderate variations in temperature over the past 9,000 years, with some regional variation. Pollen evidence suggests that annual temperatures in south-east Australia may have been slightly higher between 9,000 and 5,000 years ago as the Earth shifted into the Holocene warm phase (Macphail 1979; Lloyd and Kershaw 1997; Anker *et al*. 2001). However, records from Victoria suggest that it may actually have been winter temperatures that were higher, with summer temperatures being slightly lower (McKenzie and Busby 1992).

Tree ring records from Tasmania indicate cooler conditions than present occurred during the Little Ice Age that occurred from around 1300 to the mid-19th century (Briffa 2000; Cook *et al*. 2000). This is supported by coral records from New Caledonia, which suggest a 1.4ºC cooling around 1730 (Hendy *et al*. 2002). However, coral records from northern and western Australia for the same period give evidence of sea surface temperatures as warm as the early 1980s (Gagan *et al*. 2004), demonstrating that there has been regional variation in past temperature change, possibly as a result of significant shifts in the ocean-atmosphere system (Lough 2001; Hendy *et al*. 2002; Lough *et al*. 2006).

2.6.3 Climate variability

Higher resolution, continuous palaeo-records give evidence of decadal and sub-decadal scale climate variation. For example, palaeo-climate data (Mann *et al*. 2005; Cobb *et al*. 2003; D'Arrigo *et al*. 2005; Tudhope *et al*. 2001; Hughen *et al*. 1999) indicate that ENSO has operated for many thousands of years. The tropical cyclone palaeo-record for Cairns and the Great Barrier Reef for events spanning the last 5,000 years suggests that the historical record underestimates by a factor of ten the frequency of the most severe tropical cyclones likely to strike the Cairns region, and that the historical record of cyclones in Cairns and the east coast of Queensland coincides with a period of relative quiescence in tropical cyclone activity (Lough 2001; Nott and Hayne 2001; Nott 2003; Lough *et al*. 2006).

Chapter 3 Causes of past climate change

The climate of the Earth changes continually on a range of timescales due to 'internal' and 'external' factors. Internal factors are natural and arise from complex interactions within the climate system. In general, internal variability on short time-scales (days to weeks - what we know as 'weather') is generated by atmospheric instability. Variability on longer time-scales (intraseasonal, interannual and decadal to centennial) can be enhanced by complex interactions between the atmosphere and other components of the climate system (mostly the oceans, see e.g. Power *et al*. 1995, but also the terrestrial biosphere and the cryosphere).

Natural external factors include the Earth's rotations that produce diurnal and seasonal cycles, variations in the amount of radiant energy emitted by the Sun (e.g. sunspot cycles have a period of about 11 years), volcanic eruptions and changes in the Earth's orbital parameters (e.g. due to Milankovic cycles, which have a dominant period of 100,000 years). Substantial global warming at the end of ice ages over the past half million years was triggered by changes in the Earth's orbit and subsequently enhanced by natural increases in greenhouse gases.

Humans are also responsible for external factors which are referred to as 'anthropogenic'. For example:

- Changes in atmospheric composition (e.g. in concentrations of stratospheric ozone and greenhouse gases: carbon dioxide, methane, nitrous oxide, chlorofluorocarbons and tropospheric ozone).
- Release of atmospheric particulates (e.g. sulfate aerosols, black carbon).
- Modification of the terrestrial ecosystems (e.g. by land clearance and agricultural practices).

Radiative forcing is the term given to an externally imposed change in the radiation balance (the balance between incoming solar radiation and outgoing heat radiation) such as changes in atmospheric concentrations of greenhouse gases (See section 4.1.3).

The largest change in radiative forcing in the climate system since 1750 has been due to the increase of carbon dioxide (Figure 3.1) followed by an increase in concentrations of other greenhouse gases (IPCC 2007a). There is now "very high confidence level that the globally averaged net effect of human activities since 1750 has been one of warming, with a radiative forcing of +1.6 W/m^2 (with an uncertainty range of +0.6 to +2.4 W/m^2)".

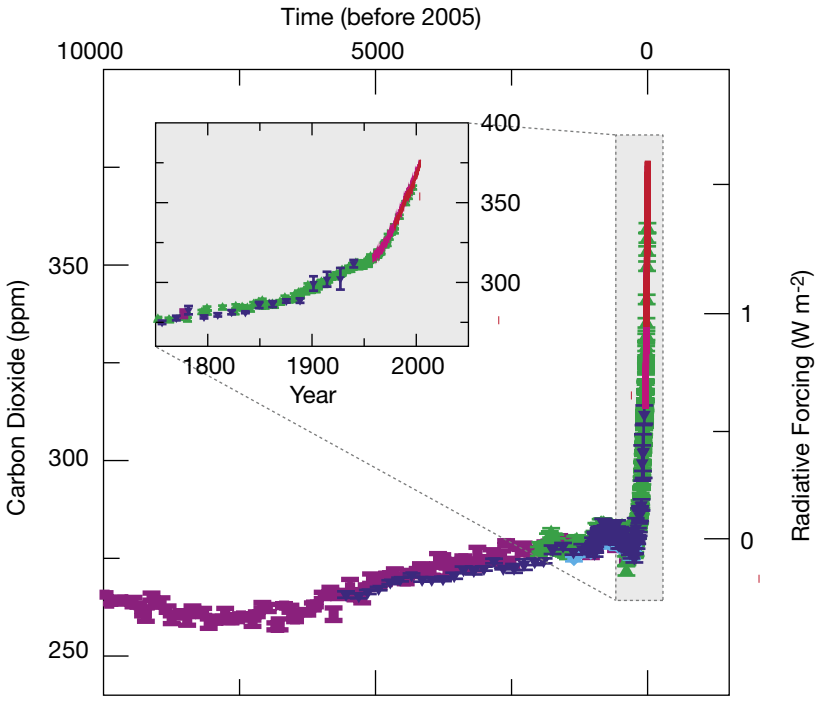

Figure 3.1: Atmospheric concentrations of carbon dioxide over the last 10,000 years (large panel) and since 1750 (inset panel). Measurements are shown for air extracted from ice cores (symbols with different colours for different studies) and atmospheric samples (red lines). The corresponding radiative forcings are shown on the right hand axes of the large panel (from IPCC (2007a) Figure SPM-1).

3.1 Detection and attribution of observed climate change

Detection of climate change is "the process of demonstrating that climate has changed in some defined statistical sense, without providing a reason for that change" (IPCC 2001). A change (the 'signal') is *detected* in observations if its likelihood of occurrence by random chance from internal variability alone (the 'noise') is small enough to be regarded as unlikely. To filter out the noise and detect a statistically significant trend, the climate record has to be of sufficient length. 'Sufficient' will vary according to the magnitude of the trend (i.e. smaller signals are harder to detect) and the importance of the noise (i.e. it is more difficult to detect changes in highly variable quantities such as rainfall as opposed to temperature). Because detection studies are necessarily statistical in nature, they are never absolutely certain. Detection does not, by itself, establish the cause of the climate change.

Attribution is "the process of establishing the most likely causes of the detected change with some defined level of confidence" (IPCC 2001). From a practical perspective, IPCC (2001) recommended that attribution of anthropogenic climate change requires:

- The detection of a change to a significant statistical level
- Demonstration that the detected change is "consistent with the estimated responses to the given combination of anthropogenic and natural forcing"; and
- Demonstration that the detected change is "not consistent with alternative, physically-plausible explanations".

Climate models are the major tools used to determine the causes of observed climate change. Climate model simulations can be used to explain recent climatic changes and separate the impact of anthropogenic factors from natural forcings. However, many observed variations are at least partly random in nature and are not expected to be replicated. Indeed, climate models exhibit effectively stochastic (random) behaviour as does the climate system (e.g. Power and Colman 2006). So to attribute a signal in model studies to any external forcing it is a common practice to use an ensemble of several simulations to filter out the naturally occurring internal climate variability within the model from the underlying trends. The differences between simulations reflect the model's estimate of the natural internal variability of the climate system.

Evidence of a human influence on recent climate has accumulated steadily during the past two decades. Despite clear evidence of changes in the composition of the global atmosphere, the first IPCC Assessment Report (IPCC 1990) contained little observational evidence of a detectable anthropogenic influence on climate. However, six years later the Second Assessment Report (IPCC 1996) concluded that "*the balance of evidence*" suggested there had been a "discernible" human influence on the climate of the 20th century. Considerably more evidence accumulated during the subsequent five years, leading the Third Assessment Report (IPCC 2001) to the stronger conclusion that "*most of the observed warming over the last 50 years is likely to have been due to the increase in greenhouse gas concentrations*".

More detection and attribution studies were carried out in the subsequent years and the Fourth Assessment Report (IPCC 2007a) concluded that "*most of the observed increase in globally averaged temperatures since the mid-20th century is very likely due to the observed increase in anthropogenic greenhouse gas concentrations. Discernible human influences now extend to other aspects of climate, including ocean warming, continental average temperatures, temperature extremes and wind patterns*".

3.2 Attribution of observed climate changes in Australia

3.2.1 Temperature

Australian surface temperatures have warmed significantly over the past century. Warming since the middle of the 20th century is likely to be mostly due to anthropogenic increases in greenhouse gases.

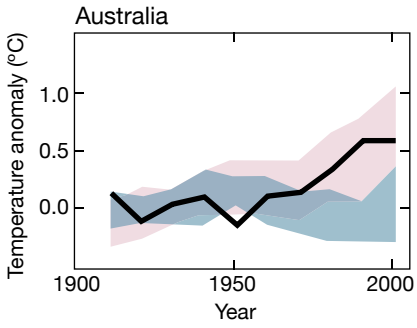

Figure 3.2: Comparison of Australia-wide observed continental changes in surface temperature (black line, decadal averages) with results simulated by climate models using natural only (blue shaded band) and natural plus anthropogenic forcings (pink shaded band). Changes are relative to the average for 1901-1950. Both shaded bands show the 5–95% range of values evident in the simulations (from IPCC (2007a) Figure SPM-4).

Temperature has increased over most of Australia since 1950 (Figures 2.1 and 2.2 and discussion in Chapter 2). As part of the IPCC Fourth Assessment Report, 19 simulations from five climate models from a number of different research groups around the world using only natural forcings and 58 simulations from 14 climate models using both anthropogenic and natural forcings were analysed. Only the ensemble of simulations that includes the anthropogenic forcing in addition to the natural forcing is able to capture the observed warming during the second half of the century (Figure 3.2). The ensemble incorporating natural forcing tracks the decadal averages of the Australia-wide observed temperature only until the 1970s but does not capture the subsequent acceleration of the warming.

This new result confirms an earlier study based on a smaller range of climate models but examining a variety of simple temperature indices. Australian temperature changes over the 20th century appear "very unlikely" to be due to natural climate variations alone, and it was "likely that there has been a significant contribution to the observed warming during the second half of the century from increasing atmospheric greenhouse gases and sulfate aerosols" (Karoly and Braganza 2005a). This work, in turn, advanced earlier work that noted consistency between observed trends and the response of climate models to enhanced greenhouse forcing (Pittock 1988; Power *et al*. 1998b).

It was also demonstrated that the recent increase in temperatures was not a consequence of rainfall change (unlike past changes) and therefore inconsistent with natural climate trends (Nicholls *et al*. 1996; Nicholls 2003; Power *et al*. 1998a,b). Indeed, once the rainfall-related component of the temperature variations is removed, "trends in the residual variations of maximum, mean and minimum temperature over the last 50 years are not explained by natural climate variations and are consistent with the response to increasing greenhouse gases and sulfate aerosols in climate models" (Karoly and Braganza 2005b).

This latter approach is able to enhance the signal-to-noise ratio for anthropogenic temperature change signals in the Australian region and shows that there is a clear anthropogenic warming signal in observed regional temperature trends, even for regions as small as the south-east of Australia. At small regional scales it is not always possible to attribute these regional features to a specific cause as more than one factor may be contributing to the change in the climate. An exception is the central part of the south-east of Australia which has warmed during the second half of the 20th century but by a much smaller amount than the rest of the continent. This reduced rate of warming was related to changes in the Southern Annular Mode. (Hendon *et al*. 2007).

3.2.2 Rainfall

The rainfall decrease in south-western Australia since the mid-1970s is likely to be at least partly due to anthropogenic increases in greenhouse gases. It is not yet possible to attribute rainfall decreases in eastern Australia, and rainfall increases in north-western Australia to human activities.

The possible causes of the rainfall decrease in the south-west of Western Australia in the mid-1970s have been studied extensively (Ryan and Hope 2005, 2006). The rainfall decline has been related to changes in the large-scale winter weather systems that bring rain to south-west Western Australia. The number of synoptic weather patterns that bring wet conditions decreased in the mid-1970s accompanied by an ongoing increase in the number that bring dry conditions (Charles *et al*. 2004). This reduction in June and July has contributed 50% of the rainfall decline in the mid-1970s (Hope *et al*. 2006). Changes in the convergence of moisture into the region by the wind also contribute to the rainfall decline (Timbal 2004). On a broader scale, a drop of 20% in the strength of the upper level winds has lead to a reduction in the likelihood of storm development over south-west Western Australia compared to the pre-1970s (Frederiksen and Frederiksen 2007). Although climate model simulations can occasionally produce a decline as substantial as that observed in the south-west without changes in external forcings (Cai *et al*. 2005b), the consensus is that "it is unlikely that the observed drying is a result of natural fluctuations in the climate" (Ryan and Hope 2006), and it is likely that the natural fluctuations inherent in the climate system and changes in greenhouse gas concentrations have contributed to the observed rainfall decline in south-west Western Australia (Timbal *et al*. 2006). Averaging over all IPCC (2007a) model simulations, it is found that 50% of the reduction is attributable to anthropogenic forcing that has a structure that is reminiscent of the Southern Annular Mode (see Chapter 5) and its impact on rainfall in south-west Western Australia (Cai *et al*. 2003a; Cai and Cowan 2006, 2007). The role of land cover changes is recognised as a possible secondary contributor but is unlikely to be the major factor in the rainfall reduction over south-west Western Australia (Pitman *et al*. 2004; Timbal and Arblaster 2006).

The more recent rainfall decline in the east of the continent (see Figure 2.5 and Chapter 2) is only now being studied extensively and is yet to be attributed to external causes (Nicholls 2006). However, the rainfall decline in the south-east of South Australia and the south-west of Victoria bears some characteristics consistent with the earlier rainfall decline in the south-west of Western Australia and has similarly been linked to large-scale changes in mean sea level pressure (Timbal and Jones 2007). The fact that the change is occurring much later may be due to the movement of the subtropical ridge (Drosdowsky 2005). However, the rainfall decline in this part of the continent appears more complex. In particular the influence of the tropical Indian Ocean is important (Meyers *et al*. 2007) but appears to have disappeared during the recent dry decade, possibly as a consequence of the increase of mean sea level pressure across the southern half of the continent (Timbal and Murphy 2007).

The largest rainfall trend observed in Australia is the increased summer rainfall in the north-west of the continent (see Figure 2.4 and Chapter 2). The attribution of these changes remains an important area of research. Two factors that are potentially relevant have been identified: warming of the Australian continent might have helped to drive to a strengthening of the monsoon, resulting in increased rainfall (Wardle and Smith 2004); and an increase in anthropogenic aerosols in the atmosphere in the latter part of the 20th century predominantly linked to extensive haze of much of Asia might have altered atmospheric circulation over northern Australia (Rotstayn *et al*. 2007). Further work on these and other possible causes are required.

3.2.3 Drought

Droughts have been accompanied by higher temperatures due to anthropogenic warming.

Recent Australian droughts (1994, 2002-03 and 2006-07) have not become drier than droughts that occurred earlier in the 20th century. However, the recent droughts have been accompanied by higher temperatures (Nicholls 2004; Murphy and Timbal 2007).

The distinction between 'meteorological drought' (due to rainfall deficiency) and other forms of drought, e.g. agricultural drought or hydrological drought, is sometimes made (see Chapter 5 for further details). It is possible, for example, that a given region might be experiencing an agricultural drought even if the criteria used to define meteorological drought have not been met. For example, seasonal rainfall might be near-average but the rain did not fall during the times when it was needed by the crop. Factors other than just rainfall can also be influential in determining non-meteorological drought. It is possible, for example, that in some contexts a temperature rise might increase the water required by the crop to grow. Warming might therefore intensify agricultural drought in a region where the crop is very common. As most of the observed warming in Australia since 1950 can be attributed to human-induced increases in greenhouse gases (section 3.2.1; IPCC 2007a) the severity of agricultural drought in that region could then be partly attributed to anthropogenic warming. While this is a plausible scenario, very little research has been done to date on either the quantification of trends in drought severity in its various forms beyond simply using rainfall deficit, or in the cause of any observed trends.

3.2.4 Snow

The decline in snow cover observed in recent decades is probably due to anthropogenic warming.

The snow season in the Australian Alps has shortened in recent decades, with less snow remaining early in spring This is due to warming (i.e. more precipitation falling as rain rather than snow, and earlier melting of snow on the ground) rather than any substantial decline in precipitation (Nicholls 2005). Since most of the observed warming in Australia since 1950 can be attributed to human-induced increases in greenhouse gases (IPCC 2007a), it can be inferred that most of the decline in snow cover is also due to human activities.

3.2.5 Changes in seasonal cycle

Little work has been done to investigate trends in indicators of seasonality. One exception, for rainfall, is the timing of the 'autumn break' or start of the wet season in northern Victoria which is largely determined by the occurrence of cut-off low pressure systems (low pressure systems that have separated from the circumpolar westerlies further south). Over the past decade, the autumn break is occurring later than previously or is failing to occur at all (Pook *et al*. 2006). The attribution of this change has not yet been made.

For temperature, it was found that the warmest time of the year in south-east Australia is occurring about a week later now than at the start of the 20th century (Alexander *et al*. 2005). No studies have yet attempted to attribute these changes to particular external causes.

3.2.6 Extremes

There has been an increase in the frequency of warm days/nights and a decrease in the frequency of cool days/nights. It is likely that these changes are mostly due to anthropogenic warming.

It is not possible to attribute a single extreme event to any particular external forcing; however, the trend in the frequency of extremes is potentially attributable to external causes (see Box 3.1). Extreme temperatures have changed in Australia, with a tendency for increased numbers of warm days and nights and fewer cool days and nights (Figure 2.3; Nicholls and Collins 2006; Alexander *et al*. 2007). This result is similar to what has been observed throughout eastern Asia and western Pacific (Griffiths *et al*. 2005). The frequency of extremes is affected by changes in mean temperatures (Griffiths *et al*. 2005), and given that regional-scale mean temperatures are likely to have changed as a result of human influence on the climate system, it is reasonable to conclude that the changes in frequency of extremes in Australia can also be partly attributed to human factors.

Extremes in daily rainfall also display trends in the same direction as the mean rainfall trends, however, the trend in the extremes is often greater than for the mean, indicating that the frequency of extreme events is changing faster than the mean (Alexander *et al*. 2007).

3.2.7 Other modes of variability

Most attribution studies have concentrated on secular trends, but considerable research also has been carried out to determine the causes of interannual and interdecadal variations in the Australian climate. Many of these studies have focussed on the effects of the El Niño – Southern Oscillation on Australian rainfall and temperature (e.g. Power *et al*. 1999, 2006; Meinke *et al*. 2005). Some studies also investigated the impact of variations in the Indian Ocean sea surface temperature on interannual variations of the Australian climate (Cai *et al*. 2005a; Meyers *et al*. 2007) and the impact of the Southern Annular Mode on the Australian climate (Cai and Cowan 2006; Hendon *et al*. 2007; Meneghini *et al*. 2007). Such seasonal-to-interannual variations are most likely the result of internal natural variability of the climate system.

3.2.8 Oceans

Rapid warming in the Tasman Sea is likely to be driven by Antarctic ozone depletion through an upward trend of the Southern Annular Mode.

Climate change in the oceans surrounding Australia is less definitive than over the land, due mainly to the shorter period for which observations are available. While some changes are evident, it is difficult to attribute the cause or the link to anthropogenic forcing.

One exception is the fast warming rate off Tasmania's Maria Island, where continuous ocean temperature measurements since the late 1940s exist and which reveal a trend that is three times greater than the global warming rate. Warming off Maria Island since the late 1970s represents a fast Tasman Sea warming rate and is principally driven by Antarctic ozone depletion. Ozone depletion causes the atmospheric circulation to change in a way that is reminiscent of changes linked to a positive phase of the Southern Annular Mode (Cai 2006; Cai and Cowan 2007). Thus both internal and external forcing can drive Southern Annular Mode-like features to the atmospheric circulation over the southern hemisphere. Ozone depletion as a result of human activities also causes circulation changes in the stratosphere, largest during the spring months, with a strengthening of the circumpolar westerlies and a weakening of the mid-latitude westerlies closer to the surface. These wind changes are largest during summer (Thompson and Solomon 2002; Gillett and Thompson 2003; Miller *et al*. 2006; Cai and Cowan 2007), when the East Australian Current is strongest and extends furthest to the south. The wind changes drive a stronger East Australian Current, moving more warm water south, leading to the warming in the Tasman Sea.

Box 3.1 Can individual extreme events be explained by climate change?

A wide range of extreme weather events is possible even in an unchanging climate, so it would be difficult to attribute an individual event, by itself, to a changed climate. Extreme weather results from a combination of factors. For example, the formation of a tropical cyclone requires a warm sea surface and specific atmospheric circulation conditions. Because some factors may be strongly affected by human influences (e.g. sea surface temperatures) but others may not, this will complicate the detection of a human influence on a single, specific extreme event.

However, it may be possible to determine whether anthropogenic forcing has changed the probability of occurrence of a specific type of extreme weather event. The value of a probability-based approach ("is there a change in the likelihood of an event that results from human influence?") is that it can be used to estimate the influence of external factors, such as increases in greenhouse gas concentrations, on the frequency of specific types of weather events (e.g. frosts, heatwaves, heavy rainfalls or floods). A climate model, either forced only with historical changes in natural factors such as volcanic activity and solar output, or by both human and natural factors, can be used to indicate whether, over the 20th century, human influences have increased the risk of any type of extremes. However, careful statistical analyses are required, since the likelihood of individual extremes could change due to changes in variability as well as changes in the mean climate. Such analyses rely on climate model-based estimates of variability, and thus an important additional requirement is that climate models adequately represent climate variability.

Global warming can increase the likelihood of a record high temperature in a given region. This means that a record high temperature that may seem extraordinary in an unchanging climate seems less extraordinary if global warming is taken into account (Power and Nicholls 2007).

In the future, climate model simulations project that there will be changes in the incidence of many types of extreme weather events, including an increase in extreme rainfall events, due to human influences on the atmosphere (IPCC 2007). There is evidence of increases in extreme rainfall events in at least some regions in recent decades. However, there is as yet no conclusive evidence that these increases are necessarily linked to increasing greenhouse gas concentrations.

Chapter 4 Global climate change projections

4.1 Scenarios of greenhouse gas emissions, concentrations and radiative forcing

4.1.1 Emissions

The greenhouse gas emissions discussed here are those due to human activities, such as energy generation, transport, agriculture, land-clearing, industrial processes and waste. To provide a basis for estimating future climate change, the Intergovernmental Panel on Climate Change (IPCC 2000) prepared 40 greenhouse gas and sulfate aerosol emission scenarios for the 21st century that combine a variety of assumptions about demographic, economic and technological factors likely to influence future emissions. Each scenario represents a variation within one of four 'storylines': A1, A2, B1 and B2 (see Box 4.1). Projected carbon dioxide, methane, nitrous oxide and sulfate aerosol emissions based on these scenarios are shown in Figure 4.1.

Box 4.1 The IPCC Special Report on Emissions Scenarios (SRES) (IPCC 2000)

A1. The A1 storyline describes a future world of very rapid economic growth, a global population that peaks in mid-century and declines thereafter, and the rapid introduction of new and more efficient technologies. Major underlying themes are convergence among regions, capacity building and increased cultural and social interactions, with a substantial reduction in regional differences in per capita income. The A1 storyline develops into three scenario groups that describe alternative directions of technological change in the energy system. They are distinguished by their technological emphasis: fossil intensive (A1FI), non-fossil energy sources and technologies (A1T), or a balance across all sources (A1B) (where balanced is defined as not relying too heavily on one particular energy source, on the assumption that similar improvement rates apply to all energy supply and end use technologies).

A2. The A2 storyline describes a very heterogeneous world. The underlying theme is self reliance and preservation of local identities. Fertility patterns across regions converge very slowly, which results in continuously increasing population. Economic development is primarily regionally oriented and per capita economic growth and technological change more fragmented and slower than other storylines.

B1. The B1 storyline describes a convergent world with the same global population as in the A1 storyline (one that peaks in mid-century and declines thereafter) but with rapid change in economic structures toward a service and information economy, with reductions in material intensity and the introduction of clean and resource efficient technologies. The emphasis is on global solutions to economic, social and environmental sustainability, including improved equity, but without additional climate initiatives.

B2. The B2 storyline describes a world in which the emphasis is on local solutions to economic, social and environmental sustainability. It is a world with continuously increasing global population, at a rate lower than A2, intermediate levels of economic development, and less rapid and more diverse technological change than in the B1 and A1 storylines. While the scenario is also oriented towards environmental protection and social equity, it focuses on local and regional levels.

An illustrative scenario was chosen for each of the six scenario groups – A1B, A1FI, A1T, A2, B1 and B2. All were considered equally sound by the IPCC.

The SRES scenarios do not include additional climate initiatives, which means that no scenarios are included that explicitly assume implementation of the United Nations Framework Convention on Climate Change or the emissions targets of the Kyoto Protocol.

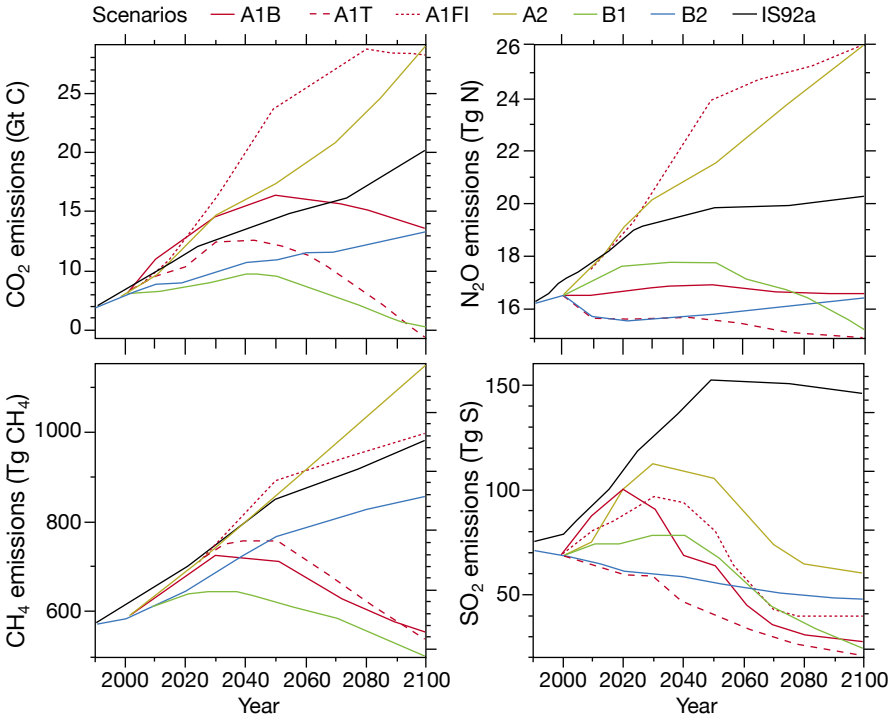

Figure 4.1: Anthropogenic emissions of carbon dioxide (CO_2), methane (CH_4), nitrous oxide (N_2O) and sulfur dioxide (SO_2) for six SRES scenarios (see Box 4.1) and the IS92a scenario from the IPCC Second Assessment Report in 1996 (IPCC 2001).

4.1.2 Concentrations

Carbon cycle models are used to convert emissions into atmospheric concentrations, allowing for uptake of emissions by the land and ocean, land and ocean climate feedbacks, and transport and chemical reactions in the atmosphere. The carbon dioxide (CO_2) lifetime in the atmosphere is difficult to quantify because it is continuously cycled between the atmosphere, ocean and biosphere, which involves a range of processes with different timescales. Around half the CO_2 emitted is removed on a time-scale of 30 years, a further 30% is removed within a few centuries, and the remaining 20% may stay in the atmosphere for thousands of years (Denman *et al*. 2007). Methane's atmospheric lifetime is about 8.4 years, nitrous oxide is around 114 years, 45 to 100 years for chlorofluorocarbons, 1 to 18 years for hydrochlorofluorocarbons and 1 to 270 years for hydrofluorocarbons (Denman *et al*. 2007).

Carbon cycle models give estimates of atmospheric CO_2 concentrations for the year 2100 ranging from 500 to 1200 ppm, compared to the 1990 concentration of 352 ppm (Meehl *et al*. 2007). Methane concentrations are projected to change from 1700 ppb in 1990 to 1400 to 3500 ppb by 2100, and nitrous oxide concentrations are projected to increase from 308 ppb in 1990 to 360 to 460 ppb by 2100 (Meehl *et al*. 2007). Concentrations of tropospheric ozone, hydrofluorocarbons and perfluorocarbons are also projected to increase.

Carbon cycle models project a reduction in the ability of the land and ocean to absorb anthropogenic CO_2, causing an increasingly large fraction of anthropogenic CO_2 to stay airborne. For example, for the A2 emission scenario, this positive feedback leads to additional atmospheric CO_2 concentration of 20 and 220 ppm by 2100 (Meehl *et al*. 2007).

This report does not explicitly address possible mitigation responses or pathways to greenhouse gas stabilisation as, by construction, none of the SRES factor in these issues (Box 4.1). However the lowest CO_2 emission scenario considered here, B1, peaks in mid-century, and declines thereafter to sufficient levels to come close to stabilisation of CO_2 concentrations (at around 550ppm) by century end. Methane and nitrous oxide concentrations also decrease and stabilise respectively over this period (refer to IPCC 2001 Technical Summary, p 65). To a first approximation, therefore, B1 may be considered representative of a stabilisation scenario to 550 ppm CO_2 by 2100. An important caveat on this is that carbon cycle feedbacks, which are currently very uncertain, must not be significantly larger than those considered in the original generation of this scenario (IPCC 2000). Details on mitigation pathways required for greenhouse gas stabilisation at a range of levels are given in the Working Group III contribution to the IPCC Fourth Assessment Report (IPCC 2007c).

4.1.3 Radiative forcing

Increasing concentrations of greenhouse gases affects the radiative balance of the Earth. The balance between incoming solar radiation and outgoing heat radiation defines the Earth's radiation budget (Bryant 1997). This balance determines the Earth's average temperature. Radiative forcing is the term given to an externally imposed change in the radiation balance, such as changes in atmospheric concentrations of greenhouse gases.

The greenhouse gas concentrations projected using the SRES are converted to a radiative forcing of the climate system using radiation codes (usually located within climate models themselves). Positive forcing warms the Earth, while negative forcing cools the Earth. CO_2 dominates the radiative forcing and has a warming effect. By the year 2100, the radiative forcing is about 4 Wm^{-2} for B1, 5 Wm^{-2} for A1T, 6 Wm^{-2} for B2, 7 Wm^{-2} for A1B, 8 Wm^{-2} for A2 and 9 Wm^{-2} for A1FI, compared to about 2 Wm^{-2} in 1990 (Fig 10.26 in Meehl *et al*. 2007).

Water vapour is another particularly important greenhouse gas. However direct human emissions of water vapour are negligible. Rather it is the *response* of water vapour to atmospheric warming which dictates its importance for climate change. A warmer atmosphere holds more water vapour, thereby increasing greenhouse trapping and resulting in further warming. This *positive feedback* therefore acts to amplify the warming initiated by increases in anthropogenic greenhouse gases such as carbon dioxide and methane.

4.2 Using global climate models to estimate future climate change

4.2.1 Global climate models

The complexity of processes in the climate system means we cannot simply extrapolate past trends to forecast future conditions. Climate models are the best tools we have for forecasting weather and climate. Perhaps the most familiar application is in daily weather forecasting. Models are also used for three-month climate forecasts for regions like Australia, which can assist agribusiness and other industries to plan for the months ahead. Another application is projecting the effect of human activities on climate over the coming decades, and explaining the causes of climate change over past decades. This includes increasing greenhouse gases and aerosols and stratospheric ozone depletion, e.g. the SRES (IPCC 2000) scenarios.

A climate model is a mathematical representation of the Earth's climate system. The mathematical equations are based on well-established laws of physics, such as conservation of mass, energy and momentum. They include the fact that the infrared radiation absorption bands are partially saturated, leading to a non-linear response to increasing greenhouse gas concentrations. The realism of climate models has been tested against a wealth of observational data from the natural world (for example, representation of spatial and temporal distribution of temperature, humidity, rainfall, pressure and winds). This provides a major source of confidence in the use of models for climate projection (see section 4.2.3). The ability of a model to simulate interactions in the climate system depends on the level of understanding of the geophysical and biochemical processes that govern the climate system. Our understanding of these processes has steadily improved, along with our ability to represent them in climate models. The increase in available computing power has allowed these processes to be represented in models with greater complexity and detail. Continued growth in computer power is essential for model improvement.

4.2.2 CMIP3 database of climate simulations

A new set of experiments from 23 models from research groups around the world is now available, representing a major advance for the evaluation of models and the generation of climate projections.

The availability of a new set of systematic model experiments from the Coupled Model Intercomparison Project 3 (CMIP3) database represents a major advance both for the evaluation of models and the generation of climate projections. The database includes more models (23) and more simulations of emission scenarios using each model. The model output is freely available to the research community, which has resulted in unprecedented levels of evaluation and analysis. The models in the CMIP3 database represent the current state-of-the-art in climate modelling, with generally more sophisticated representations of physical and dynamical processes, and finer spatial resolution.

The CMIP3 database provides monthly temperature and precipitation data for all 23 models. However, monthly data for other climate variables are available for *fewer* than 23 models, e.g. solar radiation for 20 models, wind speed for 17 models and relative humidity for 14 models (see Table 5.1 in Chapter 5). Some models have single simulations for the 20th and 21st centuries, while others have multiple simulations (ensembles). For models with multiple simulations, ensemble-mean changes in climate have been computed. The simulations of 20th century climate were driven by observed changes in greenhouse gases and aerosols. Some simulations included direct and indirect effects of anthropogenic aerosols, some included ozone depletion, and some included volcanic aerosols and solar forcing. Radiative forcing is not a directly observed quantity and is particularly uncertain for aerosols. Table 4.1 gives information about the various forcings used in each simulation and the spatial resolution of each model. The 21st century simulations were driven by the SRES A2 and A1B emission scenarios (IPCC 2000).

Table 4.1: The 23 global climate models used for simulations of 20th and 21st century climate, available from the CMIP3 database managed by the Program for Climate Model Diagnosis and Intercomparison (PCMDI) available at http://www-pcmdi.llnl.gov/ipcc/info_for_analysts.php. The reference numbers in column 1 are used in Table 5.1 in Chapter 5. The forcing factors are: G – Well-mixed greenhouse gases, O – Ozone, SD – Sulfate direct, SI – Sulfate indirect, BC – Black carbon, OC – Organic carbon, MD – Mineral dust, SS – Sea salt, LU – Land use, SO – Solar irradiance and V – Volcanic aerosol. Also given are global mean warming over the 21st century for the A1B emission scenario (see section 4.2.5; not available for BCCR model), and a skill score for Australia (see section 4.2.3).

No	Originating Group(s), Country	Model	Horizontal grid spacing (km)	Forcings used in model simulations	Warming (°C)	M Skill Score
1	Bjerknes Centre for Climate Research, Norway	BCCR	~175	G, SD	N.A.	0.590
2	Canadian Climate Centre, Canada	CCCMA T47	~250	G, SD	2.47	0.518
3	Canadian Climate Centre, Canada	CCCMA T63	~175	NOT AVAILABLE	3.03	0.478
4	Meteo-France, France	CNRM	~175	G, O, SD, BC	2.81	0.542
5	CSIRO, Australia	CSIRO-MK3.0	~175	G, O, SD	2.11	0.601
6	CSIRO, Australia	CSIRO-MK3.5	~175	G, O, SD	3.17	0.607
7	Geophysical Fluid Dynamics Lab, USA	GFDL 2.0	~200	G, O, SD, BC, OC, LU, SO, V	2.98	0.671
8	Geophysical Fluid Dynamics Lab, USA	GFDL 2.1	~200	G, O, SD, BC, OC, LU, SO, V	2.53	0.672
9	NASA/Goddard Institute for Space Studies, USA	GISS-AOM	~300	G, SD, SS	2.02	0.564
10	NASA/Goddard Institute for Space Studies, USA	GISS-E-H	~400	G, O, SD, SI, BC, OC, MD, SS, LU, SO, V	2.08	0.304
11	NASA/Goddard Institute for Space Studies, USA	GISS-E-R	~400	G, O, SD, SI, BC, OC, MD, SS, LU, SO, V	2.12	0.515
12	LASG/Institute of Atmospheric Physics, China	IAP	~300	G, SD	2.77	0.639
13	Institute of Numerical Mathematics, Russia	INMCM	~400	G, SD, SO	2.40	0.627
14	Institut Pierre Simon Laplace, France	IPSL	~275	G, SD, SI	3.19	0.505
15	Centre for Climate Research, Japan	MIROC-H	~100	G, O, SD, BC, OC, MD, SS, LU, SO, V	4.31	0.608
16	Centre for Climate Research, Japan	MIROC-M	~250	G, O, SD, BC, OC, MD, SS, LU, SO, V	3.35	0.608
17	Meteorological Institute of the University of Bonn, Meteorological Research Institute of KMA, Germany/Korea	MIUB	~400	G, SD, SI	2.97	0.632
18	Max Planck Institute for meteorology DKRZ, Germany	MPI-ECHAM5	~175	G, O, SD, SI	3.69	0.700
19	Meteorological Research Institute, Japan	MRI	~250	G, SD ,SO	2.52	0.601
20	National Center for Atmospheric Research, USA	NCAR-CCSM	~125	G, O, SD, BC, OC, SO, U	2.47	0.677
21	National Center for Atmospheric Research, USA	NCAR-PCM1	~250	G, O, SD, SO, V	1.96	0.506
22	Hadley Centre, UK	HADCM3	~275	G, O, SD, SI	3.12	0.608
23	Hadley Centre, UK	HADGEM1	~125	G, O, SD, SI, BC, OC, LU, SO, V	3.47	0.674

4.2.3 Reliability of climate models

Global climate models continue to improve in their ability to represent current global and regional patterns of temperature, precipitation and other variables. Simulation of major patterns of climatic variability particularly relevant to Australia (El Niño – Southern Oscillation, the Southern Annular Mode and the Madden-Julian Oscillation) have improved as well.

An important source of confidence in models comes from their ability to represent features of the current climate. Particularly important for Australia is how well climate models represent large-scale patterns of temperature, pressure and precipitation, as well as modes of variability such as the El Niño – Southern Oscillation (ENSO), the Southern Annular Mode and the Madden-Julian Oscillation, all of which affect regional climate.

Confidence in model projections varies with spatial and temporal scale. Highest confidence is attached to results analysed at the coarsest spatial and temporal scales, such as global or hemispheric annual means, and decreases with finer scales, such as sub-continental or regional daily variability. This is partly because the magnitude of natural variability increases as scales decrease, so that regional climate change signals are more easily masked by climate variability. Furthermore, local influences on climate (such as regional topography or processes) become more important at finer spatial scales.

Important physical processes that occur at scales too small to be explicitly resolved by the models are represented in approximate form as they interact with resolved scales (referred to as model 'parameterisations'). Examples include the interaction of radiation with atmospheric molecules and aerosols, convection within the atmosphere and ocean, small scale mixing by eddies and processes associated with the formation and dissipation of clouds. Our ability to parameterise such small-scale processes is imperfect, and different representations of those processes amongst models affect the magnitude and patterns of climate change projections. The response of clouds to climate change, in particular, is an important source of uncertainty in model projections (Soden and Held 2005). Nevertheless, this does not mean that models have no reliability at finer scales. Models can skillfully represent, for example, some types of temperature extreme – features intrinsically of small spatial and temporal scales (Tebaldi *et al*. 2007). Model resolution and parameterisations continue to improve, and several 'downscaling' techniques have been developed specifically to address regional and local climate change issues (see Chapter 5).

Mean global temperature errors from IPCC models are generally less than 3ºC outside polar regions (Figure 4.2). Greatest errors occur over land at high latitudes, likely due in part to elevation errors over ice sheets. Over the oceans, greatest relative errors occur over eastern ocean basins consistent with insufficient cloud in stratocumulus decks over cold water being simulated. Despite the errors, the typical pattern correlation coefficients between individual models and the observations are very high (0.98), indicating extremely good model representations of temperature distributions. This represents considerable improvement since the IPCC Third Assessment Report (IPCC 2001). The annual cycle in temperature is also well simulated, with mean errors in most regions less than 1ºC. Even over the Northern Hemisphere land mass, where annual temperature variations are very high, typical model errors are less than 2ºC (Randall *et al*. 2007). Although confidence is greatest for variables at the global and continental scale, some models can adequately represent the magnitude of temperature variability down to sub-continental scales (Karoly and Wu 2005).

Surface temperature patterns are driven largely by direct radiative forcing and land-sea temperature gradients. Mean precipitation patterns, on the other hand, more strongly reflect the general atmospheric circulation. Figure 4.3 shows that models represent overall features well, including the inter-tropical convergence zone, subtropical dry zones and general position of mid-latitude storm tracks. The details of those patterns, however, show a number of systematic errors that are potentially important to Australian projections. Many models show an unrealistic double inter-tropical convergence zone over the tropical Pacific, and the equatorial Pacific 'cold tongue' extends too far westward (Cai *et al*. 2003b,c; Dai 2006). Such errors in temperature and precipitation patterns also negatively affect the representation of the seasonal cycle and ENSO. Models generally also show too much light rain (1-10 mm per day) compared to observations, and underestimate the contribution and frequency for heavy rain (>20 mm per day; Watterson and Dix 2003; Dai 2006), likely to adversely affect projections of features such as heavy rain events. Recent increases in spatial resolution have, however,

improved the simulation of mid-latitude cyclones, and hence mid-latitude storm tracks (Bengtsson *et al*. 2006).

Significantly for simulation of variability in the Australian region, in recent years there has been an improvement in the ability of models to represent the spatial pattern and frequency of ENSO. For example, models are better able to reproduce the characteristic two-to-seven year frequency of ENSO. Problems remain, however, in simulating the asymmetry between El Niño and La Niña episodes, and the tendency for ENSO events to commence around March-May and persist through to December-February (Randall *et al*. 2007).

The importance of the Madden-Julian Oscillation for Australian regional climate includes its impact on tropical rainfall variability, onset and break events in the Australian monsoon, and possibly for its role in triggering ENSO events. Although models represent some gross features of Madden-Julian Oscillation variability, its magnitude is generally underestimated in the IPCC models (Lin *et al*. 2006), and errors persist in its structure and propagation (Hendon 2005). The Southern Annular Mode is a leading mode of extratropical variability in the southern hemisphere, and has important signatures on Australian rainfall. Models generally represent the spatial structure of Southern Annular Mode well (Cai *et al*. 2003a), although they differ in their ability to represent its amplitude and temporal and zonal structures (Raphael and Holland 2006). The IPCC Fourth Assessment Report concluded that

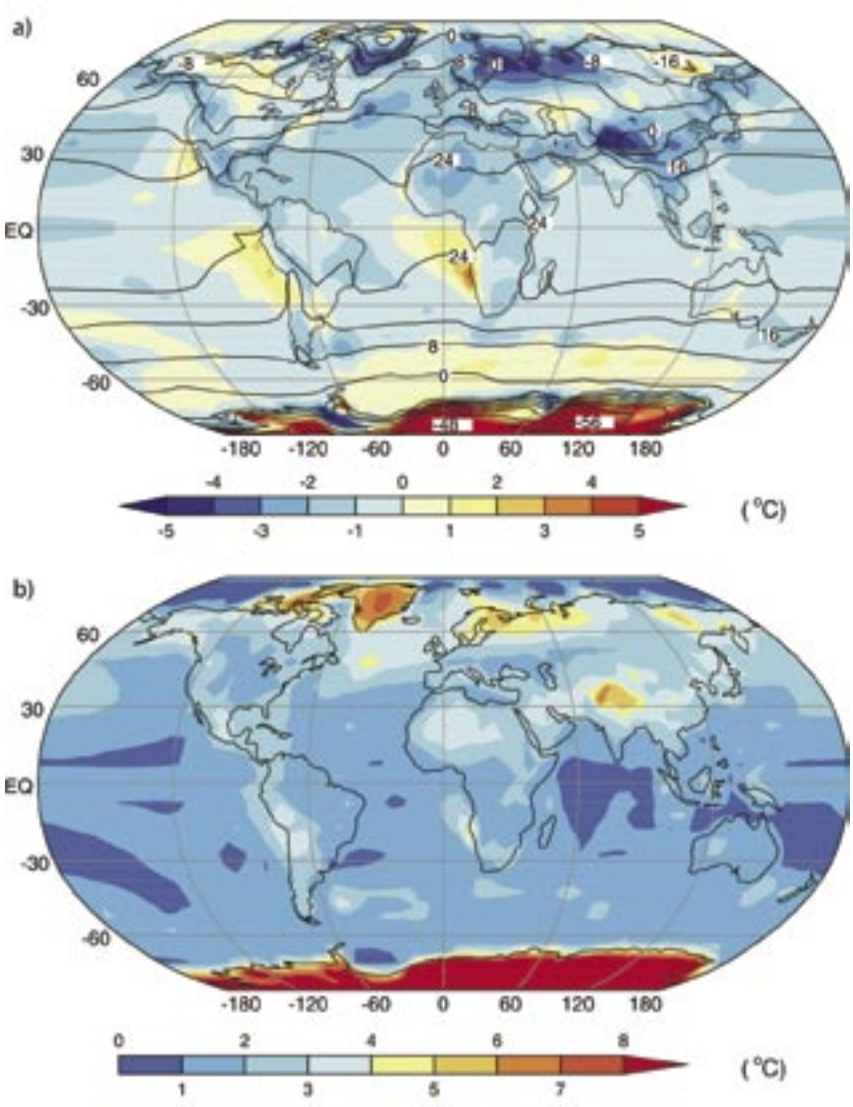

Figure 4.2: (a) Observed annual mean surface temperature (labelled contours) and the multi-model mean error for all 23 CMIP3 models, simulated minus observed (colour-shaded contours). Results are for 1960-1990 over land and 1980-1999 over the ocean. **(b)** Size of the typical model error, defined as the root-mean-square error computed over all simulations (from Figure 8.2 in Randall *et al*. 2007).

models were able to skillfully simulate many modes of climate variability, increasing confidence in their use for projecting climate change.

A simple measure of the ability of each model to simulate the Australian climate has been undertaken for the 23 models. This uses the non-dimensional measure of similarity 'M' (Watterson 1996) determined from the maps of simulated and observed seasonal-mean temperature, precipitation and sea level pressure. Observed temperature and precipitation data (on a 0.25 degree grid, approx. 25 km) come from the Australian Bureau of Meteorology, and observed pressure data (the 'ERA40' dataset) come from the European Centre for Medium Range Weather Forecasting. All data are interpolated to a common 0.25 degree Australian land grid. A single M value between 1 (perfect match) and 0 (no-skill) is obtained for each case, based on pattern correlations and root-mean-square errors. The average M skill scores for the three different variables across four seasons are given in Table 4.1. Fourteen models have skill scores between 0.6 and 0.7. Even the poorest performing model over Australia (GISS-EH) has some skill overall, with an average score of 0.3. These skill scores are used to weight climate projections from each model in Chapter 5. We assume that models with higher skill scores are likely to give more reliable projections of future climate.

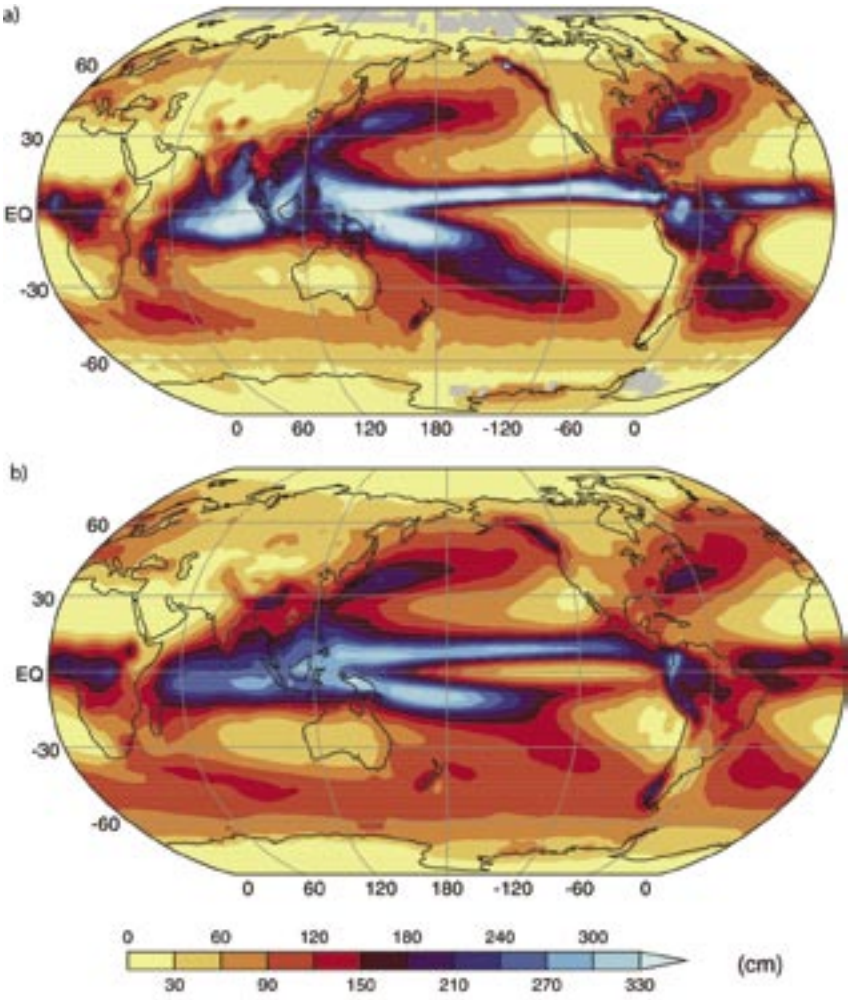

Figure 4.3: (a) Observed climatological annual mean precipitation and **(b)** multi-model mean precipitation from all 23 CMIP3 models. Observations are from Xie and Arkin (1997) updated for the period 1980-1999. Units are cm/year. (From Figure 8.5 in Randall *et al*. 2007)

4.2.4 Treatment of model uncertainties

Projections of global and regional climate change contain a large number of uncertainties. Predictability is limited by factors such as human behaviour and the uncertainties inherent in complex systems, such as chaotic behaviour and rapid changes in state. Uncertainty over future human behaviour affects emission scenarios, including future mitigation policies discussed in Section 4.1. Chaotic behaviour affects climate variability and change on a range of scales, from everyday variability (well understood) to long-term rapid shifts in climate (less common and not well understood but observable in palaeo-climate proxy records). Such behaviour is a long-term property of climate (and all complex systems) and may potentially increase under global warming (Schneider *et al*. 2007).

Structural uncertainty describes assumptions and system definitions, including how much of the actual system being simulated is included within a given modelling structure. Value uncertainty considers values, both as input and also how parameters and processes are represented within a model.

As mentioned in Chapter 1, techniques for combining model projections and producing conditional probabilities need to be very carefully managed. Over time, climate science has moved from producing single scenarios of some future state, often characterised as twice pre-industrial atmospheric CO_2, to large ensembles of transient climate change that can be portrayed as probability distributions.

The relationship between individual scenarios and ranges of change is shown in Figure 4.4 (Jones 2000; Ahmad *et al*. 2001). These show projected ranges with varying degrees of associated confidence. The well-calibrated range of uncertainty is typically quantified through a modelling exercise, whereas the judged range is more often constructed through expert judgement or other decision-analytic techniques (Ahmad *et al*. 2001). The total range of uncertainty acknowledges that uncertainties are often under-estimated by experts (Morgan and Henrion 1990).

The application of probabilities to the well-calibrated and even to the judged range of uncertainty can be justified if the above uncertainties are sufficiently well understood and managed, subject to the proviso that all such probabilities are understood to be conditional. The context, in this case, is that the IPCC has provided judged ranges of uncertainty each with attached likelihood representing their judgement that the 'true' answer is captured within that range (e.g. that climate projections correctly represent the response to specified forcing conditions) for variables such as global average warming and sea level rise. The derivation of estimates by the IPCC for global average warming is described in section 4.2.5 and conditional probability distributions are described in section 4.2.6. Chapter 5 describes the construction of regional projections of change for a range of variables, many of which include probability distributions.

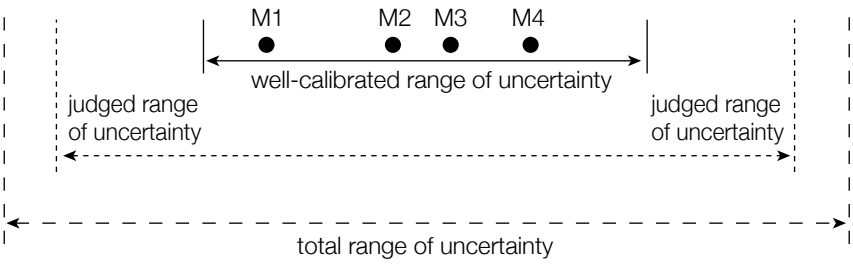

Figure 4.4: Schematic depiction of the relationship between well calibrated scenarios, the wider range of judged uncertainty that might be elicited through decision-analytic techniques and the full range of uncertainty, drawn wider to represent typical under-estimation in human judgements (Adapted from Jones 2000; Ahmad *et al*. 2001).

4.2.5 Global climate change projections for the 21st century

The 23 models in the CMIP3 dataset were driven by the B1, A1B and A2 emissions scenarios described in Box 4.1. This is a much larger set of simulations than was available for the IPCC Third Assessment Report in 2001, allowing better quantification of multi-model average changes, as well as uncertainty between models. Figure 4.5 shows the range of global warming for each of these scenarios, plus a hypothetical scenario applying constant year 2000 greenhouse gas concentrations. The IPCC (2007a) assessed the range of warming by the period 2090-2100, relative to 1980-1999, for the six SRES marker scenarios (B1, A1T, B2, A1B, A2 and A1FI) based on the 23 climate models, plus results from a hierarchy of independent models (complex, intermediate and simple) and observational constraints. Important uncertainties, including the possibility of significant further amplification of climate change due to carbon cycle feedbacks, are provided by the results of the Coupled Carbon Cycle Model Intercomparison Project (Friedlingstein *et al*. 2006). The lower end of the warming range (grey bars in Figure 4.5) corresponds to the mean warming minus 40%, while the upper end of the range is the mean warming plus 60%. The IPCC (2007a) global-average warming by 2090-2100 is 1.1-6.4ºC (Table 4.2).

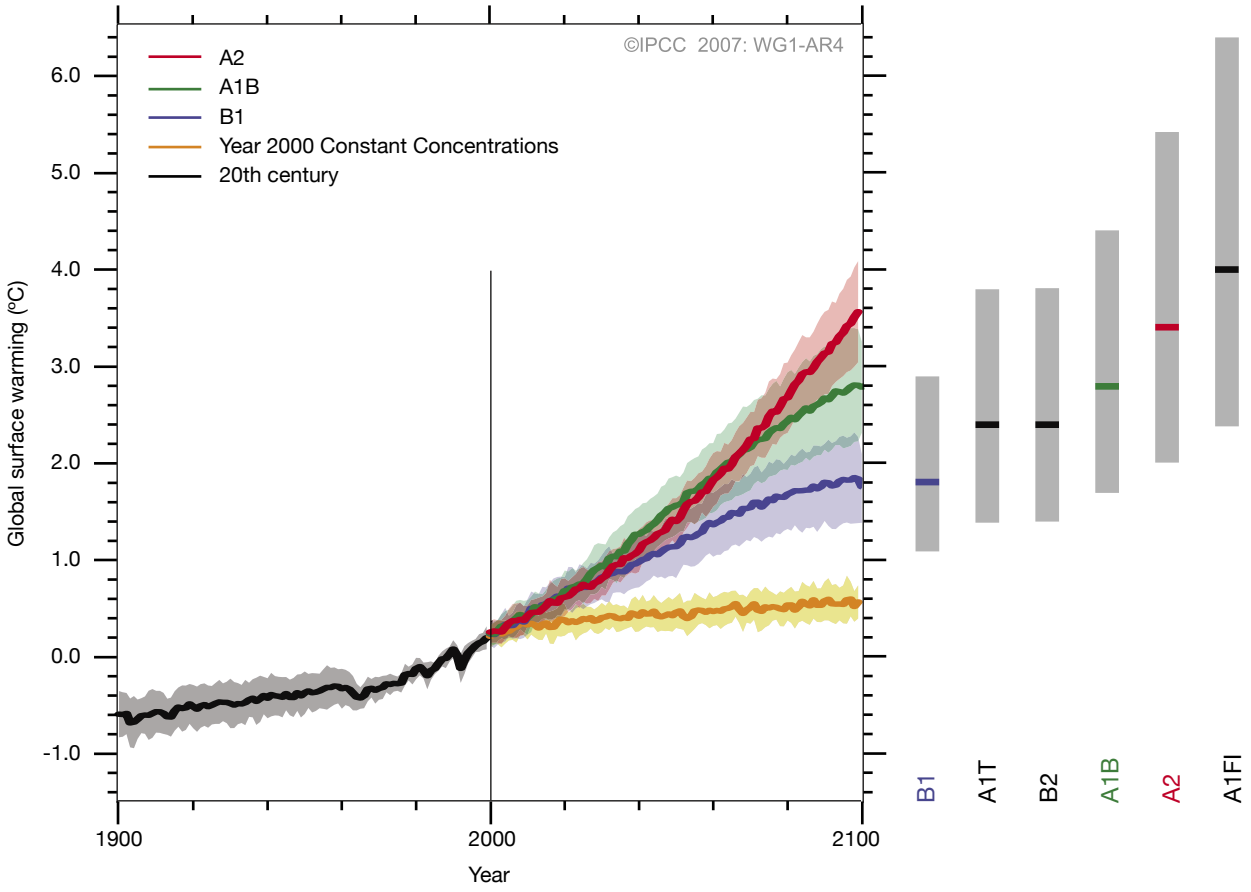

Figure 4.5: Global average warming (relative to 1980-99) for the scenarios A2, A1B and B1, shown as continuations of the 20th century simulations. Shading denotes the plus/minus one standard deviation range of individual model annual averages. The orange line is for the experiment where greenhouse gas concentrations were held constant at year 2000 values. The grey bars (right) indicate the multi-model mean warming (solid line within each bar) and the likely range of warming by the year 2100 for the six SRES marker scenarios, based on the A2, A1B and B1 simulations, plus results from independent models and observational constraints.(From IPCC (2007a) Fig SPM-5.)

Table 4.2: Best estimates and likely ranges of global warming for 2090-2099, relative to 1980-1999, for six SRES emission scenarios. (IPCC 2007a Table SPM-3).

Scenario	Best estimate	Likely range
B1	1.8°C	1.1-2.9°C
B2	2.4°C	1.4-3.8°C
A1T	2.4°C	1.4-3.8°C
A1B	2.8°C	1.7-4.4°C
A2	3.4°C	2.0-5.4°C
A1FI	4.0°C	2.4-6.4°C

Equivalent global warming estimates for 2030, 2050 and 2070 were not provided by the IPCC (2007a). Since these values are essential for the projections in Chapter 5, they have been derived in a manner consistent with the approach used by the IPCC for 2100 (Table 4.3). The multi-model mean global warmings for 2030, 2050 and 2070 were read from Figure 4.5 (or corresponding results from simple models). Note that these projections represent the anthropogenic change due to a specific change in radiative forcing for a period centred on a given year. Natural variability will influence actual values in any single year or decade.

The IPCC global warming ranges for 2100 (Meehl *et al*. 2007) are based on expert judgement in which multiple lines of evidence are taken into account. These include not only model results, but also estimates of climate sensitivity based on observed climate changes (coupled with estimates of radiative forcing) and palaeo-climate reconstructions. Warming outside these ranges cannot be excluded (Meehl *et al*. 2007, p 810). The range was described by the IPCC as 'likely'. From IPCC definitions, the likelihood of the true value being within the range is estimated to be at least 66% and less than 90%, but this percentage was not justified by the IPCC in this case. The IPCC concludes that the lower bound of the range is much better constrained than the upper bound. This is because the lower bound on climate sensitivity is better constrained and uncertainties in carbon cycle feedback are much less important for small temperature changes than for large ones (Meehl *et al*. 2007, p 810).

The ranges given in Table 4.3 were obtained simply by using -40% and +60% increments relative to the mean, as for 2100. This is supported by the statement of Meehl *et al*. (2007, p 809) that "projection uncertainties increase close to linearly with temperature in most studies", however the contribution of carbon cycle uncertainties may be smaller for the earlier times.

The IPCC also describes other 'Bayesian' approaches that estimate considerably smaller uncertainties of the 'real world' warming (Meehl *et al*. 2007). In particular, if one assumes that the model results are distributed about the 'true' value and improving in skill, then the uncertainty in the estimate of this value tends to decrease as the number of models considered increases, as is typical of statistical inference (Lopez *et al*. 2006). This issue will be also raised with respect to Australian regional changes in Chapter 5. In the results that follow, both the 'best estimates' and the likely ranges of uncertainty are derived directly from the global climate model ensemble, although the fitted range closely approximates the 'likely' range of global temperature change specified by the IPCC (Meehl *et al*. 2007). *Therefore, it must be borne in mind that, in particular, the upper limits of warming presented here and in Chapter 5 are conservative. There is a significant possibility that warming may occur in excess of these values, particularly later in the century, although the likelihood of this occurrence is impossible to estimate at this stage.*

It is worth noting that observed carbon dioxide concentrations, global mean temperatures and sea level rise have been tracking the upper end of the IPCC scenario range from 1990 to 2006 (Rahmstorf *et al*. 2007). Although this 17-year period is very short, it suggests that the mid and low projections may be less likely than the high projections, with significant implications for risk management.

Table 4.3: Global warming estimates [and representative ranges] relative to 1990 for selected years and emission scenarios. (Based on IPCC 2007a Figure SPM-3 and Meehl *et al*. 2007).

	2030	2050	2070
B1	0.75 [0.45-1.2]	1.1 [0.66-1.76]	1.5 [0.9-2.4]
B2	0.9 [0.54-1.44]	1.29 [0.77-2.06]	1.8 [1.08-2.88]
A2	0.8 [0.48-1.28]	1.4 [0.84-2.24]	2.25 [1.35-3.6]
A1B	0.9 [0.54-1.44]	1.53 [0.92-2.45]	2.13 [1.28-3.41]
A1T	1.0 [0.6-1.6]	1.7 [1.0-2.72]	2.2 [1.32-3.52]
A1F1	0.87 [0.52-1.39]	1.8 [1.08-2.88]	2.9 [1.74-4.64]

4.2.6 Deriving probability distributions for global warming

Varying global warming projections from climate models can be represented using probability distributions. These distributions are required for probabilistic regional climate change projections generated in Chapter 5.

Since probabilities were not provided by the IPCC (2007a), they have been derived using an approach that is similar to that used for local changes in Chapter 5. While this is based on an assessment of global climate model results for scenario A1B, described further by Watterson (2007), the results are quite consistent with the ranges of the previous section.

For the 22 individual models for which A1B simulations are available, the warming trend over the 21st century is evaluated by regression. The 100-year warming of each model from this analysis is given in Table 4.1. Further simulations of the same model would give somewhat different changes, and this will be particularly true of local results in Chapter 5. This uncertainty in the 'true' change of the model, as could be obtained by averaging over many simulations, can be estimated from the standard regression error. A probability density function (PDF) for the true individual model result is then a simple normal or Gaussian distribution, whose range is given by this error. Summing these individual normal distributions – one for each model (evenly weighted) – produces a combined probability density function, the 'Sum' curve plotted in Figure 4.6. The model with the largest warming stands out, here, but elsewhere there is some merging of the individual curves. The Sum PDF has the same mean as the warming in Table 4.2 (2.8ºC), and a similar range. If one randomly chose a new simulation from this set of models, this PDF would apply.

If we attempt to better represent the range of results from a typical model, or indeed the real world, it is reasonable to have a much smoother PDF. Figure 4.6 depicts the bell-shaped 'Normal' distribution, with the same mean and standard deviation as the Sum. The Normal 'fit' is however symmetric, even though the model results are somewhat 'skewed', with no small warmings. The IPCC ranges (Table 4.2) are also skewed. The 'Beta' distribution shown in Fig. 4.6 allows such skewness, but retaining the same mean and standard deviation. The tails of the Beta distribution in Figure 4.6 are constructed to extend slightly beyond the modelled range, and they also extend just beyond the range in Table 4.2 for this case (1.7-4.4ºC).

This Beta distribution gives a reasonable representation of simulated global warming for this emission scenario based on current climate models. Consistent with the ranges in Table 4.3, the same Beta distribution as in Figure 4.5 has been used to produce a PDF for the other years and scenarios, by scaling or stretching it by the ratio of the warming for the case and 2.8ºC.

For the purpose of providing probabilistic information in this report, we will assume that this set of PDFs also represents the uncertainty in real-world global warming for the various cases. As described in Chapter 5 and Watterson (2007), the projections for Australia will depend also on how the global warming PDFs are used, and the particular statistics presented. As noted at the end of section 4.2.5, *there is a significant possibility of future climate changes lying outside the projected ranges presented in this report, particularly so for changes associated with temperature increases at the upper end of the range, particularlly later in the century, although the likelihood of this occurrence is impossible to estimate at this stage.*

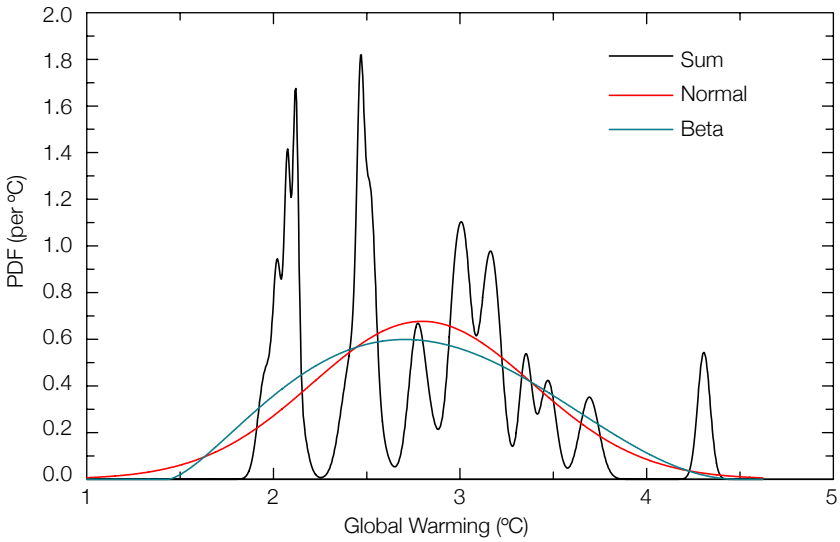

Figure 4.6: Probability distribution functions for the global mean warming for A1B over the 21st century, calculated from 22 models.

4.3 Global patterns of projected climate change of Australian relevance

It is important to place the Australian region projections contained in Chapter 5 in context of the large-scale patterns of change found in global models. Such patterns often display very large-scale coherence, and many of these large-scale changes can be understood from basic theoretical or physical constraints of the climate system, in particular related to increased ability of the atmosphere and increased moisture holding capacity (e.g. Held and Soden 2007). *Such constraints provide important extra confidence in projected regional changes, over and above that derived simply from the confidence placed in global climate models.*

The IPCC (2007a) report drew the following conclusions regarding regional patterns of climate change for the late 21st century:

- Greatest warming will occur over land and at high northern latitudes, and less warming will occur over the southern oceans and North Atlantic, consistent with observations during the latter part of the 20th century (Figure 4.7).
- Sea level pressure is projected to increase over the subtropics and mid-latitudes, and decrease over high latitudes due to a poleward expansion and weakening of the Hadley Circulation and a poleward shift of the storm tracks (Figure 4.7).
- Precipitation will generally increase in the wet tropics (such as the monsoon regimes) and over the tropical Pacific in particular, with general decreases expected in the subtropics, and increases at high latitudes due to the intensification of the hydrological cycle (Figure 4.7).
- Globally averaged mean water vapour, evaporation and precipitation are projected to increase.
- It is very likely that the duration, intensity and frequency of (i) heatwaves will increase, and (ii) cold periods and frosts will decline.
- Intensity of precipitation events is projected to increase, particularly in tropical and high latitude areas that experience increases in mean precipitation.
- Even in areas where mean precipitation decreases (most subtropical and mid-latitude regions), precipitation intensity is projected to increase but there would be longer periods between rainfall events.
- More frequent intense tropical cyclones, and associated extreme wind and rain are projected.
- A tendency for drying of the mid-continental areas during summer is expected to increase the risk of droughts in those regions.
- No consistent discernible change in ENSO frequency or intensity is evident in the projections.
- Snow cover and sea ice extent are expected to decrease, glaciers and ice caps are expected to lose mass, and this will contribute to further sea level rise.

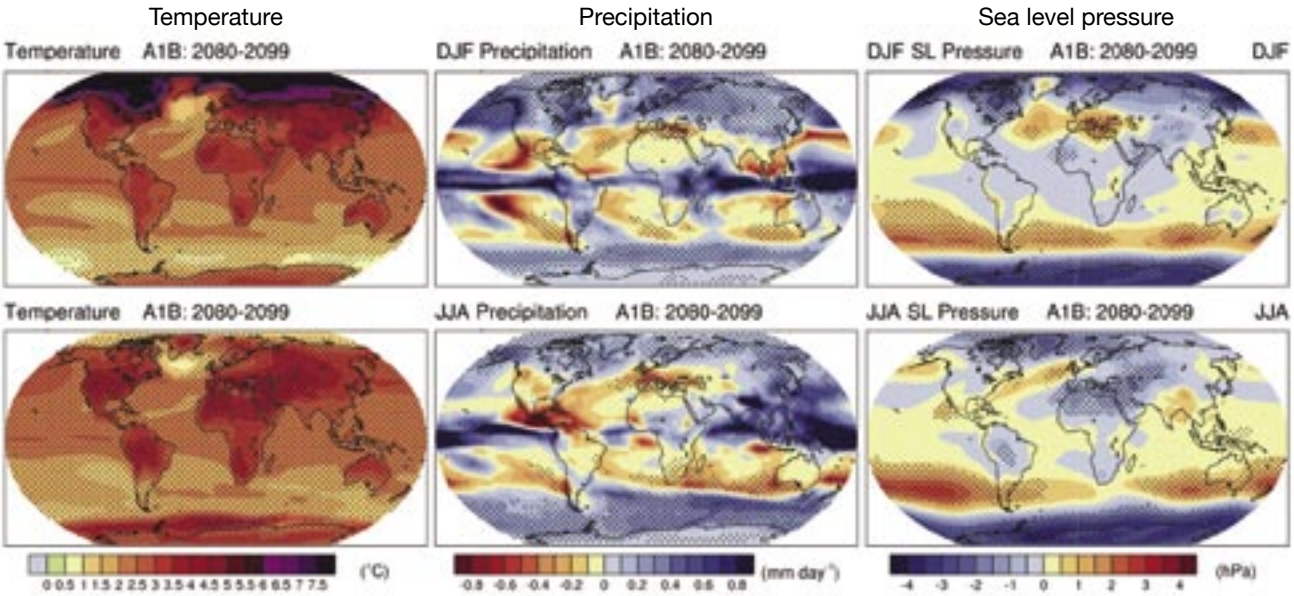

Figure 4.7: The global-average changes in surface temperature, precipitation and mean sea level pressure from 2080-2099, relative to 1980-1999. Based on the results of 20 climate models using the A1B scenario as an example, in December through February (DJF) and June through August (JJA), with shading indicating where the multi-models mean exceeds the inter-model standard deviation. (From Meehl *et al*. 2007 Figure 10.9.)

Chapter 5 Regional climate change projections

This chapter provides projections of regional changes in a wide range of climate variables important to Australia. This includes seasonal average temperature and daily temperature extremes (e.g. frosts and heatwaves), seasonal average precipitation and daily precipitation extremes, and annual average potential evaporation, relative humidity, solar radiation, wind speed and snow. Projections for drought frequency, fire weather, tropical cyclones, coastal storm surges, hail, tornadoes, thunderstorms and storm tracks are also provided, as is information on future changes in sea level, the El Niño – Southern Oscillation, and the Southern Annular Mode and. Key climate variables and how they were derived are listed in Table 5.1.

For annual or seasonal average changes in temperature, mean precipitation, humidity, radiation, wind speed, potential evaporation and sea surface temperature, projections are provided in a probabilistic form. The site-specific probability distribution represents the range of model results. The CMIP3 database of simulations is used (See Table 4.1), but relevant data for some climate variables were available only for a subset of the CMIP models (see Table 5.1). Annual and seasonal projections were prepared for the six SRES 'marker' emission scenarios (B1, A1T, B2, A1B, A2 and A1FI) and for climate change centred on 2030, 2050 and 2070, relative to 1990. The set of results for these variables is large and only selected results are presented in the chapter text. A more complete set of results is included in Appendix A to this report, and in the Technical Report supplementary material available at www.climatechangeinaustralia.gov.au. Appendix B includes results for selected sites, including capital cities.

In choosing results to show for the near term (2030), model to model variation is highlighted rather than differences between the various emission scenarios. Over the next few decades, the variation in emissions of greenhouse gases and aerosols represented by the SRES scenarios makes only a small contribution to uncertainty in global warming (and by extension regional warming and other changes in climate). This is because near-term changes in climate are strongly affected by inertia in the climate system due to past greenhouse gas emissions, whereas climate changes later in the century are more dependent on the particular pattern of greenhouse gas emissions that occur through the century. These near-term changes are hard to avoid and are relevant to adaptation planning. For projected changes centred on 2050 and 2070, variations due to differences between models *and* differences between emission scenarios are illustrated to highlight the greater dependence of longer term climate change on human behaviour.

It was not possible to treat other variables in a probabilistic manner. This was due to either the necessary data being unavailable (often due to the more specialised nature of the results being considered), our assessment that the assumptions underlying the probabilistic approach may not be applicable (particularly relevant for some aspects of extremes), or that understanding of the topic was such that a qualitative assessment was all that was warranted. As may be seen in Table 5.1, results for these other variables are usually less comprehensive with respect to emission scenarios, model to model variations and time periods.

A description of the new probabilistic approach follows. Details of any other methods of analysis are introduced in the individual subsections as required.

Table 5.1: Variables, years, models and emission scenarios underpinning the regional climate change projections presented in this report. The available SRES marker scenarios are specified, with '6' indicating A1FI, A2, A1B, A1T, B1, B2. Where fewer than the full set of 23 models are used, the available models are indicated in italics (using the numbering system of Table 4.1).

Variable	Year			Models	Scenarios
	2030	2050	2070		
Average temperature*	x	x	x	23 (all in Table 4.1)	6
Hot days	x		x	23 (all in Table 4.1)	A1B, B1, A1FI
Warm nights	x	x	x	9 (*4, 7, 8, 13, 14, 16, 19, 21, 20*)	A2, A1B, B1
Extreme temperature: frost		x		10 (*2, 4, 5, 7, 8, 11, 14, 16, 18, 19*) and downscaling	A2, B1
Average precipitation*	x	x	x	23 (all in Table 4.1)	6
Precipitation intensity	x	x	x	9 (*4, 7, 8, 13, 14, 16, 19, 21, 20*)	A2, A1B, B1
Dry days	x	x	x	9 (*4, 7, 8, 13, 14, 16, 19, 21, 20*)	A2, A1B, B1
Extreme daily precipitation		x		13 (*2, 3, 4, 5, 7, 9, 12, 13, 14, 16, 17, 18, 19, 20, 21*)	B1,A1B, A1FI
Snow		x		9 (a)	B1, A1FI
Relative humidity*	x	x	x	14 (*2, 3, 5, 6, 9, 10, 11, 12, 13, 14, 15, 16, 19, 20*)	6
Solar radiation*	x	x	x	20 (*1, 2, 3, 4, 5, 6, 7, 8, 10, 11,12, 15, 16, 17, 18, 19, 20, 21, 22, 23*)	6
Potential evaporation*	x	x	x	14 (*2, 3, 5, 6, 9, 10, 11, 12, 13, 14, 15, 16, 19, 20*)	6
Drought	x		x	2 (b)	B1, A1FI
Average wind*	x	x	x	19 (*2, 3, 4, 6, 7, 8, 9, 10, 11, 12, 13, 14, 15, 16, 17, 18, 19, 22, 23*)	6
Extreme daily wind				4 (*7, 13, 18, 19*)	
Fire		x		2 (*5, 6*)	B1, A1FI
Sea level rise				Literature review	
Ocean thermal expansion	x	x	x	17 (*1, 5, 6, 7, 8, 9, 10, 11, 12, 14, 15, 16, 17, 18, 19, 22, 23*)	A1B
Oceanic storm surges				Literature review	
Sea surface temperature*	x	x	x	12 (*2, 3, 5, 9, 10, 11, 13, 17, 19, 21, 22, 23*)	6
Ocean acidification			x	1 (*6*)	A2
East Australian Current				Literature review	
Tropical cyclones	x		x	1 (*5*) and downscaling (RAMS)	A2
Tornadoes				Literature review	
Hail	x		x	1 (*5*)	A2
East coast lows				Literature review	
ENSO				1 (*6*)	B1, A1B, A2
Southern Annular Mode				Literature review	
Southern storm tracks				Literature review	

* Model weighting based on present climate performance. Projections include threshold probabilities

(a) See section 5.2.6 for discussion of the models used.

(b) See section 5.4 for discussion of the models used.

The probabilistic approach

Various methods have been developed for preparing regional climate change projections and representing uncertainty (e.g. Giorgi and Mearns 2002; Dessai *et al*. 2005; Tebaldi *et al*. 2005; Whetton *et al*. 2005). Like many of these studies, the work presented here assumes that an ensemble of global climate model results gives a representation of the expected change of the real world to a specific emission scenario. The best estimate of the change is the ensemble average or 'multi-model mean'. Variations in this estimate relate to whether some climate models are given more weight than others based on their assessed reliability, and how that assessment is made and applied. The most common approach has been to assess how well each of the available models simulates the present climate of the region (e.g. Dessai *et al*. 2005), on the assumption that the more accurately a model is able to reproduce key aspects of the regional climate, the more likely it is to provide reliable guidance for future changes in the region. The method of weighting models is presented shortly.

Results from different models can be combined in various ways to estimate the range of possible real world climate responses, particularly when this is sought in the form of a probability density function or PDF, which quantifies the likelihood of each possible response. Our approach to deriving these ranges was introduced in section 4.2.4, where PDFs for global mean warming were presented. To progress from these to Australian changes, we use an extension of the 'pattern-scaling' approach of previous CSIRO projections (Whetton *et al*. 2005). This assumes that the local response in a climate variable is proportional to the global warming.

For a given model, we regress local climate changes against the global warming for the 21st century, and the slope of the regression equation gives the mean local change per degree of global warming. This conveniently decouples the local change from the emission scenario underlying the global warming. This means the local change can be scaled by a range of global warming values, for different times or different emission scenarios. This principle is supported by the similarity of the direct model output and the scaled CMIP3 multi-model means, as shown by Meehl *et al*. (2007), and by studies such as Mitchell (2003). Scaling remains an assumption with respect to changes in the real world. The similarity in shape of our global mean warming PDFs, for the various emissions scenarios and times through the 21st century, makes the pattern-scaling approach particularly convenient. The derivation of PDFs for the local responses and the method of combining these with global warming are described in the following sections.

Since the IPCC global warming best estimates (Table 4.2) are relative to the period 1980-1999, the regional projections in this report are against the same base years. For convenience, the baseline is often called 1990. Projections are given for 2030, 2050 and 2070, but of course individual years can vary markedly within any climate period, so the values can be taken as representative of the decade around the single year stated, i.e. projections for 2030 are representative of 2026-2035. Even then, natural variability may also modify the actual means for the decade (see e.g. Power and Colman 2006; Power *et al*. 2006 and section 5.2.2), particularly for a small region. This is included in the presentation of the projections for 2030. Strictly, the changes are relative to 'normal' conditions for 1980-1999, as simulated by the models within the changing atmosphere of the 20th century. The actual means over Australia in those years may have been somewhat different.

Weighting of models

In preparing the CSIRO (2001) projections, simulations of present average (1961-1990) patterns of precipitation, surface air temperature ('temperature') and sea level pressure were examined. Models that performed poorly overall were not included in the projections. This approach is supported by recent research (Whetton *et al*. 2007). A similar approach to CSIRO (2001) is used in this report, except that all models are given a weighting (M scores in Table 4.1) based on current climate performance across the three variables, rather than omitting models that perform poorly.

The weightings are described in section 4.2.3. These values are used to weight each model in the construction of the local response PDFs. Since the weights vary between 0.3 and 0.7, there is less discrimination of models from these than the CSIRO (2001) approach of using, in effect, weights of 0 (omit) or 1 (accept). In practice, the large number of models means that the final projections are not particularly sensitive to the inclusion of these non-uniform weights, as will be shown for annual precipitation. Note that the single set of weights is used for all variables and at each location, normalised by the number of models for which relevant data were available. Naturally, weights chosen in a different manner, such as if performance over a smaller region was considered, may lead to somewhat different projected changes from those presented here.

Construction of PDF of local response

For each model, variable and grid point, the local change per degree of global warming is obtained using a linear regression between the variable and global warming for the period 2001-2100 from the simulation for scenario A1B (or A2 in cases where A1B was not available). Using all years in this way (rather than differences between decades) minimises the effect of natural decadal variability, which can be large for individual grid points and seasons. Averages over multiple runs from the same model are used if more than one run is available. Results are then interpolated to a common one degree grid (about 100 x 100 km). Note that for some variables, data are not available for some models.

The PDF of local climate response can be derived from the standard regression error for an individual model result. This is a simple 'bell-shaped' curve, called a Normal or Gaussian distribution. One representation of the ensemble of model results is the weighted sum of these curves (using the model weighting of Table 4.1), illustrated in Figure 5.1 by the curve labelled 'Sum'. This is comparable to the representation in the Reliability Ensemble Averaging (REA) approach used by Moise and Hudson (2007) and others. Peaks corresponding to individual model results can still be seen in Sum. As usual, the vertical scale of this PDF is such that the integral of the PDF across the range (or the area under the curve) is 1.

As discussed in section 4.2.4, a probability density function representing the range of the 'real world' local response should ideally be smooth. Several ways of constructing a smooth PDF based on the model results, as represented by the Sum curve, have been considered. A standard approach is to fit the Normal distribution, by matching the mean and standard deviation from the Sum curve. This is illustrated in Figure 5.1. Two potential disadvantages of the Normal distribution are that it is unbounded in range and symmetric about the mean. The four-parameter 'Beta' distribution, described in more detail by Watterson (2007), is an attractive alternative. Two of the parameters give the range of the PDF, and these are set to extend just outside the two extreme model results, sufficiently to allow a smooth approach to zero of the Beta distribution. The other two parameters can be determined so that the mean and standard deviation match those of the Sum curve. As in the case of Figure 5.1 (and Figure 4.4), the Beta distribution will be skewed (non-symmetric) if the model data are skewed. Also shown is a 'Uniform' distribution, whose range matches that allowed in the CSIRO (2001) approach – given by the second smallest and second largest model values. In Figure 5.1, it is evident that the extreme results are clear outliers.

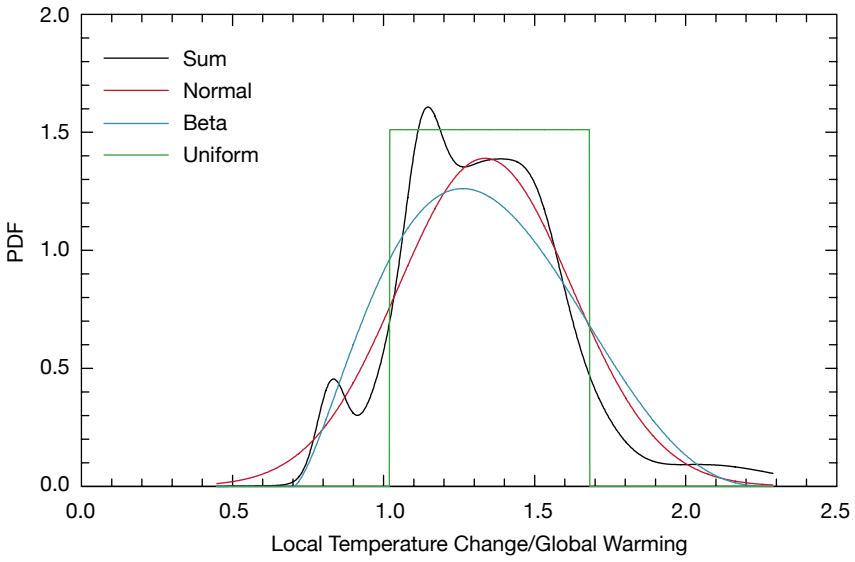

Figure 5.1: Probability distribution functions for the local temperature change per degree of global warming (non-dimensional) for December-February at Alice Springs (the point 134ºE, 24ºS) calculated from the 23 models. This shows variation in the distribution obtained using four different curve fitting methods – Normal, Sum, Beta and Uniform.

Calculation of net changes

To produce net projected changes for a particular time and emission scenario, the local changes per degree of global warming must be multiplied by a global mean warming value. There is uncertainty in both factors, of course. In CSIRO (2001) the range of global warming was taken from IPCC (2001) – the values roughly equivalent to those given in Table 4.2. Multiplying the end points by those of the Uniform distribution gave the range of possible change. Here, PDFs are used for both the local change and the global warming. Assuming these variables to be statistically independent, the PDF of the product can be determined. Following Watterson (2007) this has been done by integrating across a two-dimensional joint PDF. This gives the net change.

The Beta form has been used as the standard for the PDFs of both local response and global warming (section 4.2.5). In practice there is usually little difference in the PDF for net change if either the Sum or Normal forms for the local response are used instead. While the joint PDF for the net change would be of use in some applications, we focus on statistics derived from it, in particular percentiles determined from the corresponding cumulative distribution function. The 50th percentile, or median, is used as the 'best (or central) estimate' of the projected change. It shows little dependence on the form of PDF used. The 10th and 90th percentiles are given as a guide to the uncertainty range. The values are dependent on the assumptions made, the method used, and the set of model results analysed. The dependence would be greater for more extreme percentiles (not shown). A modification of this 'probabilistic pattern-scaling method' for the case of precipitation is described in section 5.2, where further illustrations of the fitting methods are given.

5.1 Temperature

Annual and seasonal average temperature changes will be represented using the probabilistic pattern-scaling approach, in sections 5.1.1 to 5.1.3. Other aspects, including smaller scale features and daily extremes are considered in later sections.

The simulated warming over oceans surrounding Australia is smaller than for the land due to the effects of ocean heat uptake and enhanced evaporation. In determining the local changes, only land points are used. Given varying resolutions and coastlines among the models, true coastal land points on the common one degree grid will not be within a land grid cell in every model. As a rule, the scaled PDF has been determined at land points where land is specified in at least half the models under consideration. The coastal values are not particularly sensitive to this fraction, but there is no suggestion that small-scale coastal effects can be deduced from these rather coarse grid global models.

5.1.1 Median warming by 2030

The best estimate of annual warming over Australia by 2030 is around 1.0ºC, with warmings of around 0.7-0.9ºC in coastal areas and 1-1.2ºC inland. Mean warming in winter is a little less than in the other seasons, as low as 0.5ºC in the far south.

The best estimate of the global mean warming for 2030 does not vary much among the emission scenarios. The range is about 0.75ºC (for B1) to 1.0ºC (for A1T) (Table 4.1). Therefore we focus on the mid-range A1B case which has a global warming of 0.9ºC by 2030. Results for other scenarios are available at www.climatechangeinaustralia.gov.au. The global mean warming PDF for this case and the local temperature change PDF for each season and each location are combined to produce a range or PDF for the net change. The median, or 50th percentile, determined from the range is presented here as the central or best estimate of the local response.

As seen in Figure 5.2, for most locations the mean warming is 0.7-0.9ºC in coastal areas and 1-1.2ºC inland. In winter, warming is projected to be a little smaller than in the other seasons, as low as 0.5ºC in the far south. Warming is usually smaller near the coasts than further inland, an exception being in the north-west, where the warming exceeds 1.3ºC in spring. The annual result has a similar pattern to the seasons, with the warming being largest in the interior and the north-west.

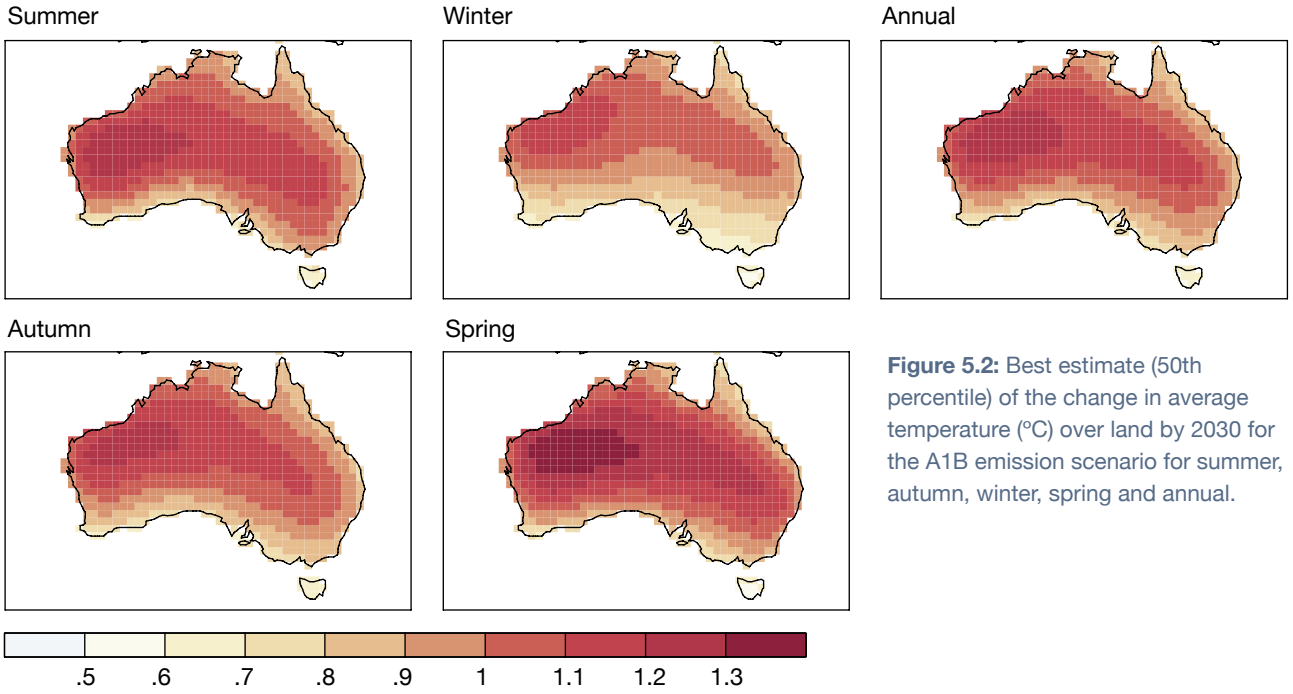

Figure 5.2: Best estimate (50th percentile) of the change in average temperature (ºC) over land by 2030 for the A1B emission scenario for summer, autumn, winter, spring and annual.

5.1.2 The uncertainties in the warming by 2030

For most of Australia, and in each season and the annual case, the range in warming allowing for uncertainty in climate response is about 0.6ºC to 1.5ºC for the A1B emission scenario. Allowing for emission scenario uncertainty, warming is still at least 0.4ºC in all regions and can be as large as 1.8ºC in some inland regions. Natural variability in decadal temperatures is small relative to these projected warmings.

The best estimate of the warming for Australia around 2030 is 0.7 to 1.2ºC depending on location (Section 5.1.1). Allowing for the differing SRES emission scenarios would modify this by barely 10%, either way (see Fig A1 in Appendix A).

Most of the uncertainty in the response in the near-term (i.e. in 2030) results from differences amongst models rather than differences in the emission scenarios. Two components of this uncertainty can be identified. The first is the sensitivity of the global mean warming. As discussed previously, the range considered likely in the IPCC Fourth Assessment Report for this is well represented by the PDF in Chapter 4. The second component is the variation in local change per degree of global warming among the models. This can be due to aspects of regional simulation. In the case of temperature, models may simulate differing land-sea contrasts and differing circulations and their changes. The PDF for the product of these factors represents the range associated with the two uncertainties.

Figure 5.3 is the PDF for a particular case – Alice Springs temperature change in summer – for which the Beta PDF for local change was shown in Figure 5.1. The net change PDF is shown in Figure 5.3 ('Forced'). The median is 1.17ºC. The full range is considerable, but with 80% probability it is within the 10th and 90th percentiles, 0.77ºC and 1.73ºC.

In general, the uncertainty range will be shown using the 10th and 90th percentile values (Figure 5.4). For most of Australia, and in each season and the annual case, the resulting range is projected to be about 0.6 to 1.5ºC for the A1B scenario. Allowing for emission scenario uncertainty (see Fig A1 in Appendix A), warming is still at least 0.4ºC in all regions and can be as large as 1.8ºC in some inland regions.

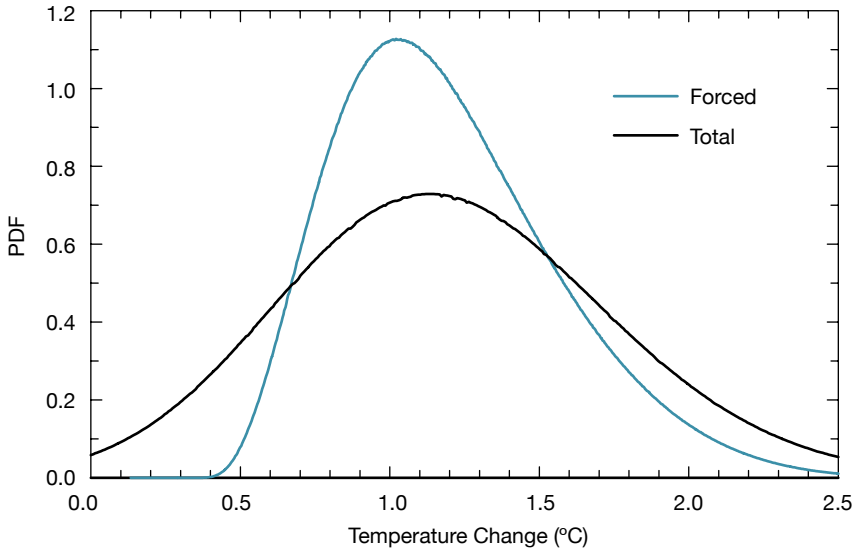

Figure 5.3: Probability density function for temperature change in summer, at Alice Springs in 2030 based on 23 models. The 'Forced' curve is of the change due to global warming alone; 'Total' is where decadal variability is included.

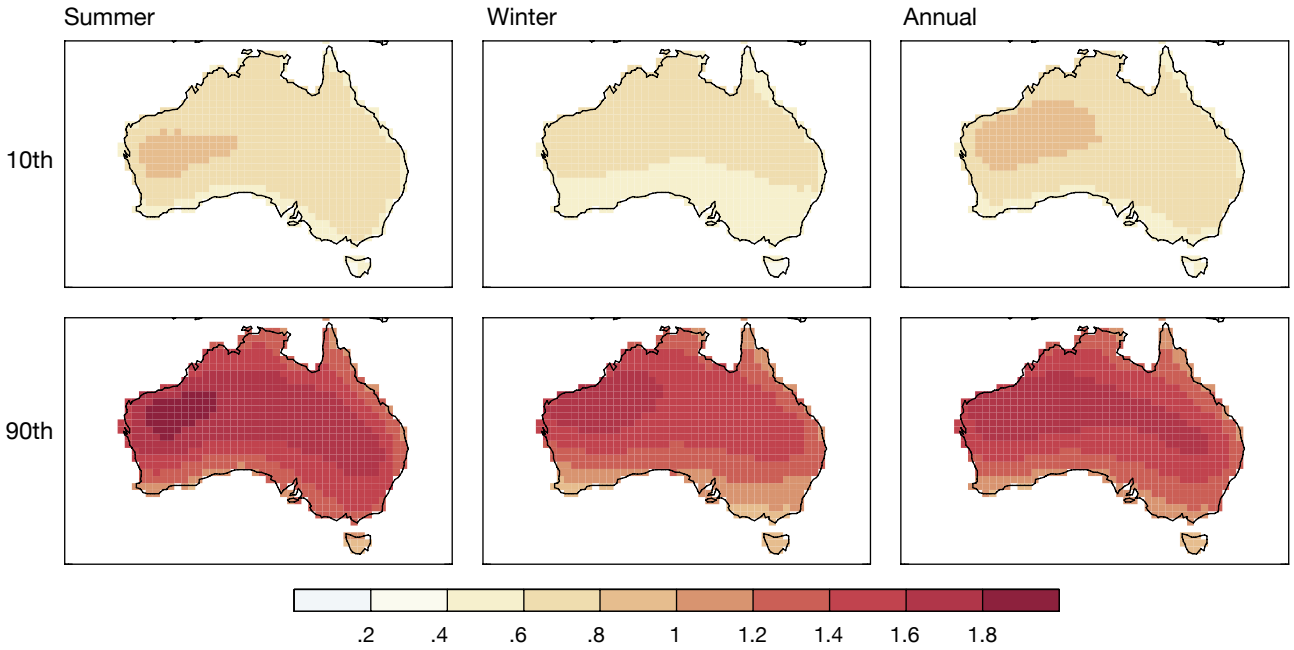

Figure 5.4: Range of warming (°C) by 2030 under the A1B scenario for the 10th to 90th percentile value for summer, winter and annual. (Note the modified colour scale compared to Figure 5.2.)

The actual observed temperature change for the decade around 2030 may differ considerably from this, as a result of natural variability in the (real-world) climate system. This may be comparable to the variability of the past, and the range of change may be spread accordingly. Accurate estimation of the natural variability based on observations is difficult. It is instructive to consider the variability simulated by the CSIRO Mark 3.5 climate model, in an 1100-year simulation for steady, pre-industrial conditions. Since there is a small increase in mean temperature after the first half, the standard deviation of 10-year means for temperature is based on the earlier 500-year period. This is plotted for two seasons and annual in Figure 5.5.

For the annual case, the variability is barely 0.2ºC and relatively small compared to the expected warming by 2030. For summer and winter, variability is larger, particularly in summer. This variability can be incorporated into the PDF using a similar approach to the method of combining global warming and local change. The variability can be represented using a Normal distribution. Combining this with the PDF for change at Alice Springs in summer produces the 'Total' PDF shown in Figure 5.3. There is no change to the best estimate. However, in this case there is a small possibility that the variability in a decade could completely counter the forced change (with the total change being zero). The usual forced range is extended by approximately 0.2ºC, about half the standard deviation for variability. For changes after 2030, decadal-scale natural variability in temperature is small compared to the uncertainty in projected warming (and the best-estimate of warming), particularly in the annual case.

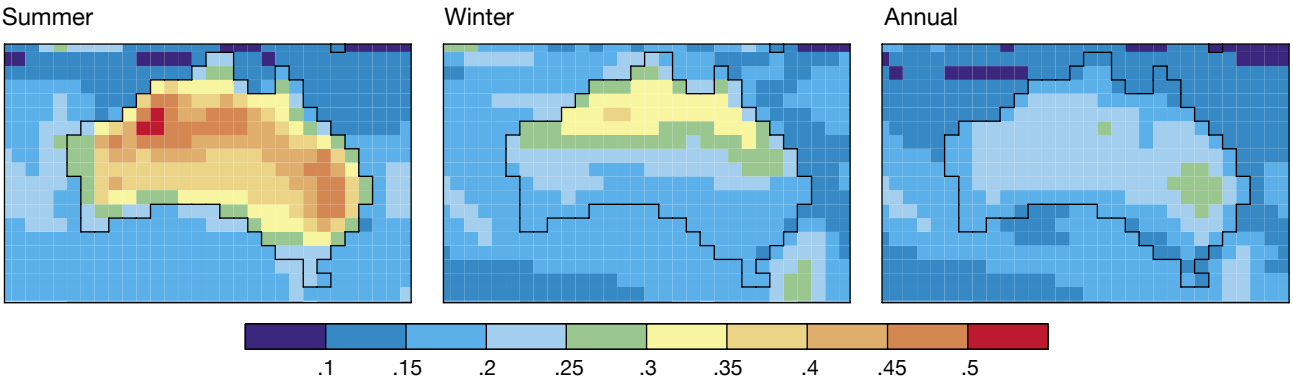

Figure 5.5: Standard deviation of decadal means of temperature (ºC) during a 500-year period simulated by CSIRO Mark 3.5 for summer, winter and annual. The model coastline is shown.

5.1.3 Projected warming for 2050 and 2070

Later in the century, the warming is more dependent upon the assumed emission scenario. By 2050, annual warming over Australia ranges from around 0.8 to 1.8ºC (best estimate 1.2ºC) for the B1 scenario and 1.5 to 2.8ºC (best estimate 2.2ºC) for the A1FI scenario. By 2070, the annual warming ranges from around 1.0 to 2.5ºC (best estimate 1.8ºC) for the B1 scenario to 2.2 to 5.0ºC (best estimate 3.4ºC) for the A1FI scenario. Regional variation follows the pattern seen for 2030, with less warming in the south and north-east and more inland. In 2070, the risk of exceeding 4ºC exceeds 30% over inland Australia under the A1FI scenario, whereas under the B1 scenario the risk of exceeding 2.0ºC is less than 20% around the coast, except in the north-west.

Beyond the first few decades of the current century, the change becomes increasingly dependent on the assumed emission scenario. To illustrate this dependence, this section highlights results for the B1 emission scenario, which amongst the SRES scenarios has the least global warming for 2050 and beyond (see Table 4.3), and A1FI, which has the greatest warming. Results for other emission scenarios are provided in Appendix A. As the relatively small seasonal variations in warming can be inferred from those for 2030, the focus here will be on the annual case (full seasonal results are available at www.climatechangeinaustralia.gov.au and results for selected sites in Appendix B). The set of projected best estimate annual warmings is plotted in Figure 5.6.

2050

By 2050, the best estimate for annual warming over Australia ranges from around 1.2ºC for the B1 scenario to 2.2ºC for the A1FI scenario (Section 5.1.1).

The range of projected Australian warming possible in 2050 is considerably larger than is shown in Figure 5.6 if the 10th-90th percentile uncertainty and differences between emission scenarios are included (Figure 5.7). The annual warming for Australia is around 0.8 to 1.8ºC for the B1 scenario, whereas for the A1FI scenario it is 1.5 to 2.8ºC. Warming for other emission scenarios lies between these two ranges. Regional variation follows the pattern seen for 2030, with less warming in the south and north-east and more inland.

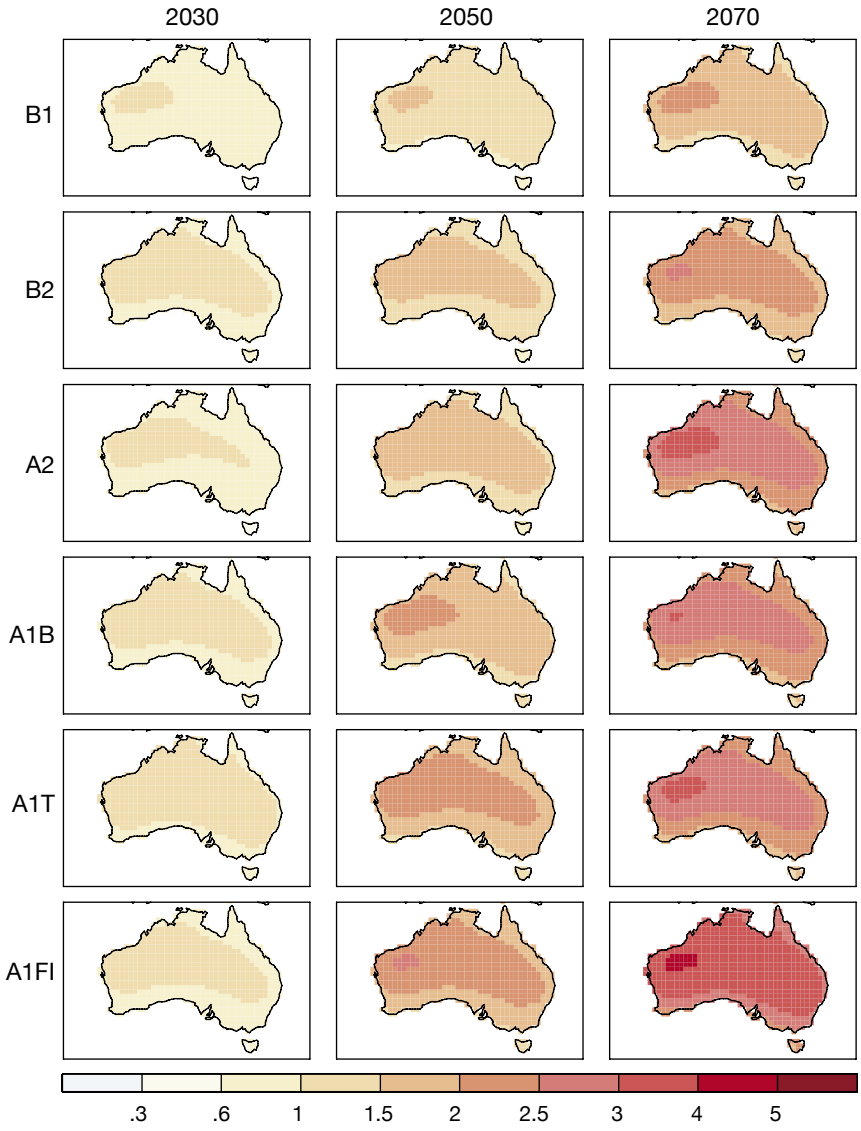

Figure 5.6: Best estimate (50th percentiles) of projected change of annual mean temperature (ºC) for 2030 (left column), 2050 (middle) and 2070 (right). Results for all six emission scenarios are given, from top to bottom.

2070

By 2070, the best estimate for annual warming over inland Australia ranges from around 1.8ºC for the B1 scenario to around 3.4ºC for the A1FI scenario (Section 5.1.1). Allowing for model to model variations (see results in Appendix A), the annual warming for Australia is around 1.0 to 2.5ºC for the B1 scenario, and around 2.2 to 5.0ºC for the A1FI scenario. Again regional variation follows the pattern seen for 2030, with less warming in the south and north-east and more inland.

For 2070 we also consider the probability of exceeding four selected thresholds (Figure 5.8). For the B1 scenario there is less than 20% chance of a 2ºC warming being reached around the coast by 2070, except in the north-west, while a 1ºC warming is virtually certain for all but the south coast (80-90% chance) and Tasmania (50-60% chance). For the A1B scenario, a 2ºC warming is very likely to be reached over much of Australia, with less than 30% chance along the south coast and Tasmania. For the A1FI scenario, even the south coast has a significant risk of reaching warming of 3ºC under this scenario, and there is around a 30% chance for 4ºC being exceeded in inland areas. There is clearly a substantial decrease in risk of high warmings under the B1 scenario, representing significant curtailment of the growth of future emissions, compared to that under A1B or A1FI.

The spatial patterns of temperature change for the best estimate case using the probabilistic method are similar to spatial patterns of change projected previously by CSIRO (2001). The patterns include greater inland warming and lower coastal warming. Winter shows the least warming, while spring and summer show the greatest warming in both cases. The current approach and set of models has

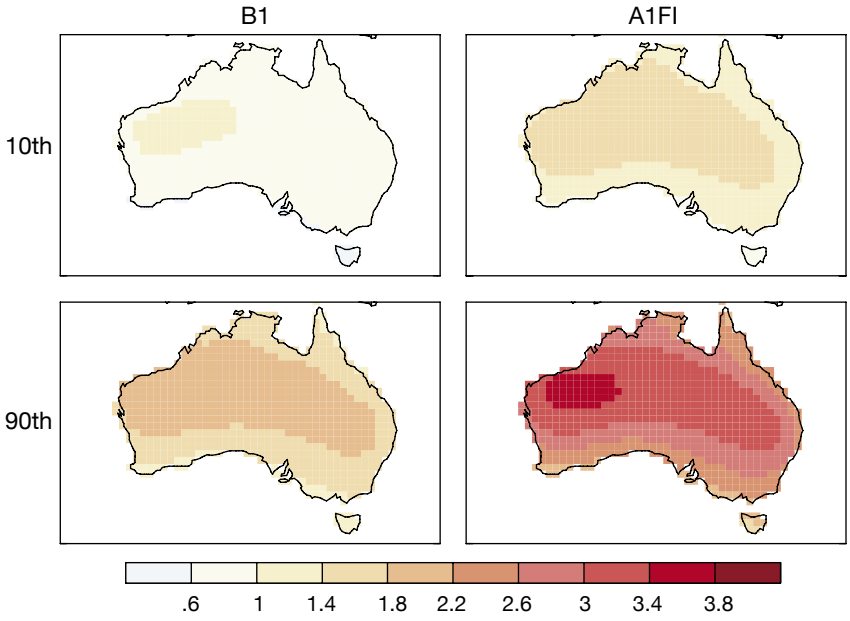

Figure 5.7: Range of annual warmings (°C) for 2050: 10th and 90th percentiles for the B1 (low) and A1FI (high) scenarios.

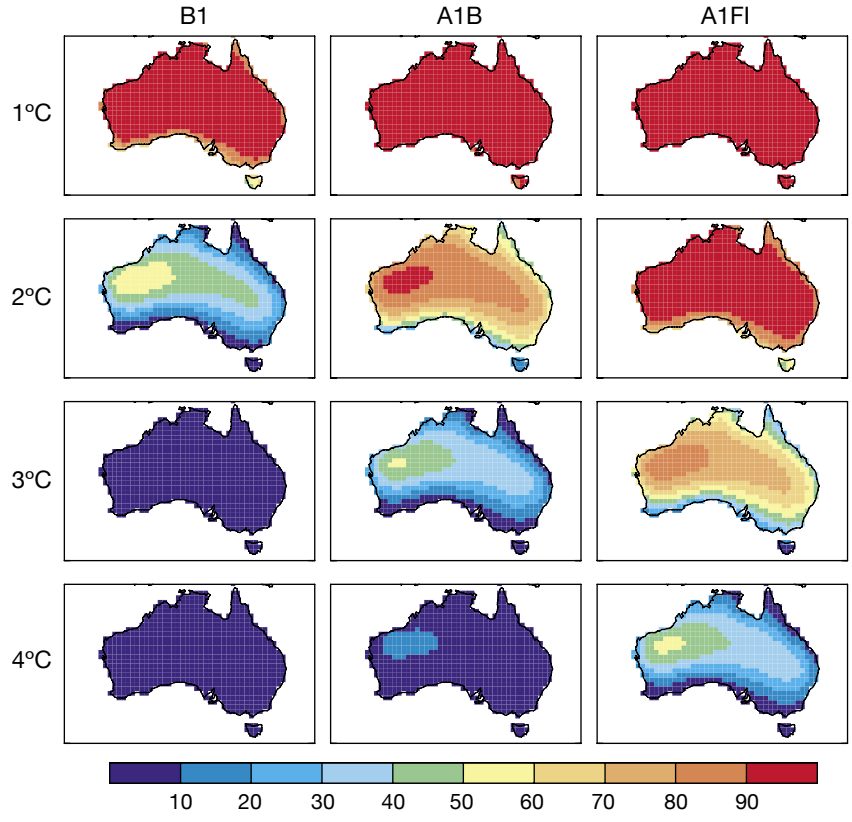

Figure 5.8: Risk (probability, in %) of exceeding each of four thresholds (1°C, 2°C, 3°C and 4°C) in the annual mean warming at 2070 under the B1 (low), A1B (middle) and A1FI (high) scenarios.

produced a range of warming which is narrower than in CSIRO (2001). This is most noticeable for 2070, where the range is 1 to 5ºC while in CSIRO (2001) the range was 1 to 6ºC. Because of the change of methods, direct comparisons are not possible, but the narrower range appears to be partly due to improved consistency between models. Suppiah *et al*. (2007) prepared projected climate changes for Australia based on 15 of the CMIP3 models using the method of CSIRO (2001) and also obtained some narrowing of the ranges of warming. Furthermore, because of the way global and local ranges of warming were combined in CSIRO (2001) (limits were simply multiplied) the end points of the ranges in CSIRO (2001) are likely to represent more extreme points than the 10th and 90th percentiles.

5.1.4 Local variations to projected warming

Projected warming may vary significantly from that given by the global climate models in mountainous areas and near the coast. This has been demonstrated through the application of fine-resolution spatial downscaling techniques.

Climate models have coarse spatial resolution (around 250 km between grid-boxes) and provide grid-box average results (Skelly and Henderson-Sellers 1996). Therefore sub-grid heterogeneity is not captured. These local details may be very important for understanding the impact of projected climate change on the natural and human environment. One simple way of estimating how the temperature PDF might vary within a grid box under global warming is to simply shift the PDF of past variability at that point to a higher average value by an amount that matches the warming expected for the whole grid box.

More advanced techniques relying on the observed statistical linkage between large-scale weather patterns and local observations can be used to downscale the information from large grid-boxes to locations of interest. Such an approach, based on meteorological analogues, has been developed for temperature (Timbal and McAvaney 2001) and adapted to precipitation (Timbal *et al*. 2003). It has been recently applied for selected locations across the southern half of the Australian continent using a subset of 10 models from the CMIP3 database for which daily outputs were archived.

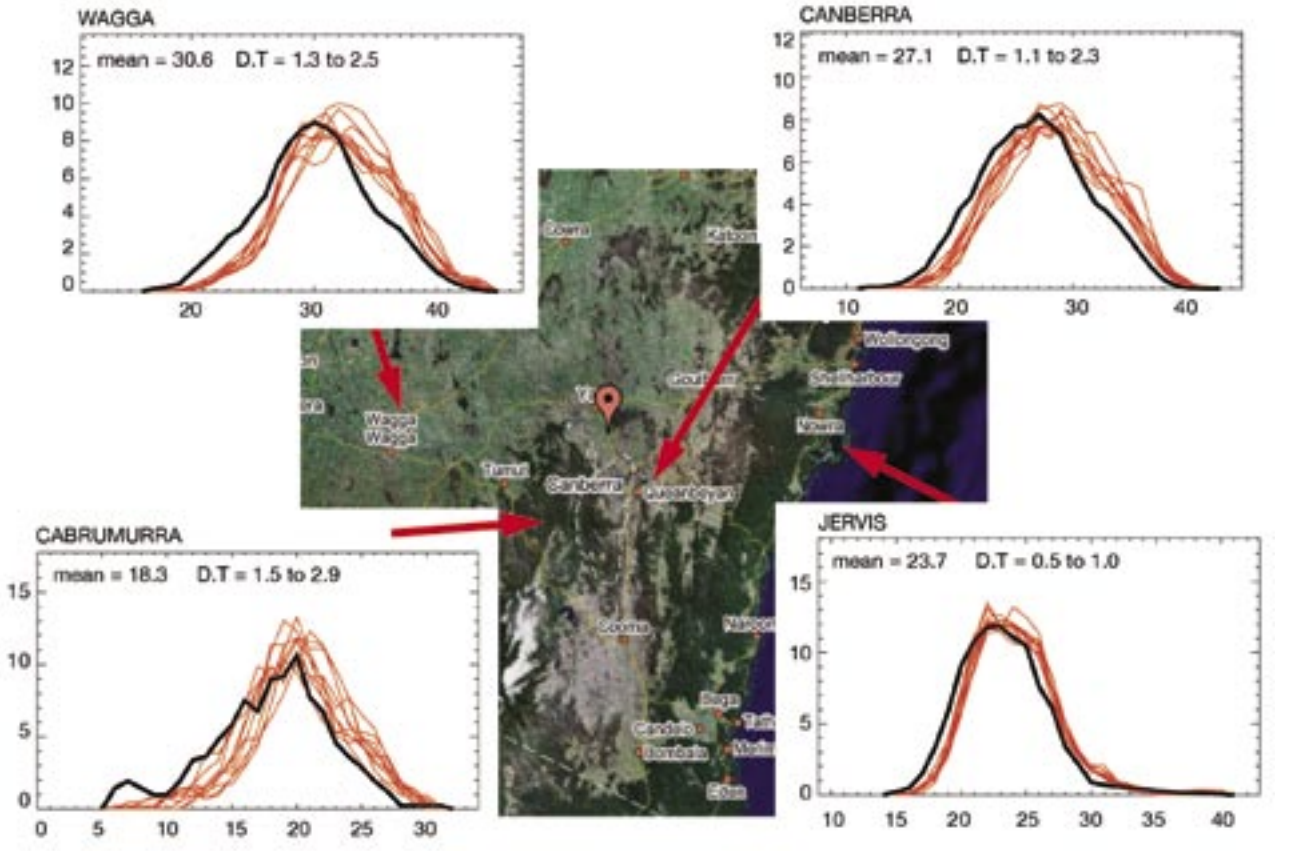

Figure 5.9: Projected changes in the observed probability distribution functions of maximum temperature in summer for 2050 (using emission scenario A2) in four neighbouring locations in south-east New South Wales with contrasting climates: Jervis Bay (a coastal location), Canberra (150 km inland, in the Great Dividing Range but at low elevation), Cabramurra (inland, at high elevation) and Wagga Wagga (on the western side of the Great Dividing Range) using the statistical downscaling technique described in the text. Observations are shown as thick black lines, 10 individual climate models from the CMIP3 database are shown as red lines.

Figure 5.9 shows probability density functions of temperature change for four locations in south-east New South Wales that could easily fit within a single grid box. This area encompasses part of the Great Dividing Range.

The results show notable differences from one part of the grid box to another: in Jervis Bay the warming is between 0.5 and 1.0ºC, while in Canberra the warming is more than twice as large (between 1.1 and 2.3ºC). The warming is slightly larger further inland (Wagga Wagga) and even larger at higher elevation (Cabramurra). The increased warming away from the coast is commonly depicted by global climate models, but the additional warming with elevation is less documented as usually it is not captured by global climate models which have a limited ability to reproduce the effect of mountains due to coarse resolution.

The projected warming is broadly similar to direct model outputs for the area (between 1.4 and 1.8ºC) as shown for the same scenarios and time span (Figure 5.6). Although direct model outputs only provide a hint that coastal warming is lower than further inland, the downscaled results provide a more contrasting response. This is not however a direct comparison as some differences arise from using mean (rather than maximum) temperature and showing annual (rather than summer) averages as well as using the full range of CMIP3 database models (rather than the subset of 10).

It is also possible to estimate the chances that the warming will exceed selected thresholds such as 1.5°C. This probability varies markedly across the grid box as would be expected from the warming range projected at each location: it is less than 5% in Jervis Bay but reaches 80% in Canberra and Wagga Wagga, and it exceeds 95% in Cabramurra.

5.1.5 Extreme temperature: hot days and warm nights

Associated with the warming is a projected strong increase in frequency of hot days and warm nights.

Changes in the frequency of hot summer days is of potential importance to the occurrence of heat stress, and energy demand for cooling. Livestock and crops are also affected by extreme high temperatures. Daily maximum temperature data were available for six climate models. For these models, the ratio of the change in maximum to mean temperature is greater than one in the south and less than one in the north (Figure 5.10). This tends to be related to changes in cloud cover, whereby reduced cloud cover leads to greater increases in maximum temperature than mean temperature, and the opposite occurs for increased cloud cover. During summer, the maximum temperature increases by up to 5% more than the mean over

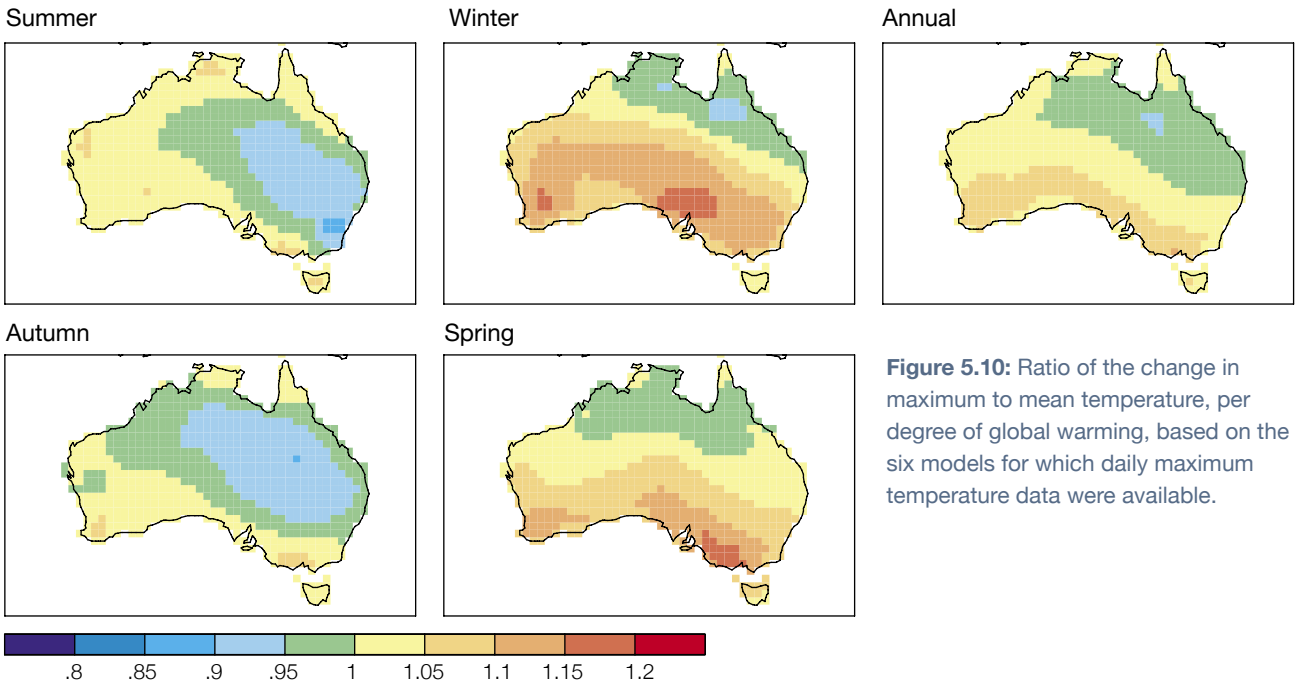

Figure 5.10: Ratio of the change in maximum to mean temperature, per degree of global warming, based on the six models for which daily maximum temperature data were available.

Western Australia, most coastal areas and Tasmania, but increases by up to 10% less than the mean over New South Wales, southern Queensland and southern Northern Territory.

The current annual average number of days above 35ºC was calculated for 14 sites, including eight capital cities, using daily temperature records from the Bureau of Meteorology (Table 5.2). These averages are based on a common 30 year period from 1971-2000. They tend to be higher than the 'present' averages for capital cities in Table 1 of the CSIRO (2001) projections because the 2001 figures were based on longer-term averages up to the year 2000, e.g. the 'present' average for Melbourne was based on data from 1855 to 2000.

Projected changes in the frequency of extreme daily maximum temperatures were calculated by applying projected warmings presented in sections 5.1.1-5.1.3 to observed daily maximum temperatures at the selected sites and then counting the number of days per year above 35ºC. The mean warming (based on 23 models) was multiplied by the ratio of maximum to mean warming (based on six models) in Figure 5.10, to allow for the fact that maximum temperatures increase faster than the mean in the south and slower in the north. Table 5.2 gives results for days above 35ºC for 2030 under A1B, and 2070 under A1FI and B1. Substantial increases in the frequency of hot days occur at all sites, particularly under A1FI in 2070 (e.g. in Melbourne, a 20-40% increase by 2030, a 30-90% increase for the B1 scenario by 2070 and a 70-190% increase for the A1FI scenario by 2070). Note that this approach assumes no change in variability. However, the statistical downscaling approach (used in sections 5.1.4 and 5.1.6) does allow for changes in variability, and has been applied to hot day occurrence at one site (Adelaide). Results were consistent with those provided by the simpler approach.

Table 5.2: Average number of days per year above 35ºC at selected sites for the 'current' climate (average for 1971-2000), and for 2030 and 2070. In each case, the low scenario is the 10th percentile, the median is the 50th percentile and the high scenario is the 90th percentile. For 2030, results are presented for the A1B emission scenario only since there is little difference between warmings for this and other emission scenarios. For 2070, results are presented for the A1FI and B1 emission scenarios. Warmings are those for the relevant location provided by sections 5.1.1-5.1.3 in this report, with an adjustment for the difference between the increase in daily maximum and mean temperatures.

	Current	2030 A1B low	2030 A1B median	2030 A1B high	2070 B1 low	2070 B1 median	2070 B1 high	2070 A1F1 low	2070 A1F1 median	2070 A1F1 high
Adelaide	17	21	23	26	24	26	31	29	36	47
Alice Springs	90	102	109	118	112	122	138	132	155	182
Brisbane airport	1.0	1.5	2.0	2.5	2.1	3.0	4.6	4.0	7.6	20.6
Broome	54	71	86	107	89	119	173	147	220	281
Cairns	3.8	5	7	9	8	12	22	19	44	96
Canberra	5	7	8	10	8	10	14	12	18	26
Darwin	11	28	44	69	49	89	153	141	227	308
Dubbo	25	31	35	39	35	40	51	44	61	87
Hobart	1.4	1.6	1.7	1.8	1.7	1.8	2.0	2.0	2.4	3.4
Melbourne	9	11	12	13	12	14	17	15	20	26
Mildura	32	36	39	43	39	45	51	48	60	76
Perth airport	28	33	35	39	36	41	46	44	54	67
St George	47	56	63	72	64	74	91	80	103	135
Sydney	3.5	4.1	4.4	5.1	4.5	5.3	6.6	6	8	12
Wilcannia	63	71	77	82	79	85	96	92	106	129

Changes in the frequency of warm nights have not been considered using a site specific approach. However, climate modelling groups worldwide submitted a standard set of 'extremes indices' to the CMIP3 data archive, one of which included 'warm nights', defined as the percentage of days when the minimum temperature is greater than 90th percentile of values for 1961-1990. This definition was based on that of Frich *et al*. (2002). A projected increase in warm nights is found Australia-wide (Figure 5.11), with increases between 15-50% at the end of the 21st century. This is consistent with a projected rise in warm nights globally (Tebaldi *et al*. 2006) with the Australian average increase at the end of the century approximately 10% larger than the global average. The pattern of change is shown in Figure 5.11 for the mid-range A1B scenario, with strongest increases in the north.

5.1.6 Extreme temperature: frost

Frost decreases in frequency as the warming progresses, but the decrease in frost can be less marked than would be expected from the mean warming alone. For locations in the Murray-Darling Basin, a simulated increase in the day to day variability of minimum temperature reduced the impact of the mean warming on frost frequency.

Changes in the frequency of frost are of potential importance to agriculture (for frost damage and vernalisation), cold stress for livestock, road safety and energy demand for heating. Daily minimum temperature data were available for six climate models. For these models, the ratio of the change in minimum to mean temperature is less than one in the south, particularly in winter and spring, and greater than one in the north (Figure 5.12). This tends to be related to changes in cloud cover, whereby reduced cloud cover leads to smaller increases in minimum temperature than mean temperature, and the opposite occurs for increased cloud cover. In winter and spring, minimum temperatures increase 10-15% more slowly than mean temperatures in the south, and up to 5% faster than mean temperatures in the north. Over Victoria, spring minimum temperatures rise 15-20% more slowly than the mean. Where minimum temperatures rise more slowly than the mean, decreases in frost frequency would also occur more slowly.

The diurnal temperature range (DTR) is the difference between the maximum and minimum temperature on a given day. Projected changes in maximum and minimum temperature shown in Figures 5.10 and 5.12 indicate an increase in the diurnal temperature range in the south, and a decrease in the north. The most significant feature is the increase in DTR in the south in winter and spring.

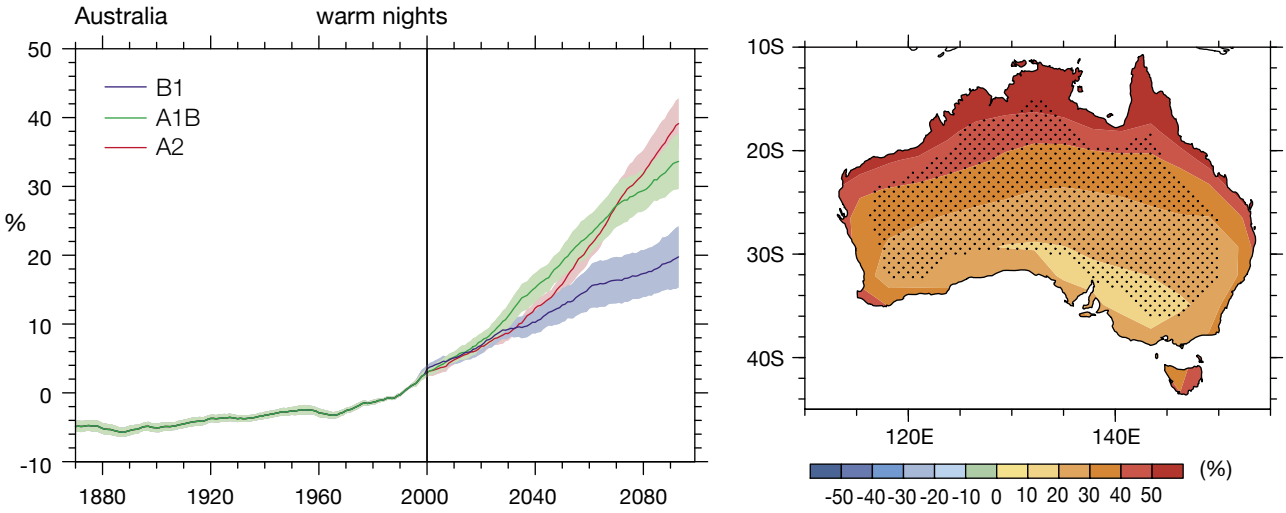

Figure 5.11: Area-average time series (left panel) of warm nights over Australian land points from the CMIP3 multi-model dataset. The ensemble mean (solid lines) of nine models is shown for the SRES B1, A1B and A2 scenarios, with shading representing inter-model uncertainty. The right panel is the ensemble mean projected changes (2080-2099 minus 1980-1999) in warm nights from the CMIP3 multi-model dataset for A1B. Stippling indicates that 5 out of 9 models agree that the change is significant. (After Tebaldi *et al*. 2006.)

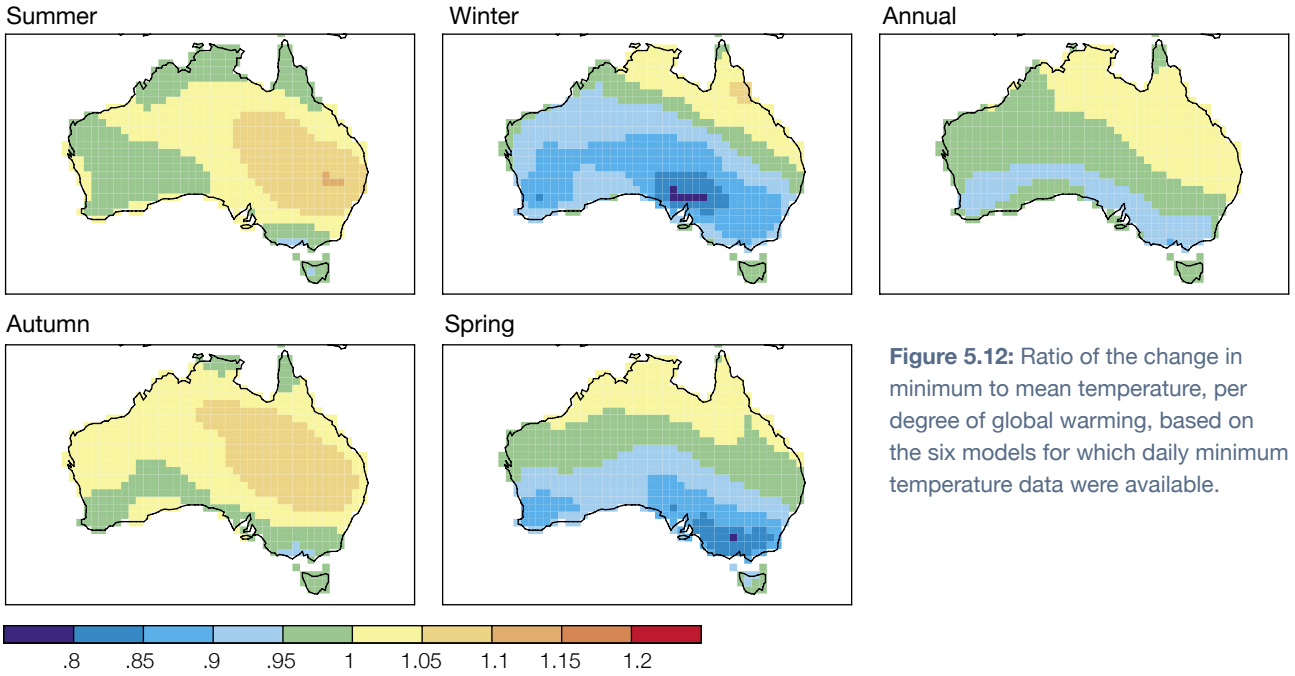

Figure 5.12: Ratio of the change in minimum to mean temperature, per degree of global warming, based on the six models for which daily minimum temperature data were available.

Due to coarse resolution and smoothed mountain features, climate models have difficulty reproducing the observed occurrence of frost. This is illustrated in Figure 5.13 which displays the number of frost occurrences as obtained from the direct output of climate models and from the statistical downscaling of the same models for 16 selected high quality stations scattered across the Murray-Darling Basin. The statistical downscaling presented in section 5.1.4 and applied to the same subset of CMIP3 climate models corrects the global climate model biases and gives realistic frost frequency at each location.

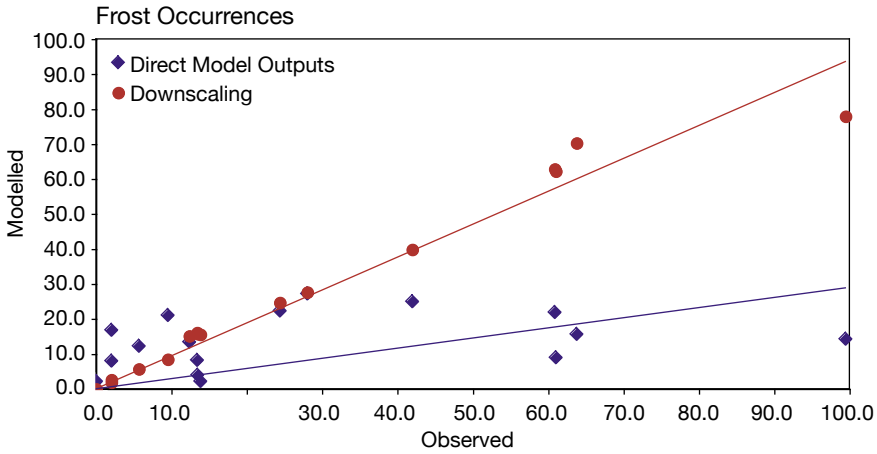

Figure 5.13: Relationship between the calculated frost occurrences by climate models across the Murray-Darling Basin and those observed. Each point represents the total number of frosts per year during winter at 16 high-quality stations as observed and modelled by the nearest grid-point from climate models (blue) and obtained from downscaling the same climate models (red). Each model calculation is based on an average of 10 CMIP3 climate models integrated over the 20th century using daily data for 40 years from 1961 to 2000.

The magnitude of the frost reduction by 2050 (Table 5.3) depends on the magnitude of the warming (and hence the emission scenario) and the location. Frost reduction is also much larger in areas where frost is already marginal (e.g. Cobar: median reduction of 50% for the B1 scenario, and 61% for the A2 scenario) but frost is more resilient when it currently occurs more frequently (e.g. Canberra: median reduction of 14% for the B1 scenario, and 17% for the A2 scenario). The 10th to 90th percentile range of uncertainty is large, and is likely to be an under-estimation of the full range of uncertainties as only 10 models were available to apply the downscaling.

It is useful to compare downscaling projections with results obtained with a simple shift of the observed PDFs by the projected mean warming, as well as direct model outputs of daily temperatures. Table 5.4 shows that using the direct model output the reduction in frost frequency is larger, in particular for locations where frost is either a regular or frequent occurrence in winter. Results provided by a simple shift of the observed PDF gives a measure of the over-estimation of the frost reduction excluding changes in variability. With downscaling, the effects of changes in the mean and variance oppose each other and reduce the magnitude of the frost changes. A plausible mechanism to explain the increase temperature variability and the resilience of frost occurrences is the projected increase in diurnal temperature range due to reduced cloud cover and rain in the south (see sections 5.2 and 5.3.1).

Table 5.3 Observed annual average number of frost days, and projected percentage changes in frost days by 2050 using two emissions scenarios (A2 and B1) for four locations in the Murray-Darling Basin: Canberra (Australian Capital Territory), Nhill (Victoria), Cobar (New South Wales) and Charleville (Queensland). Results are obtained using statistical downscaling of 10 models.

	Observed	B1 scenario (2050)			A2 scenario (2050)		
		10%	50%	90%	10%	50%	90%
Canberra	63.8	-5%	-14%	-27%	-8%	-17%	-27%
Nhill	13.5	-18%	-28%	-53%	-24%	-35%	-47%
Cobar	2.0	-24%	-50%	-71%	-44%	-61%	-77%
Charleville	13.4	-34%	-45%	-55%	-44%	-59%	-70%

Table 5.4 Reduction in frost occurrences by 2050 for emission scenarios A2 and B1 at selected stations in the Murray-Darling Basin. Stations are clustered according to the observed number of frost occurrences; very rare (5 or less per year), rare (6 to 14), regular (15 to 30) and frequent (in excess of 40). Results are compared between direct model outputs (DMO), statistical downscaling and changing the observed temperature distribution by the mean warming (Obs + ΔT).

	A2 scenario (2050)			B1 scenario (2050)		
	D.M.O	Downscaled	Obs + ΔT	D.M.O	Downscaled	Obs + ΔT
Very rare	-59%	-61%	-67%	-48%	-52%	-61%
Rare	-56%	-46%	-69%	-42%	-36%	-59%
Regular	-46%	-39%	-67%	-35%	-31%	-56%
Frequent	-48%	-24%	-48%	-40%	-19%	-37%

5.2 Precipitation

Unlike changes in radiation and temperature, precipitation changes are not directly influenced by rising greenhouse gases. However, a warmer atmosphere can hold more water vapour, and hence produce heavier precipitation. Also, changing the temperature patterns across the planet means that the wind patterns (the circulation) will change the rain patterns. A key change to the atmospheric circulation is poleward expansion of the Hadley circulation, the exchange of air from the tropics to mid-latitudes. This, together with an intensification of the hydrological cycle, tends to produce lower relative humidity and precipitation in the subtropics (the desert regions), extending to the mid-latitudes in some seasons (see Chapter 4).

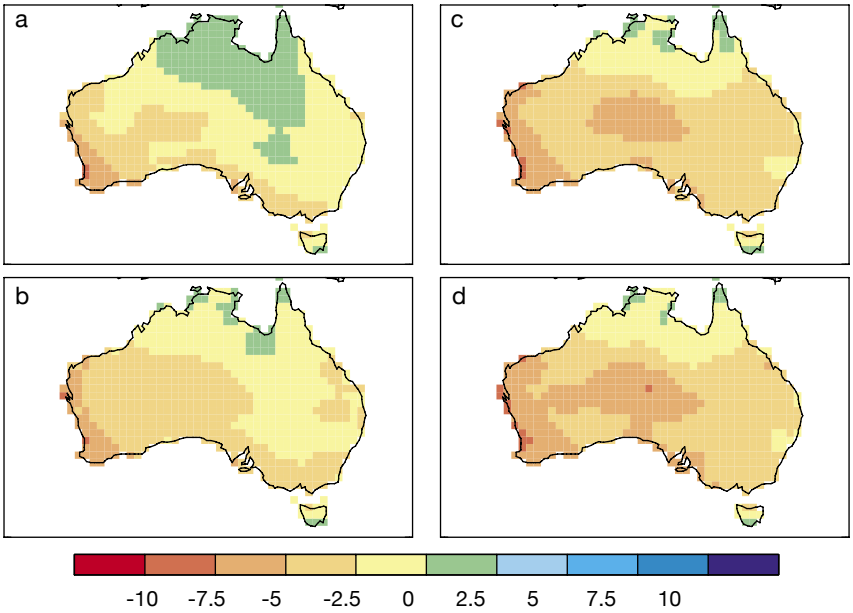

Figure 5.14: Change in annual precipitation across Australia scaled by amount of global warming (unit % per °C) averaged over the CMIP3 models, using four different approaches: **(a)** means for 2070-2099 relative to 1990-2005; **(b)** the multi-model mean trend in precipitation in mm per day, as a percentage of the multi-model mean for the standard period 1961-1990; **(c)** the mean of trend as a percentage; **(d)** as **(c)** but using the model weights (from Table 4.1).

Regional precipitation variations can be quite sensitive to small differences in the circulation and other processes, as is evident from the large natural variability of precipitation over Australia. Different models may therefore simulate somewhat different rainfall changes. As in the CSIRO (2001) projections, it will not be possible to make definitive statements on the direction of precipitation change in many cases. However the probabilistic pattern-scaling approach, applied to mean precipitation in sections 5.2.1 to 5.2.3, can provide a likely range of change, as well as a best estimate, of future precipitation. For many impact applications the percentage change in precipitation is of more interest than the absolute amounts, so the analysis will focus on percentage changes relative to 1990.

The best estimate of change depends closely on the local change per degree of global warming, so it is worthwhile focusing on this initially. Figure 5.14 compares four methods of calculating the local change. Using the simulations from 23 models available for the A1B scenario, the simple multi-model mean change in annual precipitation is shown in Fig. 5.14a for 2070-2099 relative to 1990-2005. Small increases occur in the north-central region, with larger decreases in the south.

To produce local changes per degree of global warming, precipitation (in mm per day) has been regressed against global warming over the 21st century, just as for temperature. Taking a simple average over 23 models produces the 'local trend' as a percentage, shown in Figure 5.14b. The difference, compared to the previous result, is greater drying except in the far south. This may reflect slightly different patterns of change in the mid-century, possibly associated with aerosol variations in the A1B scenario. With aerosol represented very differently among the models, we do not attempt to extract any specific signal associated with it in the analysis. The standard variable is precipitation as a percentage (from each individual model), and the simple average of these trends is shown in Figure 5.14c. The difference relative to 5.14b is again greater drying, except in the far north. Presumably, models with increases in precipitation tend to have relatively large precipitation in the base climate. Finally, the weighted mean of the percentage trends, using the standard model weights of Table 4.1, is shown in Figure 5.14d. The result is slightly drier than 5.14c everywhere. Evidently the more skilful models are more likely to produce a decrease. This final result (5.14d), with an annual precipitation decrease over nearly all of Australia, strongly influences the best estimates of change from the probabilistic projections that follow.

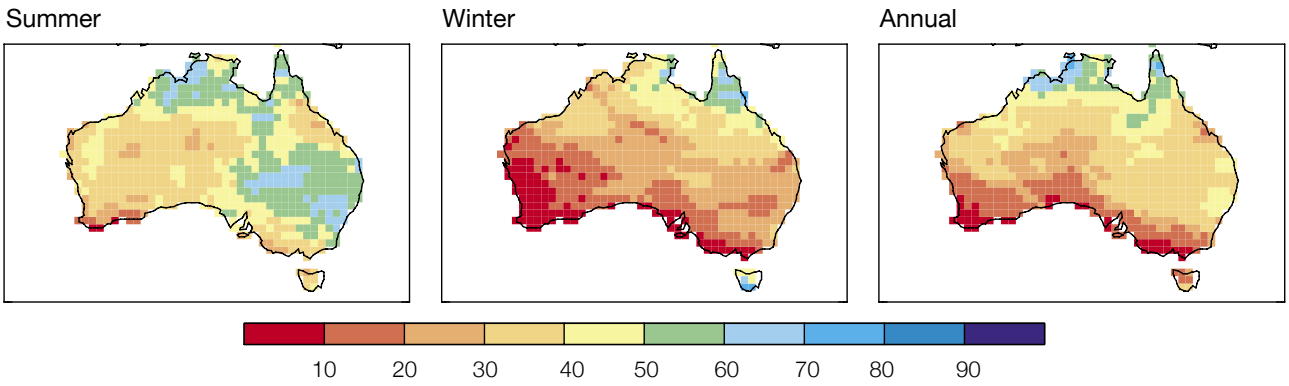

Figure 5.15: Percentage of models agreeing on an increase in precipitation for summer, winter and annual.

While the mean annual change in precipitation is mostly negative, there are some models that simulate an increase. This is seen in Figure 5.15, which shows the percentage of models projecting an increase in the (percentage) trends. In the north, half the models have an increase in the annual case, and in summer. Nearly all models produce a decrease in the south-west and along the south coast in winter.

We illustrate the spread of model trends for local change using annual results for the grid point representative of Melbourne. Most models produce a decrease, and the two lowest values (–12% and –9% per degree of global warming) are from the two CSIRO models. The largest increase is 3% per degree of global warming. The Sum PDF, constructed as for temperature using the weighted sum of individual model PDFs, is shown in Figure 5.16. Because of the relatively large regression uncertainties for precipitation, the Sum is already rather smooth, but also extends to large negative values (well beyond the Uniform case). The Normal curve shortens the left tail, but extends the curve further to the right. The Beta PDF is a smooth, bounded compromise, with a slightly negative skewness.

As for temperature, the product of a local change PDF and a global warming PDF gives a full PDF for net change

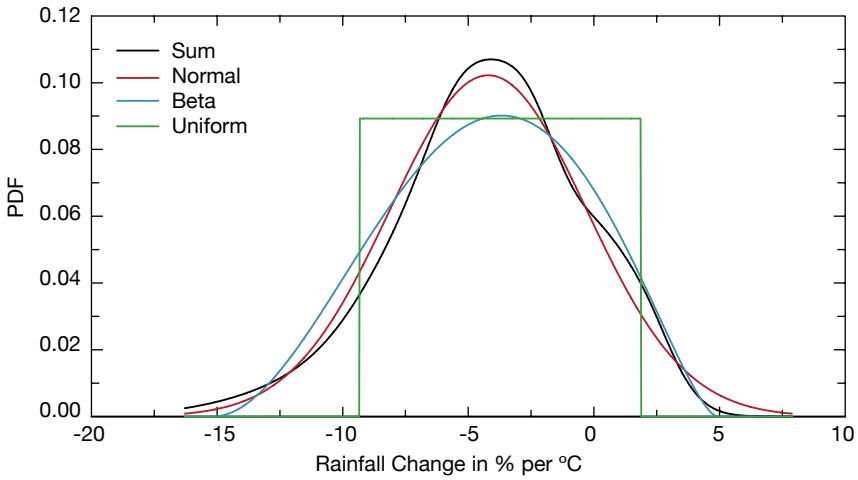

Figure 5.16: Probability distribution functions for the change in annual precipitation in % per °C of global warming at Melbourne (the point 147°E, 37°S) calculated from the 23 models, using four fitting methods (see also introduction to Chapter 5).

taking into account both sources of uncertainty. This is an enhancement over the simple products of ranges used in the CSIRO (2001) brochure. This usual linear theory seems quite adequate for increases in precipitation. It has long been recognised, however, that the larger decreases cannot continue at the same rate if warming increases, as they would eventually exceed the base climate precipitation, i.e. decreases cannot exceed 100%. Using percentage changes can alleviate this problem but does not avoid it.

The solution proposed by Watterson (2007) and adopted here is to consider percentage decreases to be compounding. For instance, if precipitation decreases 20% for 1°C global warming, then for 3°C it will decrease to 0.8 × 0.8 × 0.8, or 0.51 of the initial value; i.e. a 49% decrease, rather than the linear assumption of 60%. This is consistent with an exponential relationship between precipitation and warming. The effect is to contract the range of negative change, if it nears –100% (which rarely occurs, in fact, for changes to 2070). The linear and exponential approaches meet, smoothly, at the zero change point (e.g. in Figure 5.17), so can be readily combined. This 'mixed' scaling approach is used in all further results for precipitation.

The net change for the Melbourne point, using the Beta global warming PDF (Figure 4.5) for A1B in 2070,

is illustrated in Figure 5.17. The cumulative distribution functions for the first two fitting methods are very similar to that for the standard Beta case, with respect to the 10th, 50th and 90th percentile values presented. This provides some confidence in the results. A difference for the Uniform case is evident in this instance. The extreme negative change represented here (10th percentile) is a little larger than would result from the simple product of ranges under the CSIRO (2001) approach.

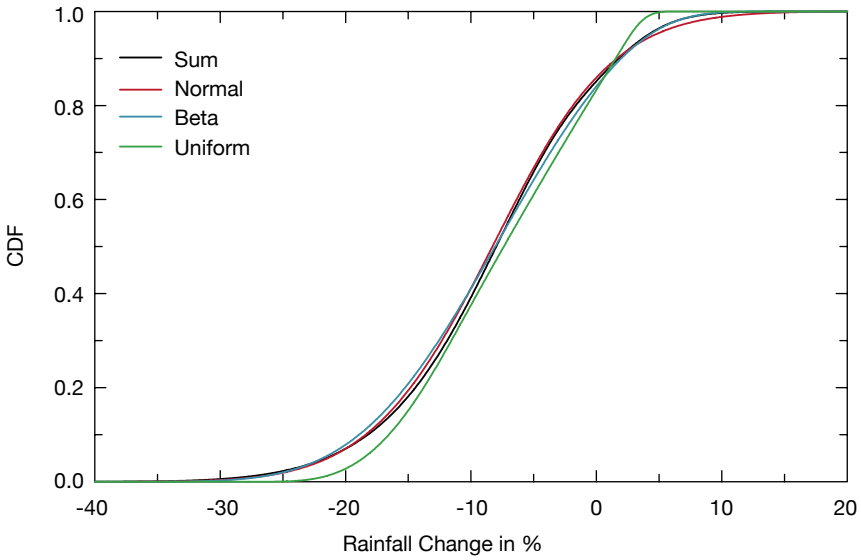

Figure 5.17: Cumulative distribution function for the net change in annual precipitation change at Melbourne in 2070 for the A1B scenario, for each of the four fits of scaled precipitation shown in Figure 5.16. The mixed scaling approach is used in each case.

5.2.1 Median precipitation change by 2030

Best estimates of annual precipitation change represent little change in the far north and decreases of 2% to 5% elsewhere. Decreases of around 5% prevail in winter and spring, particularly in the south-west where they reach 10%. In summer and autumn decreases are smaller and there are slight increases in the east.

Precipitation is assessed using the same PDFs for global warming as in section 5.1.1 for temperature, with the A1B emissions case as the standard for early in the century (selection of other emissions scenarios has very little impact on projections over this period). For 2030, the best estimates (50th percentile) of precipitation change relative to 1990 for each season and annually are shown in Figure 5.18. Best estimates of annual precipitation change represent little change in the far north and decreases of 2% to 5% elsewhere. In summer and autumn decreases are smaller and there are slight increases in the east. Decreases of around 5% prevail in winter and spring, particularly in the south-west where they reach 10%. These are still smaller, however, than the decreases that were observed there in previous decades (see section 2.2.1).

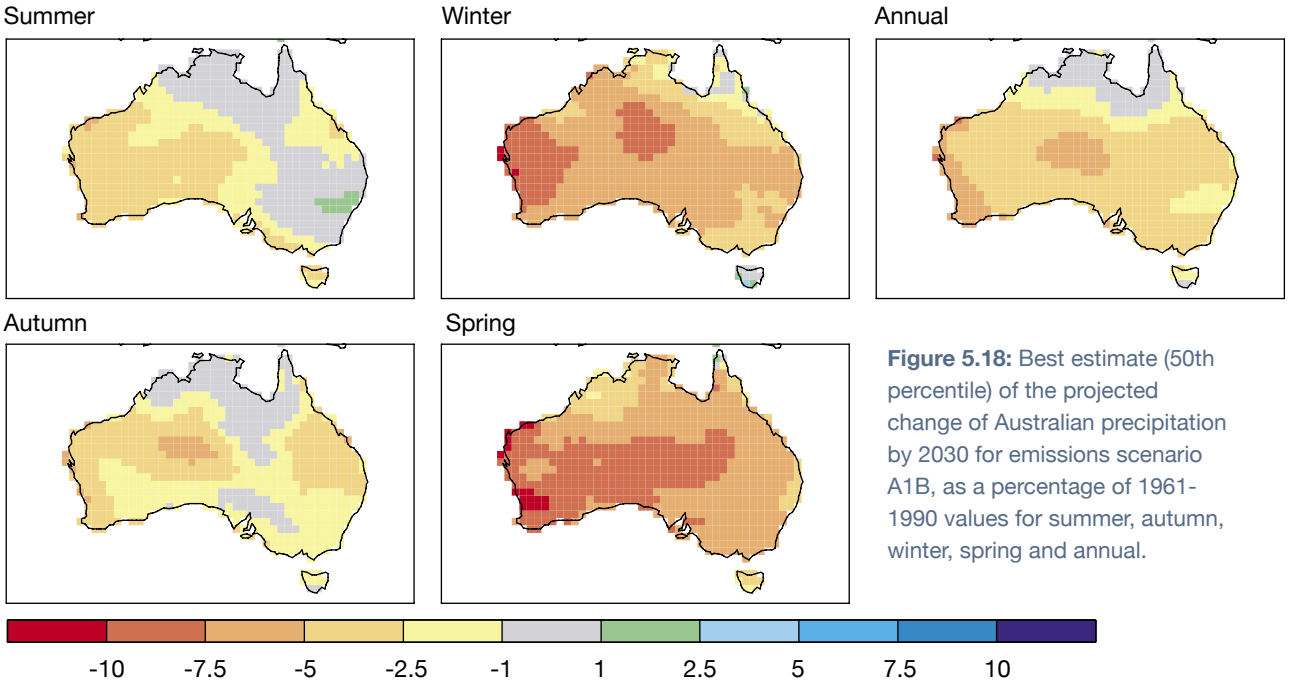

Figure 5.18: Best estimate (50th percentile) of the projected change of Australian precipitation by 2030 for emissions scenario A1B, as a percentage of 1961-1990 values for summer, autumn, winter, spring and annual.

5.2.2 The uncertainties in the precipitation change by 2030

The range of precipitation change in 2030 allowing for model to model differences is large. Annually averaged, the 10th to 90th percentile range is around -10% to +5% in northern areas and -10% to little change in southern areas. Winter and spring changes range from decreases of around 10% to little change in southern areas of the south-east of the continent, decreases of 15% to little change in the south-west, and decreases of around 15% to possible increases of 5% in eastern areas. In summer and autumn, the range is typically -15% to +10%. Decadal-scale natural variability in precipitation is comparable in magnitude to these projected changes and may therefore mask, or significantly enhance, the greenhouse-forced changes.

As an indication of the range of greenhouse-gas induced change in precipitation, the 10th and 90th percentile values are plotted in Figure 5.19 for A1B and for winter, summer and the annual average. Results for other scenarios and seasons are in Appendix A and results for selected sites in Appendix B. The 10th percentile represents the most negative changes based on the range of results from 23 models, and at every point over Australia these are decreases in all seasons. The largest percentage decreases occur in the north in winter, although this is from a dry base. The 90th percentile values are the most positive changes. These are always increases, except for very little winter and annual change along the south coast. This is to be expected given that most models simulate a decrease there in winter (compare with Figure 5.15b).

Expressing the 10th and 90th percentile values as a range, the range of annual change is around -10% to +5% in northern areas and -10% to little change in southern areas. Winter and spring changes range from decreases of around 10% to little change in southern areas of the south-east of the continent, from decreases of 15% to little change in the south-west, and from decreases of around 15% to possible increases of 5% in eastern areas. In summer and autumn, the range is typically -15% to +10%.

While decade to decade variation in mean temperature due to natural variability was estimated to be relatively small compared to the enhanced greenhouse change in the decade centred on 2030 (section 5.1.2), the same is not true for precipitation. In the control simulation (no change in greenhouse gases) with the CSIRO

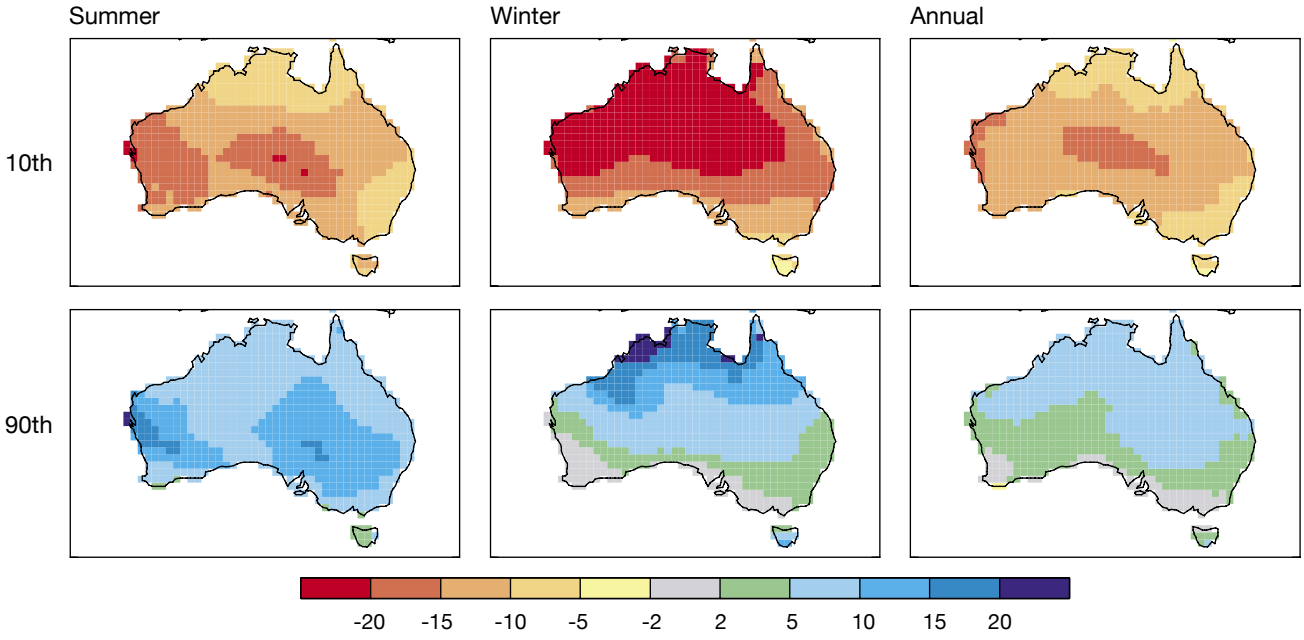

Figure 5.19: Projected Australian precipitation change (%) by 2030 for scenario A1B from the 10th to 90th percentile value for summer, winter and annual. (Note the modified colour scale compared to Figure 5.18.)

Mark 3.5 model, decadal averages of precipitation show substantial natural variability. It is convenient to present this in terms of the coefficient of variability, the standard deviation divided by the mean, shown as a percentage. As seen in Figure 5.20, even the annual case has natural variations of 10% or more over much of Australia. Restricting the averages to individual seasons produces variations often well over 20%.

Clearly these variations are substantial compared to the greenhouse-gas induced change for 2030, even for the larger changes among the range plotted in Figure 5.19. The addition of these, through the method used for temperature (Figure 5.3), would produce substantially larger potential changes for individual decades.

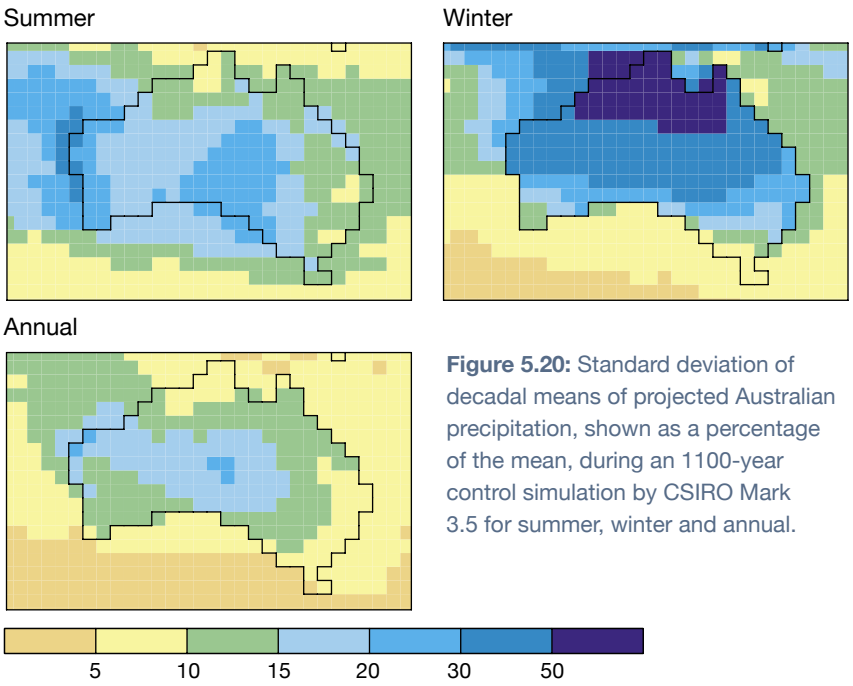

Figure 5.20: Standard deviation of decadal means of projected Australian precipitation, shown as a percentage of the mean, during an 1100-year control simulation by CSIRO Mark 3.5 for summer, winter and annual.

5.2.3 Projected change for 2050 and 2070

Later in the century, projected precipitation changes are larger and more sensitive to emission scenarios.

By 2050, under the B1 scenario, the range of annual precipitation change is -15% to +7.5% in central, eastern and northern areas, with a best estimate of little change in the far north grading southwards to a decrease of 5%. The range of change in southern areas is from a 15% decrease to little change, with best estimate of around a 5% decrease. Under the A1FI scenario changes in precipitation are larger. The range of annual precipitation change is -20% to +10% in central, eastern and northern areas, with a best estimate of little change in the far north grading to around a 7.5% decrease elsewhere. The range of change in southern areas is from a 20% decrease to little change, with best estimate of around a 7.5% decrease. Seasonal changes follow the pattern seen for 2030, but are larger under A1FI in 2050. The projected decreases in the south-west in winter and spring range up to 30%.

In 2070, precipitation changes under the B1 scenario are comparable to those seen for 2050 under the A1FI scenario. Those under the A1FI scenario are substantially larger. The range of annual precipitation change is -30% to +20% in central, eastern and northern areas, with a best estimate of little change in the far north grading to around a 10% decrease in the south-west. The range of change in southern areas is from a 30% decrease to a 5% increase, with best estimate of around a 10% decrease. Seasonal changes are larger, with the projected decreases in the south-west up to 40%.

Later in the century, projected precipitation changes are larger and more dependent on the choice of emission scenario. The best estimates for annual precipitation changes in 2050 and 2070 (and 2030) for each emission scenario are shown in Figure 5.21. The seasonal results and 90th and 10th percentile values are included in Appendix A. The full range of change for annual precipitation in 2050 from the various scenarios is also depicted in Figure 5.22. Results for selected sites are in Appendix B.

2050

By 2050 under the B1 scenario the range of annual precipitation change is -15% to +7.5% in central, eastern and northern areas, with a best estimate of little change in the far north grading southwards to a decrease. The range of change in southern areas is from a 15% decrease to little change, with best estimate of around a 5% decrease. In summer and autumn the range in most regions is -15% to

+10%, with a best estimate of little change or slight decrease. In winter and spring, changes in the south-west range from decreases of 20% to little change with a best estimate of around a 10% decrease, in southern areas of the south-east of the continent they range from a decrease of 15% to little change with a best estimate of around 5%, and in eastern areas they range from a decrease of 15% to an increase of 7.5%, with a best estimate of a 5% decrease.

Under the A1FI scenario, changes in precipitation are larger. The range of annual precipitation change is -20% to +10% in central, eastern and northern areas, with a best estimate of little change in the far north grading to around a 7.5% decrease elsewhere. The range of change in southern areas is from a 20% decrease to little change, with best estimate of around a 7.5% decrease. In summer and autumn, the range in most regions is -20% to +15%, with a best estimate of little change or a 5% decrease. In winter and spring, changes in the south-west range from decreases of 30% to little change with a best estimate of around a 15% decrease, in southern areas of the south-east of the continent they range from a decrease of 20% to little change with a best estimate of around 10%, and in eastern areas they range from a decrease of 20% to a possible increase of 10%, with a best estimate of a 7.5% decrease.

2070

In 2070, larger precipitation changes are projected to occur. Those under the B1 scenario are comparable to those seen for 2050 under the A1FI scenario. Those under the A1FI scenario in 2070 are substantially larger. The range of annual precipitation change is -30% to +20% in central, eastern and northern areas, with a best estimate of little change in the far north grading to around a 10% decrease in the south. The range of change in southern areas is from a 30% decrease to 5% increase, with best estimate of around a 10% decrease. In summer and autumn, the range in most regions is -40% to +30%, with a best estimate of little change (in the east) or a decrease of up to 10%. In winter and spring, changes in the south-west range from decreases of more than 40% to little change with a best estimate of around a 20% decrease, in southern areas of the south-east of the continent they range from a decrease of 35% to little change with a best estimate of around 15%, and in eastern areas they range from a decrease of 40% to a possible increase of 15%, with a best estimate of a 15% decrease.

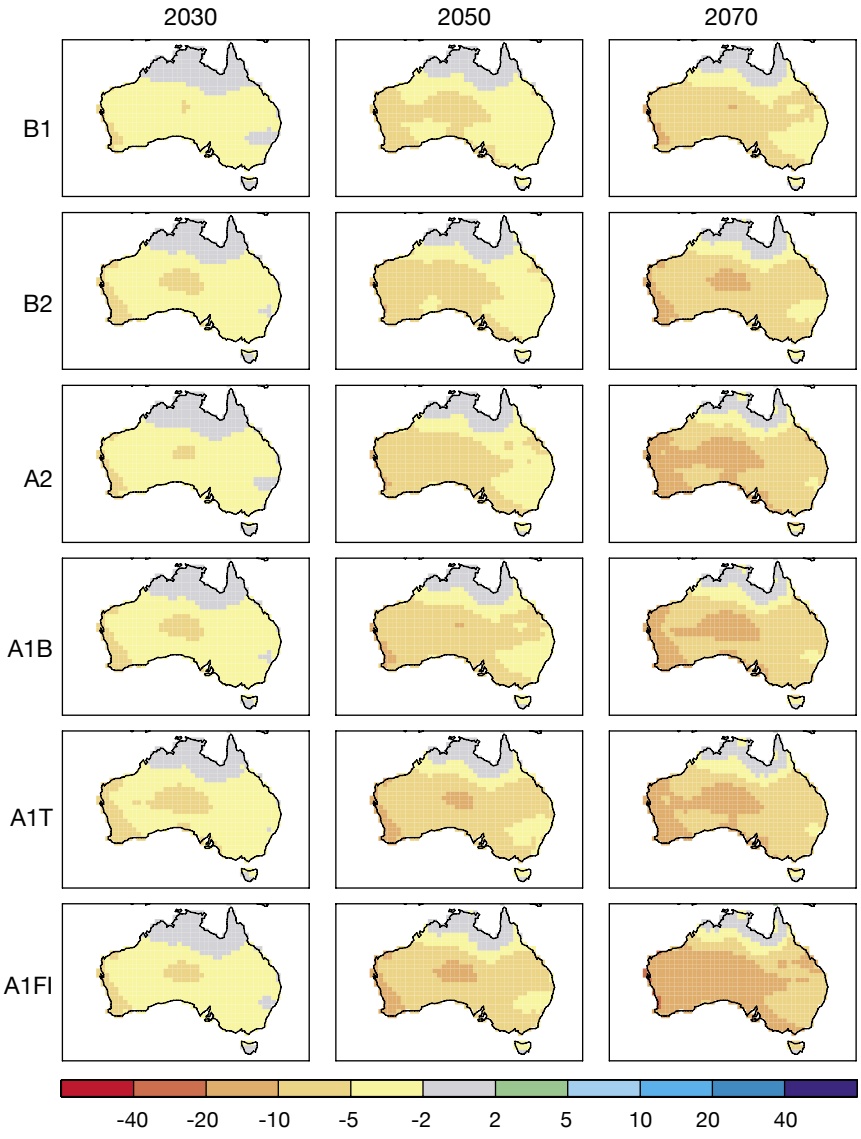

Figure 5.21: Best estimate (50th percentiles) of percentage change in annual precipitation, for 2030 (left column), 2050 (middle) and 2070 (right). Results for all six SRES scenarios are given.

The probability of exceeding selected thresholds, in percentage terms, can be determined directly from the cumulative distribution function (e.g. Figure 5.17, for Melbourne). An obvious threshold for precipitation change is zero, with the 'risk' of values below this (a decrease) being a statistic of interest for Australian water supplies. In Figure 5.23 this risk is shown for 2070 for each of the B1, A1B and A1FI emission scenarios. The risk is over 60% in the far south and south-west, but less than 40% in the north. Not surprisingly, the map largely matches the percentage of models with a decrease (compare with Figure 5.15c).

If a threshold other than zero is chosen, however, the cumulative distribution functions for net change must be calculated for each warming case. Figure 5.23 also shows results for thresholds of a decrease of 10% and 20%.

For the A1B case in 2070 (Figure 5.23), the risk of an annual precipitation decline of at least 10% is greater than 10% for most of Australia, and reaches 30% in the far south-west and centre. In the scenario with larger warming (A1FI) the risks are greater. The chance of a 20% decrease reaches 50% around Perth.

Figure 5.23 also shows the probability of an annual precipitation increase of at least 10%. This reaches 30% only in the far north under the A1FI scenario.

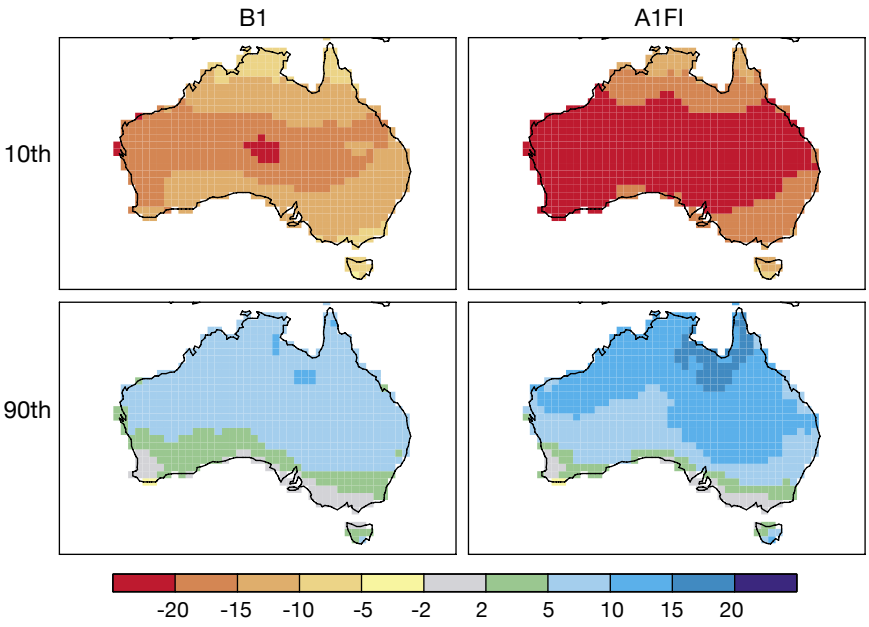

Figure 5.22: Range of change in annual precipitation (in percentage of 1961-1990) for 2050 for the B1 and A1FI scenarios from the 10th to 90th percentile values. (Note that the scale is modified from 5.21.)

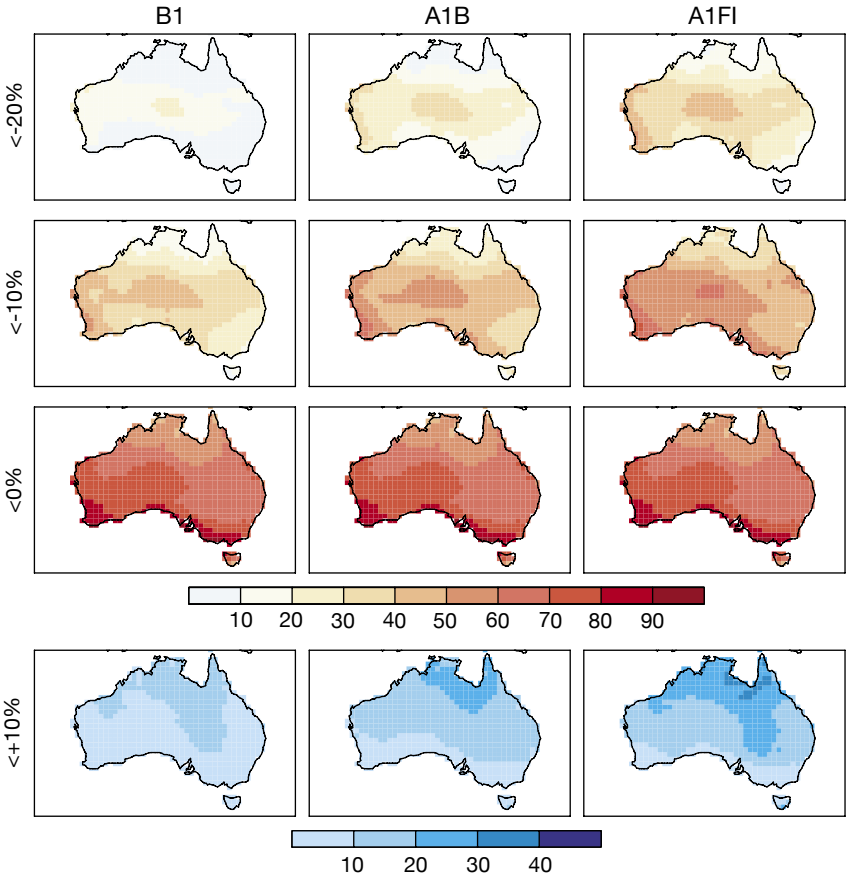

Figure 5.23: Risk (probability, in %) of annual mean precipitation in Australia decreasing by 2070 by at least 20% (first row), 10% (second row) and 0% (third row). The fourth row shows the probability of rainfall increases of at least 10%. The columns are emission scenarios B1 (left column), A1B (middle) and A1FI (right).

The spatial patterns of precipitation change are similar in key aspects to that in the previous projections (CSIRO 2001). The spatial patterns in winter and spring are very similar, with both projections showing marked decreases in the south and east, with these strengthening from winter into spring. There remains considerable uncertainty over the direction of summer rainfall change in many areas, although in the current projections, a small tendency for summer increase is now more localised in eastern Australia than in CSIRO (2001). Overall, there is stronger bias to precipitation decrease in the current projections, with this being most evident in autumn and in the annual average. These differences in pattern are primarily due to the use of a new set of models rather than the new PDF and model weighting methods, since the differences are also evident when the new set of models are analysed using the methods of CSIRO (2001) (Suppiah *et al*. 2007). Quantitative ranges of uncertainty are difficult to compare, but in many cases appear to have narrowed from CSIRO (2001). For example, winter and spring ranges of change in the south-west do not include the possibility of any significant increase, whereas those in CSIRO (2001) did. Changes in the range of uncertainty will be affected by the use of a larger set of models, but the new methods will also have had an impact (see equivalent discussion for temperature in section 5.1.3).

5.2.4 Local variations to projected change

As for temperature, statistical downscaling studies have shown that projected precipitation change can vary significantly at fine spatial scales, particularly in coastal and mountainous areas.

As discussed earlier, sub-grid heterogeneity can be important, in particular for precipitation which has high spatial variability. The same statistical downscaling technique described in section 5.1.4 was used for precipitation and applied to the same subset of CMIP3 models. This result was illustrated for the south-west of Western Australia which has suffered one of the

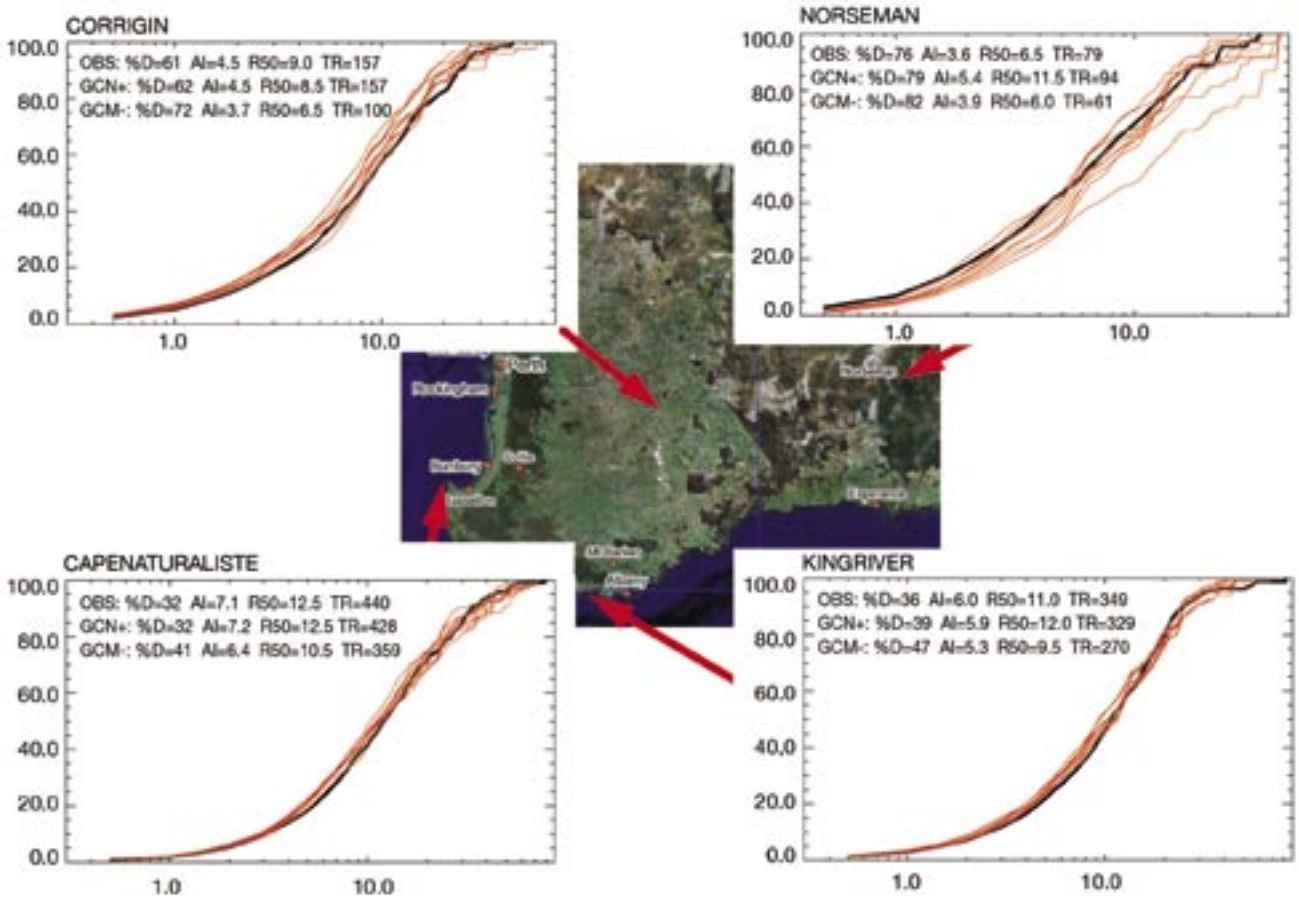

Figure 5.24: Projected changes in the observed cumulative probability distributions of precipitation in winter for 2050 (using emission scenario A2) in four locations in the south-west of Western Australia, with contrasting climate: Cape Naturaliste (along the west coast), King River (along the south coast), Corrigin (in the heart of the wheat belt) and Norseman (further inland). Observations are shown as a thick black line, based on the 1970 to 1989 period. Ten individual climate models from the CMIP3 database are shown as red lines. The x-axis in mm uses a logarithmic scale while the y-axis is expressed in percent. Some statistics extracted from the cumulative distribution are provided for the current climate (first line in each insert) and for the range of future projections (largest precipitation on the second line and smallest precipitation on the third line). The meaning of each statistic is discussed in the text.

worst precipitation declines in recent history (Ryan and Hope 2005, 2006).

Projections based on the A2 scenario for winter precipitation (Figure 5.24) indicate a reduction in the total precipitation (TR on the graphs) alongside a reduction in the average precipitation intensity (AI), a reduction of the precipitation intensity for the middle of the distribution (R50) and an increase in the percentage of dry days (%D). There is a high level of consistency amongst models. All suggest a total precipitation decline in south-western Australia from the coast (between 3% and 22% in Cape Naturaliste and King River) to the inland wheat belt (between 0% and 36% in Corrigin). However, further inland (Norseman) the precipitation is slightly more likely to increase (as projected by six models) than decrease (projected by only four models). This difference between the south-west corner and further inland is consistent with the projections shown earlier, but with a sharper contrast. Thus, as for temperature, statistical downscaling has the ability to show additional detail consistent with the broad picture provided by global climate models directly.

5.2.5 Daily precipitation intensity, frequency of dry days and extreme precipitation

An increase in daily precipitation intensity (rain per rain-day) and the number of dry days is likely. Extreme daily precipitation (highest 1%) tends to increase in the north and decrease in the south with widespread increases in summer and autumn, but not in the south in winter and spring when there is a strong decrease in mean precipitation.

As well as changes to average precipitation, the character of daily rainfall may change, e.g. the frequency of wet days (or dry days), precipitation intensity (rain per rain-day) and the intensity of extreme precipitation. Changes to extreme events would have the potential to increase erosion and flood frequency, with implications for agriculture, forestry, river flow, water quality, insurance risk and the design standards of bridges, roads, dams, storm-water and other infrastructure.

In this section we examine projections for changes in precipitation intensity and dry day frequency using standard indices prepared by modelling groups for inclusion in the CMIP3 data archive. Following the definition of Frich *et al*. (2002), precipitation intensity is annual total precipitation divided by the number of wet days (days with more than 1 mm), and the number of dry days is the number of days with less than 1 mm of precipitation. Extreme precipitation is considered through explicit analysis of daily model output (see later in this section).

Changes in precipitation intensity and dry days are shown in Figures 5.25 and 5.26, respectively. Both of these indices show strong increases in Australia over the 21st century, suggesting that the future precipitation regime will have longer dry spells interrupted by heavier precipitation events. Much larger increases are found over Australia than globally, more than 50% larger for both indices.

The 99th percentile of daily precipitation is an indicator of more extreme precipitation intensity, representing the highest 1% of precipitation events. For each season and each grid point, the 99th percentile daily value was computed for two 20-year periods (1981-2000 and 2046-2065) for 15 climate models for the A1B scenario (no other data were available). Patterns

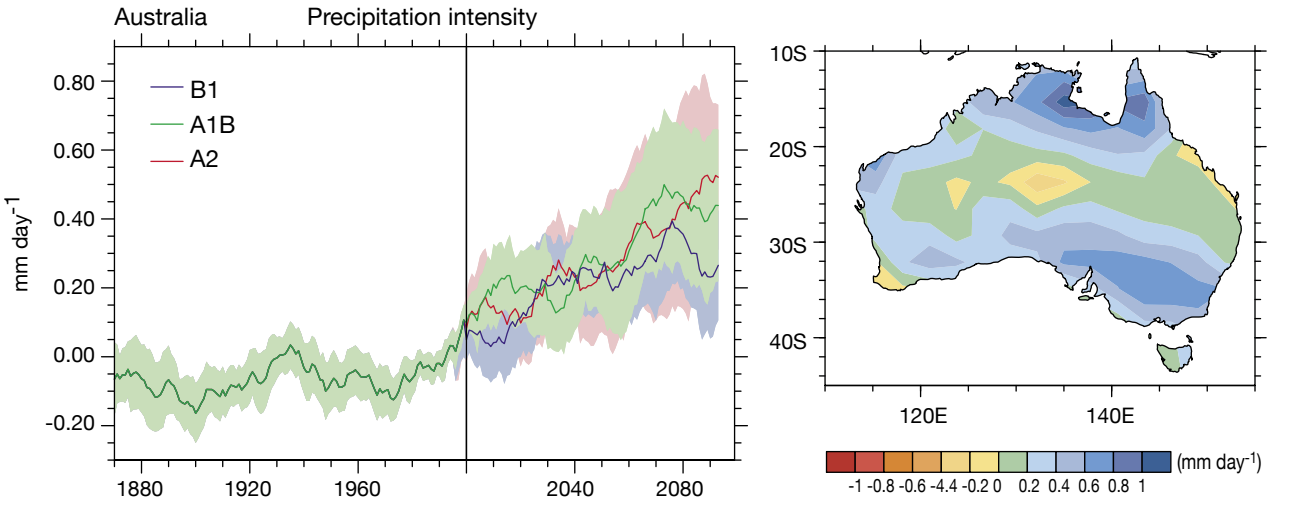

Figure 5.25: Area average time series of the change in precipitation intensity (kg m-^{2}s-^{1}) over Australia from the CMIP3 multi-model dataset (left panel). The mean (solid lines) of nine models is shown for the SRES B1, A1B and A2 scenarios, with shading representing intermodel uncertainty. The right panel gives mean projected changes (2080-2099 minus 1980-1999) in precipitation intensity (mm/day) for the A1B scenario. (After Tebaldi *et al*. 2006.)

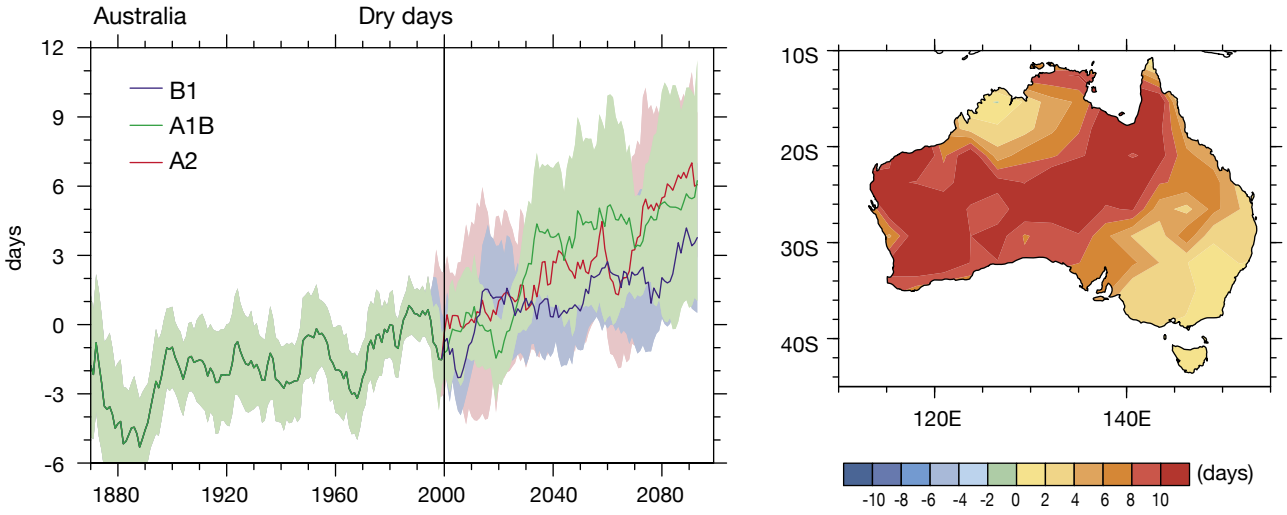

Figure 5.26: Area average time series of the change in the number of dry days over Australia from the CMIP3 multi-model dataset (left panel). The mean (solid lines) of nine models is shown for the SRES B1, A1B and A2 scenarios, with shading representing inter-model uncertainty. The right panel gives mean projected changes (2080-2099 minus 1980-1999) in dry days for the A1B scenario. (After Tebaldi *et al*. 2006.)

of regional change per degree of global warming were calculated, and median changes were computed empirically (the eighth highest value at each grid point).

Figure 5.27 shows the percentage changes in annual average and seasonal average 99th percentile daily precipitation intensity. For comparison the corresponding change in median annual and seasonal precipitation is also given. Annually and in all seasons there are significant areas showing increases in extreme precipitation intensity, particularly in summer and autumn. Increases in extreme precipitation are much more common than increases in mean precipitation (which mostly decreases). Decreases in extreme values tend to occur where there is a strong decrease in mean precipitation, such as south-west Australia in winter. These results show a tendency for extremes to become more intense, except where mean precipitation declines substantially.

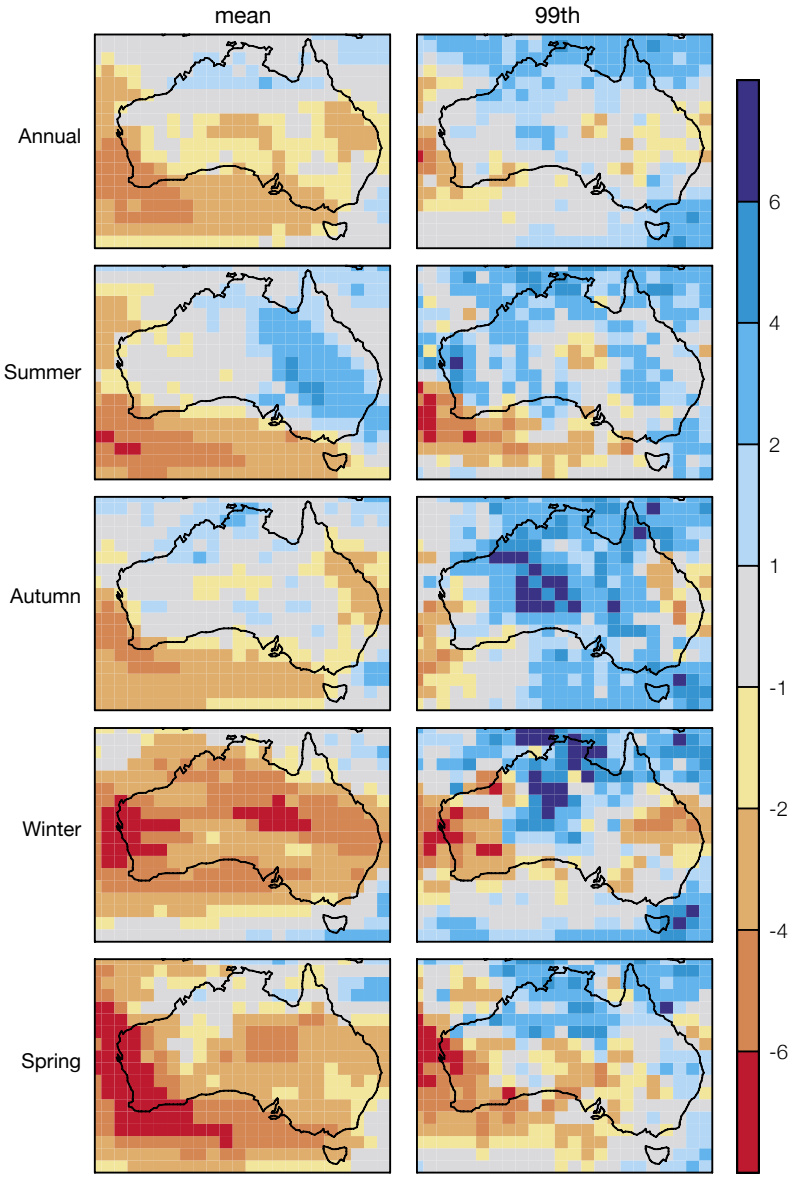

Figure 5.27: Percentage changes in annual average and seasonal average mean rainfall (left column) and 99th percentile daily precipitation intensity (right column) in 2050 under the A1B emission scenario for the median of 15 models.

5.2.6 Snow

Snow area, depth and duration are likely to decline.

Simulations of future snow conditions in the Australian mainland alpine regions were prepared for the years 2020 and 2050, based on temperature and precipitation change projections published by CSIRO in 2001, using a climate-driven snow model (Hennessy *et al*. 2003). Two scenarios were considered. The low impact scenario used the lowest projected warming combined with the highest estimate of increased precipitation. The high impact scenario used the highest projected warming with the highest estimate of decreased precipitation (Table 5.5). Results are not available for the projected changes in temperature and precipitation given in sections 5.1.2, 5.1.3, 5.2.2 and 5.2.3, but the scenarios used are broadly consistent with these, although the range in warming for 2050 is slightly broader than would be indicated the current projections.

The results can also be presented in terms of snow depth and/or snow duration for nominated locations (Table 5.6). At all sites, the low impact scenario for 2020 only has a minor impact on snow conditions. Average season lengths are reduced by around five days. Reductions in peak depths are usually less than 10%, but can be larger at low elevation sites (e.g. Mt Baw Baw and Wellington High Plains). The high impact scenario for 2020 leads to reductions of 30-40 days in average season lengths. At higher sites such as Mt Hotham, this can represent reductions in season duration of about 25%, but at lower sites such as Mt Baw Baw the reduction can be more significant (up to 60%). Impacts on peak depth follow a similar pattern: moderate impacts at higher elevation sites, large impacts at lower elevation sites. There is also a tendency for the time of maximum snow depth to occur earlier in the season under warmer conditions, e.g. about 20 days earlier at Mt Thredbo under the high impact scenario.

Table 5.5: Projected changes in alpine temperature, precipitation and snow cover for 2020 and 2050, relative to 1990. (Source: Hennessy *et al*. 2003.)

	Projected change in temperature (ºC)	Projected change in precipitation (%)	Area with at least one day snow cover (%)	Area with at least 30 days snow cover (%)	Area with at least 60 days snow cover (%)
Low impact (2020)	+0.2	+0.9	-10	-14	-18
High Impact (2020)	+1.0	-8.3	-39	-54	-60
Low impact (2050)	+0.6	+2.3	-22	-30	-38
High impact (2050)	+2.9	-24.0	-85	-93	-96

Table 5.6: Simulated average duration (days) of at least 1 cm of snow cover at selected ski resorts (some with results for low, mid and high elevations) and sites of biological significance.

Site (elevation)	Present	2020	2050
Lake Mountain (1,400 m)	74	30-66	1-48
Mt Baw Baw (1,560 m)	80	32-71	1-53
Mt Buller low (1,383 m)	33	7-25	0-15
Mt Buller mid (1,560 m)	76	36-67	1-56
Mt Buller high (1,740 m)	108	70-102	7-89
Mt Buffalo low (1,477 m)	70	29-63	0-50
Mt Buffalo mid (1,516 m)	80	39-73	1-59
Mt Buffalo high (1,723 m)	113	78-108	10-96
Mt Wellington High plains (1,560 m)	82	38-75	2-59
Mt Nelse (1,829 m)	133	101-128	27-117
Falls Creek low (1,504 m)	77	41-71	2-59
Falls Creek mid (1,643 m)	105	68-99	8-87
Falls Creek high (1,797 m)	125	92-120	18-108

Site (elevation)	Present	2020	2050
Mt Hotham low (1,400 m)	51	15-44	0-29
Mt Hotham mid (1,650 m)	98	59-92	4-77
Mt Hotham high (1,882 m)	129	97-124	21-114
Mt Perisher low (1,605 m)	90	53-87	4-69
Mt Perisher mid (1,835 m)	131	100-125	30-115
Mt Perisher high (2,021 m)	151	122-146	56-136
Mt Thredbo low (1,350 m)	32	8-26	0-17
Mt Thredbo mid (1,715 m)	113	80-108	13-97
Mt Thredbo high (2,023 m)	153	122-148	56-138
Mt Selwyn (1,604 m)	81	43-74	3-60
Whites River Valley (1,746 m)	118	88-113	18-103
Mt Jagungal (2,061 m)	156	128-151	65-141
Mt Kosciuszko (2,228 m)	183	153-178	96-169

5.3 Solar radiation, relative humidity and potential evaporation

5.3.1 Solar radiation

Projections of solar radiation change generally show little change, although a tendency for increase in southern areas of Australia is evident, particularly in winter and spring. The projected range of change is typically -1% to +2% in 2030. The magnitude of changes is larger in 2050 and 2070, particularly under the higher emission scenarios.

Changes in solar radiation would have impacts on a range of sectors, e.g. agriculture and livestock, forestry, ecosystems, human health, and building design and degradation. Solar radiation data are available from the CMIP3 archive for 20 different climate models. Best estimate annual results for each emission scenario in 2030, 2050 and 2070 are given in Figure 5.28 with the corresponding 10th and 90th percentile results given in Figure 5.29. Site-specific results are given in Appendix B. Seasonal results are available at www.climatechangeinaustralia.gov.au.

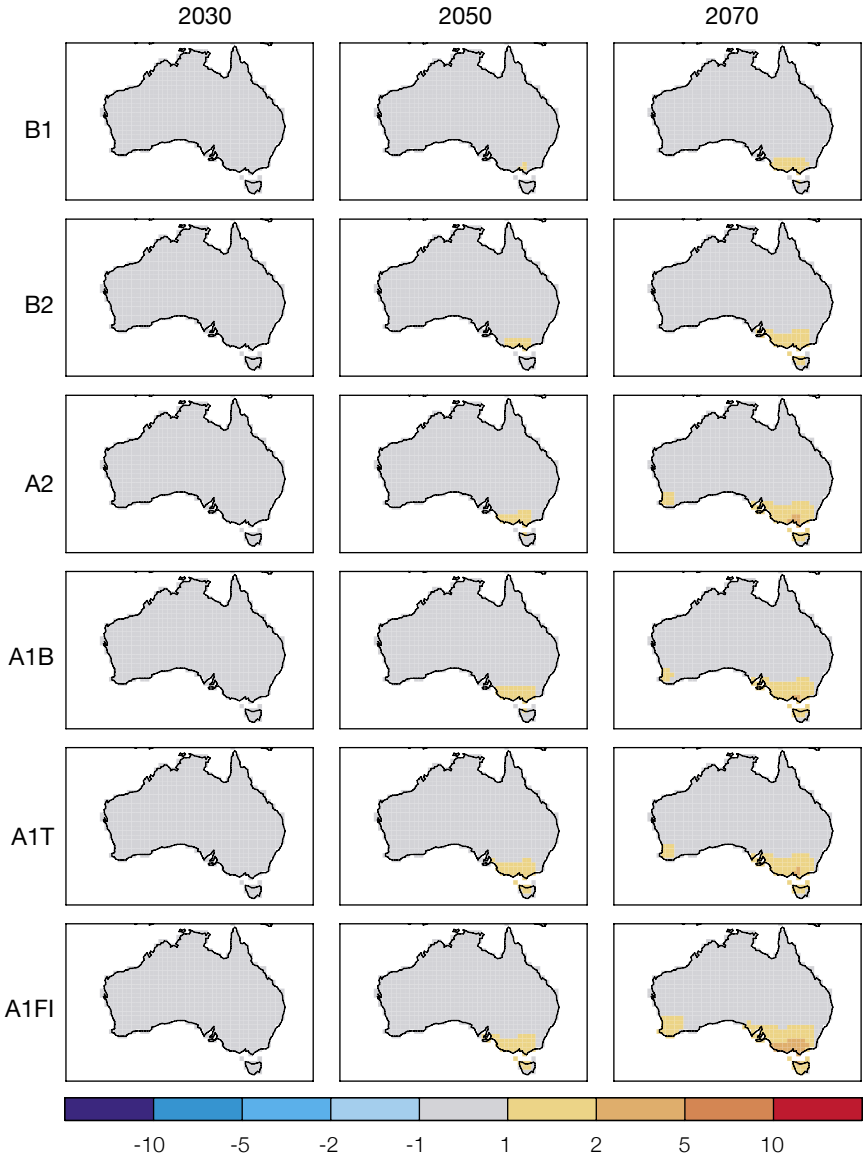

Figure 5.28: Annual changes in median (50th percentile) solar radiation (%) for 2030, 2050 and 2070, relative to 1990, for six emission scenarios, based on 20 climate models.

Best estimate annual radiation changes are small (±1%) over most of Australia by 2030, 2050 and 2070, regardless of emission scenario. The only exception is the increase of 1-2% over Victoria by 2050, and over both south-west Australia and Victoria by 2070 (Figure 5.28) under A1FI. Such increases are consistent with the decreases in precipitation that are projected for these regions. The 10th to 90th percentile range of uncertainty (Figure 5.29) in the south and west is -1% to +2% by 2030 and -2% to +4% by 2050 and -3% to +6% by 2070 allowing for emission scenario uncertainty. The uncertainty range is slightly smaller along the south coast and Tasmania, and slightly larger in the north and east.

Summer changes are very similar to the annual patterns except for a tendency for increases along the north coast. Autumn changes are small over the whole continent out to 2070. Winter increases over southern Australia reach 2% to 6% for A1FI by 2070. Spring changes are similar to the annual patterns, with increases of 2% to 5% extending up the east coast by 2070.

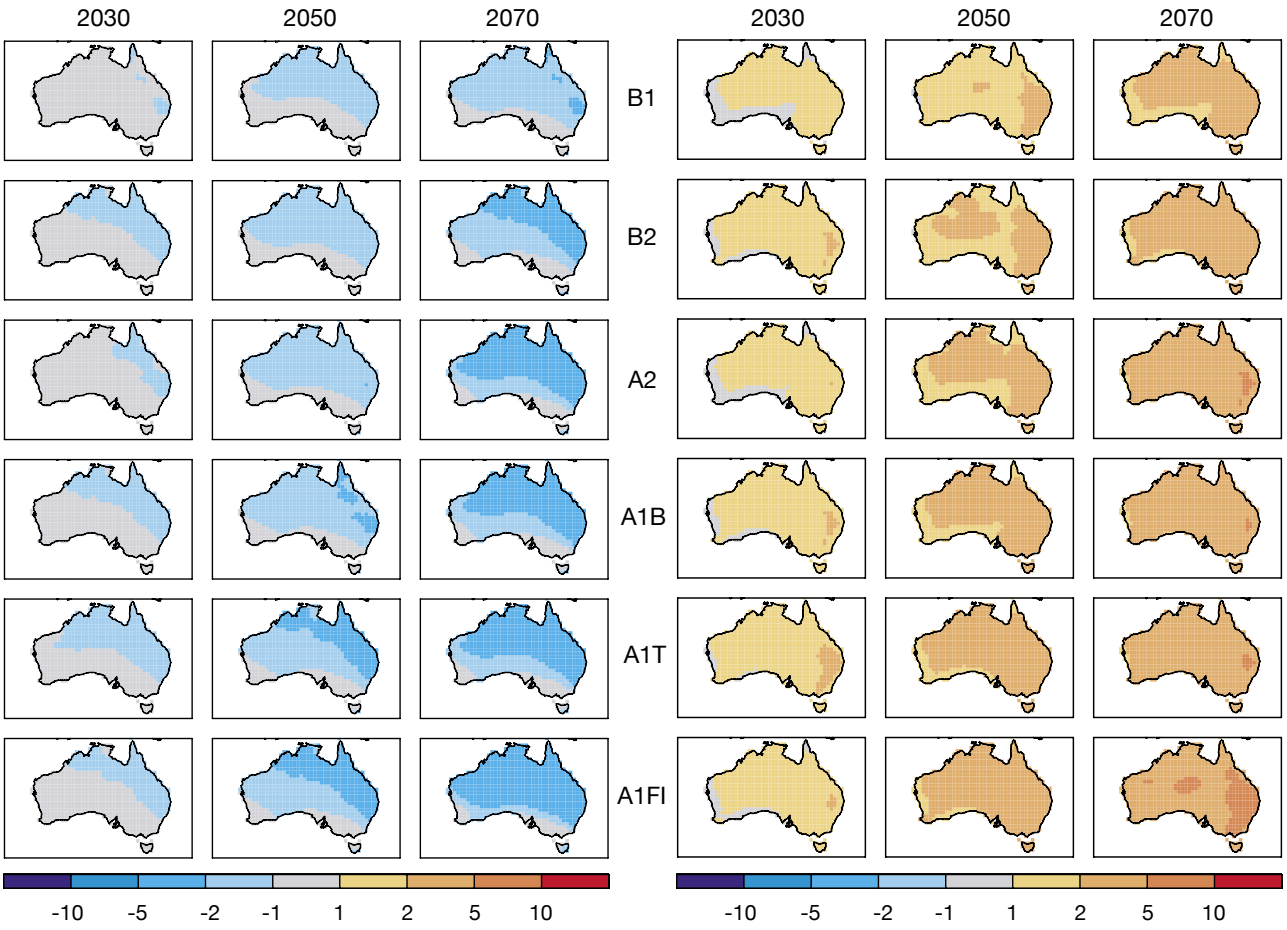

Figure 5.29: 10th percentile (left) and 90th percentile (right) annual changes in solar radiation (%) for 2030, 2050 and 2070, relative to 1990, for six emission scenarios, based on 20 climate models.

5.3.2 Relative humidity

Small decreases in relative humidity are projected over most of Australia. The range of change in annual humidity by 2030 is around -2% to +0.5% with the best estimate being a 1% decline. The projected changes are larger for 2050 and 2070, particularly under the higher emission scenarios.

Changes in relative humidity would have implications for evaporation rates, agriculture, building design, and human comfort and health. Relative humidity data are available from the CMIP3 archive for 14 different climate models. Best estimate annual results for each scenario and 2030, 2050 and 2070 are given in Figure 5.30 with the corresponding 10th and 90th percentile results given in Figure 5.31. Site-specific results are given in Appendix B. Seasonal results are available at www.climatechangeinaustralia.gov.au

Annual humidity tends to decrease over Australia, with largest decreases in the south and west, and little change along the east coast and in Tasmania (Figure 5.30). This pattern is broadly consistent with that of precipitation change (Figure 5.21). By 2030, there is little difference between the emission scenarios, with decreases of up to 1% in the south and west. By 2050, the B1 and B2 scenarios have much weaker patterns of change than A1T, A1B and A1FI, with decreases of up to 2% in the south and west. By 2070, the difference between emission scenarios is much greater: B1 gives decreases of up to 1% in the north and east, and 1-2% in the south and west, while A1FI gives decreases of 1-2% in the north and east and 2-4% in the south and west.

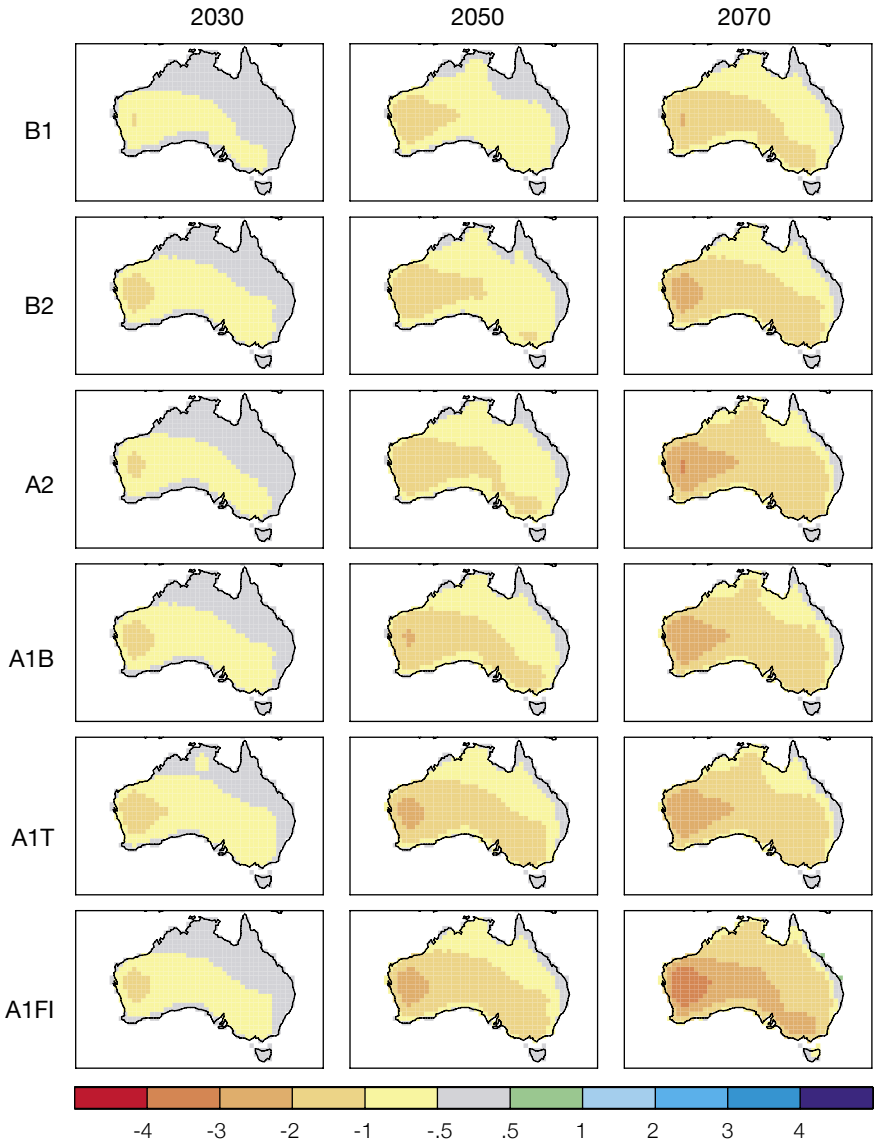

Figure 5.30: Median (50th percentile) annual changes in relative humidity (%) for 2030, 2050 and 2070, relative to 1990, for six emission scenarios, based on 14 climate models.

The 10th to 90th percentile range of uncertainty over most of Australia is -2% to +0.5% by 2030, -3% to +0.5% by 2050 and -5% to +2% by 2070 for the A1B scenario (Fig 5.31). Slightly smaller changes occur for B1 in 2050 and 2070 and larger changes for A1FI. Largest decreases occur in winter and spring (Figure 5.32).

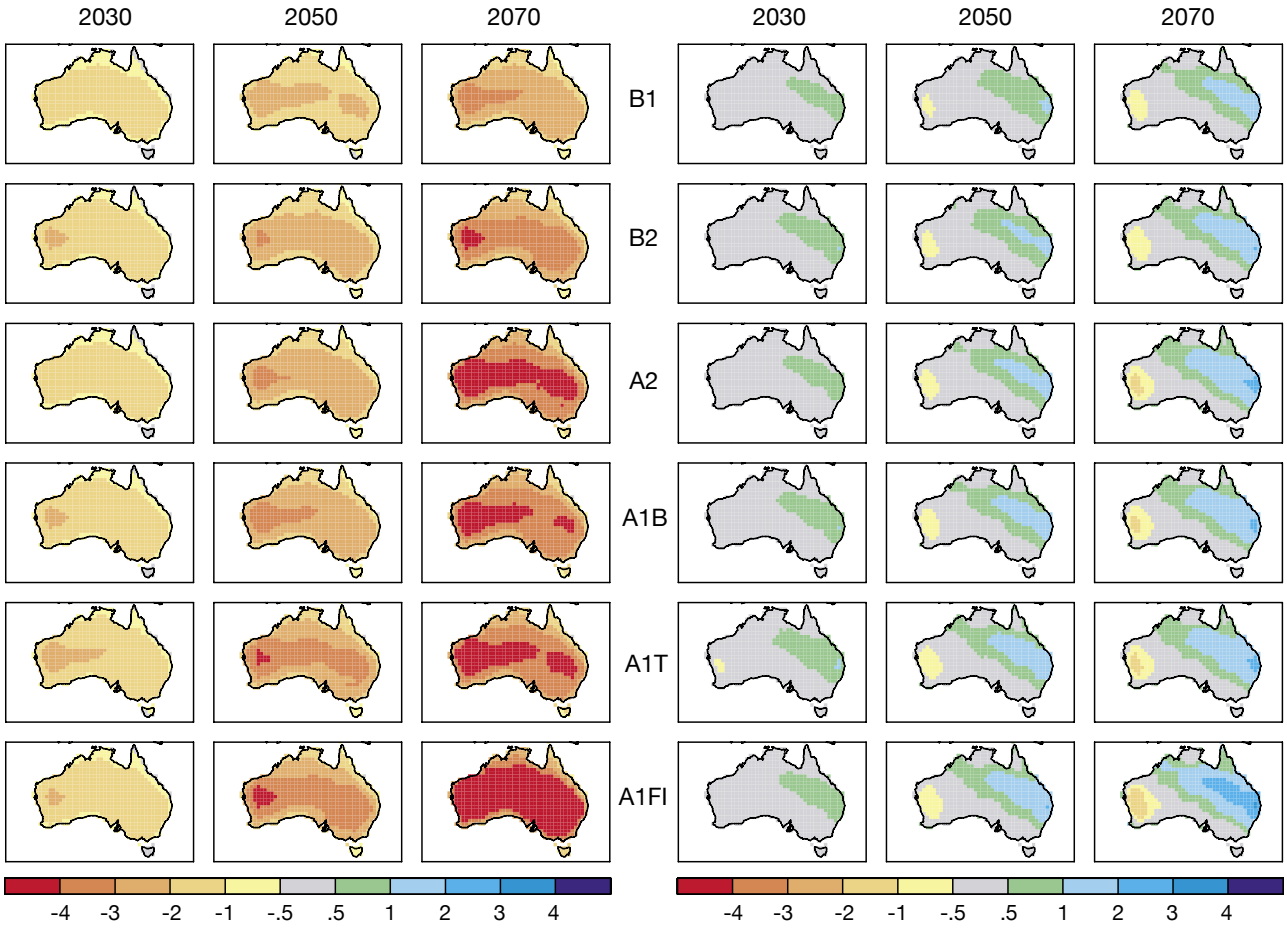

Figure 5.31: 10th (left) and 90th (right) percentile annual changes in relative humidity (%) for 2030, 2050 and 2070, relative to 1990, for six emission scenarios, based on 14 climate models.

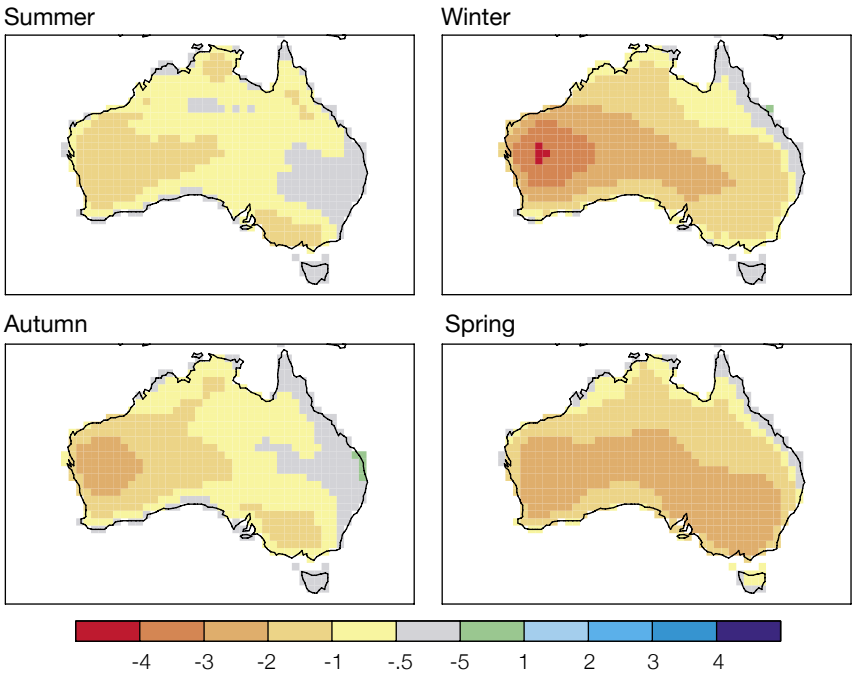

Figure 5.32: Seasonal changes in best estimate (50th percentile) relative humidity (%) by 2070, relative to 1990, based on 14 climate models, in summer, autumn, winter and spring.

5.3.3 Potential evapotranspiration

Simulated annual potential evapotranspiration increases over Australia. Largest increases are in the north and east, where the change by 2030 ranges from little change to a 6% increase, with the best estimate being a 2% increase. By 2070, the B1 scenario gives increases of 0 to 6% (best estimate around 3%) in the south and west and 2% to 8% (best estimate around 6%) in the north and east, while the A1FI scenario gives increases of 2% to 10% (best estimate of around 6%) in the south and west and 6% to 16% (best estimate around 10%) in the north and east.

Evapotranspiration is the combination of evaporation of water from soil and transpiration from vegetation, and is a key driver of the hydrological cycle. Potential evapotranspiration is that which occurs from a saturated surface, given specified atmospheric conditions, and thus gives a measure of maximum possible evapotranspiration under those conditions. Potential evapotranspiration differs significantly from pan evaporation (see Box 5.1).

Many models are available to estimate evapotranspiration. For this report, potential evapotranspiration is calculated using the Complementary Relationship Areal Evaporation model (Morton 1983). This method has been used in constructing Australia's current evaporation climatology (Bureau of Meteorology 2001) and in estimating projections of future climate change (Walsh *et al*. 2000). Changes in potential evapotranspiration were calculated from the 14 climate models that provide the required input data – air temperature, relative humidity and downward solar radiation at the surface. The Morton (1983) model does not require input of wind speed data. As a substitute, it calculates evapotranspiration using a vapour transfer coefficient which is dependent on atmospheric pressure but not on wind speed. This approach generates a near-zero mean annual closure error (Hobbins *et al*. 2001), thereby supporting Morton's parameterisation of the wind function.

Box 5.1 Pan evaporation and potential evapotranspiration

The decreasing trend in pan evaporation over recent decades in several countries seems contrary to projected trends in global climate model-based estimates of potential evapotranspiration (Hobbins *et al*. 2004). This was called the pan evaporation 'paradox' (e.g. Roderick and Farquhar 2002).

Unlike pan evaporation, which measures the quantity of water evaporated from a *small* open water surface, the potential evapotranspiration reported here represents the evapotranspiration (from soil, vegetation, and water surfaces) that would occur when moisture supply was not limited over a large area. The two measures are related, but pan evaporation is not a direct measure of potential evapotranspiration, and vice versa, since their relationships are dependent upon the type of environment in which they were measured (Kirono *et al.* 2007).

It has already been noted that high-quality pan evaporation data averaged over 60 Australian sites from 1970 to 2005 show a decline of 2.5 mm/yr^2 which is not statistically significant (Chapter 2; Jovanovich *et al*. 2007). An independent study based on high-quality data from 28 Australian sites from 1970 to 2004 found that potential evapotranspiration averaged over the dry sites (annual precipitation < 400 mm) and over the wet sites (annual precipitation > 400 mm) *increased* by 1.4 and 2.1 mm/yr^2, respectively (Kirono *et al*. 2007). The increasing trends in observed potential evapotranspiration are not statistically significant but consistent with the projected increases simulated by climate models.

Best estimate annual projections for potential evapotranspiration for each scenario and 2030, 2050 and 2070 are given in Figure 5.33 with the corresponding 10th and 90th percentile results given in Figure 5.34. Seasonal best estimate results are given in Figure 5.35. Site-specific results are given in Appendix B.

Simulated annual potential evapotranspiration increases over Australia, with largest increases in the north and east (Figure 5.33). By 2030, changes in the north and east typically vary from little change up to 6% increase, with best estimate values of around a 3% increase. Changes are weaker in the south-west. The increases are largest in winter in the south (Figure 5.35).

By 2050, the effect of the emission scenario is more evident. Under the B1 and B2 scenarios, changes are only slightly stronger than in 2030, but under the A1T, A1B and A1FI scenarios the range of increase in the north and east is 3 to 8% (best estimate around 6%), and in the south and west 0 to 6% (best estimate around 3%). By 2070, the difference between emission scenarios is greater still: B1 gives increases of 0 to 6% (best estimate around 3%) in the south and west and 2 to 8% (best estimate around 6%) in the north and east, while A1FI gives increases of 2 to 10% (best estimate of around 6%) in the south and west and 6 to 16% (best estimate around 10%) in the north and east.

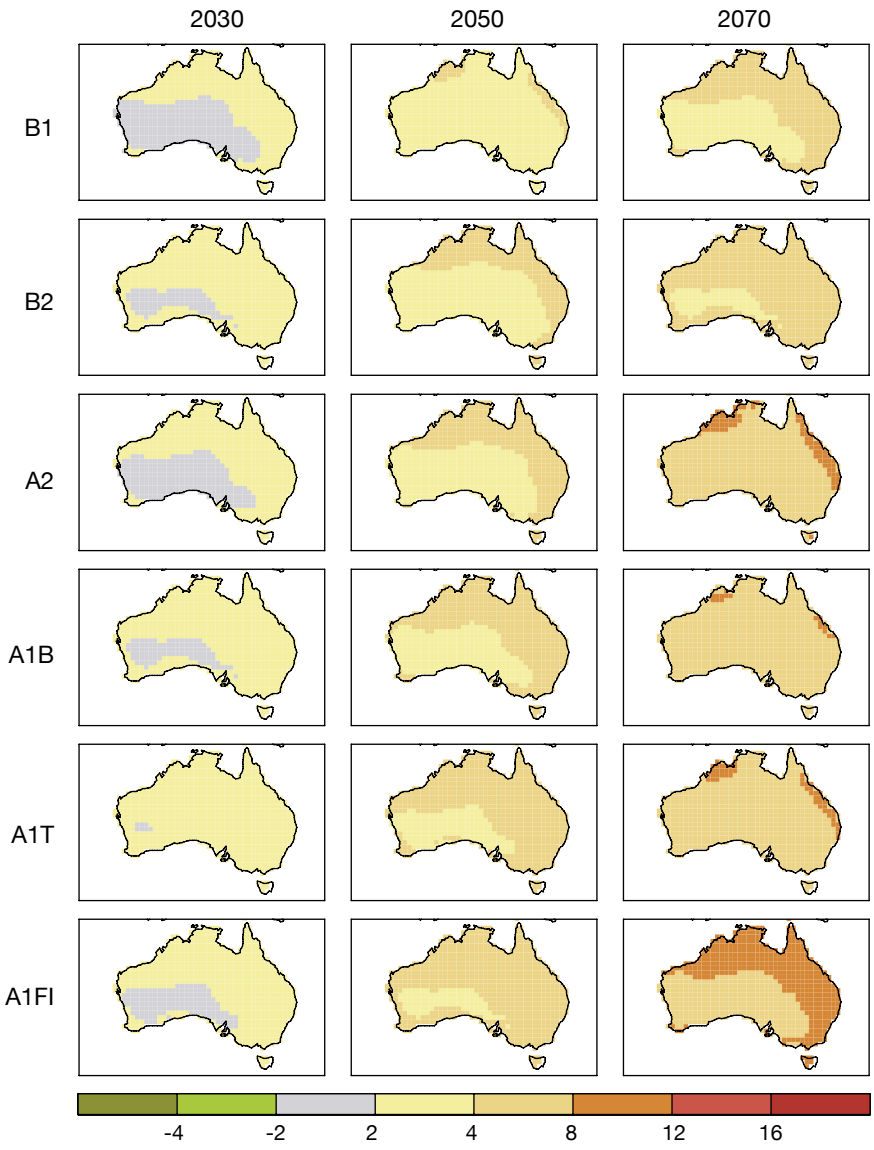

Figure 5.33: Median (50th percentile) changes in annual potential evapotranspiration in 2030, 2050 and 2070, relative to 1990, for six SRES emission scenarios, based on 14 models.

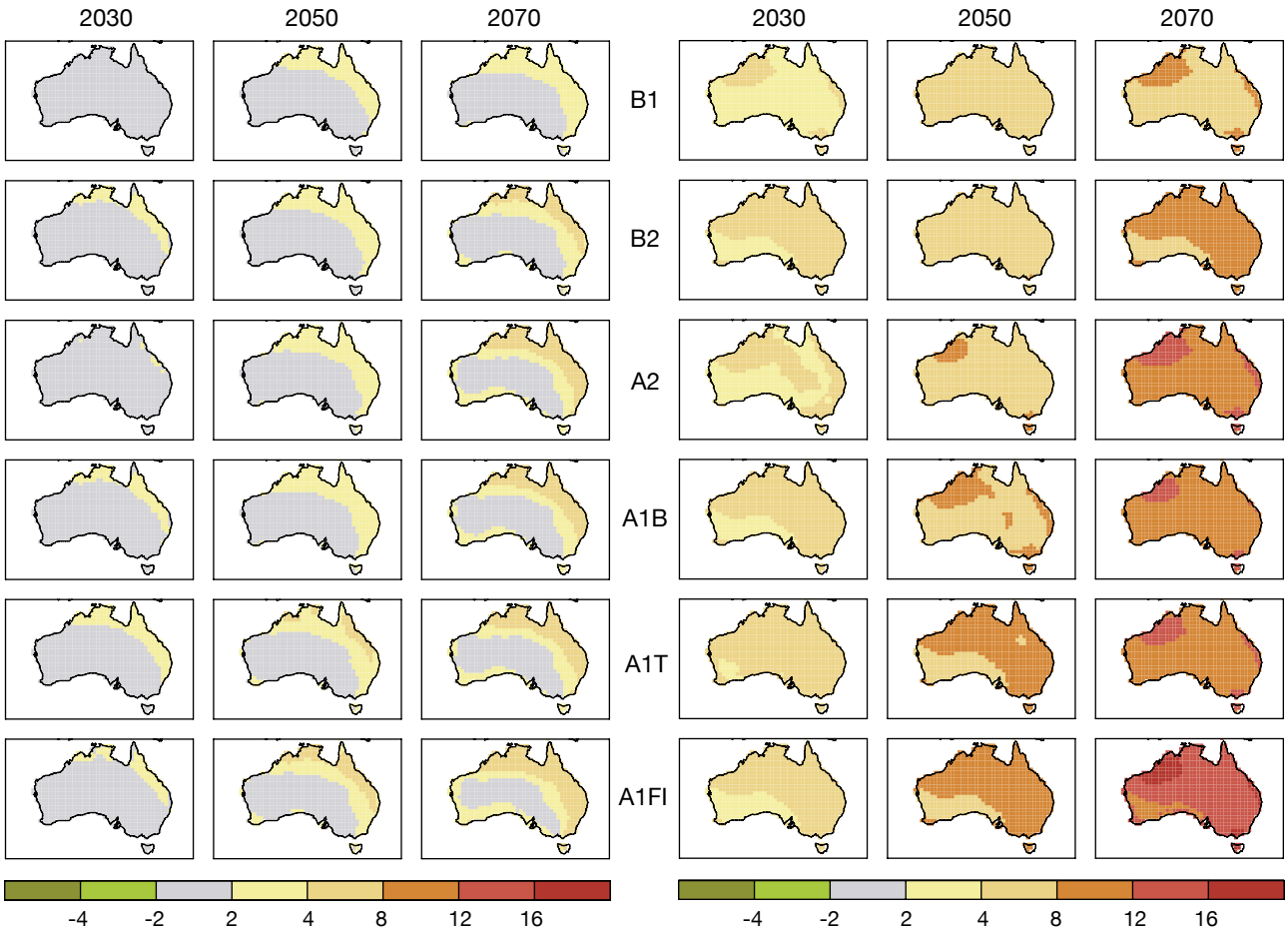

Figure 5.34: 10th (left) and 90th (right) percentile changes in annual potential evapotranspiration in 2030, 2050 and 2070, relative to 1990, for six SRES emission scenarios, based on 14 models.

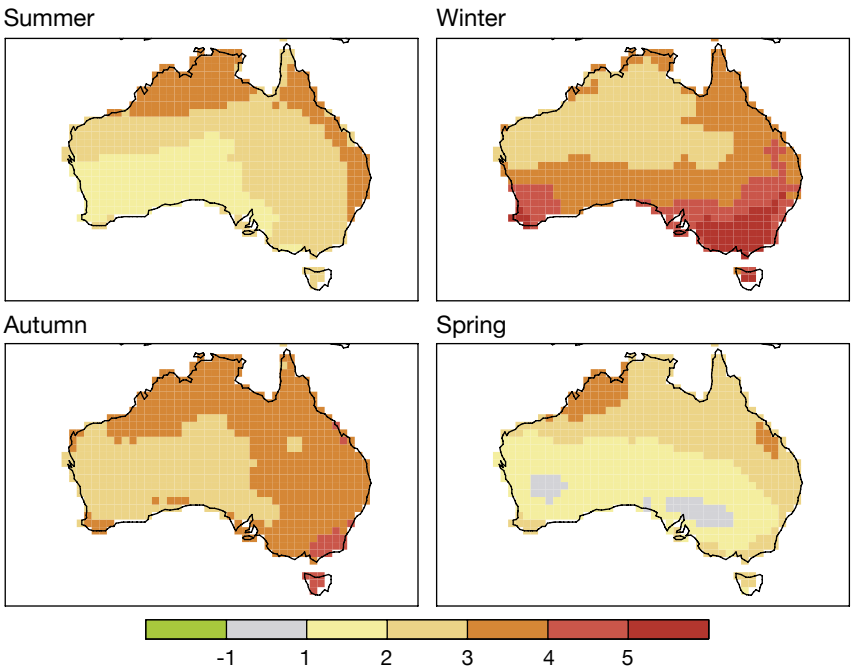

Figure 5.35: Changes in median (50th percentile) potential evapotranspiration (%) by 2030, relative to 1990 under the A1B emission scenario, based on 14 climate models in summer, autumn, winter and spring.

5.4 Drought

Drought occurrence is projected to increase over most of Australia, but particularly in south-western Australia.

In Australia, the droughts of 1982-1983, 1991-1995 and 2002-2003 cost A$3 billion, A$5 billion and A$10 billion, respectively (Adams *et al*. 2002; Bureau of Meteorology 2006a). The total drought assistance provided by the Government to farmers and communities from 2001 to 2006 exceeded A$2.3 billion (DAFF 2006).

Droughts can be grouped into four types (AMS 1997):

1. **Meteorological drought:** A period of months to years when atmospheric conditions result in low rainfall. This can be exacerbated by high temperatures and evaporation, low humidity and desiccating winds.
2. **Agricultural drought:** Changes in the seasonal temperatures and/or the distribution or amount of rainfall that constrain agricultural production.
3. **Hydrological drought:** Prolonged moisture deficits that affect surface or subsurface water supply, thereby reducing streamflow, groundwater, dam and lake levels. This may persist long after a meteorological drought has ended.
4. **Socio-economic drought:** The effect of drought on the productivity and profitability of businesses, and resulting impacts on incomes, employment and social well being.

A drought index based on rainfall deficiency alone would fail to account for the effect of projected increases in potential evaporation, and the interaction between rainfall and the moisture holding capacity of soils. Hence, we have assessed projected changes in agricultural drought. While there have been no Australian studies of the impact of climate change on hydrological or socio-economic drought, there have been a number of Australian studies assessing socio-economic aspects of climate variability and drought (Nelson and Kokic 2004; Kokic *et al*. 2007; Nelson *et al*. 2005).

For this report, soil moisture deficit was calculated using a soil moisture balance model (Jones *et al*. 2001) driven by daily inputs of rainfall and potential evaporation from the Queensland Department of Primary Industries database (http://silo.eoc.csiro.au/) on a 25 km grid over Australia (Mpelasoka *et al*. 2007). The soil moisture capacity was specified as 150 mm; that is, when the soil moisture reaches 150 mm, excess moisture becomes run-off. (Of course, soil moisture capacity across Australia ranges from around 50 mm to 300 mm, and the effect of this variation is being included in a new drought study using output from three CMIP3 climate models. An alternative approach would be to calculate soil moisture using the Aussie Grass model (Carter *et al*. 2000), which includes the effect of carbon dioxide fertilization on vegetation). The accumulated monthly soil moisture deficit is the amount of moisture needed to return the soil to its full capacity at the end of each month. For example, if the accumulated January soil moisture is 100 mm, the deficit is 50 mm.

Agricultural drought was defined as a period of extremely low soil moisture. The start and end dates were based on the Bureau of Meteorology decile definitions for starting and ending a meteorological drought. Hence, agricultural drought was identified by examining 3-month periods to see whether they lie below the first decile (lowest 10% on record). Once a 3-month period was classified as a drought, it remained in the drought category until the deficiency was removed. Drought was considered removed if the soil moisture for the past three months was above the seventh decile (highest 30% on record).

Drought projections were based on simulated changes in rainfall and potential evaporation from the Canadian (CCCma1) and CSIRO (Mark 2) global climate models. These models simulate mainly annual rainfall decreases within the range of CMIP3 models. The projections were applied to observed daily data from 1974 to 2003. The IPCC (2001) low and high climate global warming values for the SRES emission scenarios allowed results from the models to be scaled for the years 2030 and 2070. Projections based on the IPCC (2007a) range of global warming are not available. The simulations show up to 20% more drought-months over most of Australia by 2030, with up to 40% more droughts by 2070 in eastern Australia, and up to 80% more in south-western Australia (Mpelasoka *et al*. 2007).

In a separate study carried out by researchers in the United Kingdom, projected changes in the Palmer Drought Severity Index (PDSI) for the SRES A2 scenario indicate an increase over much of eastern Australia between 2000 and 2046 (Burke *et al*. 2006). The PDSI uses temperature and rainfall information in a formula to determine dryness, and is commonly used in the United States.

5.5 Wind

Changes in the frequency and intensity of severe wind due to climate change have not previously been quantified for the Australian region. However, changes in extreme wind have the potential to bring about large social, economic and ecological impacts. Extremes in wind contribute directly to hazardous conditions causing damage to the built and natural environment. They also create hazardous conditions over oceans, being responsible for the generation of storm surges and large waves which can cause coastal inundation and increase coastal erosion. Even modest changes in wind speed can have a major impact on erosion by altering the wave climate.

In this section, projections for annual and seasonal average winds are developed using the pattern-scaling methodology described earlier in this chapter. The relationship between extreme daily wind speed changes and average wind speed changes is also investigated for a selection of models.

5.5.1 Average wind speed projections

Model to model uncertainty in average wind speed change is high, but there is a tendency for increases in most coastal areas in 2030 (range of -2% to +7.5% with a best estimate 2-5%) except for band around 30ºS in winter and 40ºS in summer where there are decreases (-7.5% to +2%, with a best estimate of -2% to -5%).

Later in the century changes of wind strength can be larger in magnitude, depending on the emission scenario.

Data for wind speed at 10 m above the ground were available for 19 of the CMIP3 models. Wind speed changes for different emission scenarios and times during the 21st century have been determined using the same procedure as applied to average temperature. While it is acknowledged that directional changes are also important for processes such as coastal erosion and storm surge (e.g. McInnes *et al*. in preparation), a large scale analysis of the directional changes in the CMIP3 models has not been undertaken at this time.

2030

Figure 5.36 shows the 50th percentile (best estimate) changes to mean 10 m wind speed for each season and annually for 2030 under the A1B scenario. Figure 5.37 shows the corresponding 10th and 90th percentile values for summer, winter and annually. Site-specific results are given in Appendix B, and full results are available at www.climatechangeinaustralia.gov.au.

The annual average picture of wind speed change shows little change (±2%). In summer, increases are evident around much of the Australian coastline except Bass Strait, with changes ranging between -2% and 7.5% (best estimate increases of 2% to 5%). A band of wind speed decrease is located to the south of the continent extending from the Great Australian Bight to the

southern Tasman Sea (changes between -7.5% and +2%, with best estimate decreases of 2% to 5%). This is consistent with a southward contraction of the westerlies that are dominant in this region. A consequence of global warming is for the westerlies which are associated with the southern hemisphere storm track to strengthen but contract further polewards (e.g. Yin 2005; Lambert and Fyfe 2006). In autumn, wind speeds increase over southern Western Australia and decrease over the north-west of the continent. In winter, the structure of the change is more east-west with wind speed decreases occurring between about 30 and 35°S (-10% to +2% with a best estimate decrease of 2% to 5%), except for in the south-east of the continent where increases in wind speed occur over southern Victoria, Tasmania and Bass Strait (-2% to +7.5% with a best estimate change of +2% to +5%). Wind speed also increases between about 20 and 30°S (-2% to +7.5% with a best estimate increase of 2% to 5%), except the north-west coastline. In spring, wind speed increases in eastern Queensland, north-east New South Wales, eastern Tasmania, and parts of South Australia and the Northern Territory where changes range between -2% to +10%, with a best estimate change of 2% to 5%.

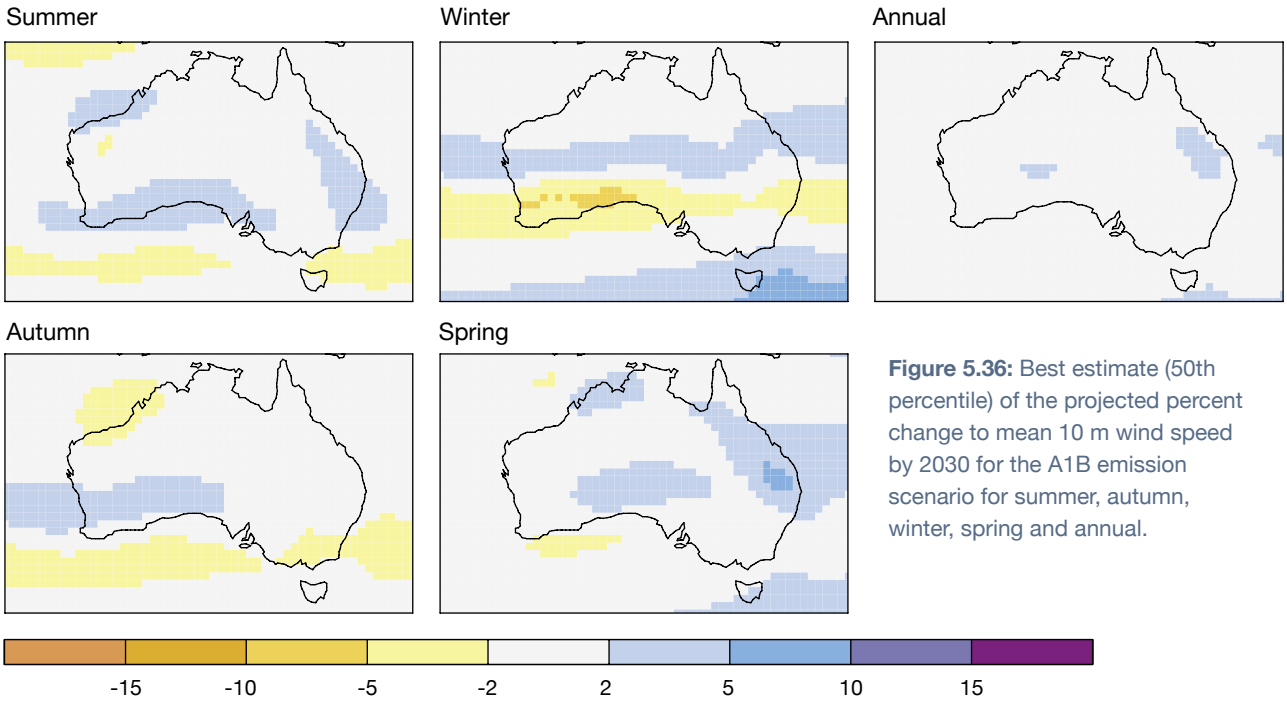

Figure 5.36: Best estimate (50th percentile) of the projected percent change to mean 10 m wind speed by 2030 for the A1B emission scenario for summer, autumn, winter, spring and annual.

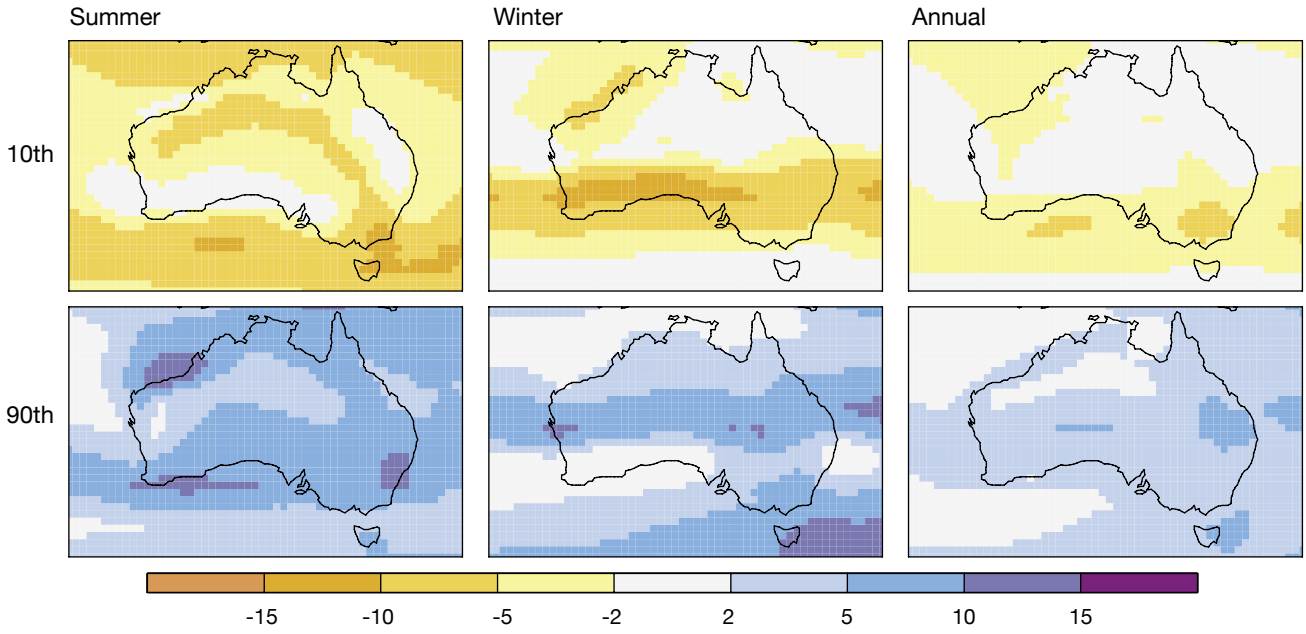

Figure 5.37: Projections of the estimate of net percent change to mean 10 m wind speed by 2030 for scenario A1B from the 10th and 90th percentile values for summer, winter and annual.

Figure 5.37 shows that the response varies from decreasing winds over almost the entire region, as given by the 10th percentile results, to increasing winds over the entire region, as given by the 90th percentile results, highlighting the large uncertainty. The strongest decreases in summer, of between about 5 and 10%, are to the south and north of the continent, especially for Tasmania and Victoria, and in the 30 to 40ºS band in winter. The 90th percentile changes in summer show the strongest wind increases of between 5% and 10% occurring over the northern coast between 110 and 140ºW, on the southern coast, and between 30 and 35ºS on the eastern coast. In winter, the strongest wind speed increases, of between about 5% and 10%, are located over Victoria and Tasmania and the northern half of the subtropical ridge between 20 and 30°S, although the east coast of Tasmania undergoes increases between 10% and 15%.

2050 and 2070

As with the projections of other climate variables, beyond the first few decades of the century the magnitude of the change becomes increasingly dependent on the emission scenario. This is illustrated by considering the 50th percentile values under the six SRES marker emission scenarios. The response patterns for 2050 and 2070 (and 2030) are shown in Figure 5.38. Seasonal results are avilable at www.climatechangeinaustralia.gov.au.

By 2050, the A1T and A1FI emission scenarios produce the strongest response in wind speed. By 2070, A1FI produces the strongest response.

The inter-model variability as captured by the range of change from the 10th to the 90th percentile is larger than the variation in response due to the different emission scenarios. This is illustrated in Figure 5.39 which shows that the lowest changes in wind speed for 2050, consisting of predominantly decreasing wind speed for the 10th percentile change under the B1 scenario. Conversely, the highest values of change in wind speed show increasing winds everywhere for the 90th percentile change under the A1FI scenario.

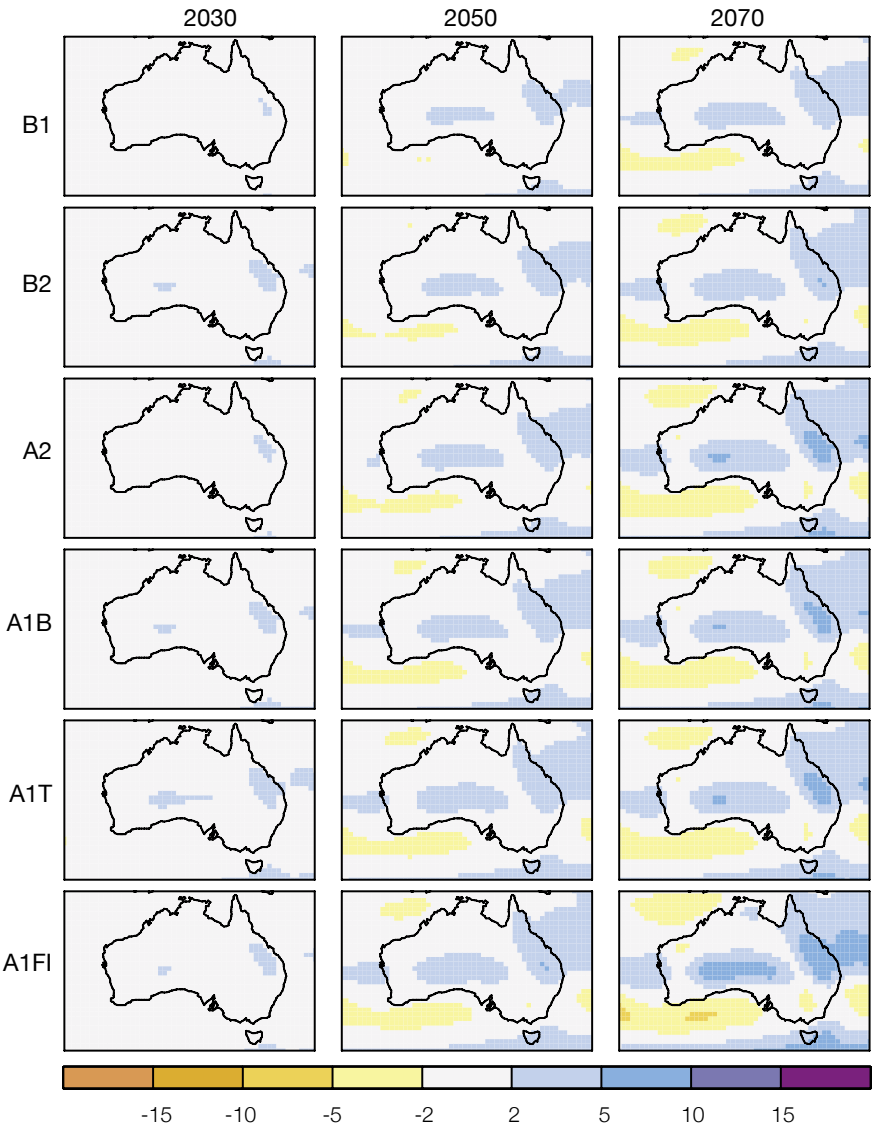

Figure 5.38: Best estimate (50th percentiles) of percent change in mean 10 m wind speed for 2030 (left column), 2050 (middle) and 2070 (right). Results for all six SRES scenarios are given.

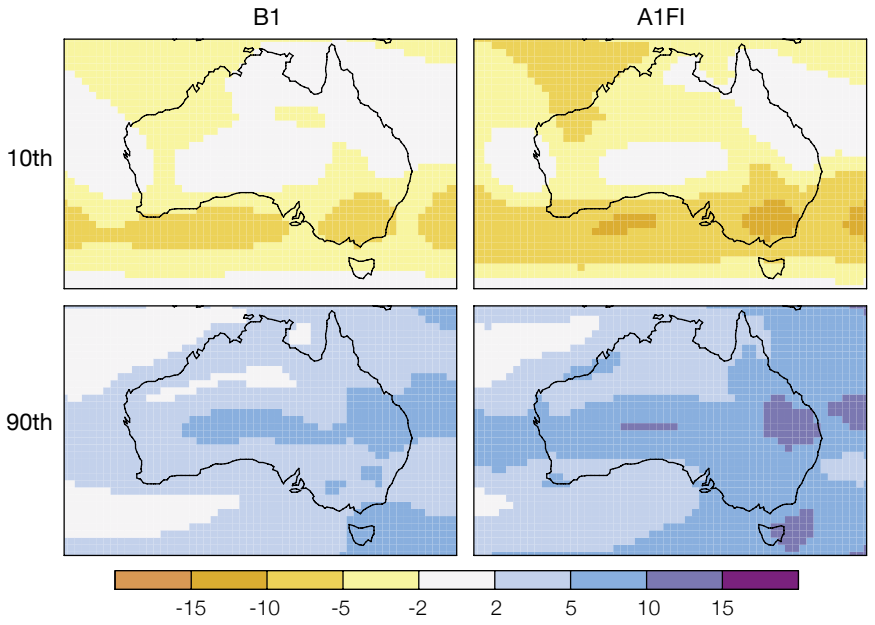

Figure 5.39: Range of annual percent change in mean 10 m wind speed (% relative to 1990 climate) for 2050 for the B1 and A1FI emission scenarios for the 10th and 90th percentile results.

An alternative way of viewing changes to wind speed is by considering the probability of a particular threshold of wind speed change being reached. Figure 5.40 shows maps of probability that wind speed will increase for the A1B scenario for all seasons. For most of coastal Australia in summer, there is a greater than 50% chance that average wind speed will undergo an increase, and in many areas the probability is at least 70%. In autumn, the north-east and south-west of the continent have a greater than 50% chance of experiencing a wind speed increase while in the north-west and south-east there is a greater than 50% chance that there will be a decrease in mean wind speeds. In winter, Tasmania and much of the north of the continent (except the north-west shelf) have a greater than 70% chance of experiencing wind speed increase. The probability of wind speed increase is as high as 90% over southern Tasmania. In spring there is greater than 50% chance of wind speeds increasing over the Queensland and Northern Territory coasts and Tasmania with the risk as high as 90% along Queensland's eastern coastline.

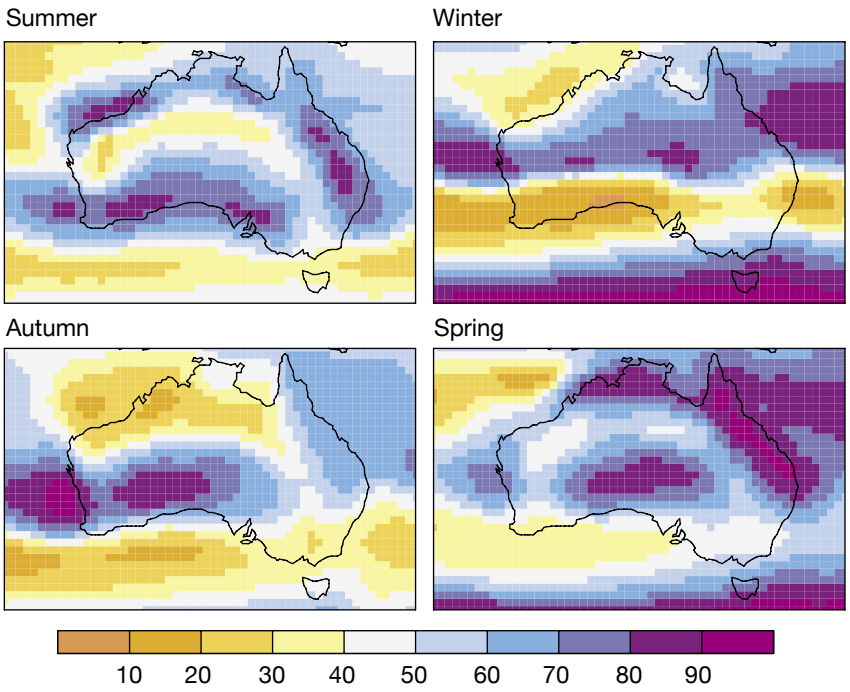

Figure 5.40: Risk (probability in %) that wind speed will decrease in 2070 for summer, autumn, winter and spring.

5.5.2 Extreme wind speed projections

In winter, changes to extreme daily wind speed are similar to the changes to seasonal mean wind speed based on the results of a limited set of models. However there is little relationship between summer mean and extreme wind speed changes. Extreme winds in summer are likely to be governed more by small scale systems that are not adequately captured by the resolution of the climate models. On the other hand, winter extreme wind events are more likely to be governed by larger scale systems (e.g. trade winds, mid-latitude cyclones) that are better captured at the resolution of the models.

Owing to the small number of models for which daily wind data were available, this section is focused on the relationship between the change in extreme wind speed and change in mean wind speed in the models for which both extreme daily and monthly wind speed data could be accessed. The aim was to determine whether the extreme winds change in a manner that is consistent with mean wind change. The analysis is directed at northern and southern Australia to delineate the possible different behaviour of extreme wind change relative to mean wind change in the tropics as compared with the mid-latitudes.

Four models recorded data enabling the calculation of extreme winds (see Table 5.1). The extreme winds were calculated from the daily wind fields in each model to yield the 90th, 95th and 99th percentile winds. The percentiles were calculated seasonally and annually. For the four seasons, a moving window was used in which the 90 days that comprise the season in any given year were combined with those days from the previous year and the following year to give a total of 270 days from which the value of the 99th percentile wind was estimated from the second and third highest values in the set of data points, and similarly for the lower percentiles. For the annual percentiles, values for a single year were sufficient for the calculation. Once a time series of percentile winds was created at each grid point, these data were linearly regressed against the model's globally averaged warming values to develop maps of local wind change per degree of global warming as described previously.

The analysis was conducted over two regions, one covering the mid-latitude region of Australia (from 110-155ºE and 30-44ºS) and one covering the tropical region of Australia (from 110-155ºE and 8-30ºS). The output from each model was interpolated to a common grid with a longitudinal resolution of 5 degrees and a latitudinal resolution of 4 degrees (the grid of the INM-CM3.0 model, which provided the coarsest of the four model datasets analysed). For each dataset on the common grid, the changes in extreme wind speeds were regressed against the changes in mean wind speed to investigate the nature of the changes between the two regions. Results are presented for only the 99th percentile winds since the behaviour of the lower percentile values was broadly similar.

The results for the tropics are shown in Figure 5.41 for the annual, summer and winter changes. Results for autumn broadly follow those for summer and those for spring follow the winter results. For summer and autumn, which are characterised by a broad spread of points across the four quadrants of a regression plot, there is low correlation between the changes in extreme wind speeds and the changes in mean wind speeds. Most commonly the extreme winds are found to decrease regardless of whether the mean winds underwent increase or decrease. For winter and spring there is a higher correlation between the two sets of data indicating that more commonly the change in the extreme winds was of the same direction as the mean winds. Frequency distribution functions for each of the models for the extreme and mean wind speed changes were considered (not shown). These show that, in general, changes in extreme wind speed are smaller than changes in mean wind speed. The four models agree on a tendency for decreases in extreme wind speed for summer and autumn, whereas the direction of the change in mean wind speeds across the region is not clear. In winter and spring the models agree on a tendency for increases in mean wind speed, whereas the direction of the change in extreme wind speeds across the region is not clear.

The results for the mid-latitudes for the annual, summer and winter changes are shown in Figure 5.42. Overall, the changes in extreme winds are more highly correlated with the changes in the mean winds than in the tropics, with the highest correlations occurring in winter. This indicates that the changes in extreme wind speeds are linked to changes in the dominant wind patterns in this region although, as for the tropics, changes in extreme wind speed are generally smaller than changes in mean wind speed. The four models agree on a tendency for decreases in extreme wind speed for summer, whereas the direction of the average change across the region in the other seasons is not clear.

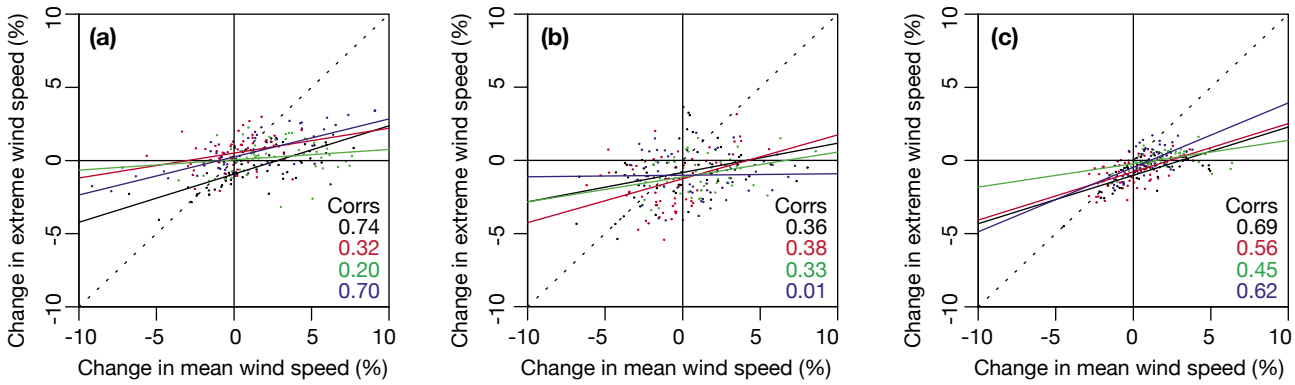

Figure 5.41: Relationships between changes in extreme (99th percentile daily) wind speed and changes in mean wind speed for tropical Australia (8 to 30ºS) for (a) summer, (b) winter and (c) annual data. Changes are percentage changes per ºC of global warming. Changes are shown for the GFDL-CM2.0 model (in black), the MRI-CGCM2.3.2 model (in red), the INM-CM3.0 model (in green) and the ECHAM5/MPI-AOM model (in blue). For each model, analyses of datasets containing data for each INM-CM3.0 model grid point are presented. Linear regression best fit lines of changes in extreme wind speed versus changes in mean wind speed with correlation coefficients are also shown.

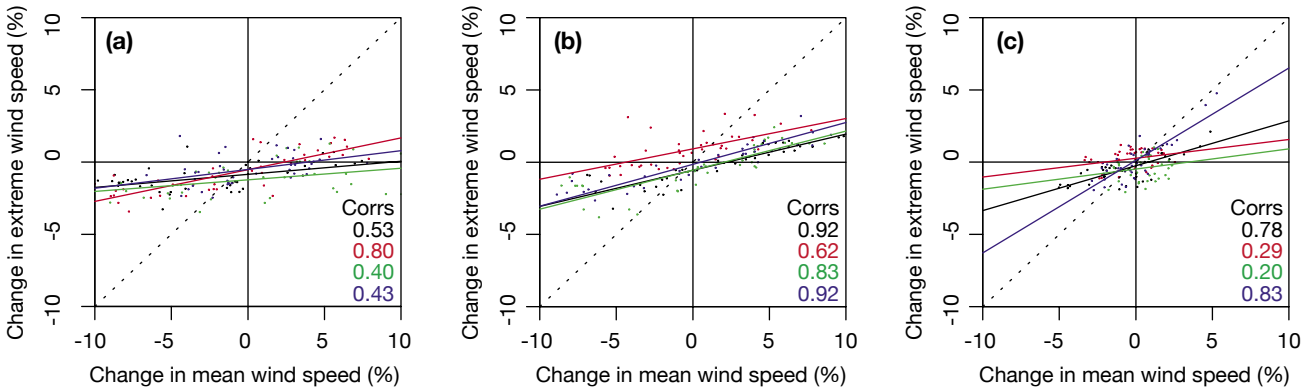

Figure 5.42: As for Figure 5.41 but for mid-latitude Australia (30 to 44°S).

The lowest correlations between mean and extreme wind occur in the tropics in summer while the highest correlations occur in winter in the mid-latitudes. The relationship between extreme winds and mean winds in the tropics compared with the mid-latitudes and between summer and winter may be related to the different weather systems responsible for extreme winds between the two regions and seasons. In both the tropics and mid-latitudes, extreme wind events are more likely to be related to smaller scale systems such as tropical cyclones and intense convective events which may be associated with tropical storms in the tropics and frontal activity or low pressure systems further south. Note that the models are not of fine enough resolution to adequately resolve these systems but can produce lower resolution systems that contain many of their features such as relatively extreme winds and rainfall, albeit to a less extreme extent than in the real world. The systems are less likely to be correlated with the climatological mean winds in summer in these regions which are comprised mainly of the north-west monsoon over the north-west and trade wind easterlies over the north-east in the tropics and the mid-latitude westerlies in the south. On the other hand, in winter, the extreme wind events are more likely to be related to the climatological mean winds in these regions. For example, the extreme westerlies associated with a severe cold front in the south are related to the climatological mean westerlies of this region. Similarly an extreme easterly wind event is associated with the predominant trade easterlies in the tropics.

5.6 Fire weather

A substantial increase in fire weather risk is likely at most sites in south-eastern Australia. Such a risk may exist elsewhere in Australia, but this has yet to be examined.

Bushfires are an integral part of Australia's environment. Its natural ecosystems have evolved with fire, and its landscapes and their biological diversity have been shaped by both historical and recent patterns of fire (Cary 2002). South-eastern Australia has the highest bushfire risk in spring, summer and autumn. This region has the reputation of being one of the three most fire-prone areas in the world, along with southern California and Mediterranean Europe.

Fire risk is influenced by a number of factors, including fuels, terrain, land management, fire suppression and weather. The Forest Fire Danger Index (FFDI) is used operationally to provide an indication of fire risk based on near-surface daily maximum temperature, daily total precipitation, 3 pm relative humidity and 3 pm wind speed. The FFDI has five intensity categories: low (less than 5), moderate (5-12), high (13-25), very high (25-49) and extreme (at least 50).

When the FFDI is extreme, a Total Fire Ban Day is usually declared. During the Canberra fires on 19 January 2003, the FFDI exceeded 100 (Figure 5.43).

Fire danger indices were calculated using daily weather records from 1974-2003 for 17 sites in south-eastern Australia (Hennessy *et al*. 2006). It was not possible to calculate changes in fire danger based on any of the CMIP3 models in Table 4.1. The results presented here are based on the study by Hennessy *et al*. (2006) using two climate change simulations with CSIRO's Cubic Conformal Atmospheric Model (CCAM), which has 50 km resolution over Australia. One simulation (denoted CCAM Mark2) was driven by boundary conditions from the CSIRO Mark 2 coupled ocean-atmosphere model, while the other simulation (denoted CCAM Mark3) was driven by boundary conditions from the CSIRO Mark 3.0 model. Data from these simulations were then used to generate climate change scenarios per degree of global

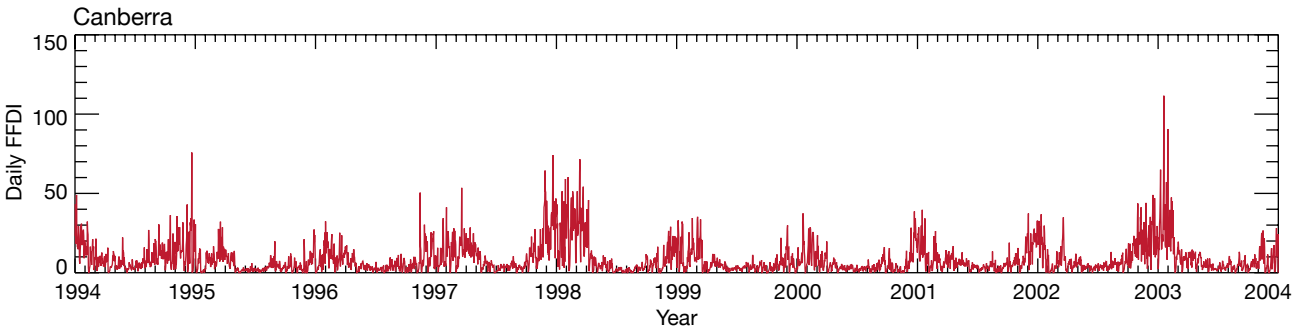

Figure 5.43: Forest Fire Danger Index (FFDI) for Canberra, reconstructed from daily temperature, humidity, wind and rainfall data from 1994-2004 (Lucas *et al*. 2007).

warming, including changes in daily weather variability. These changes were scaled by the IPCC (2001) global warming ranges for 2020 and 2050, then applied to the daily weather records from 1974-2003 at 17 sites in south-eastern Australia. Fire danger indices were then calculated for the modified 30 year datasets centred on 2020 and 2050 (Hennessy *et al*. 2006).

An increase in fire weather risk is simulated at most sites, including the average number of days when the FFDI rating is very high or extreme. The combined frequencies of days with very high and extreme FFDI ratings increase 4-25% by 2020 and 15-70% by 2050 (Table 5.7). For example, Canberra has an annual average of 25.6-28.6 very high or extreme fire danger days by 2020 and 27.9-38.3 days by 2050, compared with a present average of 23.1 days. The increase in fire weather risk is generally largest inland. Tasmania is relatively unaffected. It is likely that the higher fire weather risk in spring, summer and autumn will increasingly shift periods suitable for prescribed burning toward winter.

Table 5.7: Annual average number of days when the Forest Fire Danger Index (FFDI) rating is very high or extreme under present conditions (1974-2003) and for the years 2020 and 2050 for locations in south-east Australia. Results are for two different CSIRO global climate simulations: CCAM Mark2 and CCAM Mark3. The low and high values for each year reflect the low and high IPCC (2001) global warming values for that year. (Source: Hennessy *et al*. 2006.)

Site	Present	CCAM Mark2				CCAM Mark3			
		2020 low	2020 high	2050 low	2050 high	2020 low	2020 high	2050 low	2050 high
Canberra	23.1	25.6	27.5	27.9	36.0	26.0	28.6	28.9	38.3
Bourke	69.5	75.2	83.3	84.0	106.5	73.9	80.3	80.6	96.2
Cabramurra	0.3	0.3	0.4	0.4	0.7	0.4	0.4	0.5	1.0
Cobar	81.8	87.9	96.2	96.6	118.3	86.6	92.8	93.0	108.6
Coffs Harbour	4.4	4.7	5.1	5.1	6.3	4.7	5.6	5.6	7.6
Nowra	13.4	13.9	14.7	14.8	17.5	14.2	15.6	15.6	19.9
Richmond	11.5	12.9	14.0	14.1	17.5	13.1	14.3	14.4	19.1
Sydney	8.7	9.2	9.8	9.8	11.8	9.5	11.1	11.3	15.2
Wagga	49.6	52.7	57.3	57.6	71.5	52.8	57.4	57.7	71.9
Williamtown	16.4	17.2	18.2	18.4	20.9	17.3	19.4	19.4	23.6
Bendigo	17.8	19.5	21.3	21.4	27.3	19.7	21.9	22.0	29.8
Laverton	15.5	16.4	17.3	17.3	21.2	16.6	17.8	17.8	22.3
Melbourne	9.0	9.8	10.7	10.8	13.9	9.8	11.1	11.2	14.7
Mildura	79.5	83.9	89.5	89.9	104.8	84.6	90.7	90.9	107.3
Sale	8.7	9.3	10.0	10.1	12.1	9.6	10.7	10.8	14.0
Hobart	3.4	3.4	3.4	3.4	3.4	3.4	3.5	3.5	3.5
Launceston	1.5	1.5	1.5	1.6	2.0	1.6	1.9	1.9	3.1

5.7 Sea level rise

An increase in mean sea level and changes in sea level extremes will mainly affect the terrestrial landscape, increasing the risk of inundation of low-lying coastal terrain. However, increases in coastal inundation can impact upon marine ecosystems through changes to coastal wetlands and tidal plains that provide breeding grounds for marine life.

5.7.1 Mean sea level rise

Global sea level rise is projected by the IPCC to be 18-59 cm by 2100, with a possible additional contribution from ice sheets of 10 to 20 cm. However, further ice sheet contributions that cannot be quantified at this time may increase the upper limit of sea level rise substantially. Global climate models indicate that mean sea level rise on the east coast of Australia may be greater than the global mean sea level rise.

Mean sea level rise occurs as a result of two main processes - the melting of land-based ice, which increases the height of the ocean, and a decrease in ocean density, which increases the volume and hence the height of the ocean. Increases in ocean density in most parts of the world, including Australia, occur largely due to increases in the heat content of the ocean rather than reductions in salinity and so the density change component is often referred to as thermal expansion. The amount of thermal expansion is non-uniform due to the influence of ocean currents and spatial variations in ocean warming.

From 1961-2003, the rate of sea level rise was 1.8 mm per year, with a rise of 3 mm per year from 1993-2003. This rate of increase is an order of magnitude faster than the average rate of rise over the previous several thousand years. Around Australia the rate of sea level rise was about 1.2 mm per year during the 20th century (Church *et al*. 2006).

This rise in sea level has mainly been attributed to thermal expansion of the upper ocean. Overlying this global sea level rise is a large regional variability. The oceans surrounding Australia are particularly influenced by two dominant climate variations: the El Niño – Southern Oscillation (ENSO) and the Southern Annular Mode (SAM). These two climate variations overlay the global mean sea level rise, resulting in significant regional variability in the magnitude and trend of sea level rise in the oceans surrounding Australia. For example, ENSO results in sea level variability in the western Indian Ocean and eastern tropical Pacific Ocean, while the SAM is a major driver of sea level variability in the Southern and mid-latitude Indian and Pacific Oceans. The impact of ENSO and SAM results in a regionally complex pattern of sea level rise and variability in the Indian and Pacific Oceans.

Throughout the 21st century and beyond, sea levels across the world's oceans are expected to continue rising due to thermal expansion of sea water, melting of land-based glaciers and ice caps and contributions from the ice-sheets of Antarctica and Greenland. Relative to the 1990 level, global average mean sea level is projected to increase by 18 to 59 centimetres by 2100 (Table 5.8). If ice flow rates from Greenland and Antarctica during 1993-2003 were to continue to grow linearly with global warming, then the upper ranges of sea level rise would increase by a further 10 to 20 cm (IPCC 2007a). There is a risk that the contribution of ice sheets to sea level rise this century will substantially higher than this (IPCC 2007a; Hansen 2007).

Table 5.8: IPCC Fourth Assessment Report estimates of global average sea level rise by 2100, relative to 1990 (from IPCC (2007a) Table SPM-3) for six IPCC emissions scenarios. Larger changes are possible (see text).

Emissions scenario	Central estimate	Estimate range
B1	28 cm	18-38 cm
A1T	33 cm	20-45 cm
B2	32 cm	20-43 cm
A1B	35 cm	21-48 cm
A2	37 cm	23-51 cm
A1FI	43 cm	26-59 cm

The spatial pattern of sea level rise in the Australian region has been investigated for 2070. The patterns of thermal expansion were available for 17 of the CMIP3 models and are shown in Figure 5.44 for the A1B emission scenario. In each case, each model's globally averaged thermal expansion has been subtracted so that the diagrams represent the regional variation of sea level either above or below the global average sea level rise projection.

Although there is wide variation in the amount of projected sea level rise, there are also similarities in some regions. For example, in 13 of the 17 models, the thermal expansion along the east coast of Australia south of 30ºS is positive relative to the global average values, leading to an additional rise of around 10 cm above the global average change. This feature has been studied in the CSIRO Mark 3.0 model (Cai 2006) and is attributed to a strengthening of the East Australian Current, which results in the movement of warmer water along the east coast (see section 5.8.3).

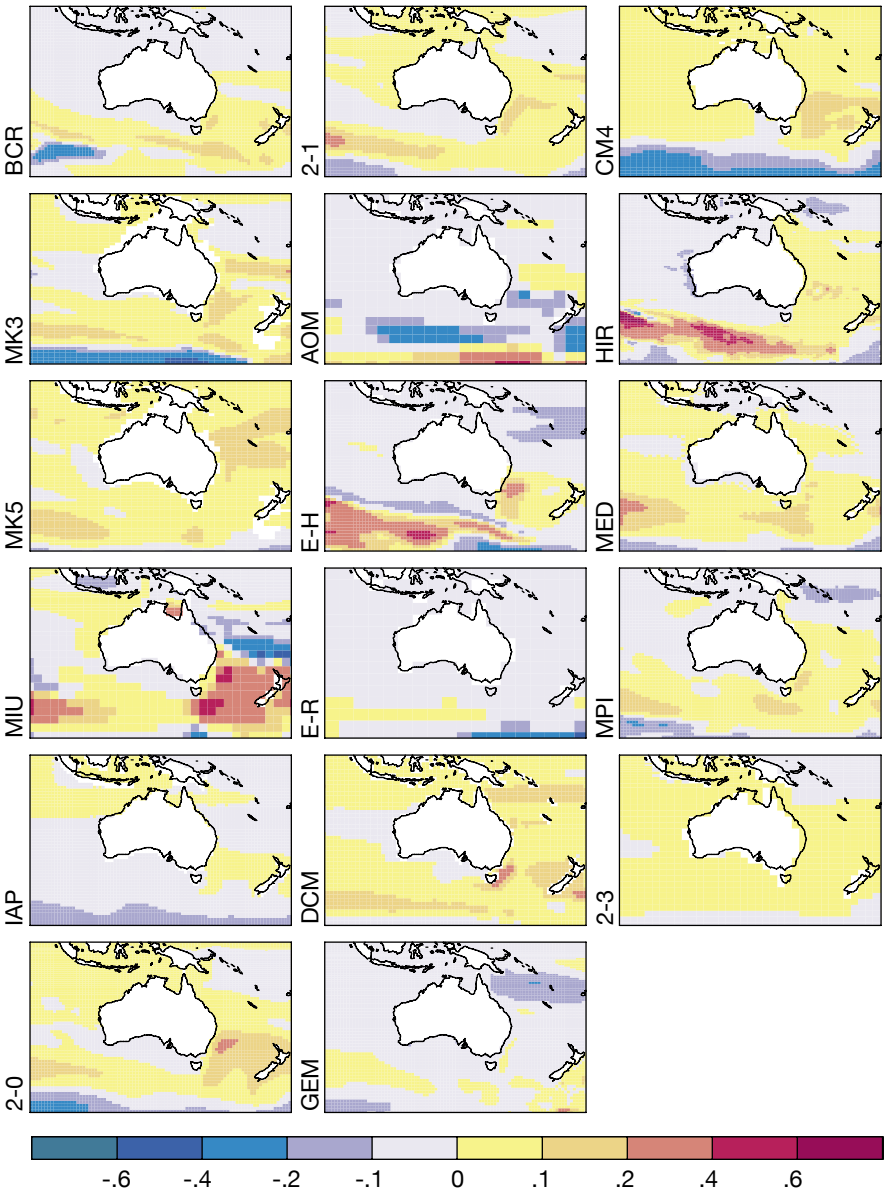

Figure 5.44: Projected regional contribution of thermal expansion to sea level by 2070 relative to the globally averaged value for each model (in metres). Calculations are based on 17 CMIP3 models for the A1B emission scenario. Units are metres. Tables 4.1and 5.1 provide details of the models used.

5.7.2 Sea level extremes

Storm surges occurring on higher mean sea levels will enable inundation and damaging waves to penetrate further inland. This would increase flooding, erosion and damage to built infrastructure and natural ecosystems. Changes to wind speed will also affect storm surge height.

Storm surge studies for portions of the Victorian and Queensland coasts demonstrate the potential for significant increases in inundation due to higher mean sea level and more intense weather systems.

As with temperature and precipitation, it may not be the mean sea level changes that have the greatest impacts, but the extreme sea level events. The effect of rising mean sea levels will be felt most profoundly during extreme storm conditions when strong winds and falling pressure bring about a temporary and localised increase in sea level known as a storm surge (see Box 5.2). Storm surges occurring on higher mean sea levels will enable inundation and damaging waves to penetrate further inland increasing flooding, erosion and damage to built infrastructure and natural ecosystems. In this section, a number of regional studies of changes to storm surge are presented.

Box 5.2 Contributions to coastal sea level from tides, storm surge and wave processes

A storm surge is a region of elevated sea level at the coast caused by the combined effect of falling atmospheric pressure and intense winds of severe weather events such as tropical cyclones. The rise in sea level due to falling pressure is about 1 cm per hectopascal fall in pressure (the so-called inverse barometer effect) although the larger contribution is due to wind, which pushes the water against the coast. Factors influencing the impact of winds on the storm surge include its strength, direction relative to the coast and the way in which the storm moves in relation to the coast.

For example, a tropical cyclone-induced storm surge would be most intense over the region of strongest onshore winds as the cyclone makes landfall. The shape of the sea floor and the proximity to bays, headlands and islands also affect the storm surge height. Wide and gently sloping continental shelves amplify the storm surge, and bays and channels can funnel and increase the storm surge height. Storm systems such as tropical cyclones and mid-latitude storms and their associated cold fronts are the main cause of storm surges. Storm surges can interact with other ocean processes such as tides and waves to further increase coastal sea levels and flooding. A storm surge will have maximum impact if it coincides with high tide. Breaking waves at the coast can also produce an increase in coastal sea levels, known as wave setup.

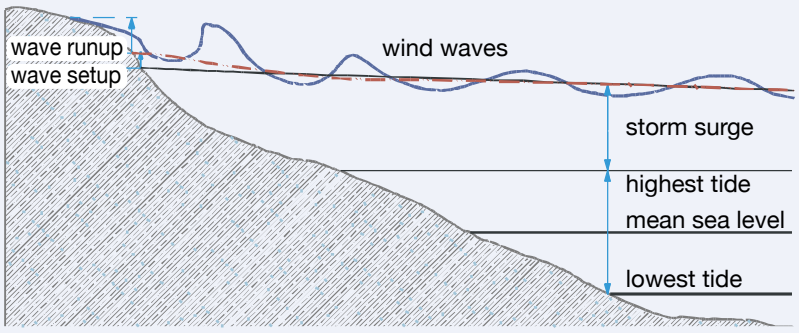

5.7.2.1 East Gippsland, Victoria

Storm surge events along the eastern Victorian coast are driven by severe weather such as cold fronts and mid-latitude cyclones. The strong winds and falling pressure elevate sea levels in the vicinity of the coast. Sea level rise will worsen the impact of these events. However, climate change may also cause changes in the frequency and intensity of the severe weather events that cause storm surges.

The south-westerlies that accompany severe cold fronts are the most common cause of elevated sea levels due to storm surge along the south coast of Australia. Scenarios of future changes to wind patterns were developed using the pattern-scaling technique of Whetton *et al*. (2005) and the results of 13 climate models. Projected changes in sea level and changes in 10 m average wind speeds are given in Table 5.9 (McInnes *et al*. 2005a,b). The range of change was formed by taking the second lowest to second highest model result at each grid point. This is a narrower range of change compared to the range obtained in the current projections using the 10th to 90th percentile, which is approximately -2% to +4% for 2030 and -6% to +15% by 2070, but the central estimates are similar. The sea level rise scenarios were based on IPCC (2001). While the latest IPCC (2007a) sea level rise scenarios are only available for 2090 to 2099, comparison with the 2001 scenarios indicates that the upper end of the range (59 cm + 20 cm for additional ice sheet response) is close to the 2001 estimate for 2095. The main difference is that the lower end of the range of change in the most recent projections is higher by about 10 cm by 2095, meaning that the low and mid-values of sea level rise in McInnes *et al*. (2005a,b) are also lower than the most recent projections.

To investigate the response of the wind speed changes, a set of storm surge events that occurred along the eastern Victorian coast were identified in 38 years of tide gauge data. These events were simulated using a hydrodynamic model under observed wind and pressure conditions, and then repeated with the projected changes to wind speed included. Astronomical tide heights were applied to the storm surge results using a joint probability approach. The low, mid and high mean sea level rise scenarios shown in Table 5.9 were applied to the storm surge heights generated from the low, mid and high wind speed scenarios respectively.

The sea level heights due to the combination of the storm tides with the corresponding mean sea level rise scenario are presented in Table 5.10 for several locations along the eastern Victorian coast. The 100-year return levels at Port Franklin and Port Albert for the 2030 low, mid and high scenarios using the wind speed and sea level rise values given in Table 5.9 differ from those for the current climate by approximately 2 cm, 11 cm and 20 cm respectively. The corresponding 2070 low, mid and high scenarios differ from current climate by 4 cm, 28 cm and 61 cm. The increase in mean sea level makes the largest contribution to this overall increase in storm surge height. For example the 2030 and 2070 high scenarios of 100-year storm surge increases of 20 cm and 61 cm respectively are comprised of 17 cm and 49 cm of mean sea level rise and 3 cm and 12 cm of storm surge increase, respectively, due to the 10% wind speed increase. The changes in sea level at Port Welshpool are similar to Ports Franklin and Albert except for the 2070 high scenario in which the increase is 56 cm. The 100-year return levels estimated for Lakes Entrance and Metung for the 2030 low, mid and high climate change scenarios differ from those for the current climate by approximately 2 cm, 10 cm and 19 cm respectively. The corresponding differences in 2070 are 4 cm , 27 cm and 58 cm. The sea level changes at Paynesville are similar to Lakes Entrance and Metung except for the 2070 high scenario in which the increase is 53 cm.

Table 5.9: Projected annual and winter wind speed changes and mean sea level rise for the Bass Strait expressed as a percentage relative to climatological wind speeds for the 1961 to 1990 period (from McInnes *et al*. 2005a).

Variable	Climate change scenario					
	2030			2070		
	Low	Mid	High	Low	Mid	High
Annual 10 m wind speed (%)	-1	1	3	-5	3	10
Mean sea level rise (m)	0.03	0.10	0.17	0.07	0.25	0.49

Table 5.10: Projected 100-year return levels of storm tides for selected locations along the eastern Victorian coast under current climate and 2030 and 2070 low, mid and high scenarios for wind speed and sea level rise as given in Table 5.10 (from McInnes *et al*. 2005b).

Location	Current Climate (m)	2030			2070		
		Low (m)	Mid (m)	High (m)	Low (m)	Mid (m)	High (m)
Port Welshpool	1.65	1.67	1.75	1.84	1.69	1.92	2.21
Port Franklin	1.87	1.88	1.98	2.07	1.90	2.15	2.48
Port Albert	1.75	1.77	1.87	1.96	1.79	2.04	2.36
Lakes Entrance	0.98	1.00	1.09	1.17	1.02	1.25	1.56
Metung	0.59	0.61	0.70	0.78	0.63	0.86	1.16
Paynesville	0.35	0.37	0.45	0.53	0.40	0.61	0.88

An example of the impact of inundation resulting from the 100-year storm surge in Corner Inlet and Gippsland Lakes is shown in Figure 5.45. In Corner Inlet, the sea level extremes are greatest across the islands and northern coastline of the inlet. The inundation in the regions of the towns of Port Franklin, Port Welshpool and Port Albert will increase in areal extent by between 15% and 30% by 2070 under a high wind speed change, high mean sea level rise scenario. Over the Gippsland Lakes, inundation resulting from sea level extremes will be greatest in existing swamp areas and in the vicinity of Lake Reeve, located along the barrier between the Lakes and the open coastline. The total area of inundation within the model domain doubles from current climate values of around 25 km^2 to just over 50 km^2 under a 2030 high wind speed change, high mean sea level rise scenario. It increases by a further 25% relative to 2030 under the corresponding scenario for 2070.

A key finding in this study is that even under a worst case (high) wind speed scenario (stronger winds in the future), the increase in storm surge height due to stronger winds will be smaller overall than the projected worst case rise in sea level. Under the best case (decreasing) wind speed changes the ensuing reductions in storm surge height will be cancelled out by the low range of projected sea level rise. The results point to a change of extreme sea level events in the future along this coastline that range from, at best, no change from current climatology to at worst, more severe.

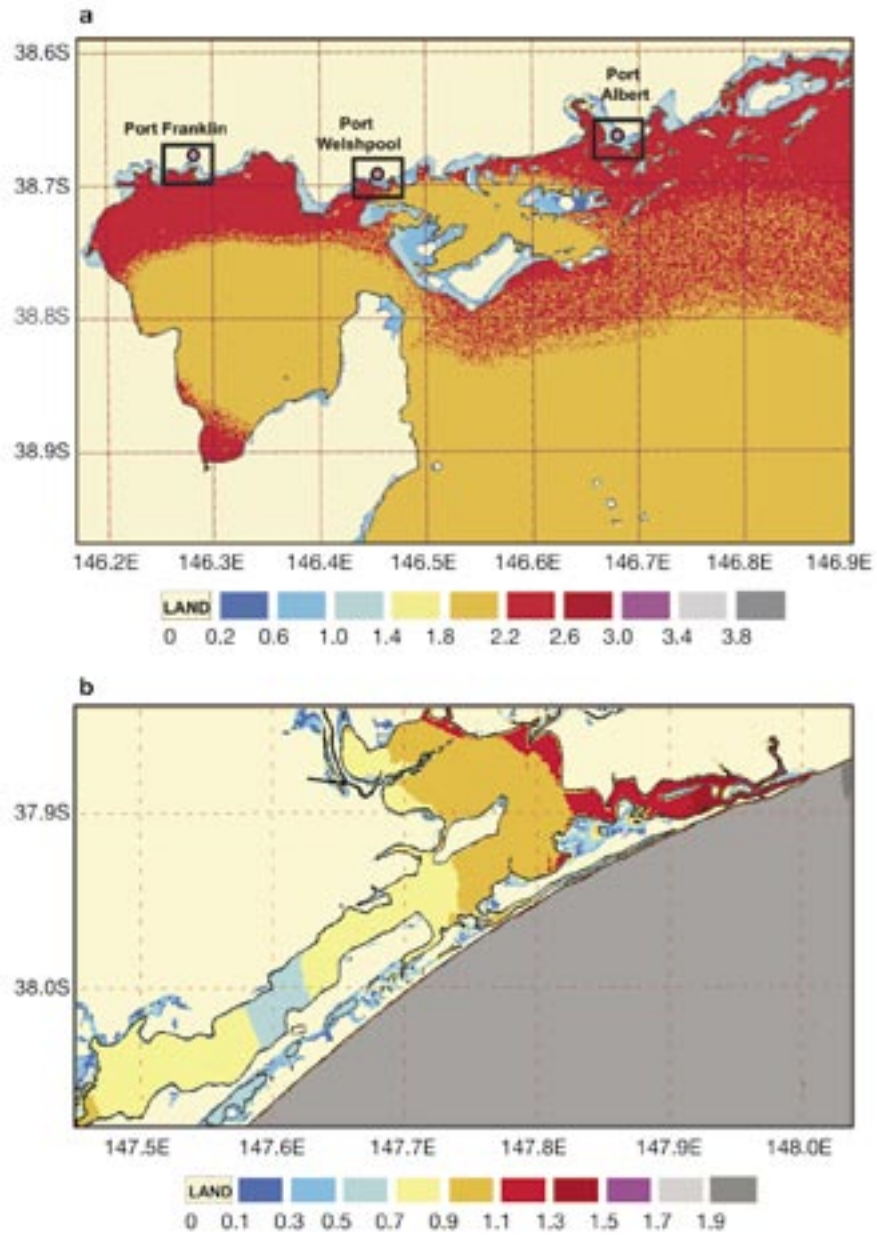

Figure 5.45: The areas around (a) Corner Inlet and (b) the Gippsland Lakes likely to experience inundation during the 1-in-100-year storm tide event estimated for a high wind speed, high mean sea level rise scenario for 2070. Sea levels are relative to current climate mean sea level over ocean regions and are relative to the topographic surface over land. (Source: McInnes *et al*. 2006).

5.7.2.2 Cairns, Queensland

Due to the localised nature of storm-surge impacts in northern Australia and the spatially sparse and relatively short sea level records along this part of the coast, stochastic sampling and dynamical modelling was used to investigate the impact of climate change on the tropical east coast around Cairns (McInnes *et al*. 2003). Using the historical record of tropical cyclones in the region, probability distribution functions were developed for cyclone speed and direction of approach and an extreme value distribution was fitted to the cyclone intensity.

The cyclone intensity distribution was increased by 10% for enhanced greenhouse conditions in 2050 following Walsh and Ryan (2000). A population of cyclones and tides were randomly selected under both climates, and modelled with a coastal ocean model at 200 m resolution (McInnes *et al*. 2003). Results show that increasing cyclone intensity by 2050 could increase the height of the 1-in-100 year event by 0.3 m. Projected sea level rise will add a further 0.05 m to 0.32 m to this figure. The areal extent of flooding increases from approximately 32 km^2 to 71 km^2 to encompass much of the Cairns downtown region (Figure 5.46).

5.7.2.3 Queensland

Storm tide statistics have been calculated at locations along the Queensland coast by Hardy *et al*. (2004) using storm surge and wave models. Changes in tropical cyclone-induced storm tides at locations on Queensland's east coast were determined using a stochastic sampling and dynamical modelling approach. The climate change scenarios used were a 10% increase in the intensity of all cyclones applied as a decrease to the central pressure of the cyclone combined with a southward shift of cyclone tracks of 1.3 degrees (about 130 km), a 10% increase in frequency of tropical cyclones and a 0.3 m sea level rise. These scenarios were chosen to explore the relative contributions of the different potential future changes even though there remains significant uncertainty about some of the changes that were applied such as the southward migration of cyclone tracks.

In southern Queensland locations such as the Sunshine Coast and Hervey Bay, the increase in the 100-year storm tide events were 0.45 m and 0.5 m respectively with the changes dominated by the sea level rise. The study did not consider weather systems other than tropical cyclones which may be expected to make an increasing contribution to the lower return periods at these more southern Queensland locations.

In the Cairns study, Hardy *et al*. (2004) estimated a 100-year storm tide level of 2.04 m which is lower than that calculated by McInnes *et al*. (2003) and Harper (1999). A key difference in the approaches taken by Hardy *et al*. to that of McInnes *et al*. is that the former selected their population of synthetic cyclones using an autoregressive model whose coefficients were derived from observed tropical cyclones over the Coral Sea from 1969 to 2001. McInnes *et al*. examined extreme value statistics from cyclones dating back to 1908 to evaluate the cyclone probabilities and this approach includes more intense cyclones than have been observed in the recent historical record (Church *et al*. 2006). Under conditions of climate change the 100-year event increased negligibly due to cyclone intensity and frequency increases.

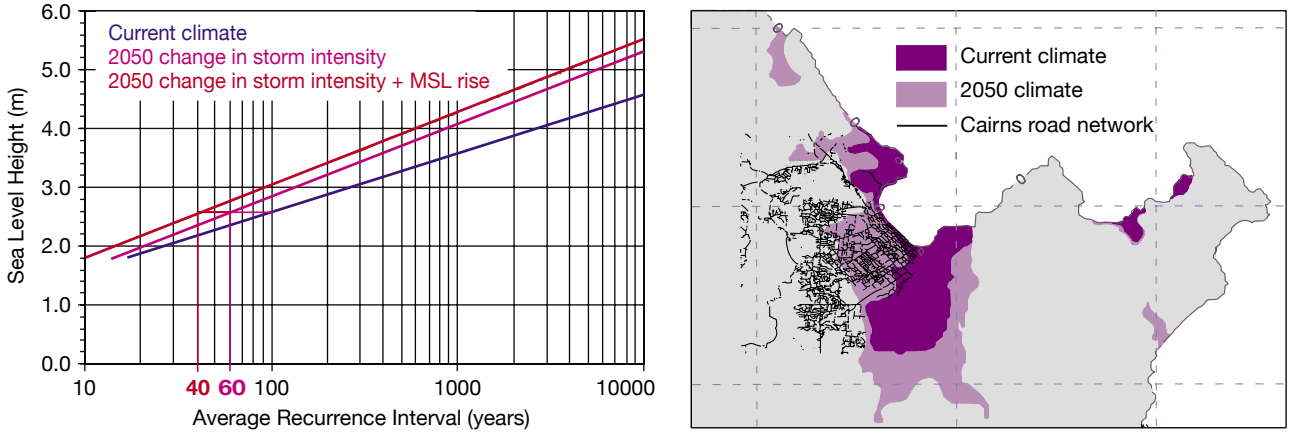

Figure 5.46: Projected (a) return period curves for storm tide, not including wave setup. (b) The inundation produced by the top 5% of storm surge model simulations (100-year return period and greater) under current climate conditions and conditions assuming a 10% increase in tropical cyclone intensity by 2050. The road network of Cairns is shown in black to highlight the urban impact of the inundation (Source: McInnes *et al*. 2003).

5.8 Marine projections

Australia is a maritime nation with sovereign rights over about 8.1 million km^2 of ocean. This region yields about 8% of the gross domestic product through activities such as fishing, tourism and recreation, shipping, and offshore gas and petroleum extraction.

The east and west coasts of Australia feature major poleward-flowing warm currents which are generally nutrient poor (oligotrophic), with regards to nitrate and phosphate. This, in combination with other stressors such as fishing, pollution and habitat degradation, make the marine environment particularly vulnerable to a changing climate. Climate variables that will influence marine impacts along with the broad areas of impact are listed in Table 5.11 and further details can be found in Hobday *et al*. (2006).

Table 5.11: Summary of potential climate change impacts on the marine environment.

Climate variable or feature	Potential or observed impact
Increased temperature	Southward migration of tropical and temperate species. Increased frequency of coral bleaching episodes. Declining kelp forests off eastern Tasmania (Edyvane 2003; Edgar *et al*. 2005).
Ocean chemistry (acidity)	Increased CO_2 absorption by the ocean decreases pH of the ocean and reduces availability of calcium carbonate which may impair the survival of organisms with calcium carbonate shells.
Ocean circulation and overturning	Changes to larval transport and upwelling regions and subsequent changes to productivity.
Increased oceanic stratification	Reduced overturning and nutrient cycling.
Cloud cover and solar radiance	Changes in the light supply to the surface ocean with influence on productivity.
Increased storminess	Increased turbidity, destruction of marine habitat such as coral reefs during extreme events.
Sea level rise	Potential loss of mangrove forests and nursery grounds for marine species.

5.8.1 Sea surface temperature

By 2030 the best estimate of sea surface temperature increase is 0.6-0.9ºC in southern Tasman Sea and off the north-west shelf of Western Australia and 0.3-0.6ºC elsewhere. Allowing for model-to-model variations the ranges are 0.4-1.0ºC off the north-west coast and to 0.4-1.4ºC in the southern Tasman Sea.

Beyond the first few decades of the 21st century, the magnitude of the sea surface temperature change will become increasingly dependent on the emission scenarios. Under the B1 scenario in 2070, the sea surface temperature increase is 0.6-1.0ºC along the south coast of Australia while elsewhere it is 1.2-1.5ºC. Under the A1FI emission scenario, the regions of highest warming are about 1.0ºC higher than those for the B1 scenario.

The ocean is a major heat sink. Observations since 1961 show that about 80% of the heat added to the climate system has been absorbed by the ocean, which has undergone a temperature increase to a depth of at least 3000 m (Levitus *et al*. 2005). Sea surface temperature projections were available for eleven of the IPCC Fourth Assessment Report climate models. Projections were developed for sea surface temperatures using the probabilistic methodology described earlier. Projections for sea surface temperature encapsulating the best estimate and the range of possible change, as represented by the 10th and 90th percentile changes, are shown in Figure 5.47 for 2030. Full results are available at www.climatechangeinaustralia.gov.au.

Figure 5.47 indicates that greater warming is likely to occur in the southern Tasman Sea off the east coast of New South Wales and off the north-west shelf of Western Australia. A possible explanation for the greater warming off the east coast may lie in the strengthening of the East Australian Current which transports warmer water further south, which has been found in the CSIRO Mark 3.0 model (Cai 2006). The best estimate of this increase is 0.6-0.9ºC and elsewhere by 0.3-0.6ºC. The 10th and 90th percentile values increase these ranges to 0.4-1.0ºC off the north-west coast and to 0.4-1.4ºC in the southern Tasman Sea.

The central estimate (50th percentile) projections of sea surface temperature for 2050 and the uncertainty, represented by the 10th and 90th percentile changes are shown in Figure 5.48 for the A1B emission scenario. Compared to the 2030 scenarios, the regions where the highest sea surface

temperature increase occurs indicates an increase in temperature that is almost twice that indicated at 2030.

Beyond the first few decades of the 21st century, the magnitude of the sea surface temperature change will become increasingly dependent on the emission scenarios. Figure 5.49 shows the central estimate (50th percentile) change in sea surface temperatures for 2070 under various emission scenarios. The 50th percentile estimate sea surface temperature increase for the B1 emission scenario in 2070 is similar to the 50th percentile changes for sea surface temperature in 2030 using the A1B scenario (Figure 5.47). Under the A1B scenario, the sea surface temperature increase is 1.5 to 1.8ºC in the southern Tasman Sea and over the north-west shelf. Along the south coast of Australia the increase is 0.9 to 1.2ºC, while elsewhere it is 1.2 to 1.5ºC. Under the A1FI emission scenario, the regions of highest warming are about 1.0ºC higher than those for the B1 scenario.

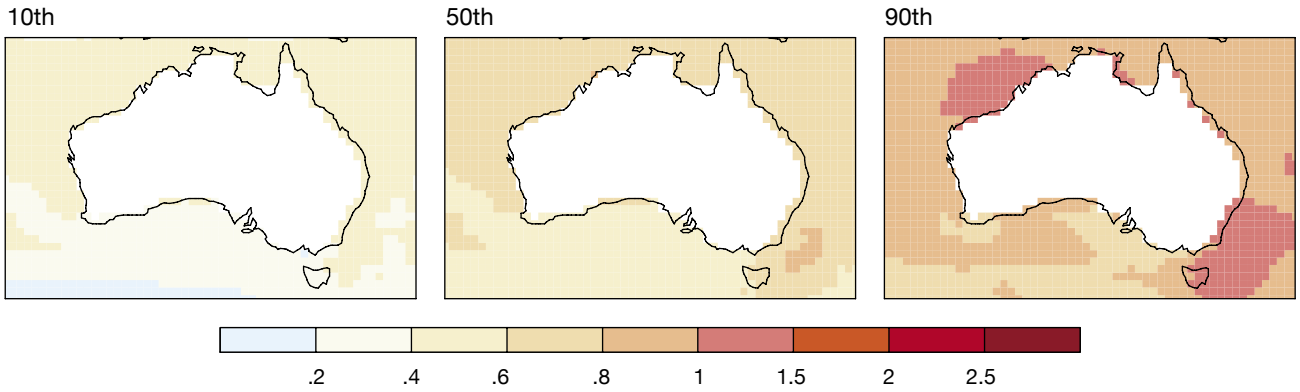

Figure 5.47: 10th, 50th and 90th percentile values for projected annual change in sea surface temperature by 2030 using the A1B emission scenario. Units are ºC.

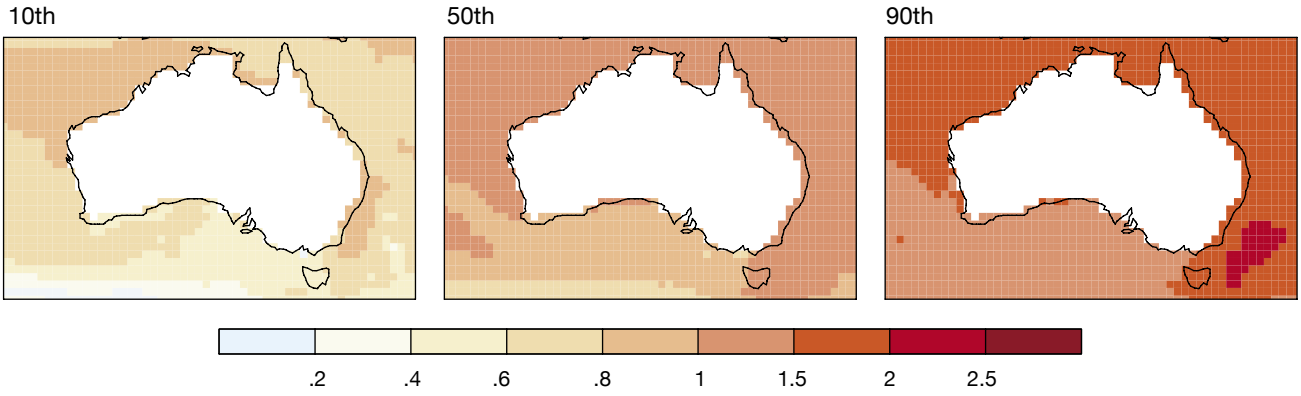

Figure 5.48: 10th, 50th and 90th percentile values for projected annual change in sea surface temperature by 2050 using the A1B emission scenario. Units are ºC.

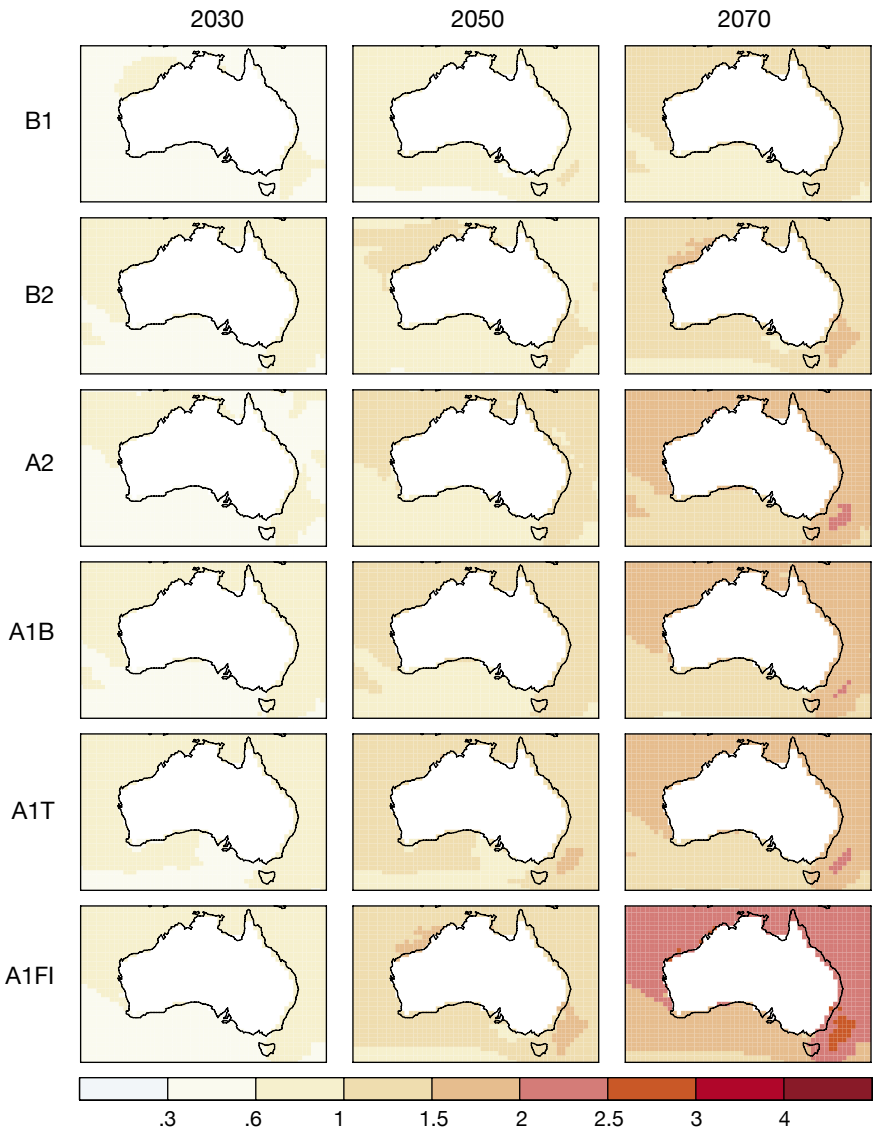

Figure 5.49: Best estimate (50th percentiles) of change of sea surface temperature relative to a 1961 to 1990 climatological average for 2030 (left column), 2050 (middle) and 2070 (right). Results for all six SRES scenarios are given.

5.8.2 Ocean acidification

Increases in ocean acidity are expected in the Australian region with the largest increases in the high to mid-latitudes. Model simulations indicate that the under-saturation of aragonite could occur by the middle of the century in the higher latitudes with potential detrimental impacts to ecosystems.

The world's oceans absorb carbon dioxide (CO_2) naturally from the atmosphere, acting as a buffer for increasing atmospheric CO_2. However, rising atmospheric CO_2 concentrations due to emissions from fossil-fuel combustion will lead to an increase in oceanic CO_2 as the ocean absorbs part of this CO_2 (McNeil *et al*. 2003). It has been estimated that the global oceans have absorbed half of the anthropogenic emitted CO_2 from the atmosphere to date (e.g. Sabine *et al*. 2004) lessening the impact on atmospheric radiative forcing. However, as oceanic concentrations of CO_2 increase, the ability of the ocean to take up CO_2 will decline (Sarmiento *et al*. 1995).

As CO_2 enters the ocean, it combines with water to form a weak acid (H_2CO_3) that dissociates into bicarbonate-generating hydrogen ions (H^+), making

the ocean more acidic and reducing the surface ocean carbonate ion (CO_3^{2-}) concentration. When under-saturation of calcium carbonate occurs in sea water, marine organisms are unable to form calcium carbonate shells (Raven *et al*. 2005). The surface pH and aragonite (a form of carbonate) saturation states are functions of temperature, salinity, alkalinity and dissolved inorganic carbon concentrations. However, future pH in the ocean will be determined mainly by atmospheric CO_2 concentrations rather than the degree of warming.

Figure 5.50 shows the average pH and aragonite concentrations projected for the 1990s and the changes between the 1990s and the 2070s from the CSIRO Mark 3.5 model. Average pH values are highest in the mid-latitudes from about 15 to 45ºS while aragonite concentrations are largest in the tropics. Declines in pH can be seen across the region by 2070 (Figure 5.50c) with the largest declines in the high to mid-latitudes. Aragonite concentrations show their largest decrease in the tropics and mid-latitudes. However because of the low concentrations present in the high latitudes, under-saturation of aragonite is likely to occur in the high latitudes first. Model simulations indicate that the under-saturation could occur within a few decades, with potential detrimental impacts to high latitude ecosystems.

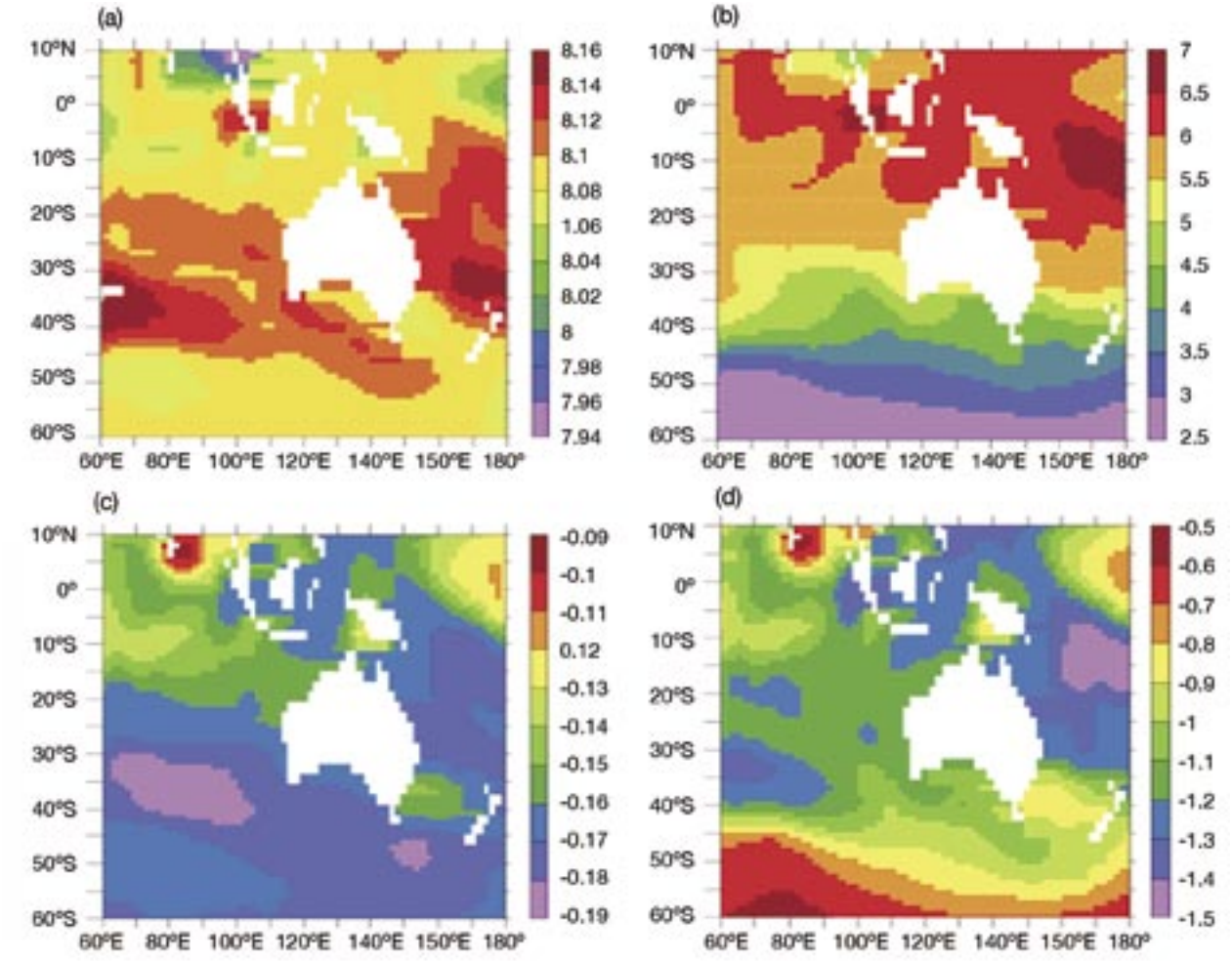

Figure 5.50: Averaged pH **(a)** and aragonite saturation **(b)** observed for the 1990s and the projected values for the 2070s for pH **(c)** and aragonite **(d)** using the CSIRO Mark 3.5 model under the A2 scenario (From Poloczanska *et al*. 2007).

5.8.3 East Australian Current

Model simulations indicate a likely strengthening of the East Australian Current through the 21st century which will result in warmer waters extending further southward and possible subsequent impacts on severe storms and marine ecosystems.

Since the late 1970s, a strengthening of the circumpolar westerlies has been observed, producing a bias towards the high-index polarity of the Southern Annular Mode. The observed changes have been attributed to ozone depletion (e.g. Thompson and Solomon 2002; Gillett and Thompson 2003). One oceanic consequence of this trend has been an increase in the Southern Ocean super-gyre circulation and an associated strengthening of the East Australian Current, particularly south of 30ºS. A consequence of the circulation change has been a strong warming trend along the path of the East Australian Current (Cai 2006).

The warming trend in the East Australian Current also occurs in four 21st century simulations of the CSIRO Mark 3.0 model carried out using the A2, A1B and B1 emission scenarios by Cai *et al*. (2005c). The analysis indicates that the strengthening of the East Australian Current may continue into the 21st century and is therefore also a consequence of global warming, since all three emission scenarios used in the climate model experiments assume a full recovery of ozone concentrations by 2050 indicating that the continuing changes to the East Australian Current are not related to ozone changes but instead are occurring due to greenhouse warming.

5.9 Severe weather

5.9.1 Tropical cyclones

Similar to studies for other basins, Australian region studies indicate a likely increase in the proportion of the tropical cyclones in the more intense categories, but a possible decrease in the total number of cyclones.

Tropical cyclone activity and intensity is variable on the intraseasonal, interannual, interdecadal and multi-decadal timescales. In the Australian region, variations in the number of tropical cyclones from year-to-year are strongly correlated with local sea surface temperature before and near the start of the cyclone season, with the strongest correlations being with October sea surface temperatures (Nicholls 1984). Australian region tropical cyclone numbers are also correlated with indices of ENSO from the central and east equatorial Pacific, indicating a remote effect on tropical cyclone numbers through the Walker Circulation. Observations show that tropical cyclone activity is lower in the Australian region during El Niño events, while La Niña events typically produce greater activity (Nicholls 1979, 1984, 1985; Kuleshov 2003).

There is substantial evidence from theory and model experiments that the large-scale environment in which tropical cyclones form and evolve is changing as a result of greenhouse warming. Theory includes potential intensity theories as well as empirical indices that attempt to relate tropical cyclone frequency to large-scale environmental conditions. The models range from global climate models to higher resolution regional models. In the models the tropical cyclones are located and tracked using objective techniques such as those described by Walsh *et al*. (2004) and Oouchi *et al*. (2006). Global climate models generally have a grid spacing that is larger than the typical scale of tropical cyclones and the modelled cyclones tend to have a larger horizontal scale and lower wind speeds than observed tropical cyclones. Higher resolution studies (Walsh *et al*. 2004; Abbs *et al*. 2006) are frequently used to investigate possible changes in tropical-cyclone climate over a region of interest, although Oouchi *et al*. (2006) have recently presented the results from a global climate model with a grid spacing of 20 km. High resolution global climate models have the advantage of being able to represent better the atmospheric processes conducive to tropical cyclone genesis while also capturing changes in the global circulation, such as ENSO, that may affect the location of tropical cyclone formation.

Projected changes in tropical cyclones are subject to the sources of uncertainty inherent in climate change projections. These include the future climate-forcing scenario, model dynamics and physics, errors in the modelled tropical cyclone climatology and regional patterns and magnitude of change for various fields and climate patterns such as ENSO. Consequently there is large uncertainty in the future change in tropical cyclone frequency projected by climate models. IPCC (2001) concluded that "there is some evidence that regional frequencies of tropical cyclones may change but none that their locations will change. There is also evidence that the peak intensity may increase by 5% to 10% and precipitation rates may increase by 20% to 30%. There is a need for much more work in this area to provide more robust results."

Since that time there has been a growing number of studies using results from medium and high resolution global climate models. The results from these studies indicate

a consistent signal of fewer tropical cyclones globally in a warmer climate (Knutson *et al*. 2006). However, there are significant regional variations in the direction of the changes and these vary between models. Substantial disagreement remains between climate models concerning future changes in tropical cyclone intensity, although the highest resolution models show evidence of an increase in tropical cyclone intensity in a warmer world.

Three recent studies have produced projections for tropical cyclone changes in the Australian region. Two suggest that there will be no significant change in tropical cyclone numbers off the east coast of Australia to the middle of the 21st century (Walsh *et al*. 2004; Leslie *et al*. 2007). The third study, based on the CSIRO simulations (Abbs *et al*. 2006), shows a significant decrease in tropical cyclone numbers for the Australian region especially off the coastline of Western Australia. In that sub-region, tropical cyclone numbers are simulated to decrease by 44% by 2070; off the east Australian coastline small decreases of only 9% are simulated. The simulations also show more long-lived eastern Australian tropical cyclones (Abbs *et al*. 2006; Leslie *et al*. 2007). In contrast, for the Western Australian coast a decrease in the number of long-lived cyclones is found (Abbs *et al*. 2006). These changes in both tropical cyclone duration and number affect the annual average tropical cyclone days for the region as shown in Figure 5.51.

Each of the above studies finds a marked increase in the severe Category 3-5 storms. An increase of 60% and 140% in the intensity of the most extreme storms for 2030 and 2070, respectively, was found using a model with a 15 km grid spacing (Abbs *et al*. 2006). Walsh *et al*. (2004) found an increase of 56% by 2050 using a 30 km model. Leslie *et al*. (2007) used a

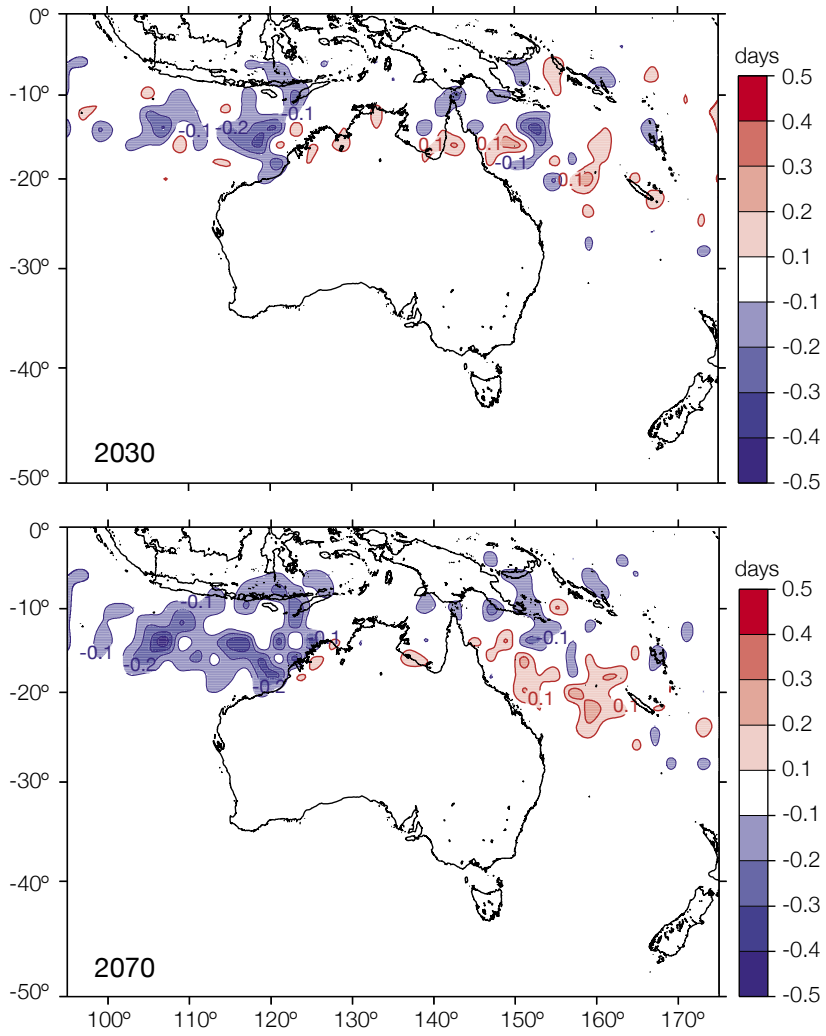

Figure 5.51: Simulated change in annual average tropical cyclone occurrence in the Australian region for 40-year time slices centred on 2030 and 2070. Blue regions indicate a decrease in tropical cyclone occurrence and red regions indicate an increase in occurrence. Results are from the CCAM Mark3 simulations forced with the SRES A2 scenario presented in Abbs *et al*.(2006).

50 km model and reported an increase of 22% by 2050, and a change in the latitudinal extent of tropical cyclones, with more storms forming closer to both the equator and the poles; a poleward extension of tropical cyclone tracks; and a poleward shift of over 2 degrees of latitude in the tropical cyclone genesis region. A poleward shift of 0.7 degrees of latitude (around 70 km) in the average tropical cyclone genesis region on both coastlines and a shift of almost 3 degrees latitude in the average decay location for east Australian cyclones were found for the year 2070 (Abbs *et al*. 2006).

Projected changes in tropical cyclone characteristics are inherently tied to changes in large-scale teleconnection patterns such as ENSO, changes in sea surface temperature and changes in deep convection. As global climate models improve, their simulation of tropical cyclones is expected to improve, thus providing greater certainty in projections of tropical cyclone changes in a warmer world.

5.9.2 Severe thunderstorms

Model results show that conditions will become less suitable for the occurrence of tornadoes in southern Australia in the cool season (May to October). There is an indication that hail risk may increase over the south-east coast of Australia.

The term thunderstorm refers to the relatively small-scale convective process that can occur when the atmosphere is moist and unstable. Rising air results in the formation of cumulonimbus clouds which develop rapidly and may be accompanied by lightning, thunder, severe wind gusts, heavy rain and large hail. The severity is in part related to the amount of moisture, and thus the energy, available through the condensation of that water in the cloud-formation process. In Australia, for a thunderstorm to be classified as severe by the Bureau of Meteorology, it needs to produce any of the following:

- Hailstones with a diameter of 2 cm or more at the ground
- Wind gusts of 90 km/h or greater at 10 m above the ground
- Flash flooding
- A tornado.

There are three simplified thunderstorm types: the single-cell, the multi-cell, and the super-cell. Of these, it is the multi-cell that is the most common, but super-cell thunderstorms account for most of the serious thunderstorm events experienced. The average annual thunder-day map for Australia is available from the Bureau of Meteorology (Kuleshov *et al*. 2002).

Neither global climate models nor regional, high-resolution models are able to capture thunderstorms. Hence, it is difficult to infer the impact of climate change on thunderstorms using a modelling approach. An alternative method is to use diagnostics of the large-scale environment that have been found to be favourable for the formation of such systems and to infer a risk of occurrence, rather than forecast, a particular event. Thunderstorms form when the atmosphere is buoyant enough to produce deep, moist convective clouds through heating or mechanical lift that causes the air to rise. Convective clouds are more likely to become organised into multi-cellular storms when the winds within the atmosphere change direction with height - these storms are more likely to produce severe weather. Rapid thunderstorm development can occur when the energy stored within the atmosphere by a temperature inversion (a 'lid') is released by heating or mechanical lift. The atmospheric parameters that are measures of these processes are:

1. for buoyancy – convective available potential energy (CAPE) or lifted index
2. for wind direction change – vertical wind shear
3. for temperature inversion – temperature lapse rate

Within such a framework it is possible, using the output from a global climate model or a reconstruction of the past global weather conditions (e.g. the NCEP/NCAR re-analysis), to obtain a climatology of risk areas. A world-wide climatology of areas favourable for severe thunderstorm and tornado formation has been produced by applying such a method to the NCEP/NCAR re-analyses (Brooks *et al*. 2003).

5.9.2.1 Cool season tornadoes

Cool season (May to October) tornadoes account for about 50% of all observed tornado events in Australia. They are mostly observed in the southern part of the continent, in particular in Western Australia and South Australia (Hanstrum *et al*. 2002). A diagnostic tool to help predict the risk of cool season tornadoes (Mills 2004) relies on two parameters: a measure of the instability of the atmosphere or the ability of the lower air to be raised in a convective development such as a thunderstorm (the surface lifted index up to 700 hPa) and a measure of the likelihood of twisting winds in the lower atmosphere (the vertical wind shear between 850 hPa and the surface).

The application of the diagnostic to a subset of four CMIP3 models (CCM-T47, CNRM, IPSL and MPI all forced with the SRES A2 scenario) for which daily outputs needed to calculate the two parameters were available, shows that favourable conditions for the formation of cool season tornadoes are likely to be reduced under global warming (Kounkou *et al*. 2007). Consistent across all models, a decrease (between 10 and 20%) of the cool season tornado risk at the end of the 21st century is projected. This is driven by a thermodynamical response: the stabilisation of the troposphere as seen by the increase of the surface lifted index. This thermal response is modulated by the dynamical response (changes in the vertical wind shear) and contributes to enhance or reduce the magnitude of the risk reduction from one model to another.

The methodology used in this study has not been proven for tornadoes during summer thunderstorms and hence it was not possible to assess the impact of climate change on this phenomenon during months other than May to October.

5.9.2.2 Large hail

A statistically significant relationship between convective available potential energy (CAPE) and hail events has been found for locations around south-eastern Australia (Melbourne and Mount Gambier), using both large-scale weather analyses and radiosonde measurements (Niall and Walsh 2005). This relationship was used to infer the likely change in hail occurrence in this region using output from the CSIRO Mark 3.0 global climate model for an environment containing double the pre-industrial concentrations of equivalent CO_2. From this, assuming that the relationship between the CAPE and hail remains unchanged under enhanced greenhouse conditions, it was concluded that there will be a decrease in the frequency of hail in these locations (Niall and Walsh 2005).

The diagnostic relationship between convective available potential energy (based on a parcel of air mixed over the lowest 100 hPa), the vertical wind shear between the surface and 6 km above ground level and the lapse rate of temperature between 2 km and 4 km above ground level, developed by Brooks *et al*. (2003), has been shown to describe the risk of large hail occurrence over eastern Australia. This relationship has been applied to output from the CSIRO Mark 3.5 model. The model captures the observed high hail-risk regions along the eastern coastline but overestimates hail risk over Victoria and Tasmania. Projections of changes in hail risk for the end of the century (based on the A2 scenario) indicate a dramatic increase along the south-eastern coastline (see Figure 5.52). The results also show a decrease in hail risk along the south coast of Australia, consistent with the projected decrease of cool season tornadoes in similar locations as described earlier, and points toward a general reduction of severe thunderstorm activity along the southern coast.

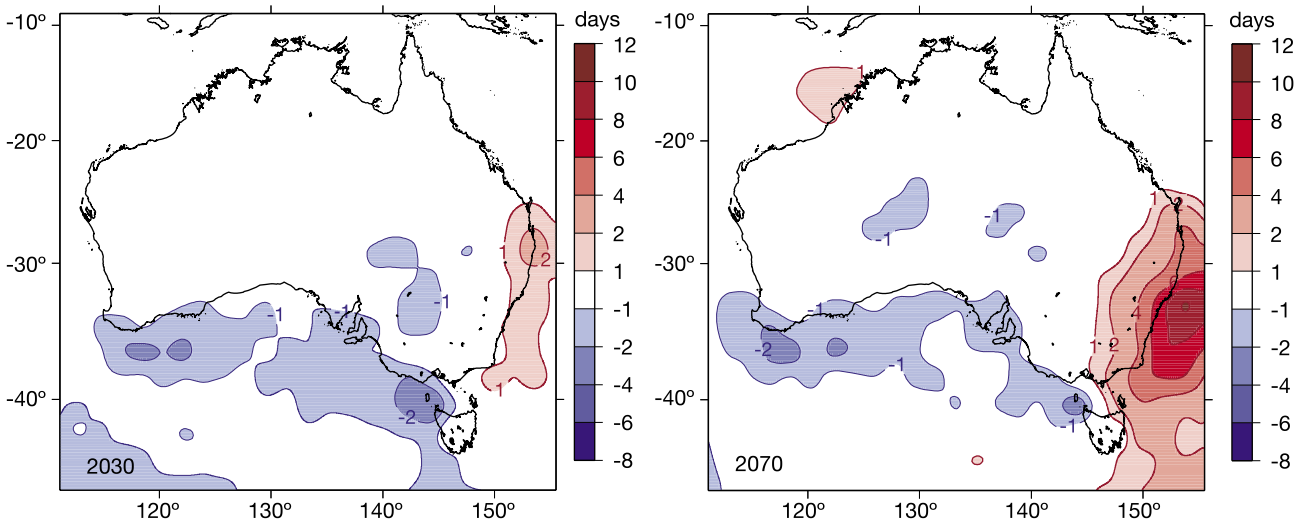

Figure 5.52: Projected changes in hail risk (hail-days per year) for 2030 and 2070 from the CSIRO Mark 3.5 model for the SRES A2 scenario. Blue regions indicate a decrease in hail risk and red regions indicate an increase in hail risk. The large-hail risk for this region is projected to almost double, increasing by between 4 to 6 days per year.

5.9.2.3 East coast lows

Model studies do not as yet indicate how the occurrence of east coast low pressure systems may change.

East coast cyclones, or east coast lows, occur primarily in autumn, winter and spring in regions of warm sea surface temperature anomaly and typically form when an upper-level short-wave trough or cut-off low moves over an area of strong low-level baroclinicity (Holland *et al*. 1987; McInnes *et al*. 1992). The coastal mountain ranges provide orographic uplift and provide a mechanism for the northward deflection of the low-level easterly flow. It is estimated that over 16% of all coastal heavy precipitation between 20 and 40ºS are directly related to east coast lows and that intensification of these events is often associated with strong zonal sea surface temperature gradients close to the coastline (Hopkins and Holland 1997). East coast lows are usually accompanied by a cut-off low at the surface, although the event that caused the Gold Coast flooding of June 2005 did not have a well-defined signature at the surface (Bureau of Meteorology 2006b). East coast lows have structural similarities to tropical cyclones in that they are highly convective and are warm-cored in the lower troposphere.

Studies of the ability of various climate models to represent the weather systems conducive to extreme precipitation and winds for locations along the New South Wales and southern Queensland coastlines find that the highest resolution models perform better than the coarser resolution global climate models (Abbs and McInnes 2004; Hennessy *et al*. 2004; McInnes *et al*. in preparation). There is an increase in the frequency of the weather systems that produce both extreme winds and extreme precipitation in a single regional climate model (Abbs and McInnes 2004). The projected changes in the frequency of east coast low events were sensitive to both the threshold used to define intensity and to the choice of model (McInnes *et al*. in preparation). For example, one regional climate model produced a decrease of 60% in the frequency of lows of 990 hPa or deeper by 2070, while a second model produced an increase of 40%.

5.10 ENSO, the Southern Annular Mode and storm tracks

5.10.1 ENSO's impact on Australia under global warming

In south-east Australia El Niño events are projected to become drier and La Niña events will tend to become wetter even if Pacific variability linked to ENSO does not increase.

Although studies involving a relatively large number of international models have been conducted (e.g. Zelle *et al*. 2005; Van Oldenborgh *et al*. 2005; Cane 2005; Philip and Van Oldenborgh 2006; Yamaguchi and Noda 2006; Joseph and Nigam 2006) the effect of global warming on ENSO is not clear, leading the IPCC (2007a) to conclude that "... there is no consistent indication at this time of discernable changes in ENSO amplitude or frequency in the 21st century".

Even if ENSO variability in the tropical Pacific does not change, ENSO's impact on Australia might (Smith *et al*. 1997). The CSIRO Mark 3.0 climate model was used to examine the ENSO response to 20th century and 21st century forcing, using three SRES scenarios (B1, A1B, and A2). The runs analysed were submitted to the CMIP3 database.

In all three 21st century scenarios, Nino3.4 sea surface temperature (i.e. the sea surface temperature averaged over the ocean surface, 190-240ºE and 5ºS-5ºN) exhibits a warming trend. ENSO variability about this trend was estimated by calculating the deviations of Nino3.4 sea surface temperature away from 30-year running averages. Interannual variability in south-east Australian precipitation was also assessed in a similar manner. The relationship between these year-to-year deviations in precipitation and Nino3.4 are depicted in Figure 5.53 for the three different scenarios for the 21st century. The corresponding data for the 20th century are depicted in each plot for reference (blue dots). In each case the level of interannual variability in both Nino3.4 and precipitation increases relative to the variability exhibited during the 20th century.

The results suggest that in south-east Australia El Niño events may become drier and La Niña events wetter even if Pacific variability linked to ENSO does not increase.

5.10.2 The Southern Annular Mode (SAM)

The Southern Annular Mode is likely to shift towards its positive phase (weaker westerly winds over southern Australia, stronger westerly winds at higher latitudes).

All climate models exhibit a trend in the Southern Annular Mode towards its positive phase when forced with increasing greenhouse gas concentrations. In fact this is one of the most robust signatures of future climate change found anywhere in the

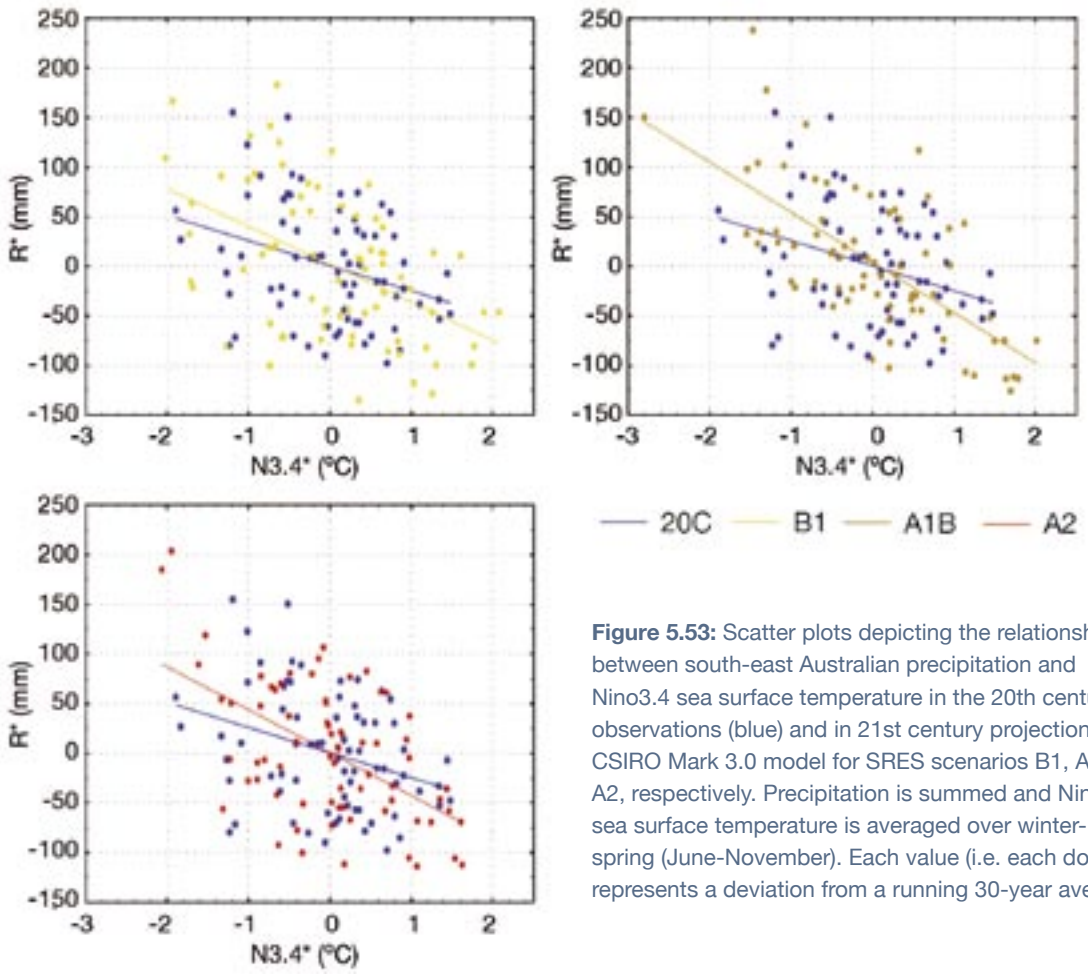

Figure 5.53: Scatter plots depicting the relationship between south-east Australian precipitation and Nino3.4 sea surface temperature in the 20th century observations (blue) and in 21st century projections of the CSIRO Mark 3.0 model for SRES scenarios B1, A1B and A2, respectively. Precipitation is summed and Nino3.4 sea surface temperature is averaged over winter-spring (June-November). Each value (i.e. each dot) represents a deviation from a running 30-year average.

globe (Miller *et al*. 2006). For recent trends however, it is likely that declining stratospheric ozone (Thompson and Solomon 2002; Gillett and Thompson 2003; Shindell and Schmidt 2004; Arblaster and Meehl 2006; Cai and Cowan 2007) and/or natural variability (Cai *et al*. 2003a, 2006; Marshall 2003) also played a role.

Although the ozone hole is projected to recover within the next 50 years, further rises in greenhouse gas concentrations will soon override the influence of ozone, with the SAM projected to keep trending upward over the 21st century (Arblaster and Meehl 2006; Miller *et al*. 2006). This is consistent with previous studies that find positive trends in the SAM in simulations forced solely with greenhouse gas concentrations (Fyfe *et al*. 1999; Kushnir *et al*. 2001; Cai *et al*. 2003a).

5.10.3 Storm tracks

Climate models indicate a decrease during the 21st century in the occurrence of winter low pressure systems over south-west Western Australia.

Changes in the Southern Annular Mode have also been associated with changes in storm tracks and synoptic weather systems in the mid-latitudes (Frederiksen and Frederiksen 2007; Hope *et al*. 2006). Changes in synoptic patterns influencing southwest Western Australia during winter in CMIP3 climate models showed a decrease in the frequency of the deep trough patterns in the latter part of the 20th century. The decrease in the number of deep troughs and an increase in number of synoptic types with high pressure regions across south-west Western Australia became more marked in simulations with increasing levels of atmospheric greenhouse gases. This response was evident during the late 21st century for all SRES scenarios, and earlier in the century under the higher emissions scenarios (Hope 2006).

Chapter 6 Application of climate projections in impact and risk assessments

Risk management is an iterative process, where a process of scoping and risk identification usually takes place before more detailed assessments are carried out. Care must be exercised when using the projections from Chapter 5 in any risk assessment, particularly when selecting climate variables, determining temporal and/or spatial resolution, and dealing with uncertainty.

Detailed risk assessments generally require purpose-built climate projections, including time series, or probabilistic representations of future climate. Various tools have been developed which represent different methods for enhancing the delivery of climate information to stakeholders both for education and for risk assessment and management. Nevertheless, significant challenges remain for communicating climate risk in ways that can be effectively used in risk management.

The major purpose behind constructing and using climate change projections is to aid decision-making in an environment of uncertainty. There are subtle but important differences between the development of climate change projections and the use of such information for impact and risk assessment.

The context of an assessment determines the information required and how it can best be used: who it is for, what it is about, where it is located and how the results are to be used. Specific methods for treating uncertainty are largely dictated by context and the needs of stakeholders. Such needs also include the development and sharing of a conceptual framework, i.e. sharing the researchers' and stakeholders' understanding of how the system in question operates, creating a viable assessment process, and communicating assumptions and confidence levels as part of the assessment process.

Climate change risk assessment and management is an emerging and inherently inter-disciplinary science. New approaches and methods for incorporating information about future climates into assessments are constantly being developed. Appropriate methods and tools are largely dictated by an assessment's context, rather than through a 'best practice' set of recipes. This chapter summarises the use of climate information to inform impact assessment and risk management.

6.1 Climate change and risk management

Climate risk is the product of the *consequences* of climate change and the *likelihood* of those consequences (Jones 2001; ISO 2002; Figure 6.1). In the past, climate change impact assessment has been dominated by analysis of the consequence component of climate change risk, especially in testing the consequences of unmitigated climate change. The estimation of impacts independently of likelihood continues to be a mainstream research activity. However, as questions regarding risk have become more sophisticated, such as 'how much climate change needs to be adapted to by when', more decision-makers are seeing climate change as a risk management issue. This development is increasing the need to assess the likelihood of specific risks. However, great care is warranted because likelihoods need to be developed appropriately: all relevant uncertainties need to be managed carefully and underlying assumptions clearly stated to avoid under- or over-confidence, incorrect framing of the problem or misapplication of the results.

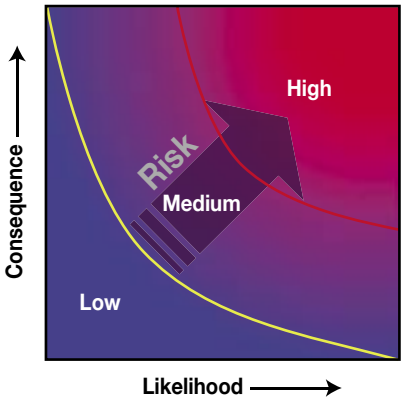

Figure 6.1: Conceptual model of the likelihood – consequence relationship

Risk management applies scientific and technical analyses to estimate the likelihood of different outcomes. The process is often conceptualised as a series of steps, which identify the context, characterise the hazards and/or potential consequences, assess the likelihood of different outcomes, evaluate risk, and, ultimately, implement appropriate method(s) for reducing risk (Box 6.1).

Box 6.1 A risk management framework

A number of frameworks exist that provide guidance on applying the principles of risk assessment and management in decision-making. In Australia, the principal framework is the Australia/New Zealand Risk Management Standard (Australian Standards 2004), which has recently been adapted to provide guidance specific to managing climate risk (AGO 2006a). The Risk Management Standard divides the process of risk management into five steps:

1. **Establish the context** – identification of the decision-making event and the associated challenges, establishment of the approach to risk management that is to be used as well as the information and data requirements (including climate projections);
2. **Risk identification** – identification of the potential climate hazards and downstream consequences of concern to stakeholders;
3. **Risk analysis** – qualitative or quantitative analysis of the likelihood of different outcomes, including the probability of exceeding stakeholder-identified thresholds;
4. **Risk evaluation** – assessment of whether risks are tolerable, prioritisation of multiple risks (if present), and judgment regarding whether risks require treatment; and
5. **Risk treatment** – selection and implementation of risk management actions (e.g. through methods such as stakeholder forums, multi-criteria analysis, cost-effectiveness).

In addition, **communication and consultation** with stakeholders occurs throughout the entire process. Clarity and transparency surrounding underlying concepts and assumptions is required. All participants need to understand the different ways in which the system is conceptualised and used by various stakeholders. **Monitoring and review** ensures that a learning-by-doing ethos is developed and communicated among all parties. Risk management should not be a one-off event, but a process that is engaged over time and updated with changing information and stakeholder preferences.

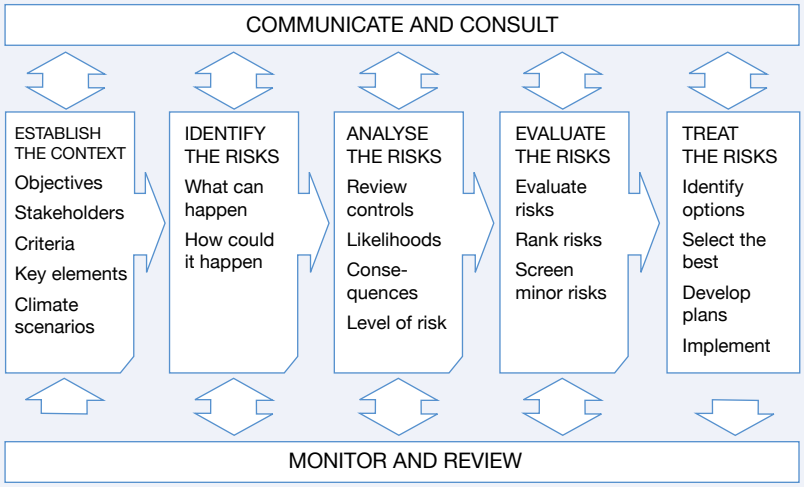

The two main strategies for managing climate risk are: *mitigation* of climate change via the abatement and sequestration of greenhouse gas emissions and *adaptation* to climate impacts emanating from the unmitigated component of climate change (IPCC 2007b,c). For each there are myriad specific policies and measures that could be implemented. Combined with the uncertainties associated with future climate change, they form a complex decision-making environment. Both public and private institutions need to navigate this complexity to manage climate risk, whether it is in assessing the benefits of avoided damages via mitigation (Preston and Jones 2006; Jones and Preston 2006) or the potential for adaptation options to reduce societal vulnerability. This has increased the demand for climate information.

Climate risks can be divided into two broad categories (Sarewitz *et al*. 2003):

1. **Event risk** – The risk of occurrence of natural hazards such as sea level rise, storm surge, or extreme rainfall events. *Consequence* is expressed as the occurrence of a discreet event of a particular size or duration and may be integrated with *likelihood* through the quantification of an event return period. For example, the identification of a 1-in-100 year storm event communicates the frequency or likelihood (once every hundred years) of an event as well as its magnitude (in terms of wind speeds or rainfall totals). Event risk is often quantified as hazard times likelihood and is typical of assessments carried out by the natural disaster and insurance communities.
2. **Outcome risk** – Risks associated with environmental or societal outcomes of climatic changes such as species extinctions, loss of agricultural productivity or heat-related human mortality. *Consequences* are expressed as impacts for one or more scenarios of climate change, and may be integrated with *likelihood* through uncertainty analysis (e.g. generation of a probability distribution) or the quantification of the likelihood of exceeding a vulnerability threshold (Jones 2001). Outcomes may also incorporate risk from non-climatic sources, allowing climate change to be assessed in a broader social and environmental context.

Both types of risk are useful to stakeholders for risk management, their choice depending on how rigorously they can be quantified and the form in which that information can be produced, subject to requirements. Risk management is iterative, where a process of scoping and risk identification usually takes place before more detailed assessments are carried out to manage specific risks identified by those initial assessments.

National to regional scale climate projections provide valuable information at this initial stage, which helps establish the context for risk management and scope the potential consequences (Box 6.1). Quantification of event risk is typically a first step in a risk analysis, which requires integrating information on climate events into impact models that predict the resulting system responses. Outcome risks, or clear links between event risks and outcomes, are generally preferred for assessing adaptation needs. Most adaptation measures are designed to reduce negative or enhance positive consequences.

More detailed risk assessments generally require purpose-built climate scenarios or probabilistic representations of future climate. These are discussed in sections 6.2 and 6.3.

When assessing climate risk, caution must be exercised to avoid over-investment in analytical precision. Due to uncertainties associated with climate change and limits to time, expertise, system knowledge, or funding, it may be difficult to derive robust estimates of risks, especially outcome risks, which may also be heavily influenced by the evolution of future adaptive capacity (Patt *et al.* 2005). In such situations, effort may be best-invested in identifying least-cost strategies for achieving risk reduction, rather than exhaustive attempts to reduce uncertainty or to rigorously quantify the risk itself. Identifying and reducing existing system vulnerabilities to climate variability may also help to manage future climate risks (Sarewitz *et al*. 2003; Allen Consulting 2005), especially where risks under current climate are consistent with future risks identified during scoping exercises.

6.1.1 Framing climate risks

A range of different assessments of climate risk can be carried out, such as:

- Impact assessments of unmitigated climate change, testing what may happen if no specific climate policies are enacted; this covers most of the assessments within the IPCC Working Group II contribution to the Fourth Assessment Report (IPCC 2007b);
- Assessing the benefits of greenhouse gas emission policies through avoided damages measured as the difference in climate-related risks associated with a reference emissions scenario (e.g. the unmitigated SRES scenarios) and those associated with a mitigation policy scenario (e.g. Jones and Preston 2006); integrated assessments will consider benefits from both adaptation and mitigation (e.g. Stern *et al*. 2007);

- Assessing adaptation needs over a range of policy and planning horizons for specific activities and regions;
- Assessing how specific development pathways or policies may be affected by climate change and developing adaptation options to make them more sustainable. Integrating adaptation options into ongoing plans and activities, especially into current risk management activities, is referred to as *mainstreaming*.

In general, the benefits of mitigation are longer-term (decades) and the benefits of adaptation are shorter term (years to decades), but not exclusively so (Figure 6.3). Key to assessing adaptation needs is planning horizons: what is the rate and magnitude of change anticipated within a given planning horizon that needs to be adapted to?

When assessing adaptation, it is important to take a whole of climate approach by representing *both* human-induced climate change and background climate variability. The change may be linear, graduated non-linear, or a step change. Many subsequent risks will follow a similar pattern. Background variability may also alter in response to climate change but this possibility needs to be investigated on a case-by-case basis.

Planning horizons mark how far into the future adaptation measures may be needed. Timing is informed by both operational and aspirational goals. Aspirational goals relate to what is desired (e.g. sustainable operations, profitability) or should be avoided (e.g. critical levels of harm, system failure). Operational goals relate to the pathway that is taken to achieve that goal.

Incremental adaptation allows a learning-by-doing approach to be taken, informing the process along the way and allowing it to adjust to new information. Up-front responses, or the need to anticipate outcomes in advance, are most relevant to adaptations that require large initial planning and investment, those with a long operational life (and where retrofitting is too expensive) or if the damage to be avoided is irreversible and/or unacceptable. The 'wait and see' response is thought in most cases to be the most expensive option and will not cope with irreversible impacts.

Figure 6.3 shows a sample of planning horizons for different activities (lower scale) and operational pathways towards achieving a specific goal (upper scale). These are not intended to represent a complete set of pathways – many paths are possible depending on circumstance. The process for deciding which adaptation(s) to implement may also assess which type of adaptation pathway is most suitable. If aspirational targets are some decades away, the capacity to carry out an assessment over a range of timescales may be needed to test variable timing of responses. This is a far more sophisticated requirement than is being applied in most existing assessments.

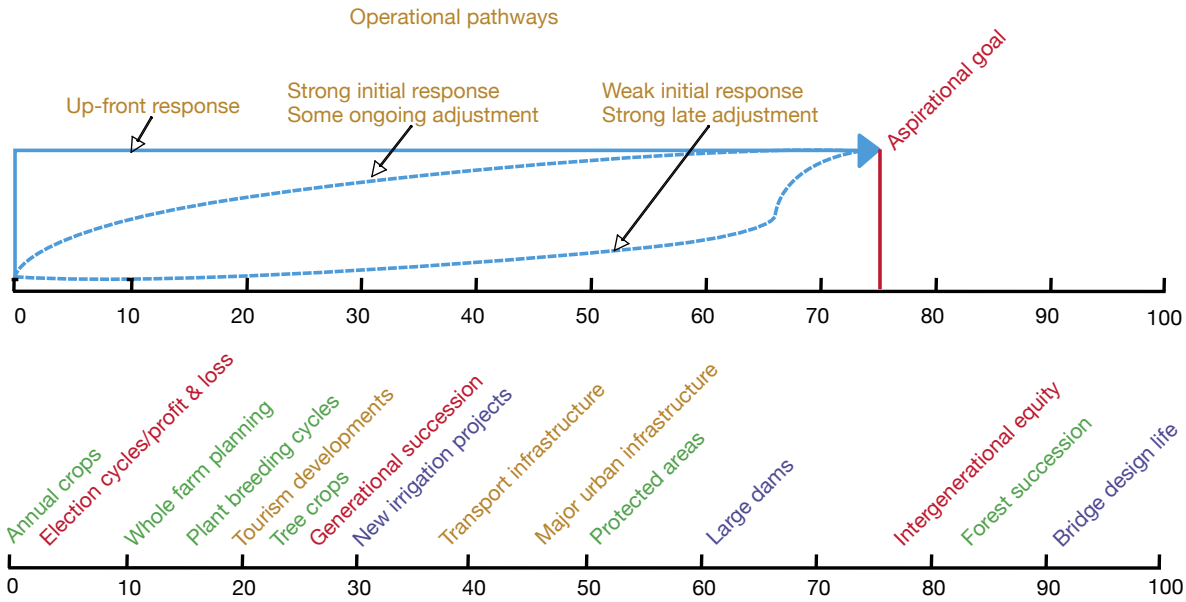

Figure 6.3: Relationship between goals and pathways for adaptation (upper diagram), related to a number of planning horizons of different timescales (lower diagram). The horizontal scale is in years.

6.2. Key issues in applying climate information

The choice of which climate information may be required for use in any impact or risk assessment is determined by the:

1. climate variable(s) of interest
2. spatial and temporal scale of the assessment
3. management of uncertainty

The first two factors, properly applied, will establish the plausibility of any resulting climate information and the third factor will establish confidence in the results.

Most projections, such as those detailed in this report, are not forecasts but are conditional upon the assumptions incorporated into the input data and model that produced those projections. Many of the assessments listed in section 6.1.1 do not require forecasts. For example, scenarios used in an assessment of unmitigated climate change risks would aim to be physically plausible under the forcing conditions consistent with that change, but would not necessarily be expected to occur. Analyses testing the sensitivity of impacts to specific climate change likewise do not require forecasts.

When assessing adaptation needs over the short to medium term, the aim should be to come as close to the anticipated range of plausible climate change as possible. However, because a whole of climate focus is taken, combining Australia's substantial ongoing climate variability with the uncertainties of climate change, uncertainties will be substantial. Assigning likelihoods to specific outcomes is becoming increasingly possible with model improvements and more sophisticated approaches and methods. However, the large inherent uncertainties remain a reason as to why off-the-shelf estimates and the uncritical use of climate projections are not advised.

6.2.1 Climate variables

A major task in any assessment is to identify the relevant climate variables, either associated with event risk or those that drive subsequent responses of societal and environmental systems (Table 6.1). Although the projections developed for this report span a broad range of variables, for any given application or risk of concern often only a subset of these is required. A robust physical relationship between the selected variables and the outcome of interest should be ensured. Appropriate variables may be identified by stakeholders, conceptual models of the system of interest, or through the use of more detailed process models where prior research and experience has elucidated the key climate drivers of the system.

The form of a selected variable will differ from system to system; for example:

- Species richness in the wet tropics is a function of maximum and minimum temperatures and rainfall during summer and winter seasons as well as intra-annual variability in temperature, rainfall and radiation (Williams *et al.* 2003).
- Maximum average January temperature is the most sensitive indicator of grape quality for a number of varieties (Webb 2006).
- Changes in alpine snow conditions depend on daily precipitation and temperature (Hennessy *et al*. 2003).

Although most event-based risks will be in response to changes in extreme conditions (IPCC 2007b), it is often difficult to provide reliable estimates of such changes. Instead, changes to mean conditions have most often been relied upon. For example, while past assessments of coastal impacts applied average sea level change in Bruun Rule-like algorithms (CIU 1992; Zhang *et al*. 2004), the interaction of higher sea levels with extreme tides resulting from natural climatic variability and/or anthropogenic climate changes are more realistic (McInnes *et al*. 2003, 2005a,b). Similarly, projections of changes in extreme rainfall events are central to understanding flood risk (Hennessy *et al.* 2004; Abbs *et al*. 2006), extreme heat for understanding heat-related mortality (McMichael *et al*. 2002), and fire weather for understanding bushfire risk (Hennessy *et al*. 2005).

To develop meaningful estimates of the risk of such climatic events, simulations using low-resolution climate models to derive average changes in climatic conditions are not sufficient. Instead, high-resolution modelling through statistical or dynamical downscaling and nested modelling techniques is often required to simulate such events (Abbs *et al.* 2006). However, there is a trade-off between the application of simple and easy to apply methods and the time, money and effort needed to provide more realistic detail that each assessment must confront. Ideally, scenarios should be constructed using the simplest information required to make the decision under consideration, but this is not always an easy task.

When identifying climate variables and selecting the relevant climate models used for generating climate scenarios, each scenario used in a risk assessment should be internally consistent. For example, all projections of rainfall and temperature changes applied in an agricultural impact model should be incorporated under a consistent set of assumptions, including the choice of global climate models, time period, and greenhouse gas emissions scenario. Arbitrary mixing-and-matching of projections degrades the realism of the outcome and limits comparability of different impact and risk assessments (Box 6.2).

Table 6.1: Common climate variables used in impact and risk assessment

Impact area	Impact	Climate variables	Examples
Agriculture	• Dryland wheat production • Grape quality	• Temperature • Rainfall	• Howden *et al*. (1999) • Howden and Jones (2001) • Luo *et al*. (2005) • Webb (2006)
Water resources	• Stream flows • Storage inflows	• Rainfall • Evaporation	• Jones and Page (2001) • Jones and Durack (2005)
Coasts	• Sustainable yields • Storm surge return periods and area inundated	• Sea level rise • Winds • Pressure	• Kirono *et al*. (2007) • CIU (1992) • Cowell *et al*. (2006) • McInnes *et al*. (2003) • McInnes *et al*. (2006)
Infrastructure	• Impacts to buildings • Road maintenance costs • Energy production	• Temperature • Rainfall • Radiation • Winds • Sea level rise	• Amitrano *et al*. (2007) • Austroads (2004) • PIA (2004) • PB Associates (2007) • Victorian Government (2007)
Terrestrial biodiversity	• Primary production • Population extinctions	• Temperature • Rainfall • Radiation	• Pickering *et al*. (2004) • Williams *et al*. (2003)
Marine biodiversity	• Coral bleaching and mortality	• Sea surface temperature	• Hoegh-Guldberg (1999) • Done *et al*. (2003)
Health impacts	• Heat-related mortality • Infectious disease	• Temperature • Rainfall • Humidity	• McMichael *et al*. (2002) • Woodruff *et al*. (2005)
Fire weather	• Fire intensity & frequency • Length of fire season • Period suitable for controlled burning	• Precipitation • Temperature • Relative humidity • Wind	• Hennessy *et al*. (2005)
Alpine snow conditions	• Snow cover • Snow depth • Snow duration	• Precipitation • Temperature	• Hennessy *et al*. (2003)

Box 6.2 Applying internally consistent climate change scenarios

Because different global and regional climate models display marked differences with respect to future climate projections, multiple models are often used to generate climate scenarios for impact assessment. This enables the uncertainty in future climate conditions to be reflected in estimates of impact and risk assessments, often by identifying of potential 'best' and 'worst' case impact scenarios. Care must be exercised to preserve the internal consistency of a model's projections of different climate variables. Variables such as temperature, rainfall, evaporation, and humidity are highly interactive, meaning a change in one variable has an effect on other variables. As such, mixing variables from different models in a single scenario may result in physically implausible (or impossible) combinations.

For example, to identify the worst possible outcome from an impact model, it may be tempting to identify the most pessimistic rainfall projection from any climate model and pair that scenario with the most pessimistic temperature projection (Figure 6.4a). However, because the projections for the variables were derived from different climate models, they may be physically inconsistent, providing a spurious estimate of future impacts. The magnitude of projected impacts would therefore be larger than that derived from internally consistent projections.

Instead, estimates of impacts should first be calculated independently for each climate model under consideration (Figure 6.4b). This results in a range of impact estimates that are representative of plausible climate futures which can then be ranked according to their relative impact. Low, high and/or intermediate outcomes, or combinations of those in probability distributions, can be selected for further application.

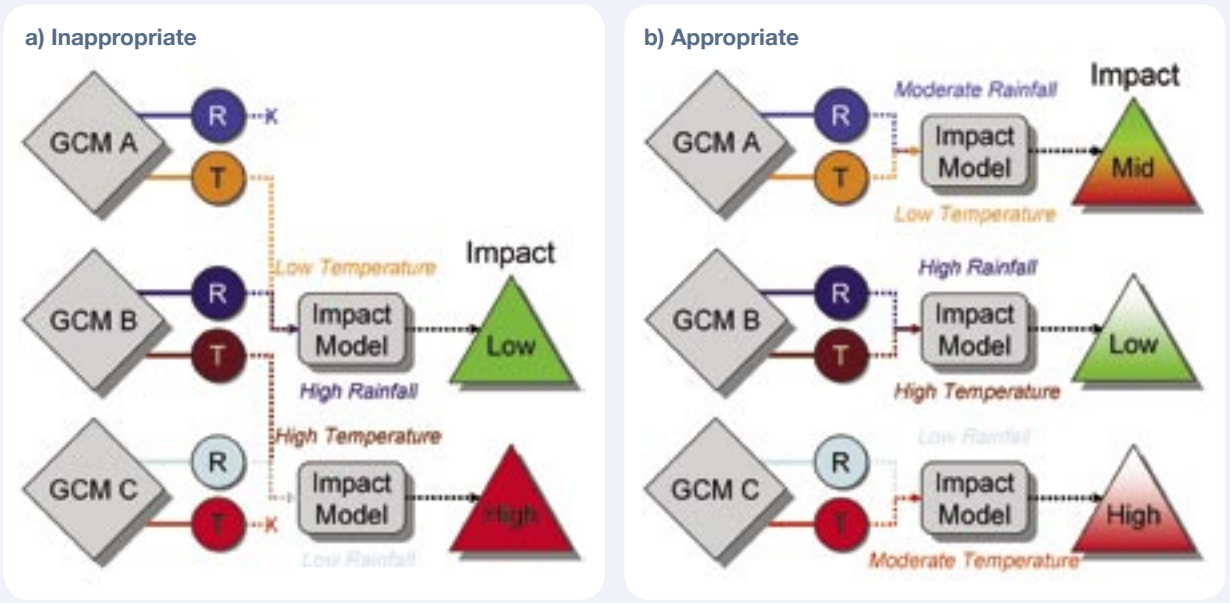

Figure 6.4. Example of appropriate and inappropriate use of climate model projections in impact assessment. For both of the above figures, rainfall (R) and temperature (T) projections from three different global climate models (GCMs) are applied in a hypothetical impact model. In **(a)**, each pair of global climate model scenarios is applied independently to the impact assessment model, resulting in a range of different climate impacts. In **(b)**, projections of rainfall and temperature from different models are paired to yield extreme scenarios of climate change, which are then applied to the impact model.

6.2.2 Spatial and temporal scales

Each assessment needs to decide the temporal and spatial scales over which that assessment will be conducted by considering the following aspects:

- the time horizon for the projected climate change or impact
- future time slice or transient time series
- the temporal resolution of the projection or assessment
- single point, multiple points or geographic areas
- the spatial resolution of the projection.

6.2.2.1 The time horizon for the projected climate change or impact

By convention, most of the climate change projections and estimated impacts developed internationally have employed time horizons of approximately one century (e.g. out to 2100), as illustrated by IPCC global temperature and sea level projections (IPCC 2001, 2007a). This reflects the limit of most greenhouse gas scenarios and climate model simulations. Australian climate projections and estimates of impacts often extend to the late 21st century (i.e. 2070) although more immediate time horizons are also routinely employed (e.g. 2025, 2030 or 2050). However, the stakeholder focus groups conducted for this report reflected the growing demand for time horizons more consistent with planning horizons for many industries and sectors, ranging anywhere from 1 to 25 years.

6.2.2.2 Fixed time or transient time series

The CSIRO (2001) projections of Australian climate change and a wide variety of impact assessments relied upon time slices centred on 2030 and 2070 (Whetton *et al*. 2005). Many specific applications, for example, both hydrological and crop models require the use of long time series to adequately capture a realistic response due to climate variability. These can be used as time slice (a changed climate for a number of decades centred on a given year) or transient inputs (a gradually changing climate spanning the present to future). Because some systems (particularly natural ecosystems and biodiversity) are affected as much by the rate of climate change as the magnitude (IPCC 2004), transient projections may be required to estimate rates of climate changes over various time periods.

6.2.2.3 Temporal resolution

Climate projections may be developed on annual, seasonal, monthly, weekly, or daily time steps. Sometimes seasonal to annual information is sufficient to develop a general understanding of future trends and dynamics. However, many complex processes, such as specific hydrological or agricultural systems, may require daily time series data as input, even though the results may be aggregated to seasonal to annual values. Preparation of high resolution data is often resource intensive. Daily data from climate models is available from a limited number of models and time periods, but this situation has improved with the latest set of climate models. Methods for preparing scenarios incorporating daily data include dynamic and statistical downscaling and perturbation of historical time series by monthly or annual change factors, the most common method used to date (Chiew 2006).

6.2.2.4 Single point, multiple points, or geographic areas

Climate projections require data presented in a range of spatial forms. For example, agricultural crop models are often location-specific and hydrological models may require information for specific nodes within the surface water system. In such instances, climate projections at specific geographic locations (grid-cells) are necessary to drive impact assessment models for one or more locations. Howden *et al*. (1999) used climate model projections to simulate climate change impacts on dryland wheat production for 11 point locations throughout the Australia wheatbelt but aggregated the result to assess national impacts. Kirono *et al.* (2007), used climate projections for the Lismore region in northern New South Wales to drive hydrological modelling of the Richmond River catchment. Hennessy *et al*. (2005) projected changes in fire weather for 17 sites in south-east Australia. Other impact assessment applications have simulated impacts over an entire region or landscape (e.g., Hennessy *et al*. 2003; Williams *et al*. 2003; Jones *et al*. 2007), thereby capturing spatial heterogeneities. For such applications, climate projections that reflect the spatial variability in future changes are needed, often as gridded data sets of varying geographic and temporal resolutions.

6.2.2.5 The spatial resolution of the projection

The spatial resolution of climate information is a core challenge for development of climate projections. Climate model output is often produced on a geographic grid of 300–400 km, yet underlying climatological gradients and land surface heterogeneity lie within these spatial scales. Capturing events such

as thunderstorms or tropical cyclones requires much finer resolution (e.g. 1–5 km; Abbs *et al*. 2006). Quantifying the impacts of climate change at relevant scales is also important for decision-making. Although climate projections are often provided at coarse resolution, many of the datasets for baseline climate, soil, runoff, topography and land use in Australia that are useful for supporting risk assessment research are available at resolutions from 1–5 km (e.g. spatial datasets generated for the 2001 National Land and Water Resources Audit) while remote sensing may allow the built environment to be resolved with centimetre-scale precision. However, if it can be shown that coarse resolution climate changes overlaid on higher resolution baseline data provide realistic simulations of change, the spatially explicit modelling of impacts can be accomplished even with coarse projections.

6.3 Treatment of uncertainty

While the role of science is to improve our understanding of how systems work, research does not always reduce uncertainty. For example, when a poorly known process becomes better quantified and added to other known uncertainties, the total quantified range may increase, fuelling the perception that uncertainty has increased. However, a qualified uncertainty has merely been quantified. For example, the addition of carbon cycle uncertainties to the range of global average warming in IPCC (2007a) have led to a greater range of global warming than in IPCC (2001). Examples of uncertainties that were reduced in the Fourth Assessment Report include the thermal component of sea level rise, the 'likely' range of climate sensitivity (IPCC 2007a) and ranges of warming for selected regions (Fig 2.6 in Carter *et al*. 2007). Advances in scientific research pertaining to current climate and projections of regional climate change for Australia are discussed in Chapters 2 to 5.

The main methods for managing the resulting uncertainties contained within climate projections research in impact and risk assessments can be grouped into contextual and statistical approaches. Contextual approaches, which reduce structural uncertainties described in section 4.2.4, are discussed in section 6.1, and statistical approaches, which reduce value uncertainties, are described below.

Some of the key uncertainties associated with climate projections, include:

- Future emissions of greenhouse gases and aerosols
- Climate sensitivity
- Regional expressions of global climate change.

Additional uncertainties arise during the impact assessment process, namely:

- System sensitivity to climatic changes
- System adaptive capacity.

These key climate uncertainties translate into an uncertainty space bounded by plausible parameters for climate sensitivity, future greenhouse gas emissions, and regional patterns of change. (These are not the only uncertainties that may need to be managed during a risk assessment – for example, environmental and socio-economic factors may both contribute to risk as stressors and modifiers of impact and resulting consequences. However, space only permits a discussion of the major climate-related uncertainties.)

This uncertainty space can be explored using a range of statistical methods that include various sampling strategies. Because of the many contributing uncertainties and possible contexts for assessment, there is no completely objective way of applying these statistical methods to manage uncertainties. Instead a hierarchy of approaches is used – these range from multi-model studies that produce probability distributions, various sampling methods applied to quantified ranges of uncertainty, and expert judgement through to the exploration of 'what if' scenarios and sensitivity studies (Box 1.1 in Chapter 1). Sometimes, an assessment will combine several of the above approaches in scenario construction.

All approaches used need to be clearly described, transparent (i.e. assumptions are clearly stated) and reproducible. Credibility with stakeholders is an important part of whether the results are ultimately accepted. One major test to determine whether a specific uncertainty, and

how it is constructed, is important to a result is to gauge its robustness under different assumptions (e.g. Jones and Page 2001; Dessai and Hulme 2007). If the result is insensitive to changes in the underlying uncertainty then that particular source of uncertainty can be overlooked. If the result is sensitive, then confidence in how well that particular aspect of uncertainty has been represented, and how it contributes to the total uncertainty, will influence how the results are interpreted and taken up. In this context, the sensitivity testing of methods and assumptions becomes an extension of more conventional sensitivity assessments, such as those that test sensitivity to changing inputs. However, such work does require the expenditure of resources, which may compete with the resources required to construct physically plausible scenarios discussed in section 6.2. Trade-offs between uncertainty management and scenario detail (e.g. spatial and temporal downscaling) in an assessment may be required.

The following descriptions portray how climate change uncertainties have been represented in a range of assessments conducted in Australia over the past decade. They are presented in a hierarchical order ranging from the use of simple scenarios through to methods that fully explore the plausible range of uncertainty.

6.3.1 Representing climate uncertainties

Most often, bounded estimates of climate change are used rather than the total uncertainty as portrayed in Figure 4.4 of Chapter 4. Figure 6.5 shows three representations of sampling within an uncertainty space. A single model, with a single emissions scenario, and low, medium, and high climate sensitivities results in three different estimates of future change, confined to one region of the uncertainty space. When additional emissions scenarios are included, a broader range of futures becomes apparent. With the inclusion of additional models, the range of potential changes becomes even wider. However, by combining uncertainties for climate sensitivity, emissions, and regional climate patterns the resulting projections can be represent the plausible uncertainty space of judged climate change (section 4.2.4).

The lower series in Figure 6.5 describes the current state of play. This report describes a range of climate models, greenhouse gas emission scenarios and climate sensitivities that can be used to represent both biophysical and socio-economic uncertainties. The difference between the sample of 144 projections compared to the sample of three projections in Figure 6.5 emphasises that any likelihoods and associated statistical measures (e.g. mean, median or standard deviation), will differ substantially depending on the assumptions and method used to characterise uncertainty (Lopez *et al*. 2006).

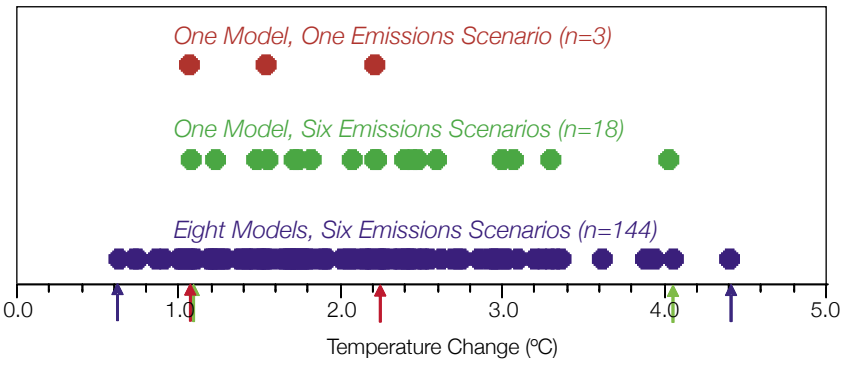

Figure 6.5: Projected changes in annual mean temperature in Canberra in 2070 based on simulations with the OzClim scenario generator (www.csiro.au/ozclim; Page and Jones 2001). Results are presented for temperature changes using one model (CSIRO Mark 3.0) with one emissions scenario (A1) and three climate sensitivities (red); one model (CSIRO Mark 3.0) with the six IPCC illustrative scenarios (green); and eight models with the six IPCC scenarios (blue). Coloured arrows on the axis identify the minimum and maximum results for each ensemble of results.

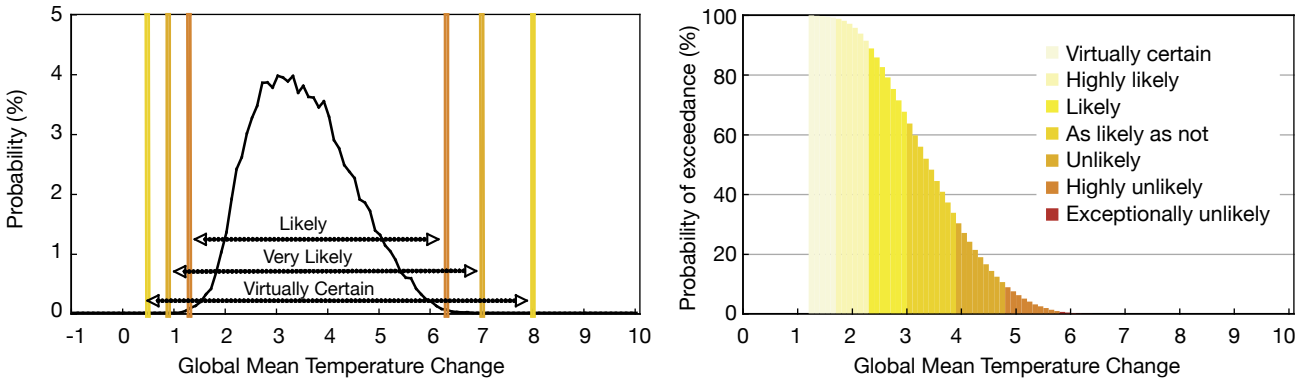

Figure 6.6: Likelihood of global average warming in 2100 consistent with the climate sensitivity, carbon cycle uncertainties and range of SRES emissions scenarios summarised in IPCC (2007a). The left hand panel shows the conditional probability of occurrence along with the likelihood that the 'real' answer (given the underlying assumptions are considered realistic) will lie within the stated range. The right hand panel shows the likelihood of exceeding a given level of change.

Other strategies include continuous random sampling of the uncertainty space (e.g. Monte Carlo and bootstrap sampling techniques), structured sampling and model weighting according to representativeness or skill as discussed in Chapter 4.

Probabilities can be expressed in two ways. One is as a probability density function as shown in Figure 4.6, where several sources of uncertainty, or a suite of model results may combine in a probability density function where the central tendencies are more likely than the extremes. This is a predictive framework that estimates conditional likelihoods of specific outcomes, often event-based risks. The other is as a cumulative distribution function that measures the likelihood of exceeding a given limit or threshold, and is more suited to the assessment of outcome risk. The first gives the conditional probability of occurrence and the second the conditional probability of exceedance (Figure 6.6). The key advantages in using cumulative probability functions, or assessing the likelihood of exceedance, are that it measures risk from a baseline and is much less sensitive to underlying uncertainties than the probability density function (Jones 2004).

6.3.2 Examples of uncertainty management in impact and risk assessments

A single projection of future climate conditions may be sufficient to illustrate the type of changes that can occur and the potential sensitivity of impacts to that change, or to test a particular method of downscaling. However, for most other purposes, it is better to apply a larger number of projections that represent a larger portion of the uncertainty space.

One commonly used approach is to apply widely divergent estimates of future changes, such as a

'best case' and a 'worst case', for example by constructing two projections combining a higher climate sensitivity (commonly yielding higher temperatures) with drier conditions, and a lower climate sensitivity with wetter conditions (e.g. NAST 2000; Hayhoe *et al*. 2004; Edmonds and Rosenberg 2005). The use of disparate emissions scenarios can further accentuate the difference in projected futures. However, while both may be plausible, they represent limited uncertainty and it is difficult to determine which, if either, might be more likely.

Alternatively, investigators can examine a broad range of climate projections from multiple climate models to identify 'low' and 'high' projections that are more reflective of the full range of uncertainty (AGO 2006a,b). For example, Figure 6.7 shows low and high projections of climate change impacts to snow conditions in the Australian Alps (Hennessy *et al*. 2003). This approach has the advantage of representing the range of uncertainty in future conditions, while communicating this information in a relatively simple manner. As discussed in Box 6.2, when applying such projections in impact assessment models, care must be taken to ensure projections are internally consistent.

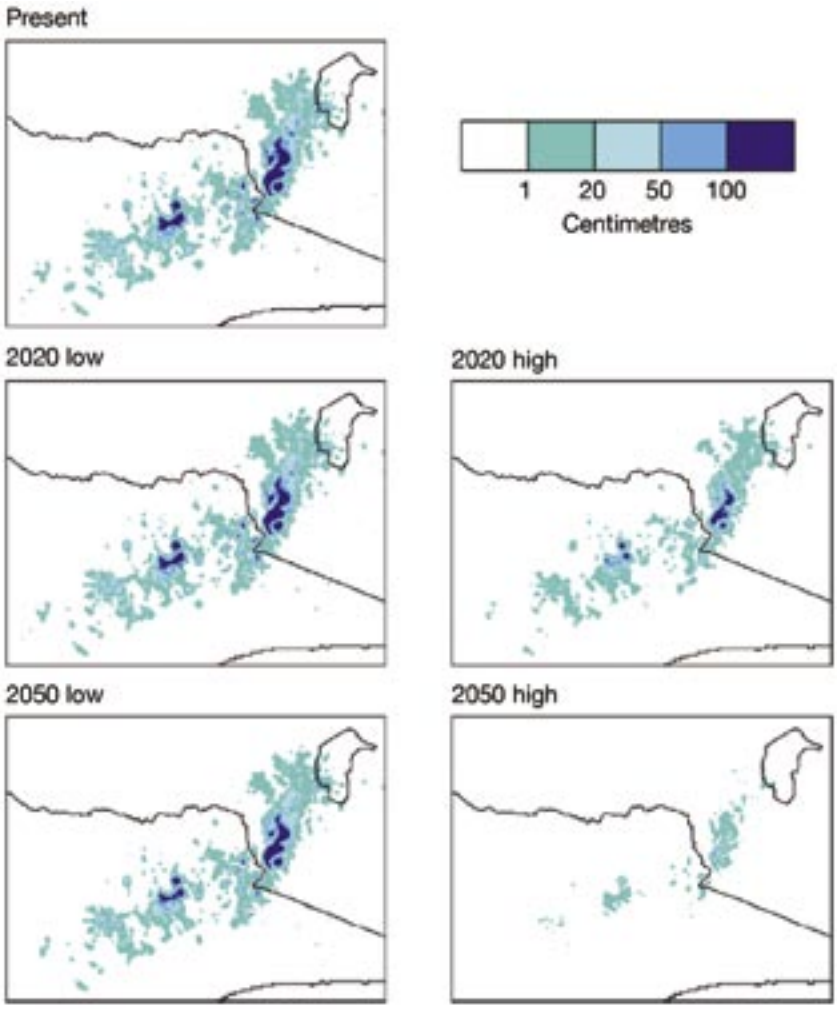

Scenario (Year)	Projected Change in Temperature (°C)	Projected Change in Precipitation (%)
Low impact (2020)	+0.2	+0.9
High Impact (2020)	+1.0	-8.3
Low impact (2050)	+0.6	+2.3
High impact (2050)	+2.9	-24.0

Figure 6.7: Projected 'low' and 'high' changes in alpine temperature and precipitation for 2020 and 2050, relative to 1990 (bottom) and associated simulated annual average maximum snow depth (cm) (top).

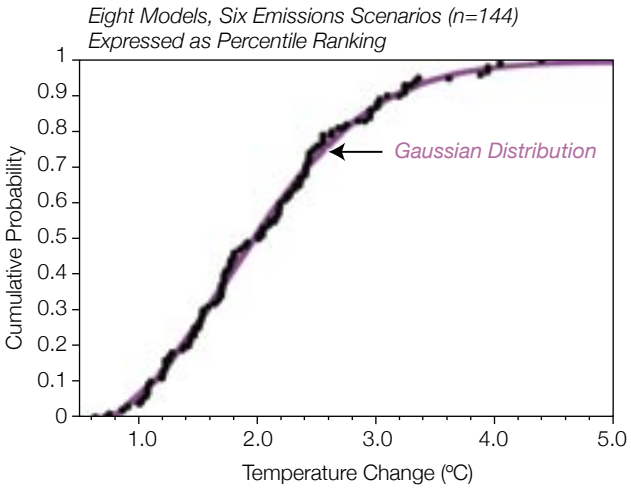

Figure 6.8: Cumulative probability distribution for annual mean temperature change in Canberra in 2070. Black circles represent 144 projections from eight climate models with three climate sensitivities and the six illustrative emissions scenarios of the IPCC. Purple curve represents a Gaussian distribution fit to the data.

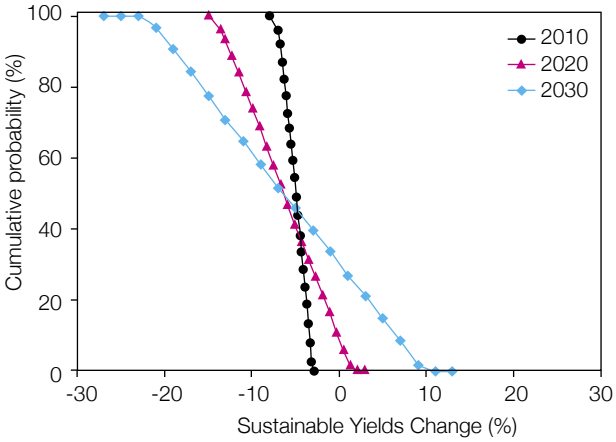

Figure 6.9: Cumulative probability distributions for changes in sustainable yields of a regional water utility. Distributions were based upon the applications of a suite of climate projections to a statistical relationship between rainfall, evaporation and yield, based upon simulations with the IQQM hydrological model (Kirono *et al*. 2007).

If information is needed on the likelihood of different changes or impacts, estimates of probability can be generated by applying frequency statistics. Results can be treated as a sample of the population of actual climate change or impacts, and probabilities can be calculated to compare the relative likelihood of different outcomes in the sample (Figure 6.8). More advanced statistical methods can be used to generate probability density functions or cumulative probability distributions from a sample of projections or impact results. These can be applied in impact assessment using Monte Carlo methods to estimate the probability of different outcomes (Kirono *et al*. 2007; Figure 6.9)

Downscaling of extreme events from model simulations can also assess the likelihood of exceeding specific extremes, such as extreme rainfall events (Figure 6.10). This frequentist analysis tests many instances of an event-based risk downscaled from a baseline and climate change simulation of the same model, consistent with the analysis of historical events. Using ensembles of models will increase the confidence in such analyses.

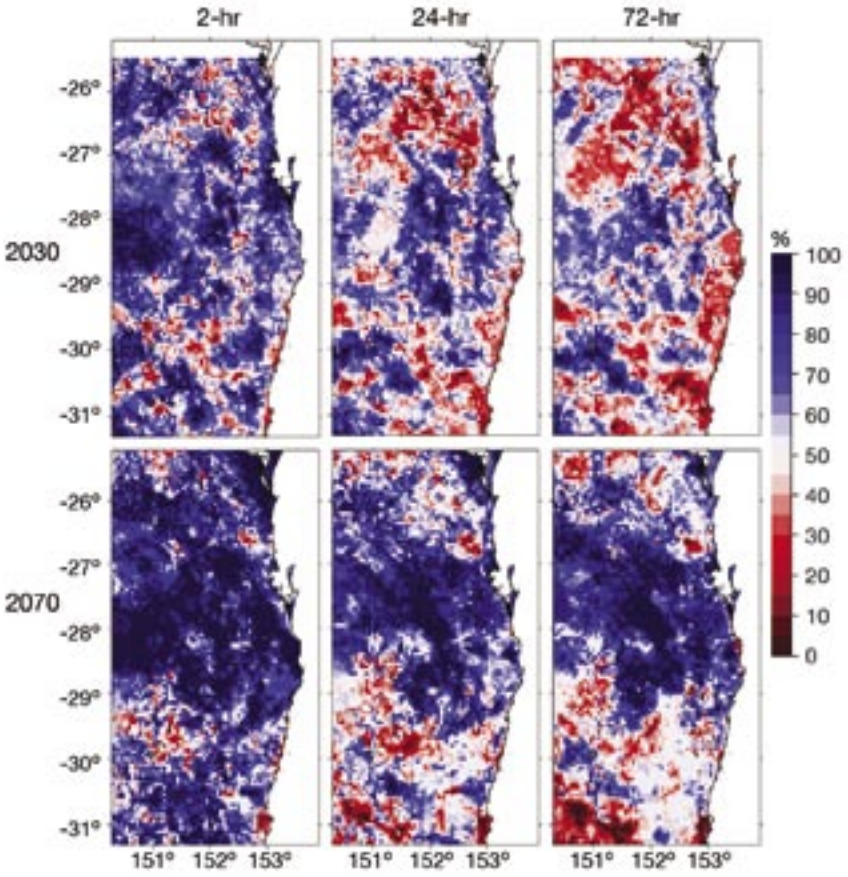

Figure 6.10: Probability of increases in extreme rainfall events in central coastal New South Wales. Probabilities are expressed as a percentage of model simulations that indicate increases in extreme rainfall (Hennessy *et al*. 2004).

A range of assessments have been carried out that combine the SRES greenhouse gas emission scenarios and model-based projections of climate change derived from those scenarios to ask 'what if' questions about impact-related risks. These assessments have applied ensembles of change and/or Monte Carlo methods to develop more robust statistical estimates of the probability of exceeding thresholds. Chapter 5 presents probabilities of exceeding different temperature and rainfall thresholds across Australia. Such techniques have been used to assess the likelihood of exceeding different impact thresholds, such as reductions in agricultural productivity or dam inflows (Howden and Jones 2001; Jones and Page 2001; Kirono *et al*. 2007). A number of studies have also examined the likelihood of exceeding thresholds for 'dangerous interference' with the global climate system (Hare and Meinshausen 2004; Jones 2004; Mastrandrea and Schneider 2004; Jones and Preston 2006). Damages avoided through mitigation can be contrasted by comparing outcomes associated with high emissions with those from a low emissions, or stabilisation scenario.

The application of methods for likelihood estimation is highly dependent upon sample size and potentially on how those underlying uncertainties are managed. Generally, as the sample size increases, estimates of the distribution become more robust. The need for a healthy sample is a challenge for some impact applications. Crop models, hydrological models and ecosystem models all tend to be complex, physically-based process models. Iterative simulations with such models with a broad range of scenarios may be prohibitive, given the time and resources involved. This challenge has been addressed in two different ways:

1. Prior screening of a population of climate scenarios to identify the 'most-likely' future climatic conditions (Jones and Mearns 2005). This projection is then used in impact assessment, yielding a 'most likely' impact.

2. Prior sensitivity analysis of the impact model of interest with a relatively small number of arbitrary projections. The population of impact outcomes can subsequently be used to generate a simple statistical impact response function that can then be comprehensively interrogated with a larger population of global climate model estimates. For example, Jones and Howden (2001) used a similar approach with APSIM in a national risk assessment. This technique has also seen several applications in hydrology (Jones and Page 2001; CSIRO and Melbourne Water 2005; Jones and Durack 2005; Kirono *et al*. 2007; Figure 6.9).

Finally, the projections presented in this document signal a further advance in estimating climate change likelihoods. Applying these techniques to impact and risk assessment should help constrain uncertainties by providing tighter 'most likely' outcomes. However, because there are a number of realistic alternatives in how such likelihoods can be applied, these alternatives can be tested in impact assessments to determine whether the results are robust or sensitive to the input assumptions (Jones and Page 2001; Dessai and Hulme 2007). This information will improve our understanding of which risks are sensitive to what variables, and also feed back into modelling studies in terms of where improvements are needed most. For example, Jones *et al*. (2005) tested water yield in the Fitzroy Basin under the assumption that regional ranges of rainfall variability were uniform, or grouped according to the distribution of model patterns of change (Figure 6.11). The resulting analysis showed that the shapes of the input uncertainties were critical and that rainfall changes over only three months of the wet season comprised 75% of the uncertainty in total catchment water yield. Such exercises, expanded to a larger range of impact types, could be used to test model-weighting schemes.

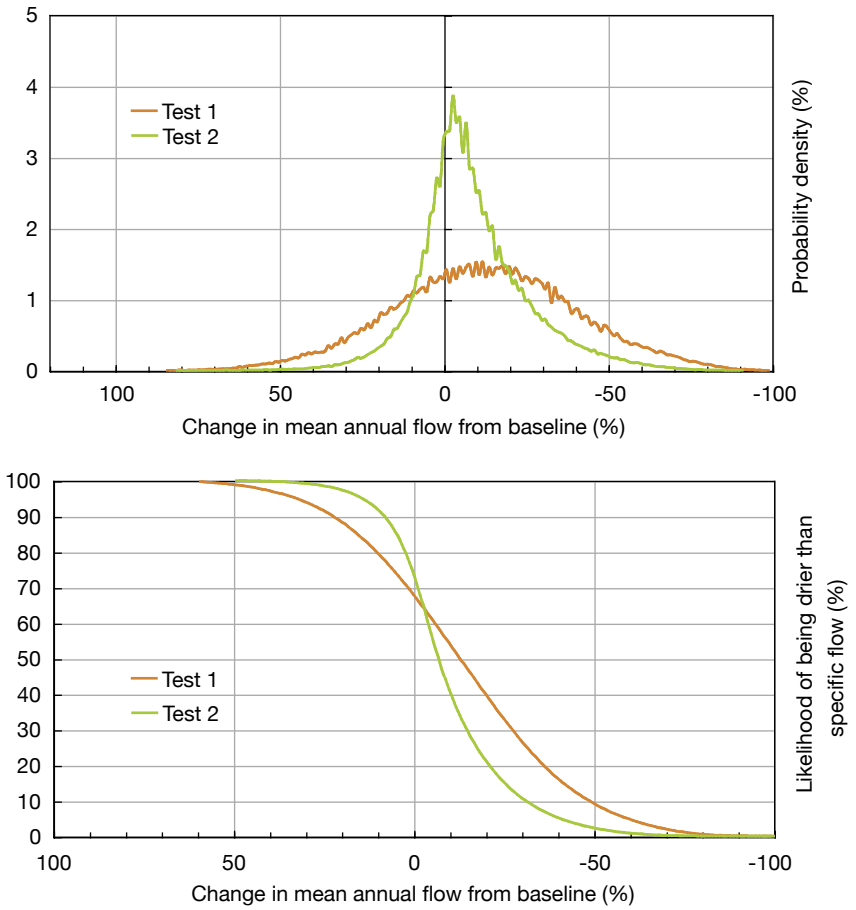

Figure 6.11: Comparison of probability distributions for change in mean annual flow for the Fitzroy River in 2030 comparing uniform sampling of rainfall changes (Test 1) with non-uniform sampling based on the climate model distribution (Test 2). The top chart shows probability density, the bottom chart shows the probability of mean annual flow being drier than a specific change (as measured from the x-axis).

6.4 Delivering climate projections to end-users and stakeholders

As the demand for climate projections has grown, various tools have been developed which represent different methods for enhancing the delivery of climate information to the public and stakeholders both for education and for risk assessment and management.

Australia's primary platform for distributing climate projections is the OzClim scenario generator. OzClim enables users to generate their own projections of average climate change for different time periods in the future, drawing from various climate models and assumptions about climate sensitivity and future greenhouse gas emissions. It also enables projection data to be exported in various file formats for subsequent use in other computing environments. MAGICC/SCENGEN can be used to explore potential climate changes at the global to regional scale under a similar range of assumptions. SimCLIM is an open-framework modelling system for integrated hazard and climate impact analysis.

In the United States, the Consortium for Atlantic Regional Assessment was recently developed as an internet-based tool providing information on historical and future climate and land-use (Dempsey and Fisher 2005). The United Kingdom (UK) Climate Impacts Programme's Adaptation Wizard is a simple on-line tool that leads users through the process of understanding climate change through to making decisions about adaptation, while the Scenario Gateway provides online access to UK climate scenarios. Together with appropriate risk assessment and management frameworks, these tools enhance the capacity for stakeholders to access climate projections, begin assessing risk and identifying risk management decisions.

The availability of climate data through such tools does not ensure that such information will be used for managing climate risk. Recent work on climate change communication has identified challenges in delivering messages to the public regarding climate change and its consequences (Table 6.2). Unless overcome, these challenges diminish perceptions of climate risk, reduce incentives for taking risk management actions and limit understanding of what actions may be useful or appropriate.

Many of these challenges were also identified in stakeholder focus groups conducted as a part of the development of the projections in this report. Stakeholder consultation was undertaken in November 2006 through focus groups in Adelaide, Perth, Brisbane Melbourne and Sydney, and through an online survey. There were 64 participants in the focus groups, and 230 responses to the survey.

Stakeholder messages regarding climate projections highlighted:

- the need for different data among diverse stakeholders.
- the need for simplicity and transparency in communication of information.
- the limited ability by stakeholders to distinguish between weather forecasts, seasonal climate forecasts and multi-decadal climate projections.
- confusion by stakeholders in managing information on climate change as new research becomes available, such as successive generations of climate change projections, and the use of different climate models, emissions scenarios and model resolutions.
- conflicting messages from different communicators.
- the need for information on how to respond to projected changes.
- the potential for demands for information to exceed available resources and technical capacity.

Such sentiments reflect two issues that exist in conflict:

1. an intense demand for increasingly detailed information, and
2. challenges in meeting demand as well as in interpreting and using that information which is available.

In addition, stakeholders identified a number of barriers to obtaining and applying climate projections, such as the ability to locate information on the internet (the most popular vehicle for obtaining information) or even the colour scheme used in graphics.

Perhaps the most effective mechanism for overcoming the challenges to using climate information in decision-making is to couple the provision of information about climate change and impacts with a particular decision-making event (CSIRO and Melbourne Water 2005; Kirono *et al*. 2007). This ensures that climate projections are developed that are relevant to the endpoint or risk of concern, and stakeholders have more intimate knowledge of the methods by which they were developed. It also ensures that uncertainty in climate projections and impacts are treated in a manner relevant to and preferred by stakeholders charged with a decision-making event. Such an approach provides the best chance that the information will be relevant to stakeholders, appropriately interpreted and effectively used.

Table 6.2: Challenges in communicating climate change projections and risk

Challenge	Solution
Diverse communicators (e.g. scientists, policy-makers, the media) with varying agendas and credibility (Boykoff and Boykoff 2004; Cameron 2005).	Emphasise the scientific confidence in climate projections; ensure transparency and consistency in communications.
Confusion about how the climate system works (Sterman and Sweeney 2002).	Provide the public with information not only regarding what climate changes are projected, but also why such changes are anticipated and how they were derived.
Difficulty in identifying specific and salient threats associated with climate change (Ohe and Ikeda 2005).	Link climate change projections with social and environmental impacts. Increase focus on projections of climate extremes where the consequences are more self-evident.
Low prioritisation of climate change relative to more immediate concerns (Moser and Dilling 2004).	Link climate change to other sustainability issues, such as energy, natural resource management, regional security and public health.
Limited understanding of how individuals' actions can reduce risk (CCSA 2005).	Link projections of climate change and impacts with risk management strategies relevant to the audience (e.g. greenhouse gas mitigation and adaptation measures).
Perceptions of the likelihood of climate projections and impacts vary by individual, population, and impact of interest (Patt and Schragg 2003; Patt and Dessai 2005)	Isolate consequence and probability in the communication of risk to minimise subjective interpretations (Manning 2003).
Poor uptake and use of existing tools for climate projections and impact assessment by stakeholders (Demeritt and Langdon 2004; Dempsey and Fisher 2005).	Better marketing of available tools and services to stakeholders as well as demonstrations of prior use and value; easy to access and use methods and tools.
Existing information on climate change is inappropriate for a particular decision-event.	Target projection development to the needs of end users and develop alternative, yet internally consistent, methods for presenting projections.

APPENDIX A

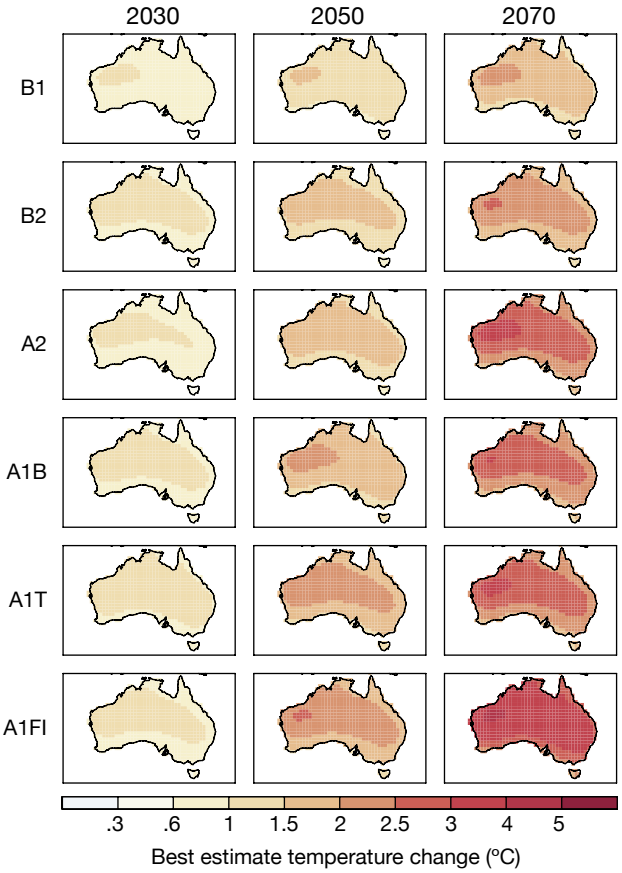

Figure A1:
Best estimate, 10th percentile and 90th percentile annual temperature change (°C) for 2030, 2050 and 2070 and six SRES emission scenarios.

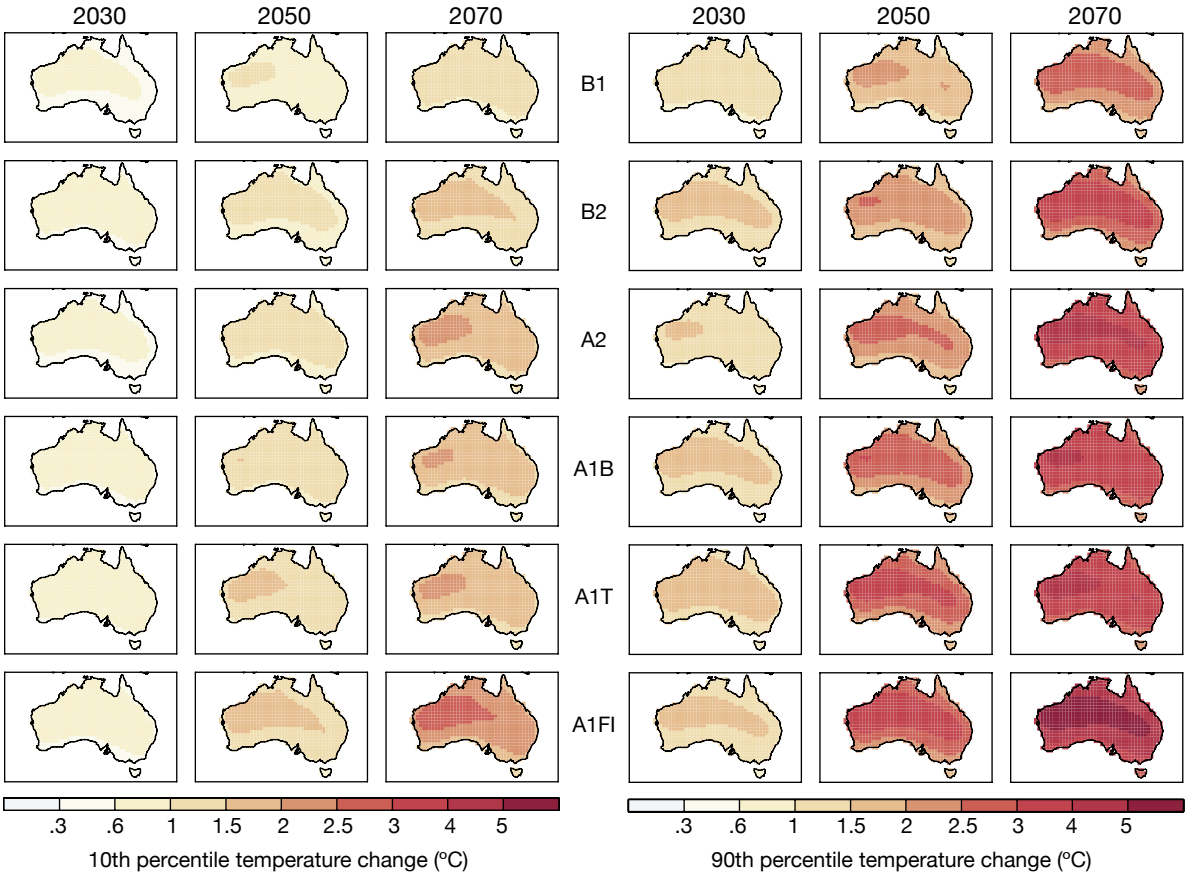

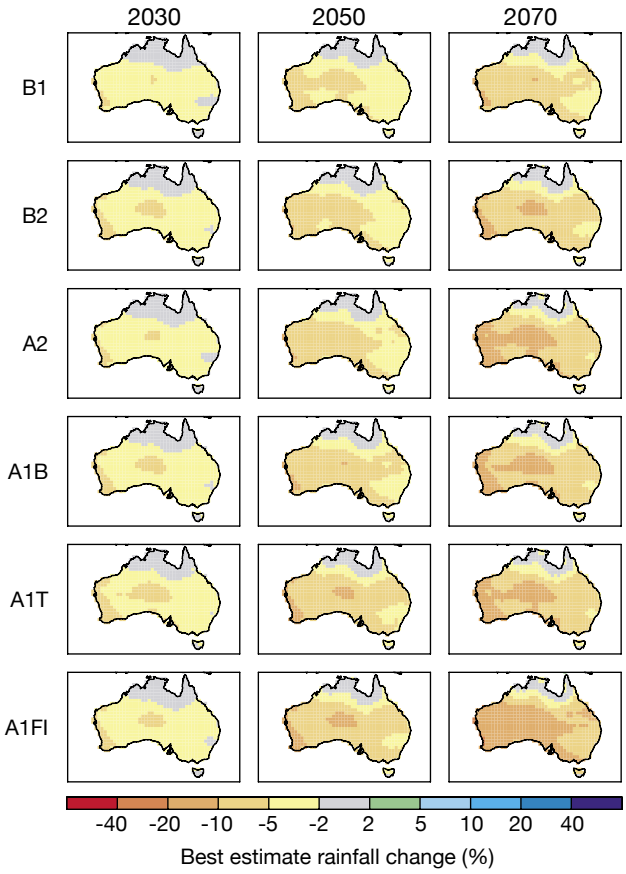

Figure A2:
Best estimate, 10th percentile and 90th percentile annual rainfall change (%) for 2030, 2050 and 2070 and six SRES emission scenarios.

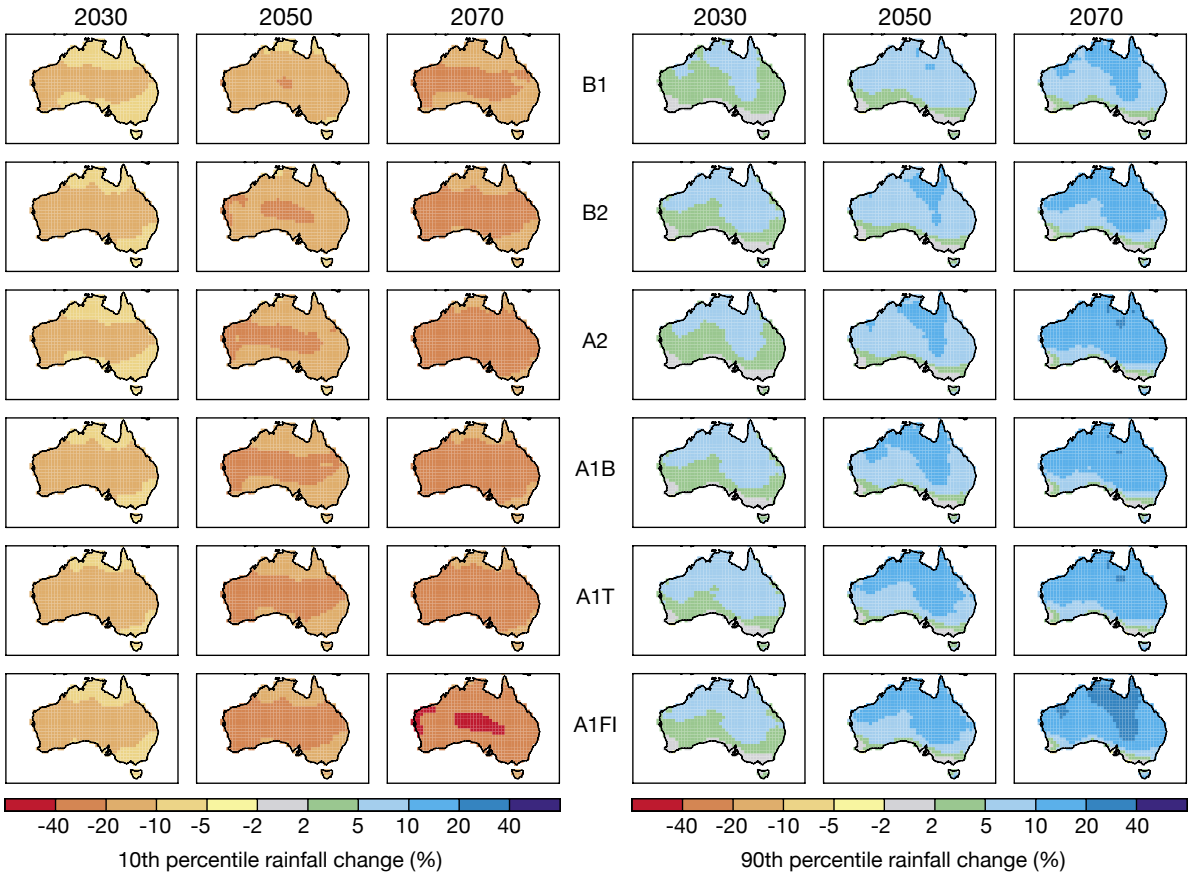

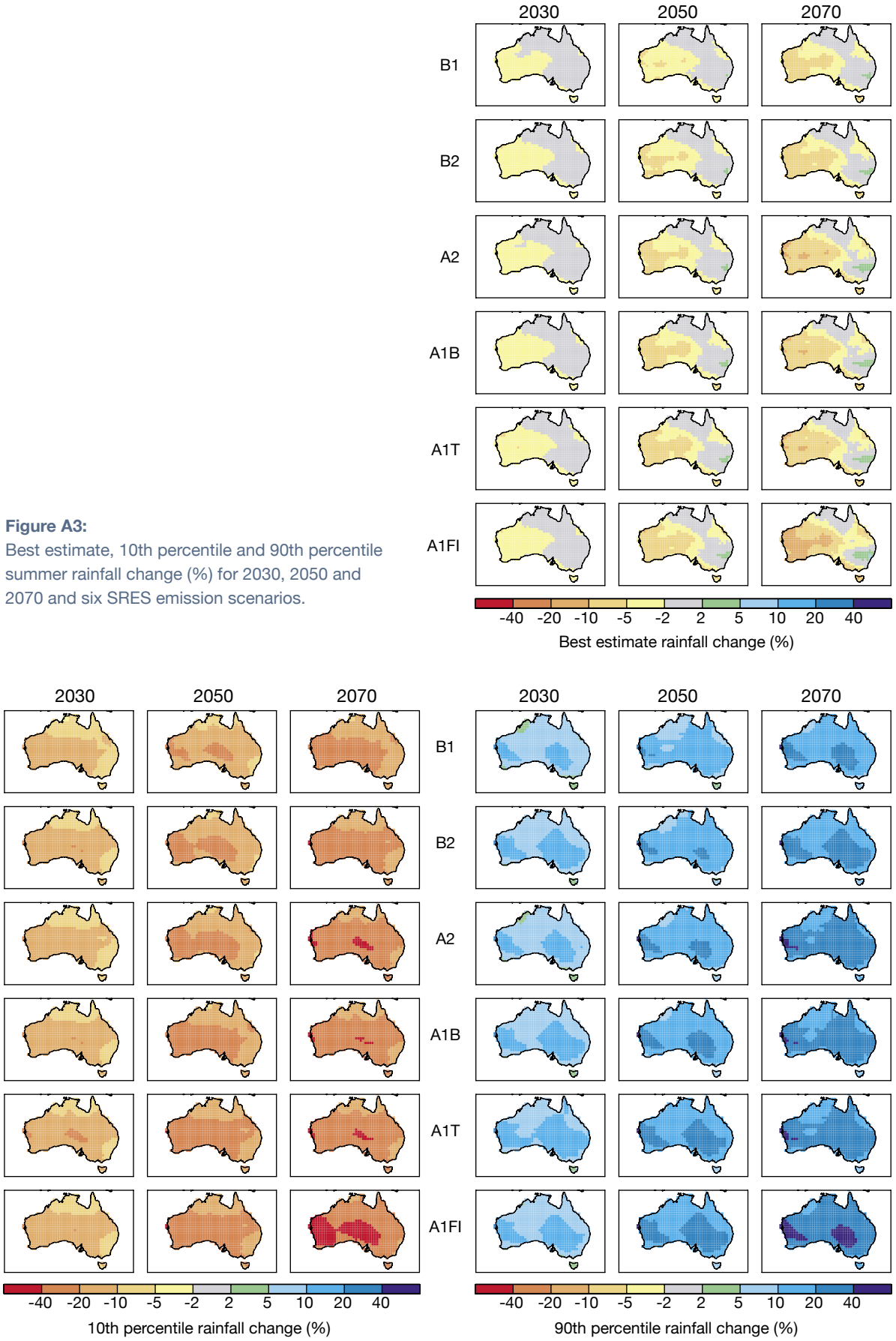

Figure A3:
Best estimate, 10th percentile and 90th percentile summer rainfall change (%) for 2030, 2050 and 2070 and six SRES emission scenarios.

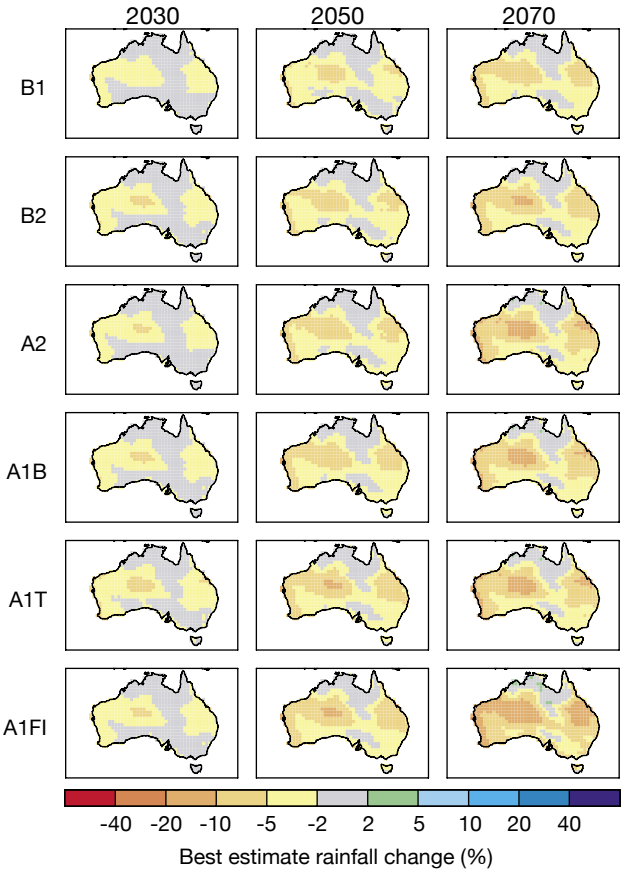

Figure A4:
Best estimate, 10th percentile and 90th percentile autumn rainfall change (%) for 2030, 2050 and 2070 and six SRES emission scenarios.

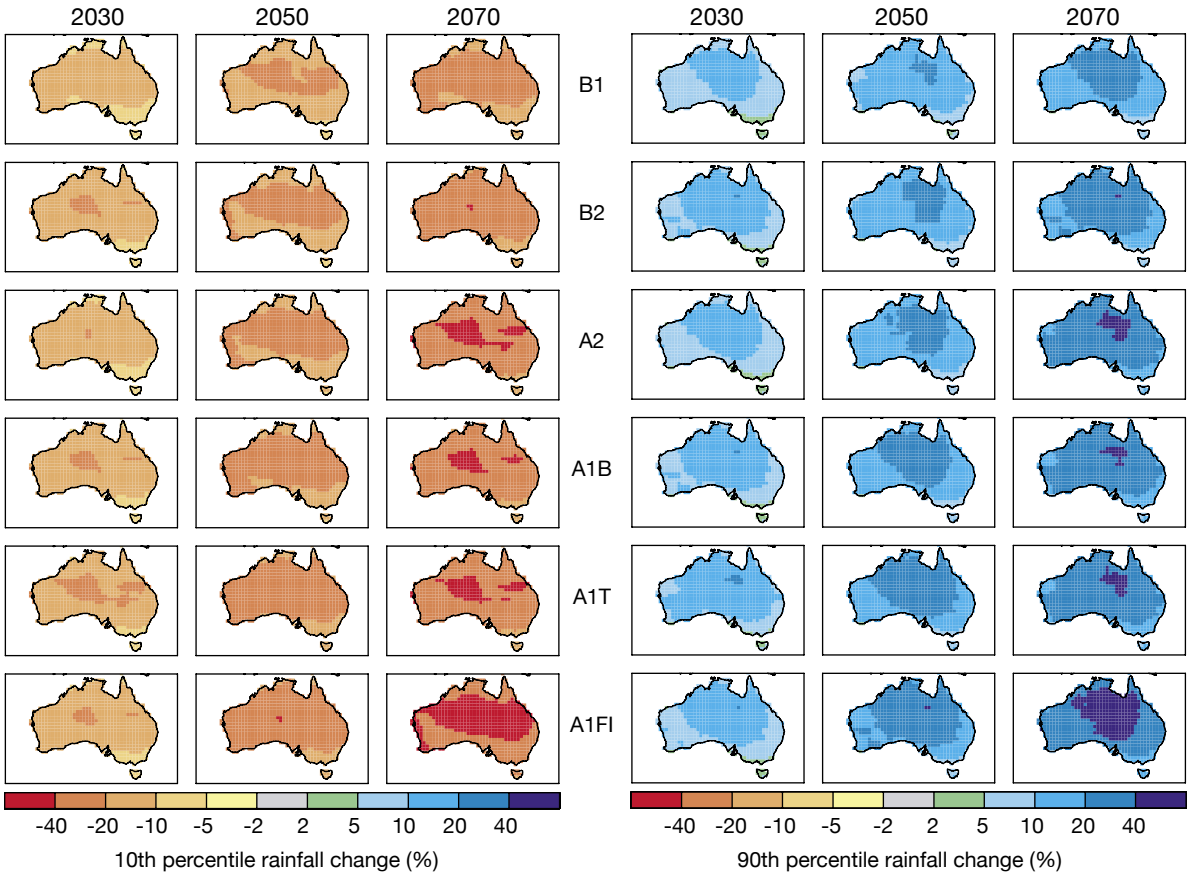

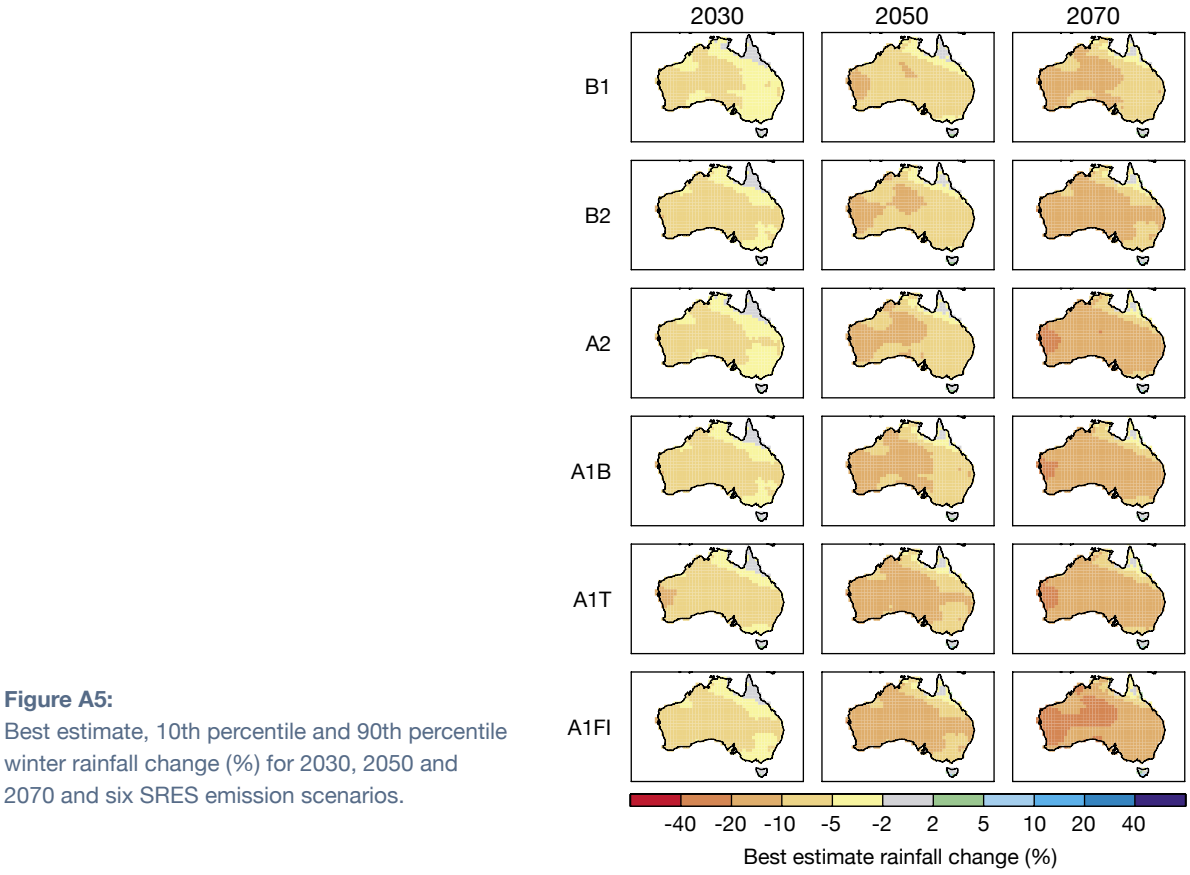

Figure A5:
Best estimate, 10th percentile and 90th percentile winter rainfall change (%) for 2030, 2050 and 2070 and six SRES emission scenarios.

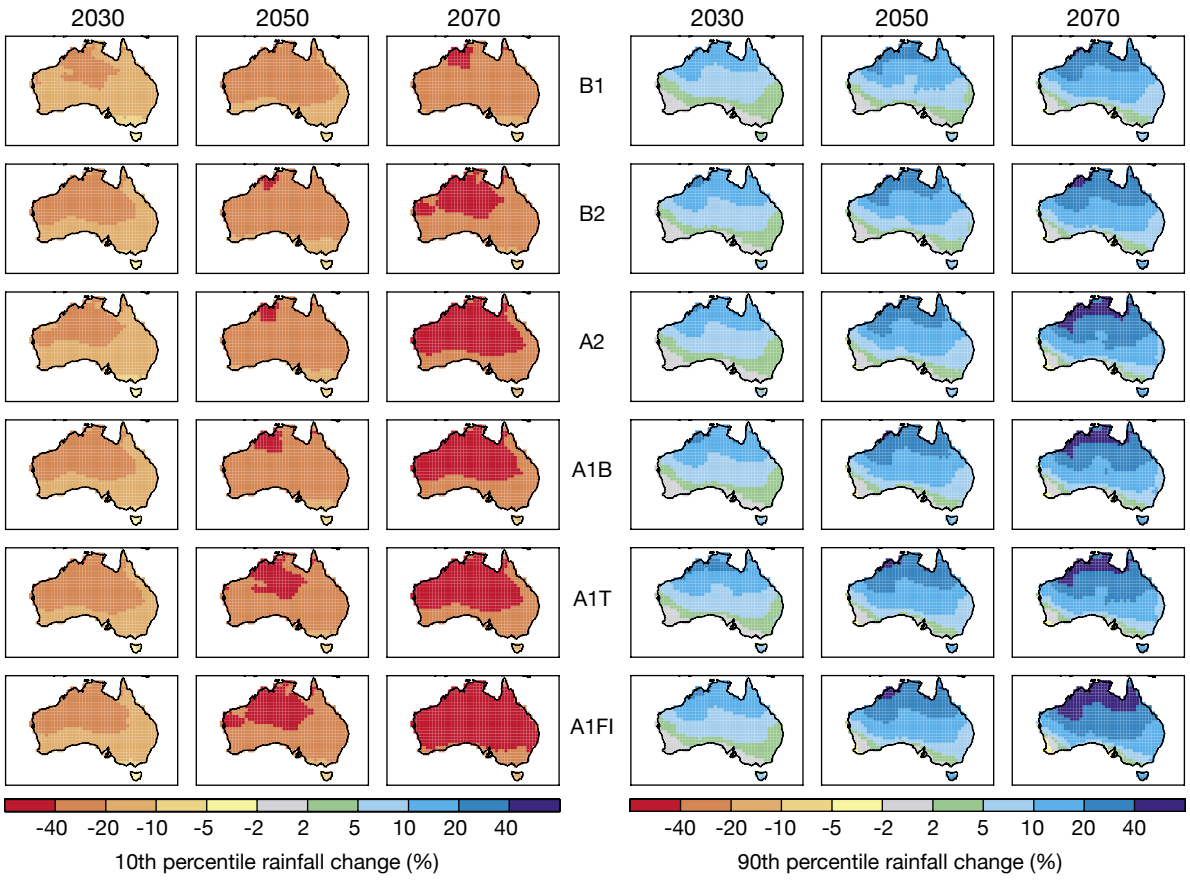

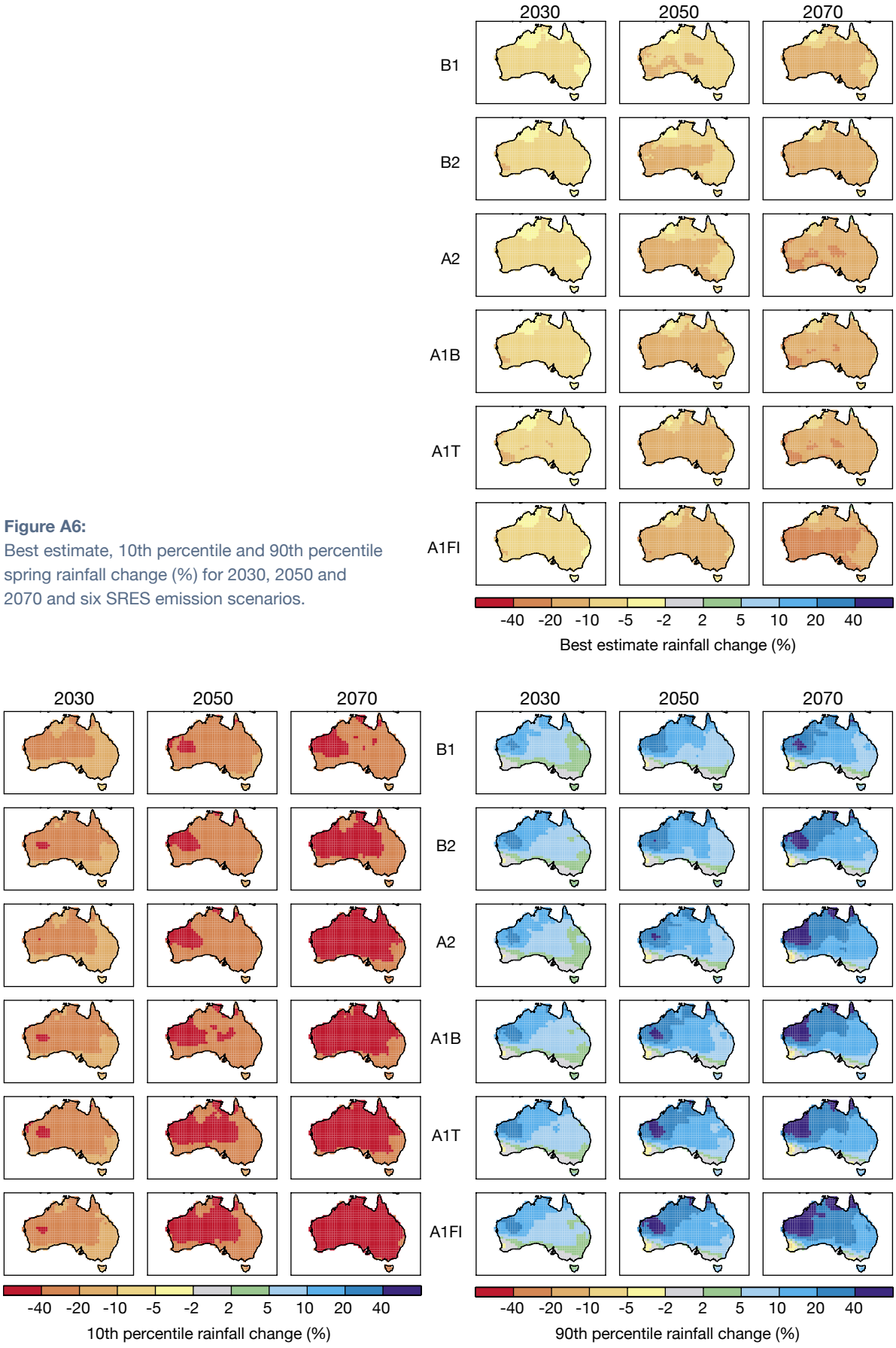

Figure A6:
Best estimate, 10th percentile and 90th percentile spring rainfall change (%) for 2030, 2050 and 2070 and six SRES emission scenarios.

APPENDIX B – CITY SUMMARIES

In this climate change projections based on the probabilistic method are given for a set of 14 selected sites. Results are indicative in that they are based on the results of global climate models for the locations and do not take into account local topographical effects (see sections 5.1.4 and 5.2.4). Changes (relative to 1990) are shown, except for days over 35ºC.

Table B1: Projected climate changes for Adelaide

Variable	Season	2030 A1B 10p	2030 A1B 50p	2030 A1B 90p	2070 B1 10p	2070 B1 50p	2070 B1 90p	2070 A1FI 10p	2070 A1FI 50p	2070 A1FI 90p
Temperature (ºC)	Annual	0.6	0.9	1.3	1	1.5	2.1	1.9	2.8	4
	Summer	0.6	0.9	1.4	1	1.6	2.3	2	3	4.4
	Autumn	0.6	0.9	1.3	0.9	1.5	2.2	1.8	2.8	4.2
	Winter	0.5	0.8	1.2	0.8	1.3	2	1.5	2.4	3.8
	Spring	0.6	0.9	1.3	1	1.5	2.2	2	3	4.3
No. days over 35ºC (current 17)	Annual	21.3	23.0	25.5	24.0	26.4	30.6	28.9	35.6	46.6
Rainfall (%)	Annual	-11	-4	+2	-18	-7	+4	-32	-13	+8
	Summer	-14	-2	+11	-23	-3	+18	-39	-5	+35
	Autumn	-11	-1	+9	-18	-2	+14	-31	-4	+28
	Winter	-15	-6	+2	-23	-10	+3	-40	-19	+6
	Spring	-19	-8	+3	-30	-12	+4	-50	-23	+8
Potential evaporation (%)	Annual	0	+2	+4	+1	+3	+7	+2	+6	+14
	Summer	0	+2	+5	0	+3	+8	-1	+6	+15
	Autumn	+1	+3	+5	+2	+5	+9	+4	+10	+17
	Winter	+1	+5	+12	+2	+8	+20	+3	+16	+39
	Spring	-1	+1	+3	-2	+1	+5	-4	+3	+10
Wind-speed (%)	Annual	-3	0	+3	-6	0	+5	-11	0	+10
	Summer	-1	+2	+6	-2	+4	+10	-3	+7	+19
	Autumn	-6	0	+5	-9	-1	+8	-18	-1	+15
	Winter	-8	-2	+4	-13	-3	+6	-25	-6	+11
	Spring	-6	0	+5	-10	0	+8	-18	-1	+16
Relative humidity (%)	Annual	-1.5	-0.7	+0.0	-2.6	-1.1	+0.1	-5.0	+2.1	+0.1
Solar radiation (%)	Annual	-0.2	+0.4	+1.2	-0.4	+0.7	+2.1	-0.7	+1.4	+4.0

Table B2: Projected climate changes for Alice Springs

Variable	Season	2030 A1B 10p	2030 A1B 50p	2030 A1B 90p	2070 B1 10p	2070 B1 50p	2070 B1 90p	2070 A1FI 10p	2070 A1FI 50p	2070 A1FI 90p
Temperature (ºC)	Annual	0.8	1.2	1.6	1.3	1.9	2.7	2.6	3.7	5.2
	Summer	0.8	1.2	1.7	1.3	2	2.9	2.5	3.8	5.6
	Autumn	0.7	1.1	1.7	1.2	1.9	2.8	2.3	3.6	5.4
	Winter	0.6	1	1.5	1.1	1.7	2.5	2	3.3	4.9
	Spring	0.9	1.3	1.8	1.5	2.1	3	2.8	4.1	5.8
No. days over 35ºC (current 89.6)	Annual	101.6	109.2	118.1	111.7	121.7	138.2	132.4	155.1	181.7
Rainfall (%)	Annual	-17	-6	+5	-26	-9	+8	-44	-17	+16
	Summer	-17	-3	+10	-27	-6	+17	-45	-11	+33
	Autumn	-20	-4	+13	-32	-6	+22	-52	-12	+42
	Winter	-25	-9	+7	-38	-14	+12	-60	-25	+23
	Spring	-26	-9	+8	-39	-14	+12	-62	-26	+24
Potential evaporation (%)	Annual	0	+2	+4	0	+4	+7	+1	+7	+14
	Summer	0	+2	+4	0	+3	+7	0	+6	+14
	Autumn	+1	+3	+5	+1	+5	+9	+2	+9	+17
	Winter	0	+3	+6	-1	+5	+10	-2	+9	+20
	Spring	-1	+2	+5	-1	+3	+8	-3	+6	+15
Wind-speed (%)	Annual	-1	+1	+4	-2	+2	+6	-3	+4	+12
	Summer	-4	0	+5	-7	0	+8	-14	-1	+15
	Autumn	-1	+1	+3	-2	+1	+5	-4	+2	+9
	Winter	-1	+3	+8	-2	+5	+14	-4	+9	+27
	Spring	-1	+2	+5	-2	+3	+8	-4	+5	+16
Relative humidity (%)	Annual	-1.8	-0.7	+0.4	-3.0	-1.2	+0.6	-5.8	-2.3	+1.2
Solar radiation (%)	Annual	-0.9	+0.2	+1.7	-1.5	+0.4	+2.8	-3.0	+0.7	+5.5

Table B3: Projected climate changes for Brisbane

Variable	Season	2030 A1B 10p	2030 A1B 50p	2030 A1B 90p	2070 B1 10p	2070 B1 50p	2070 B1 90p	2070 A1FI 10p	2070 A1FI 50p	2070 A1FI 90p
Temperature (ºC)	Annual	0.7	1	1.4	1.1	1.6	2.3	2.1	3.1	4.4
	Summer	0.6	0.9	1.4	1.1	1.6	2.3	2	3	4.4
	Autumn	0.6	0.9	1.3	1	1.5	2.2	1.9	3	4.3
	Winter	0.6	1	1.3	1.1	1.6	2.2	2.1	3.1	4.3
	Spring	0.7	1	1.5	1.1	1.7	2.5	2.1	3.2	4.8
No. days over 35ºC (current 1.0)	Annual	1.5	2.0	2.5	2.1	3.0	4.6	4.0	7.6	20.6
Rainfall (%)	Annual	-12	-3	+5	-18	-5	+9	-33	-9	+17
	Summer	-11	-1	+9	-17	-1	+15	-31	-3	+29
	Autumn	-14	-3	+10	-23	-5	+16	-39	-9	+31
	Winter	-15	-6	+4	-24	-10	+6	-42	-18	+11
	Spring	-17	-6	+6	-28	-10	+10	-47	-18	+18
Potential evaporation (%)	Annual	+2	+3	+5	+3	+6	+8	+7	+11	+16
	Summer	+2	+3	+5	+3	+6	+9	+6	+11	+17
	Autumn	+2	+4	+6	+3	+6	+10	+6	+12	+20
	Winter	+2	+4	+6	+4	+6	+10	+7	+12	+19
	Spring	+2	+3	+4	+3	+5	+7	+5	+9	+14
Wind-speed (%)	Annual	-1	+2	+6	-1	+3	+10	-2	+6	+19
	Summer	-2	+2	+7	-3	+4	+11	-5	+7	+22
	Autumn	-3	+1	+5	-4	+2	+9	-9	+3	+18
	Winter	-6	0	+6	-10	-1	+10	-20	-1	+19
	Spring	0	+5	+12	0	+9	+19	0	+17	+37
Relative humidity (%)	Annual	-1.1	-0.1	+0.9	-1.9	-0.1	+1.5	-3.6	-0.2	+3.0
Solar radiation (%)	Annual	-1.2	0.2	1.9	-2	0.4	3.1	-3.9	0.7	6

Table B4: Projected climate changes for Cairns

Variable	Season	2030 A1B 10p	2030 A1B 50p	2030 A1B 90p	2070 B1 10p	2070 B1 50p	2070 B1 90p	2070 A1FI 10p	2070 A1FI 50p	2070 A1FI 90p
Temperature (ºC)	Annual	0.6	0.9	1.2	1.1	1.5	2	2.0	2.9	3.9
	Summer	0.6	0.9	1.3	1	1.5	2.2	2	3	4.2
	Autumn	0.6	0.9	1.2	1	1.5	2.1	2.0	2.9	4.0
	Winter	0.6	0.9	1.2	1	1.5	2.1	1.9	2.8	4
	Spring	0.6	0.9	1.2	1	1.5	2	2	2.8	3.9
No. days over 35ºC (current 3.8)	Annual	5.4	6.6	9.1	7.5	12.1	22.1	18.7	44.4	96.0
Rainfall (%)	Annual	-8	0	+8	-14	-1	+13	-25	-1	+25
	Summer	-9	0	+10	-14	0	+16	-25	0	+32
	Autumn	-14	-1	+13	-22	-1	+22	-38	-2	+42
	Winter	-16	-1	+14	-25	-1	+24	-43	-2	+46
	Spring	-21	-5	+10	-33	-8	+16	-54	-16	+32
Potential evaporation (%)	Annual	+2	+3	+4	+4	+5	+7	+7	+10	+14
	Summer	+2	+3	+5	+3	+5	+9	+5	+10	+17
	Autumn	+2	+3	+5	+4	+6	+9	+7	+11	+17
	Winter	+2	+3	+5	+3	+6	+9	+7	+11	+17
	Spring	+2	+3	+4	+3	+5	+6	+6	+9	+12
Wind-speed (%)	Annual	0	+1	+3	0	+2	+4	0	+4	+8
	Summer	-3	+1	+5	-5	+2	+9	-9	+4	+17
	Autumn	-2	+1	+3	-3	+1	+6	-7	+2	+11
	Winter	-1	+1	+3	-1	+2	+5	-2	+4	+10
	Spring	0	+2	+4	0	+3	+7	0	+6	+13
Relative humidity (%)	Annual	-0.8	-0.3	+0.2	-1.3	-0.4	+0.4	-2.5	-0.8	+0.7
Solar radiation (%)	Annual	-1.1	0.0	+1.3	-1.9	0.0	+2.1	-3.7	0.0	+4.1

Table B5: Projected climate changes for Canberra

Variable	Season	2030 A1B 10p	2030 A1B 50p	2030 A1B 90p	2070 B1 10p	2070 B1 50p	2070 B1 90p	2070 A1FI 10p	2070 A1FI 50p	2070 A1FI 90p
Temperature (ºC)	Annual	0.6	0.9	1.3	1.1	1.6	2.2	2.1	3.0	4.2
	Summer	0.6	1	1.5	1.1	1.7	2.4	2.1	3.2	4.7
	Autumn	0.6	0.9	1.3	1.0	1.5	2.2	1.9	3	4.3
	Winter	0.5	0.8	1.1	0.9	1.3	1.8	1.7	2.5	3.6
	Spring	0.7	1.0	1.5	1.1	1.7	2.4	2.2	3.3	4.7
No. days over 35ºC (current 5.4)	Annual	6.9	7.9	9.9	8.1	10.5	13.0	11.8	16.9	24.7
Rainfall (%)	Annual	-9	-3	+2	-14	-5	+4	-26	-9	+8
	Summer	-8	0	+8	-12	0	+13	-22	+1	+25
	Autumn	-10	-2	+6	-16	-3	+10	-29	-6	+20
	Winter	-14	-5	+3	-22	-9	+5	-38	-16	+10
	Spring	-17	-6	+3	-27	-10	+5	-46	-19	+10
Potential evaporation (%)	Annual	+1	+3	+5	+2	+5	+8	+5	+9	+15
	Summer	+1	+2	+4	+2	+4	+7	+3	+8	+14
	Autumn	+2	+4	+7	+3	+7	+11	+7	+13	+22
	Winter	+1	+6	+13	+2	+10	+22	+5	+19	+43
	Spring	0	+2	+4	0	+3	+7	-1	+6	+14
Wind-speed (%)	Annual	-6	-1	+4	-10	-1	+7	-20	-2	+13
	Summer	-9	+1	+11	-15	+2	+18	-28	+4	+34
	Autumn	-10	-2	+4	-16	-4	+7	-31	-8	+13
	Winter	-7	-0	+6	-11	-1	+10	-22	-1	+19
	Spring	-10	-1	+6	-16	-2	+10	-31	-3	+20
Relative humidity (%)	Annual	-1.4	-0.5	+0.3	-2.3	-0.8	+0.5	-4.5	-1.6	+0.9
Solar radiation (%)	Annual	-0.7	+0.5	+1.9	-1.2	+0.7	+3.2	-2.3	+1.4	+6.2

Table B6: Projected climate changes for Darwin

Variable	Season	2030 A1B 10p	2030 A1B 50p	2030 A1B 90p	2070 B1 10p	2070 B1 50p	2070 B1 90p	2070 A1FI 10p	2070 A1FI 50p	2070 A1FI 90p
Temperature (ºC)	Annual	0.7	1	1.4	1.2	1.7	2.3	2.3	3.2	4.4
	Summer	0.7	1	1.4	1.1	1.6	2.4	2.1	3.2	4.6
	Autumn	0.7	1	1.5	1.1	1.7	2.4	2.2	3.3	4.7
	Winter	0.7	1	1.4	1.1	1.7	2.3	2.2	3.2	4.5
	Spring	0.7	1	1.4	1.2	1.7	2.3	2.3	3.3	4.4
No. days over 35ºC (current 10.8)	Annual	27.9	44.0	68.8	49.0	89.4	153.1	140.6	226.8	308.3
Rainfall (%)	Annual	-7	-0	+6	-11	-1	+10	-21	-1	+20
	Summer	-6	0	+7	-10	0	+11	-18	+1	+21
	Autumn	-11	0	+11	-18	0	+18	-32	0	+34
	Winter	-27	-4	+18	-41	-7	+31	-63	-13	+59
	Spring	-21	-5	+13	-33	-8	+22	-54	-15	+42
Potential evaporation (%)	Annual	+2	+3	+5	+3	+5	+8	+7	+10	+15
	Summer	+2	+4	+6	+3	+6	+10	+6	+11	+18
	Autumn	+2	+3	+5	+3	+6	+8	+7	+11	+16
	Winter	+1	+3	+5	+1	+5	+9	+2	+9	+17
	Spring	+2	+3	+4	+3	+5	+7	+5	+9	+14
Wind-speed (%)	Annual	-1	+1	+2	-2	+1	+4	-4	+2	+7
	Summer	-5	+1	+7	-8	+2	+12	-16	+3	+23
	Autumn	-3	0	+2	-5	-1	+3	-10	-2	+7
	Winter	-2	0	+2	-4	0	+4	-7	0	+7
	Spring	-1	+2	+5	-1	+3	+9	-2	+7	+17
Relative humidity (%)	Annual	-1.0	-0.5	+0.0	-1.7	-0.8	+0.0	-3.2	-1.5	+0.1
Solar radiation (%)	Annual	-1.1	+0.0	+1.3	-1.9	+0.0	+2.2	-3.6	+0.1	+4.3

Table B7: Projected climate changes for Dubbo

Variable	Season	2030 A1B 10p	2030 A1B 50p	2030 A1B 90p	2070 B1 10p	2070 B1 50p	2070 B1 90p	2070 A1FI 10p	2070 A1FI 50p	2070 A1FI 90p
Temperature (ºC)	Annual	0.7	1	1.5	1.2	1.7	2.5	2.2	3.3	4.8
	Summer	0.7	1.1	1.6	1.2	1.8	2.7	2.2	3.5	5.3
	Autumn	0.6	1	1.5	1.1	1.7	2.6	2.1	3.3	4.9
	Winter	0.6	0.9	1.3	0.9	1.4	2.1	1.8	2.8	4.1
	Spring	0.8	1.1	1.7	1.3	1.9	2.8	2.4	3.7	5.4
No. days over 35ºC (current 25.1)	Annual	30.7	34.7	38.7	34.9	40.4	50.5	44.3	61.4	87.2
Rainfall (%)	Annual	-10	-2	+5	-16	-4	+8	-29	-7	+16
	Summer	-8	+1	+11	-13	+2	+18	-24	+4	+35
	Autumn	-13	-2	+10	-21	-3	+16	-36	-6	+31
	Winter	-15	-5	+4	-24	-8	+7	-41	-15	+14
	Spring	-19	-6	+5	-29	-9	+9	-49	-17	+17
Potential evaporation (%)	Annual	+1	+3	+5	+2	+4	+8	+4	+9	+15
	Summer	+1	+3	+5	+2	+4	+8	+3	+9	+15
	Autumn	+2	+4	+6	+3	+6	+10	+6	+12	+20
	Winter	0	+5	+12	+1	+8	+20	+1	+15	+39
	Spring	-1	+2	+4	-1	+3	+7	-3	+5	+13
Wind-speed (%)	Annual	-5	0	+4	-8	-1	+7	-15	-1	+13
	Summer	-6	+1	+9	-9	+2	+15	-18	+5	+29
	Autumn	-7	0	+7	-12	-1	+11	-24	-1	+21
	Winter	-10	-2	+4	-16	-4	+7	-31	-8	+14
	Spring	-6	0	+7	-11	0	+11	-21	+1	+22
Relative humidity (%)	Annual	-1.6	-0.5	+0.7	-2.7	-0.9	+0.8	-5.3	-1.8	+1.5
Solar radiation (%)	Annual	-1.0	+0.3	+1.9	-1.7	+0.5	+3.2	-3.2	+1.0	+6.3

Table B8: Projected climate changes for Hobart

Variable	Season	2030 A1B 10p	2030 A1B 50p	2030 A1B 90p	2070 B1 10p	2070 B1 50p	2070 B1 90p	2070 A1FI 10p	2070 A1FI 50p	2070 A1FI 90p
Temperature (ºC)	Annual	0.4	0.6	0.9	0.7	1.1	1.5	1.4	2.1	2.9
	Summer	0.5	0.7	1	0.8	1.1	1.6	1.5	2.2	3.1
	Autumn	0.4	0.7	1	0.7	1.1	1.6	1.4	2.2	3.1
	Winter	0.4	0.6	0.9	0.7	1	1.4	1.3	1.9	2.8
	Spring	0.4	0.6	0.9	0.6	1	1.5	1.2	1.9	2.9
No. days over 35ºC (current 1.4)	Annual	1.6	1.7	1.8	1.7	1.8	2.0	2.0	2.4	3.4
Rainfall (%)	Annual	-6	-1	+3	-10	-3	-4	-19	-6	+8
	Summer	-11	-3	+4	-17	-5	+14	-31	-10	+13
	Autumn	-7	+1	+4	-11	-2	+7	-20	-4	+14
	Winter	-5	0	+6	-8	0	+9	+15	0	+18
	Spring	-11	-4	+3	-18	-6	+6	-31	-12	+11
Potential evaporation (%)	Annual	+1	+3	+6	+2	+5	+9	+4	+10	+18
	Summer	+1	+3	+5	+2	+5	+8	+3	+9	+16
	Autumn	+2	+4	+7	+4	+7	+12	+7	+14	+24
	Winter	-14	+12	+45	-23	+20	+75	-44	+38	+145
	Spring	+1	+3	+6	+1	+5	+10	+2	+9	+19
Wind-speed (%)	Annual	-2	+1	+5	-4	+2	+8	-7	+4	+16
	Summer	-11	-2	+5	-19	-3	+9	-36	-6	+17
	Autumn	-6	-1	+5	-10	-1	+8	-20	-2	+15
	Winter	0	+5	+11	0	+8	+18	-1	+15	+34
	Spring	-2	+2	+7	-3	+3	+11	-6	+7	+22
Relative humidity (%)	Annual	-0.5	-0.2	+0.1	-0.8	-0.3	+0.1	-1.5	-0.6	+0.2
Solar radiation (%)	Annual	-0.3	+0.5	+1.5	-0.5	+0.9	+2.4	-1.0	+1.7	+4.7

Table B9: Projected climate changes for Melbourne

Variable	Season	2030 A1B 10p	2030 A1B 50p	2030 A1B 90p	2070 B1 10p	2070 B1 50p	2070 B1 90p	2070 A1FI 10p	2070 A1FI 50p	2070 A1FI 90p
Temperature (ºC)	Annual	0.6	0.9	1.2	1	1.4	2	1.9	2.8	3.8
	Summer	0.6	1	1.4	1.1	1.6	2.4	2.1	3.1	4.5
	Autumn	0.6	0.8	1.2	0.9	1.4	2.1	1.8	2.7	4
	Winter	0.5	0.7	1	0.8	1.1	1.7	1.5	2.2	3.2
	Spring	0.6	0.9	1.3	1	1.5	2.1	1.9	2.9	4.1
No. days over 35ºC (current 9.1)	Annual	10.6	11.4	12.8	11.9	13.6	16.8	15.4	19.8	25.9
Rainfall (%)	Annual	-9	-4	+1	-14	-6	+1	-25	-11	+3
	Summer	-11	-1	+9	-17	-2	+14	-30	-4	+27
	Autumn	-9	-2	+6	-14	-2	+10	-25	-5	+19
	Winter	-10	-4	+2	-17	-7	+3	-30	-12	+5
	Spring	-16	-7	+1	-25	-11	+1	-43	-21	+2
Potential evaporation (%)	Annual	+1	+3	+5	+1	+4	+8	+2	+8	+16
	Summer	0	+2	+5	0	+4	+8	0	+7	+16
	Autumn	+2	+4	+6	+3	+6	+10	+6	+12	+20
	Winter	-1	+8	+20	-1	+14	+34	-2	+26	+66
	Spring	-1	+2	+5	-2	+3	+8	-3	+6	+16
Wind-speed (%)	Annual	-6	0	+4	-9	-1	+6	-18	-1	+12
	Summer	-8	0	+6	-13	0	+9	-25	-1	+18
	Autumn	-10	-3	+3	-16	-4	+6	-32	-8	+11
	Winter	-5	+1	+5	-8	+1	+9	-15	+2	+18
	Spring	-7	0	+6	-12	-1	+10	-24	-1	+19
Relative humidity (%)	Annual	-1.5	-0.7	-0.1	-2.4	-1.2	-0.2	-4.7	-2.3	-0.3
Solar radiation (%)	Annual	+0.1	+0.8	+1.8	+0.1	+1.3	+3.0	+0.3	+2.6	+5.7

Table B10: Projected climate changes for Mildura

Variable	Season	2030 A1B 10p	2030 A1B 50p	2030 A1B 90p	2070 B1 10p	2070 B1 50p	2070 B1 90p	2070 A1FI 10p	2070 A1FI 50p	2070 A1FI 90p
Temperature (ºC)	Annual	0.6	0.9	1.3	1.1	1.5	2.2	2	3	4.2
	Summer	0.7	1	1.5	1.1	1.7	2.4	2.1	3.2	4.7
	Autumn	0.6	0.9	1.4	1	1.5	2.3	1.9	3	4.4
	Winter	0.5	0.8	1.2	0.8	1.3	1.9	1.6	2.5	3.8
	Spring	0.7	1	1.4	1.1	1.6	2.3	2.1	3.1	4.5
No. days over 35ºC (current 31.8)	Annual	36.2	38.5	42.6	39.4	44.9	51.0	48.4	59.9	75.8
Rainfall (%)	Annual	-10	-3	+4	-17	-5	+6	-30	-10	+11
	Summer	-14	0	+14	-22	-1	+22	-38	-1	+42
	Autumn	-11	-1	+9	-17	-1	+15	-30	-3	+30
	Winter	-15	-6	+3	-23	-9	+5	-40	-17	+9
	Spring	-18	-7	+3	-29	-11	+5	-48	-21	+10
Potential evaporation (%)	Annual	0	+2	+4	+1	+4	+7	+1	+7	+14
	Summer	0	+2	+5	0	+3	+8	-1	+7	+15
	Autumn	+1	+3	+6	+2	+5	+9	+4	+10	+18
	Winter	+1	+5	+12	+1	+8	+21	+2	+16	+40
	Spring	-2	+1	+4	-3	+2	+6	-5	+3	+11
Wind-speed (%)	Annual	-4	0	+4	-7	0	+6	-13	0	+12
	Summer	-2	+2	+6	-3	+3	+10	-5	+6	+19
	Autumn	-7	-1	+5	-11	-1	+8	-21	-2	+16
	Winter	-8	-2	+4	-13	-3	+7	-26	-5	+14
	Spring	-6	0	+6	-10	0	+10	-20	0	+20
Relative humidity (%)	Annual	-1.6	-0.7	+0.1	-2.6	-1.1	+0.1	-5.1	-2.1	+0.2
Solar radiation (%)	Annual	-0.3	+0.4	+1.3	-0.5	+0.6	+2.1	-1.0	+1.2	+4.2

Table B11: Projected climate changes for Perth

Variable	Season	2030 A1B 10p	2030 A1B 50p	2030 A1B 90p	2070 B1 10p	2070 B1 50p	2070 B1 90p	2070 A1FI 10p	2070 A1FI 50p	2070 A1FI 90p
Temperature (ºC)	Annual	0.6	0.8	1.2	1	1.4	2	1.9	2.7	3.8
	Summer	0.6	0.9	1.3	1	1.5	2.2	1.9	2.9	4.2
	Autumn	0.6	0.8	1.2	0.9	1.4	2	1.8	2.7	3.9
	Winter	0.5	0.7	1	0.8	1.2	1.7	1.6	2.3	3.3
	Spring	0.6	0.9	1.3	1	1.5	2.1	1.9	2.9	4.1
No. days over 35ºC (current 28.1)	Annual	33.1	35.3	38.7	36.2	40.5	46.2	44.1	53.8	67.4
Rainfall (%)	Annual	-13	-6	+1	-21	-11	+1	-37	-19	+2
	Summer	-16	-4	+9	-25	-6	+14	-43	-12	+28
	Autumn	-15	-4	+8	-24	-7	+14	-41	-12	+26
	Winter	-14	-7	-1	-23	-12	-1	-39	-22	-2
	Spring	-18	-9	-2	-29	-15	-4	-48	-27	-7
Potential evaporation (%)	Annual	+1	+2	+4	+2	+4	+6	+4	+7	+12
	Summer	+1	+2	+3	+1	+3	+6	+2	+6	+11
	Autumn	+1	+3	+5	+2	+5	+9	+4	+9	+17
	Winter	+2	+5	+9	+4	+8	+15	+7	+16	+29
	Spring	0	+2	+4	0	+3	+7	+1	+6	+13
Wind-speed (%)	Annual	-3	0	+2	-5	0	+4	-9	-1	+7
	Summer	-1	+2	+7	-2	+4	+12	-5	+8	+24
	Autumn	-2	+2	+7	-4	+3	+11	-7	+6	+21
	Winter	-10	-4	+1	-17	-7	+2	-34	-14	+4
	Spring	-5	-1	+3	-9	-1	+5	-17	-3	+10
Relative humidity (%)	Annual	-1.3	-0.6	+0.0	-2.1	-1.0	-0.2	-4.0	-2.0	-0.3
Solar radiation (%)	Annual	-0.1	+0.4	+1.0	-0.2	+0.7	+1.7	-0.3	+1.4	+3.3

Table B12: Projected climate changes for St George

Variable	Season	2030 A1B 10p	2030 A1B 50p	2030 A1B 90p	2070 B1 10p	2070 B1 50p	2070 B1 90p	2070 A1FI 10p	2070 A1FI 50p	2070 A1FI 90p
Temperature (ºC)	Annual	0.7	1.1	1.6	1.2	1.8	2.7	2.4	3.6	5.2
	Summer	0.7	1.1	1.7	1.1	1.9	2.9	2.2	3.6	5.5
	Autumn	0.7	1.1	1.7	1.1	1.8	2.8	2.1	3.5	5.3
	Winter	0.7	1	1.5	1.1	1.7	2.5	2.1	3.3	4.8
	Spring	0.8	1.2	1.8	1.3	2	2.9	2.6	3.9	5.7
No. days over 35ºC (current 46.7)	Annual	56.3	63.1	72.3	63.5	74.1	91.1	80.3	102.9	135.3
Rainfall (%)	Annual	-12	-3	+5	-20	-5	+9	-35	-10	+17
	Summer	-12	-1	+10	-19	-1	+17	-33	-3	+33
	Autumn	-16	-3	+10	-26	-6	+16	-44	-11	+32
	Winter	-19	-6	+6	-29	-9	+9	-49	-17	+18
	Spring	-18	-6	+5	-28	-10	+9	-47	-18	+17
Potential evaporation (%)	Annual	+2	+3	+4	+3	+5	+7	+5	+9	+14
	Summer	+1	+3	+5	+2	+5	+8	+5	+9	+15
	Autumn	+2	+3	+6	+3	+6	+9	+5	+11	+18
	Winter	+1	+4	+8	+2	+7	+13	+4	+13	+24
	Spring	0	+2	+4	+1	+4	+7	+1	+7	+14
Wind-speed (%)	Annual	-2	+2	+6	-3	+3	+10	-5	+5	+19
	Summer	-3	+2	+8	-4	+4	+14	-8	+8	+27
	Autumn	-4	+1	+6	-6	+1	+10	-12	+3	+19
	Winter	-6	0	+7	-10	0	+12	-19	0	+23
	Spring	-4	+4	+12	-6	+6	+19	-12	+11	+37
Relative humidity (%)	Annual	-1.7	-0.5	+0.7	-2.9	-0.8	+1.2	-5.6	-1.6	+2.2
Solar radiation (%)	Annual	-1.2	+0.2	+2.0	-2.0	+0.3	+3.3	-3.8	+0.7	+6.3

Table B13: Projected climate changes for Sydney

Variable	Season	2030 A1B 10p	2030 A1B 50p	2030 A1B 90p	2070 B1 10p	2070 B1 50p	2070 B1 90p	2070 A1FI 10p	2070 A1FI 50p	2070 A1FI 90p
Temperature (ºC)	Annual	0.6	0.9	1.3	1.1	1.6	2.2	2.1	3.0	4.3
	Summer	0.6	1.0	1.5	1.0	1.6	2.5	2.1	3.1	4.7
	Autumn	0.6	0.9	1.4	1.0	1.5	2.3	1.9	3.0	4.3
	Winter	0.6	0.8	1.2	0.9	1.4	1.9	1.8	2.6	3.7
	Spring	0.7	1.0	1.5	1.2	1.7	2.5	2.2	3.3	4.8
No. days over 35ºC (currently 3.5)	Annual	4.1	4.4	5.1	4.5	5.3	6.6	6.0	8.2	12.0
Rainfall (%)	Annual	-9	-3	+3	-14	-4	+5	-25	-8	+10
	Summer	-7	+1	+9	-12	+1	+14	-21	+2	+28
	Autumn	-10	-2	+6	-16	-3	+11	-29	-6	+21
	Winter	-15	-5	+4	-23	-9	+6	-40	-16	+12
	Spring	-16	-6	+4	-25	-9	+6	-44	-17	+12
Potential evaporation (%)	Annual	+2	+3	+5	+3	+5	+8	+5	+9	+15
	Summer	+1	+3	+5	+2	+5	+8	+4	+9	+15
	Autumn	+2	+4	+6	+3	+6	+11	+7	+12	+20
	Winter	+2	+5	+9	+3	+8	+15	+6	+16	+29
	Spring	0	+2	+4	0	+3	+7	+1	+6	+13
Wind-speed (%)	Annual	-5	0	+4	-8	0	+6	-15	-1	+12
	Summer	-5	+3	+11	-9	+4	+19	-16	+8	+36
	Autumn	-9	-2	+4	-14	-3	+7	-27	-5	+14
	Winter	-7	-1	+5	-12	-2	+8	-23	-3	+16
	Spring	-8	0	+6	-14	-1	+10	-26	-1	+19
Relative humidity (%)	Annual	-1.3	-0.4	+0.4	-2.1	-0.6	+0.7	-4.0	-1.2	+1.3
Solar radiation (%)	Annual	-1.0	+0.3	+1.9	-1.6	+0.5	+3.1	-3.2	+0.9	+6.0

Table B14: Projected climate changes for Wilcannia

Variable	Season	2030 A1B 10p	2030 A1B 50p	2030 A1B 90p	2070 B1 10p	2070 B1 50p	2070 B1 90p	2070 A1FI 10p	2070 A1FI 50p	2070 A1FI 90p
Temperature (ºC)	Annual	0.7	1	1.5	1.2	1.7	2.4	2.3	3.3	4.7
	Summer	0.7	1.1	1.6	1.2	1.8	2.6	2.3	3.5	5.1
	Autumn	0.7	1	1.5	1.1	1.7	2.6	2.1	3.3	5
	Winter	0.5	0.9	1.3	0.9	1.4	2.2	1.8	2.8	4.3
	Spring	0.7	1.1	1.6	1.2	1.8	2.6	2.4	3.5	5.1
No. days over 35ºC (current 63.1)	Annual	71.3	77.2	82.3	78.6	85.1	95.7	91.7	106.1	129.4
Rainfall (%)	Annual	-13	-3	+7	-20	-5	+11	-35	-9	+21
	Summer	-16	0	+15	-25	0	+25	-43	0	+48
	Autumn	-15	-1	+12	-23	-2	+20	-40	-5	+39
	Winter	-18	-6	+6	-28	-9	+10	-46	-17	+20
	Spring	-23	-7	+8	-35	-11	+12	-56	-20	+24
Potential evaporation (%)	Annual	+1	+2	+5	+1	+4	+7	+2	+7	+14
	Summer	0	+2	+5	0	+4	+9	0	+8	+17
	Autumn	+1	+3	+6	+2	+5	+10	+4	+10	+18
	Winter	0	+4	+9	0	+6	+15	0	+13	+28
	Spring	-2	+1	+4	-3	+2	+6	-5	+3	+12
Wind-speed (%)	Annual	-2	0	+4	-4	+1	+6	-8	+1	+12
	Summer	-3	+1	+7	-5	+2	+12	-9	+5	+23
	Autumn	-4	+1	+6	-7	+1	+10	-13	+3	+19
	Winter	-9	-3	+4	-16	-4	+7	-31	-8	+13
	Spring	-4	+1	+7	-6	+2	+11	-12	+4	+21
Relative humidity (%)	Annual	-1.6	-0.6	+0.3	-2.7	-1.0	+0.5	-5.1	-1.9	+1.0
Solar radiation (%)	Annual	-0.7	+0.2	+1.3	-1.2	+0.3	+2.2	-2.3	+0.6	+4.3

References

Abbs, D.J., and K.L. McInnes, 2004: *Impact of Climate Change on Extreme Rainfall and Coastal Sea Levels over South-east Queensland. Part 1: Analysis of Extreme Rainfall and Wind events in a GCM*. Report for the Gold Coast City Council, Queensland, Australia, 48 pp.

Abbs, D.J., S. Aryal, E. Campbell, J. McGregor, K. Nguyen, M. Palmer, T. Rafter, I. Watterson, and B. Bates, 2006: *Projections of Extreme Rainfall and Cyclones*. A report to the Australian Greenhouse Office, Canberra, Australia, 97 pp.

Adams, P.D., M. Horridge, J.R. Masden, and G. Wittwer, 2002: Drought, regions and the Australian economy between 2001-02 and 2004-05. *Australian Bulletin of Labour*, **28**(4), 233-249.

AGO (Australian Greenhouse Office), 2006a. *Climate Change Impacts & Risk Management: A Guide for Business and Government*. Department of Environment and Heritage, Commonwealth of Australia, 72 pp.

AGO (Australian Greenhouse Office). 2006b. *Climate Change Scenarios for Initial Assessment of Risk in Accordance with Risk Management Guidance*. Department of Environment and Heritage, Commonwealth of Australia, 35 pp.

Ahmad, Q.K., R.A. Warrick, T.E. Downing, S. Nishioka, K.S. Parikh, C. Parmesan, S.H. Schneider, F. Toth, and G. Yohe, 2001: Methods and tools. In: McCarthy, J.J., O.F. Canziani, N.A. Leary, D.J. Dokken, and K.S. White (eds). *Climate Change 2001: Impacts, Adaptation, and Vulnerability. Contribution of Working Group II to the Third Assessment Report of the Intergovernmental Panel on Climate Change*. Cambridge University Press, Cambridge, pp 105-143.

Alexander, B.M., J.A.T. Bye, and I.N. Smith, 2005: Australian summer maximum temperature lags. *Australian Meteorological Magazine*, **54**, 103-114.

Alexander, L., P. Hope, D. Collins, B. Trewin, A. Lynch, and N. Nicholls, 2007: Trends in Australia's climate means and extremes: A global context. *Australian Meteorological Magazine*, **56**, 1-18.

Allan, R.J., J. Lindesay, and D. Parker, 1996: *El Niño Southern Oscillation and Climatic Variability*. CSIRO Publishing, 402 pp.

Allen Consulting, 2005: *Climate Change Risk and Vulnerability*. Report to the Australian Greenhouse Office, Department of the Environment and Heritage, Canberra, Commonwealth of Australia, 159 pp.

Amitrano, L., R. Hargreaves, I. Page, K. Hennessy, T. Lee, M. Snow, L. Winton, R. Woodruff, and T. Kjellstrom, 2007: *An Assessment of the Need to Adapt Buildings for the Unavoidable Consequences of Climate Change*. Report to the Victorian Department of Sustainability and the Environment, Melbourne, Victoria, Australia, 199 pp.

AMS (American Meteorological Society), 1997: Meteorological drought – policy statement. *Bulletin of the American Meteorological Society*, **78**, 847-849.

Anker, S.A., E.A. Colhoun, C.E. Barton, M. Peterson, and M. Barbetti, 2001: Holocene vegetation and paleoclimatic and paleomagnetic history from Lake Johnston, Tasmania. *Quaternary Research*, **56**, 264–274.

Arblaster J.M., and G.A. Meehl, 2006: Contributions of external forcings to Southern Annular Mode trends. *Journal of Climate*, **19**, 2896-2905.

Australian Standards, 2004: *Australian Standard: Risk Management*, Council of Standards Australia and Council of Standards New Zealand, AS/NZA 4360:2004, Standards Association of Australia, Strathfield, NSW, Australia.

Austroads, 2004: *Impact of Climate Change on Road Infrastructure*. Austroads Incorporated, Sydney, Australia, 124 pp.

Bengtsson, L.K., I. Hodges, and E. Roeckner, 2006: Storm tracks and climate change. *Journal of Climate*, **19**, 3518–3543

Boycoff, M., and J. Boykoff, 2004: Bias as balance: Global warming and the U.S. prestige press. *Global Environmental Change*, **14**(2), 125-136.

Briffa, K.R., 2000: Annual climate variability in the Holocene: interpreting the message of ancient trees. *Quaternary Science Reviews*, **19**(1-5), 87–105.

Brooks, H.E., J.W. Lee, and J.P. Craven, 2003: The spatial distribution of severe thunderstorm and tornado environments from global reanalysis data. *Atmospheric Research*, **67**, 73-94.

Bryant, E. 1997: *Climate processes and change*. Cambridge University Press, 209 pp.

Bureau of Meteorology, 2001: *Climatic Atlas of Australia: Maps of Evaporation*. Wang, Q.J., F.L.N. McConachy, F.H.S. Chiew, R. James, G.C. de Hoedt, and W.J. Wright, Australian Bureau of Meteorology, Melbourne.

Bureau of Meteorology, 2006a: *Living with Drought*. Australian Bureau of Meteorology. http://www.bom.gov.au/climate/drought/livedrought.shtml.

Bureau of Meteorology, 2006b. *The meteorology of the Gold Coast floods*: 29th-30th June 2005. (unpublished manuscript)

Burke, E.J., S.J. Brown, and N. Christidis, 2006: Modelling the recent evolution of global drought and projections for the 21st century with the Hadley Centre climate model. *Journal of Hydrometeorology*, **7**, 1113-1125.

Cai, W.J., 2006: Antarctic ozone depletion causes an intensification of the Southern Ocean super-gyre circulation. *Geophysical Research Letters*, **33**, L03712.

Cai, W.J., P.H. Whetton, and D.J. Karoly, 2003a: The response of the Antarctic Oscillation to increasing and stabilized atmospheric CO_2. *Journal of Climate*, **16**(10): 1525-1538.

Cai, W.J., M.A. Collier, P.J. Durack, H.B. Gordon, A.C. Hirst, S.P. O'Farrell, and P.H. Whetton, 2003b: The response of climate variability and mean state to climate change: preliminary results from the CSIRO Mark 3 coupled model. *CLIVAR Exchanges*, **8**(8-11), 16-17.

Cai, W.J., M.A. Collier, H.B. Gordon and L.J. Waterman, 2003c: Strong ENSO variability and a Super-ENSO pair in the CSIRO Mark 3 coupled climate model. *Monthly Weather Review*, **131**(7), 1189-1210.

Cai, W.J., H.H. Hendon and G.A. Meyers, 2005a: Indian Ocean dipole-like variability in the CSIRO Mark 3 Coupled Climate Model. *Journal of Climate*, **18** (10): 1449-1468.

Cai, W.J., G. Shi, and Y. Li, 2005b: Multidecadal fluctuations of winter rainfall over southwest Western Australia simulated in the CSIRO Mark 3 coupled model. *Geophysical Research Letters*, **32**, L12701.

Cai, W.J., G. Shi, T.D. Cowan, D. Bi, and Ribbe, J. 2005c: The response of the Southern Annular Mode, the East Australian Current, and the southern mid-latitude ocean circulation to global warming. Geophysical Research Letters, **32** (23), L23706.

Cai W., and T. Cowan, 2006: SAM and regional rainfall in IPCC AR4 models: Can anthropogenic forcing account for southwest Western Australian winter rainfall reduction? *Geophysical Research Letters*, **33**, L24708.

Cai, W.J., and T. Cowan, 2007: Trends in Southern Hemisphere circulation in IPCC AR4 models over 1950-99: Ozone-depletion vs. greenhouse forcing. *Journal of Climate*, **20**(4), 681–693.

Cameron, T.A., 2005: Updating subjective risks in the presence of conflicting information: An application to climate change. *The Journal of Risk and Uncertainty*, **30**(1), 63-97.

Cane, M.A., 2005: The evolution of El Niño, past and future. *Earth and Planetary Science Letters*, **164**, 1-10.

Carter, J., W. Hall, K. Brook, G. McKeon, K. Day and C. Paull, 2000: AUSSIE GRASS: Australian Grassland and Rangelands Assessment by Spatial Simulation. In *Applications of Seasonal Climate Forecasting in Agricultural and Natural Ecosystems: The Australian Experience*. G. Hammer, N. Nicholls and C. Mitchell (Eds.). Kluwer Academic Publishers, Atmospheric and Oceanographic Sciences Library.

Carter, T.R., R.N. Jones, X, Lu, S Bhadwal, C. Conde, L.O. Mearns, B.C. O'Neill, M.D.A. Rounsevell, and M.B. Zurek, 2007: New Assessment Methods and the Characterisation of Future Conditions. In: Parry, M.L., O.F. Canziani, J.P. Palutikof, P.J. van der Linden, and C.E. Hanson (eds). *Climate Change 2007: Impacts, Adaptation and Vulnerability. Contribution of Working Group II to the Fourth Assessment Report of the Intergovernmental Panel on Climate Change*. Cambridge University Press, Cambridge, UK.

Cary, G.J. (2002). Importance of a changing climate for fire regimes in Australia, In: *Flammable Australia: Fire Regimes and Biodiversity of a Continent*. R.A. Bradstock, J.E. Williams and A.M. Gill (Eds.). Cambridge University Press, Melbourne, pp 26-49.

CCSA (Conservation Council of South Australia), 2005: *Climate Change Resilient Communities*. Adelaide, South Australia.

Charles, S.P., B.C. Bates, I.N. Smith, and J.P. Hughes, 2004: Statistical downscaling of daily precipitation from observed and modelled atmospheric fields. *Hydrological Processes*, **18**, 1373-1394.

Chiew, H.S., 2006: An overview of methods for estimating climate change impact on runoff. 30th Hydrology and Water Resources Symposium, 4-7 December, 2006, Launceston, Tasmania, Australia.

Church, J.A., and N.J. White, 2006: 20th century acceleration in sea-level rise. *Geophysical Research Letters*, **33**, L01602.

Church, J.A., and N.J. White and J.M. Arblaster, 2005: Significant decadal-scale impact of volcanic eruptions on sea level and ocean heat content. *Nature*, **438**, 74–77.

Church, J.A., J.R. Hunter, K.L. McInnes, and N.J. White, 2006: Sea-level rise around the Australian coastline and the changing frequency of extreme sea-level events. *Australian Meteorological Magazine*, **55**, 253-260.

CIU (Coastal Investigations Unit), 1992: *Victorian Coastal Vulnerability Study.* Port of Melbourne Authority, Port Melbourne, Victoria, Australia.

Cobb, K.M., C.D. Charles, R.L. Edwards, H. Cheng, and M. Kastner, 2003: El Niño/Southern Oscillation and tropical Pacific climate during the last millennium, *Nature*, **424**, 271–276.

Cook, E.R., B.M. Buckley, R.D. D'Arrigo, and M.J. Peterson, 2000: Warm-season temperatures since 1600 BC reconstructed from Tasmanian tree rings and their relationship to large-scale sea surface temperature anomalies. *Climate Dynamics*, **16**(2-3), 79–91.

Cowell, P.J., B.G. Thom, R.A. Jones, C.H. Everts, and D. Simanovic, 2006: Management of uncertainty in predicting climate change impacts on beaches. *Journal of Coastal Research*, **22**, 232-245.

CSIRO (Commonwealth Scientific and Industrial Research Organisation), 1992: *Climate change scenarios for the Australian region*. CSIRO Division of Atmospheric Research, Melbourne, 6 pp.

CSIRO (Commonwealth Scientific and Industrial Research Organisation), 1996: *Climate change scenarios for the Australian region*. CSIRO Division of Atmospheric Research, Melbourne, 8 pp.

CSIRO (Commonwealth Scientific and Industrial Research Organisation), 2001: *Climate Change Projections for Australia*. CSIRO Atmospheric Research, Aspendale, Victoria, Australia.

CSIRO and Melbourne Water, 2005: *Implications of Climate Change for Melbourne's Water Resources*. Melbourne Water, Melbourne, 26 pp.

DAFF (Department of Agriculture, Fisheries and Forestry), 2006: *Contours*. Department of Agriculture, Fisheries and Forestry, 24 pp.

D' Arrigo, R., E. Cook, R. Wilson, R. Allan, and M. Mann, 2005: On the variability of ENSO over the past six centuries. *Geophysical Research Letters*, **32**, L03711, 1-4.

Dai, A., 2006: Precipitation characteristics in eighteen coupled climate models. *Journal of Climate*, **19**, 4605–4630.

Demeritt, D., and D. Langdon, 2004: The UK Climate Change Programme and communication with local authorities. *Global Environmental Change*, **14**, 425-336.

Dempsey, R., and A. Fisher, 2005: Consortium for Atlantic Regional Assessment: Information tools for community adaptation to changes in climate or land use. *Risk Analysis*, **25**(6), 1495-1509.

Denman, K.L., G. Brasseur, A. Chidthaisong, P. Ciais, P. Cox, R.E. Dickinson, D. Hauglustaine, C. Heinze, E. Holland, D. Jacob, U. Lohmann, S. Ramachandran, P.L. da Silva Dias, S.C. Wofsy, and X. Zhang, 2007: Couplings Between Changes in the Climate System and Biogeochemistry. In: Solomon, S., D. Qin, M. Manning, Z. Chen, M. Marquis, K.B. Averyt, M. Tignor, and H.L. Miller (eds.) *Climate Change 2007: The Physical Science Basis. Contribution of Working Group I to the Fourth Assessment Report of the Intergovernmental Panel on Climate Change*. Cambridge University Press, Cambridge, United Kingdom and New York, NY, USA.

Dessai, S., and M. Hulme, 2007: Assessing the robustness of adaptation decisions to climate change uncertainties: A case study on water resources management in the East of England, *Global Environmental Change*, **17**, 59-72.

Dessai, S., X.F. Lu and M. Hulme, 2005: Limited sensitivity analysis of regional climate change probabilities for the 21st century. *Journal of Geophysical Research-Atmospheres*, **110**, D19108.

Done, T., P. Whetton, R.N. Jones, R. Berkelmans, J. Lough, W. Skirving and S. Wooldridge, 2003: *Global Climate Change and Coral Bleaching on the Great Barrier Reef*. Final Report to the State of Queensland Greenhouse Taskforce through the Department of Natural Resources and Mines, QDNRM, Brisbane.

Drosdowsky, W., 2005: The latitude of the subtropical ridge over eastern Australia: the L index revisited. *International Journal of Climatology*, **25**, 1291-1299.

Edgar, G.J., C.R. Samson and N.S. Barrett, 2005: Species extinction in the marine environment: Tasmania as a regional example of overlooked losses in biodiversity. *Conservation Biology* **19**, 1294-1300.

Edmonds, J.A., and N.J. Rosenberg, 2005: Climate change impacts for the coterminous USA: An integrated assessment summary. *Climatic Change*, **69**, 151-162.

Edyvane, K.S., 2003: *Conservation, monitoring and recovery of threatened giant kelp (Macrocystis pyrifera) beds in Tasmania*. Final Report for Environment Australia. Department of Primary Industries, Water and Environment, Hobart, Tasmania.

Emanuel, K., 2005: Increasing destructiveness of tropical cyclones over the past 30 years. *Nature*, **436**, 686–688.

Feng, M., G. Meyers, A. Pearce, and S. Wijffels, 2003: Annual and interannual variations of the Leeuwin Current at 32ºS. *Journal Geophysical Research*, **108**(C11), 3355.

Flückiger, J., E. Monnin, B. Stauffer, J. Schwander, T.F. Stocker, J. Chappellaz, D. Raynaud, and J.-M. Barnola, 2002: High resolution Holocene N_2O ice core record and its relationship with CH_4 and CO_2. *Global Biogeochemical Cycles*, **16**, GB001417.

Frederiksen, J.S., and C. Frederiksen, 2005: *Decadal changes in Southern Hemisphere winter cyclogenesis*. CSIRO Marine and Atmospheric Research Report No. 002, 29pp.

Frederiksen, J.S., and C. Frederiksen, 2007: Inter-decadal changes in Southern Hemisphere winter storm track modes, *Tellus*, accepted.

Frich, P., L.V. Alexander, P. Della-Marta, B. Gleason, M. Haylock, A.M.G. Klein Tank, T. Peterson, 2002: Observed coherent changes in climatic extremes during the second half of the twentieth century, *Climate Research*, **10**, 103-212.

Friedlingstein, P., P. Cox, R. Betts, L. Bopp, W. Von Bloh, V. Brovkin, P. Cadule, S. Doney, M. Eby, I. Fung, G. Bala, J. John, C. Jones, F. Joos, T. Kato, M. Kawamiya, W. Knorr, K. Lindsay, H. D. Matthews, T. Raddatz, P. Rayner, C. Reick, E. Roeckner, K. G. Schnitzler, R. Schnur, K. Strassmann, A. J. Weaver, C. Yoshikawa, and N. Zeng, 2006: Climate–carbon cycle feedback analysis: results from the C4MIP model intercomparison, *Journal of Climate*, **19**, 3337-3353.

Fyfe, J.C., G.J. Boer, and G.M. Flato, 1999: The Artic and Antarctic Oscillations and their projected changes under global warming, *Geophysical Research Letters*, **26**, 1601-1604.

Gagan, M. K., E.J. Hendy, S.G. Haberle, and W.S. Hantoro, 2004: Post-glacial evolution of the Indo-Pacific Warm Pool and El Niño-Southern Oscillation. *Quaternary International*, **118-119**, 127–143.

Gallant, A., K. Hennessy and J. Risbey, 2007: A re-examination of trends in rainfall indices for six Australian regions. *Australian Meteorological Magazine*, accepted.

Gillett, N.P., and D.W.J. Thompson, 2003: Simulation of recent Southern Hemisphere climate change. Science, **302**, 273–275.

Giorgi, F., and L.O. Mearns, 2002: Calculation of average, uncertainty range and reliability of regional climate changes from AOGCM simulations via the reliability ensemble averaging (REA) method. *Journal of Climate*, **15**, 1141-1158.

Godfrey, J.S. 1989. A Sverdrup model of the depth-integrated flow for the world ocean allowing for island circulations. *Geophysical and Astrophysical Fluid Dynamics*, **45**, 89–112.

Griffiths, G.M., L.E. Chambers, M.R. Haylock, M.J. Manton, N. Nicholls, H.-J. Baek, Y. Choi, P. Della-Marta, A. Gosai, N. Iga, R. Lata, V. Laurent, L. Maitrepierre, H. Nakamigawa, N. Ouprasitwong, D. Solofa, L. Tahini, D.T. Thuy, L. Tibig, B. Trewin, K. Vediapan, and P. Zhai, 2005: Change in mean temperature as a predictor of extreme temperature change in the Asia-Pacific region. *International Journal of Climatology*, **25**, 1301-1330.

Hansen, J., 2007: Scientific reticence and sea level rise. *Environmental Research Letters*, **2**, 1-6.

Hanstrum, B.N., G.A. Mills, and A. Watson, 2002: The cool-season tornadoes of California and Southern Australia, *Weather Forecast*, **17**, 705-722.

Hardy, T., L. Mason and A. Astorquia, 2004: *Queensland climate change and community vulnerability to tropical cyclones: Ocean hazards assessment – Stage 3*. Report for Queensland Government. 56 pp.

Hare, B., and M. Meinshausen, 2004: *How Much Warming Are We Committed To And How Much Can Be Avoided?* PIK Report, No. 93, Potsdam Institute for Climate Impact Research, Potsdam, Germany, 45 pp.

Harper, B. 1999: *Storm tide threat in Queensland: history, prediction and relative risks*. Queensland Department of Environment and Heritage, Conservation technical report no. 10. 24 pp.

Harper, B.A., and J. Callaghan, 2006: *On the importance of reviewing historical tropical cyclone intensities*. Presented at the 27th Conference on Hurricanes and Tropical Meteorology, Monterey, California, April 24-28, American Meteorological Society.

Hartmann, D.L., and F. Lo, 1998: Wave-driven zonal flow vacillation in the Southern Hemisphere. *Journal of Atmospheric Sciences*, **55**, 1303–1315.

Hayhoe, K., D. Cayan, C.B. Field, P.C. Frumhoff, E.P. Maurer, N.L. Miller, S.C. Moser, S.H. Schneider, N.C. Cahill,, C.C. Cleland, L. Dale, R. Drapek, R.N. Hanemann, L.S. Kalkstein, J. Lenihan, C.K. Lunch, R.P. Neilson, S.C. Sheridan, and Verville, J.H. 2004: Emissions pathways, climate change, and impacts on California. *Proceedings of the National Academy of Science USA*, **101**, 12422-12427.

Held, I.M., and B.J. Soden, 2006: Robust responses of the hydrological cycle to global warming. *Journal of Climate*, **19**, 5686–5699.

Hendon, H.H., 2005: Air sea interaction. In: Lau, W.K.M., and D.E. Waliser (eds). *Intraseasonal Variability in the Atmosphere-Ocean Climate System*. Praxis Publishing, 436 pp.

Hendon H.H., D.J.W. Thompson, and M.C. Wheeler, 2007: Australian rainfall and surface temperature variations associated with the Southern Hemisphere annular mode, *Journal of Climate*, in press.

Hendy, E.J., M. K. Gagan, C.A. Alibert, M.T. McCulloch, J.M. Lough, and P.J. Isdale, 2002: Abrupt decrease in tropical Pacific sea surface salinity at end of Little Ice Age. *Science*, **295** (5559), 1511–1514.

Hennessy, K.J., 2004: Climate change and Australian storms. In: *Proceedings of the International Conference on Storms*, Brisbane, Australia. 5-9 July, 2004, 8 pp.

Hennessy, K.J., P.H. Whetton, J. Bathols, M. Hutchinson, and, J. Sharples, 2003: *The Impact of Climate Change on Snow Conditions in Australia*. CSIRO Atmospheric Research. Consultancy report for the Victorian Dept of Sustainability and Environment, NSW National Parks and Wildlife Service, Australian Greenhouse Office and the Australian Ski Areas Association, 47 pp.

Hennessy, K., K. McInnes, D. Abbs, R. Jones, J. Bathols, R. Suppiah, J. Ricketts, T. Rafter, D. Collins and D. Jones, 2004: *Climate Change in New South Wales, Part 2: Projected Changes in Climate Extremes*. Consultancy report for the New South Wales Greenhouse Office by the Climate Impact Group of CSIRO Atmospheric Research and the National Climate Centre of the Australian Government Bureau of Meteorology, 79 pp.

Hennessy, K., C. Lucas, N. Nicholls, J. Bathols, R. Suppiah, and J. Ricketts, 2005: *Climate Change Impacts on Fire-Weather in Southeast Australia*. CSIRO Atmospheric Research. Consultancy report jointly funded by the Commonwealth of Australia and the governments of New South Wales, Victoria, Tasmania, and the Australian Capital Territory, 91 pp.

Hennessy, K., C. Lucas, N. Nicholls, J. Bathols, R. Suppiah, and J. Ricketts, 2006: *Climate change impacts on fire-weather in south-east Australia*. Consultancy report for the New South Wales Greenhouse Office, Victorian Department of Sustainability and Environment, Tasmanian Department of Primary Industries, Water and Environment, and the Australian Greenhouse Office. CSIRO Atmospheric Research and Australian Government Bureau of Meteorology, 78 pp.

Hobday A.J., T.A. Okey, E.S. Poloczanska, T.J. Kunz, and A.J. Richardson. 2006: *Impacts of climate change on Australian marine life. Part A: Executive Summary*. Report to the Australian Greenhouse Office. 36pp

Hobbins, M.T., J.A Ramirez, T.C. Brown, and L.H.J.M. Claessens, 2001: The complementary relationship in estimation of regional evapotranspiration: the complementary relationship areal evapotranspiration and advection-aridity models. *Water Resources Research*, **37**, 1367-1387.

Hobbins, M.T., J.A. Ramirez and T.C. Brown, 2004: *Developing a long-term, high resolution, continental-scale, spatially distributed time-series of topographically corrected solar radiation*. Paper presented at the Proceedings of the 24th Annual American Geophysical Union Hydrology Days, Colorado State University, Fort Collins, Colorado.

Hoegh-Guldberg, O., 1999: Climate change, coral bleaching and the future of the world's coral reefs. *Freshwater and Marine Research*, **50**, 839-866.

Holland, G.J., A.H. Lynch, and L.M. Leslie, 1987: Australian east-coast cyclones. Part I: Synoptic overview and case study. *Monthly Weather Review*, **115**, 3024-3036.

Hope, P.K., 2006: Projected future changes in synoptic systems influencing southwest Western Australia. *Climate Dynamics*, **26**, 765-780.

Hope, P.K., W. Drosdowsky, and N. Nicholls, 2006: Shifts in the synoptic systems influencing southwest Western Australia, *Climate Dynamics*, **26**, 51-764.

Hopkins, L.C., and G.J. Holland 1997: Australian heavy-rain days and associated east coast cyclones: 1958-92. *Journal of Climate*, **10**, 621-635.

Howden, M., and R. Jones, 2001: *Costs and Benefits of CO_2 Increase and Climate Change on the Australian Wheat Industry*. Australian Greenhouse Office, Department of Environment and Heritage, Canberra, Australia.

Howden, S.M., P.J. Reyenga, and H. Meinke, 1999: *Global Change Impacts on Australian Wheat Cropping*. Working Paper Series 99/04, CSIRO Wildlife and Ecology, Canberra, Australia, 121 pp.

Hughen, K.A., D.P. Schrag, S.B. Jacobsen, and W.S. Hantoro, 1999: El Niño during the last interglacial period recorded by a fossil coral from Indonesia. *Geophysical Research Letters*, **26**, 3129-3132.

Insurance Council of Australia, 2007: *Australia's catastrophe list.* http://www.insurancecouncil.com.au/Catastrophe-Information/default.aspx

IOCI (Indian Ocean Climate Initiative), 2002: *Climate variability and change in south west Western Australia*. IOCI, Perth, 34 pp.

IPCC (Intergovernmental Panel on Climate Change), 1990: *Climate change: The Intergovernmental Panel on Climate Change Scientific Assessment*. J.T. Houghton, G.J. Jenkins, and J.J. Ephraums (eds.). Cambridge University Press, Cambridge, 365 pp.

IPCC (Intergovernmental Panel on Climate Change), 1994: *Climate Change 1994: Radiative Forcing of Climate Change and an Evaluation of the IPCC IS92 Emission Scenarios*. J.T. Houghton, L.G. Meira Filho, J.P. Bruce, Hoesung Lee, B.T. Callander, E.F. Haites, N. Harris, and K. Maskell (Eds.). Cambridge University Press, Cambridge and New York, 339 pp.

IPCC (Intergovernmental Panel on Climate Change), 1996: *Climate change 1995: The Science of Climate Change. Contribution of the Working Group I to the Second Assessment Report of the Intergovernmental Panel on Climate Change*. J.T. Houghton, *et al*. (eds.). Cambridge University Press, Cambridge, 572 pp.

IPCC (Intergovernmental Panel on Climate Change), 2000: Emissions Scenarios. Special Report of the Intergovernmental Panel on Climate Change. Nakicenovic, N., and R. Swart, (eds). Cambridge University Press, UK. 570 pp

IPCC (Intergovernmental Panel on Climate Change), 2001: *Climate Change 2001: The Scientific Basis*. Contribution of Working Group I to the Third Assessment Report of the Intergovernmental Panel on Climate Change. J.T. Houghton, Y. Ding, D.J. Griggs, M. Noguer, P. J. van der Linden, and D. Xiaosu (Eds.).Cambridge University Press, UK, 944 pp.

IPCC (Intergovernmental Panel on Climate Change), 2004: *Climate Change and Biodiversity. IPCC Secretariat*, Geneva, Switzerland, 77 pp.

IPCC (Intergovernmental Panel on Climate Change), 2007a: *Climate Change 2007: The Physical Science Basis*. Contribution of Working Group I to the Fourth Assessment Report of the Intergovernmental Panel on Climate Change. S. Solomon, D. Qin, M. Manning, Z. Chen, M. Marquis, K.B. Averyt, M. Tignor and H.L. Miller (Eds.). Cambridge University Press, Cambridge, United Kingdom and New York, NY, USA, 996 pp.

IPCC (Intergovernmental Panel on Climate Change), 2007b: *Climate Change 2007: Impacts, Adaptation and Vulnerability*. Contribution of Working Group II to the Fourth Assessment Report of the Intergovernmental Panel on Climate Change. M.L. Parry, O.F. Canziani, J.P. Palutikof, P.J. van der Linden and C.E. Hanson (Eds.). Cambridge University Press, Cambridge, UK, 1000 pp.

IPCC (Intergovernmental Panel on Climate Change), 2007c: *Climate Change 2007: Mitigation of Climate Change. Summary for Policymakers*. Contribution of Working Group III to the Fourth Assessment Report of the Intergovernmental Panel on Climate Change. IPCC Secretariat, Geneva, Switzerland, 36 pp.

ISO (International Organization for Standardization), 2002: *Risk Management. Vocabulary. Guidelines for Use in Standards*. Guide 73:2002, International Organization for Standardization, Geneva, Switzerland.

Jones, R.N., 2000: Managing uncertainty in climate change projections: issues for impact assessment. *Climatic Change*, **45**, 403-419.

Jones, R.N., 2001: An environmental risk assessment/management framework for climate change impact assessments. *Natural Hazards*, **23**, 197-230.

Jones, R.N., 2004: Incorporating agency into climate change risk assessments. *Climatic Change*, **67**, 13–26.

Jones, R.N., J.M. Bowler, and T.A. MacMahon, 1998: A high resolution Holocene record of P/E ratio from closed lakes in Western Victoria. *Palaeoclimates*, **3**, 51–82.

Jones, R.N, T.A. McMahon and J.M. Bowler, 2001. Modelling historical lake levels and recent climate change at three closed lakes, Western Victoria, Australia (c. 1890-1990). *Journal of Hydrology*, **246**(1):159-180.

Jones, R.N., and C.M. Page, 2001: Assessing the risk of climate change on the water resources of the Macquarie river catchment. In: Ghassemi, P., P. Whetton, R. Little, and M. Littleboy, (eds). *Integrating Models for Natural Resources Management Across Disciplines, Issues and Scales*, MODSIM 2001 International Congress on Modelling and Simulation, Modelling and Simulation Society of Australia and New Zealand, Canberra.

Jones, R.N., and P.J. Durack, 2005: *Estimating the Impacts of Climate Change on Victoria's Runoff Using a Hydrological Sensitivity Model*. CSIRO Atmospheric Research, Aspendale, Victoria, Australia, 47 pp.

Jones, R.N., and L.O. Mearns, 2005: Assessing future climate risks. In Lim, B. *et al*. (eds), *Adaptation Policy Frameworks for Climate Change: Developing Strategies, Policies and Measures*. United Nations Development Programme, Cambridge University Press, Cambridge, UK, pp 119-143.

Jones, R., P. Durack, C. Page, and J. Ricketts, 2005: Climate change impacts on the Water Resources of the Fitzroy River Basin. In Cai *et al*. (eds). *Climate Change in Queensland under Enhanced Greenhouse Conditions: Final Report 2004–2005*. CSIRO Marine and Atmospheric Research, Melbourne, pp 19–58.

Jones, R.N. and B.L. Preston, 2006: *Climate change impacts, risk and the benefits of mitigation: a report for the Energy Futures Forum*. CSIRO, Melbourne, 97 pp.

Jones, R.N., P. Dettman, G. Park, M. Rogers and T. White, 2007: The relationship between adaptation and mitigation in managing climate change risks: a regional approach, *Mitigation and Adaptation Strategies for Global Change*, **12**, 685–712.

Joseph, R., and, S. Nigam, 2006: ENSO evolution and teleconnections in IPCC's 20th Century climate simulations: realistic representation? *Journal of Climate*, **19**, 4360–4377.

Jovanovic, B., D.A. Jones, and D. Collins, 2007: A high quality monthly pan evaporation dataset for Australia. *Climatic Change*, accepted.

Kalnay, E., M. Kanamitsu, R. Kistler, W. Collins, D. Deaven, L. Gandin, M. Iredell, S. Saha, G. White, J. Woollen, Y. Zhu, A. Leetmaa, R. Reynolds, M. Chelliah, W. Ebisuzaki, W. Higgins, J. Janowiak, K. C. Mo, C. Ropelewski, J. Wang, R. Jenn, and D. Joseph, 1996: The NCEP/NCAR 40-year reanalysis project, *Bulletin of the American Meteorological Society*, **77**, 437-471,.

Karoly, D.J., 1990: The role of transient eddies in low-frequency zonal variations of the Southern Hemisphere circulation. *Tellus*, **42A**, 41–50.

Karoly, D.J., and Braganza, K. 2005a: Attribution of recent temperature changes in the Australian region. *J. Climate*, **18**, 457-464.

Karoly, D.J., and Braganza, K. 2005b: A new approach to detection of anthropogenic temperature changes in the Australian region. *Meteorology and Atmospheric Physics*, **89**, 57-67.

Karoly, D.J., and Q. Wu, 2005: Detection of regional surface temperature trends. *Journal of Climate*, **18**, 4337-4343.

Kidson, J.W., 1988a: Interannual variations in the Southern Hemisphere circulation. *Journal of Climate*, **1**, 1177–1198.

Kirono, D., G. Podger, W. Franklin, R. Siebert, 2007: Climate change impact on Rous Water supply. *Water Journal of the Australian Water Resources Association*, March, 68-72.

Klotzbach, P.J., 2006: Trends in global tropical cyclone activity over the past twenty years (1986-2005). *Geophysical Research Letters*, **33**, L10805.

Knutson, T. R., K. Emanuel, S. Emori, J. Evans, G. Holland, C. Landsea, K.-b. Liu, R. E. MacDonald, D. S. Nolan, M. Sugi, and Y. Wang, 2006: Possible relationships between climate change and tropical cyclone activity. Topic reports, Sixth International Workshop on Tropical Cyclones, World Meteorological Organization, pp. 464-492.

Kokic, P., R. Nelson, H. Meinke, A. Potgieter and J. Carter, 2007: From rainfall to farm incomes - transforming advice for Australian drought policy. Part I: Development and testing of a bioeconomic modelling system, *Australian Journal of Agricultural Research*, in press.

Kossin, J.P., K.R. Knapp, D.J. Vimont, R.J. Murnane, and B.A. Harper, 2007: A globally consistent reanalysis of hurricane variability and trends. *Geophysical Research Letters*, **34**, L04815.

Kounkou, R., G.A. Mills, and B. Timbal, 2007: *The impact of anthropogenic climate change on the risk of cool-season tornado occurrences*. BMRC Research Report No. 129, 79 pp.

Kuleshov, Y.A., 2003: *Tropical cyclone climatology for the southern hemisphere. Part 1: Spatial and temporal profiles of tropical cyclones in the southern hemisphere*., National Climate Centre, Australian Bureau of Meteorology, 22 pp.

Kuleshov, Y., G. de Hoedt, W. Wright and A. Brewster, 2002: Thunderstorm distribution and frequency in Australia. *Australian Meteorological Magazine*, **51**, 145-154.

Kushnir, P.J., I.M. Held, and T.L. Delworth, 2001: Southern Hemisphere atmospheric circulation response to global warming, *Journal of Climate*, **14**, 2238-2249.

Lambert, S.J. and J.C. Fyfe, 2006: Changes in winter cyclone frequencies and strengths simulated in enhanced greenhouse warming experiments: results form the models participating in the IPCC diagnostic exercise. *Climate Dynamics*, **26**, 713-728.

Leslie, L.M., D.J. Karoly, M. Leplastrier, and B.W. Buckley, 2007: Variability of Tropical Cyclones over the Southwest Pacific Ocean using a High Resolution Climate Model. *Meteorology and Atmospheric Physics (Special Issue on Tropical Cyclones)*, accepted.

Levitus, S., J. Antonov, and, T. Boyer, 2005: Warming of the world ocean, 1995-2003. *Geophysical Research Letters*, **32**, L02604.

Li, F., L. Chambers, and N. Nicholls, 2005: Relationships between rainfall in the southwest of Western Australia and near-global patterns of sea surface temperature and mean sea level pressure variability. *Australian Meteorological Magazine*, **54**, 23–33.

Lim, E.-P., and I. Simmonds, 2007: Southern Hemisphere winter extratropical cyclone characteristics and vertical organization observed with the ERA-40 reanalysis data in 1979-2001, *Journal of Climate*, **20**, 2675-2690.

Lin, J.L., G.N. Kiladis, B.E. Mapes, K.M. Weickmann, K.R. Sperber, W.Y. Lin, M. Wheeler, S.D. Schubert, A. Del Genio, L.J. Donner, S. Emori, J.-F. Gueremy, F. Hourdin, P.J. Rasch, E. Roeckner, and J.F. Scinocca, 2006: Tropical intraseasonal variability in 14 IPCC AR4 climate models. Part I: Convective signals. *Journal of Climate*, **19**, 2665-2690.

Lloyd, P.J., and A.P. Kershaw, 1997: Late Quaternary vegetation and early Holocene quantitative climate estimates from Morwell Swamp, Latrobe Valley, south-eastern Australia. *Australian Journal of Botany*, **45**, 549–563.

Lopez, A., C. Tebaldi, M. New, D. Stainforth, M. Allen, and J. Kettleborough, 2006: Two approaches to quantifying uncertainty in global temperature changes, *Journal of Climate*, **19**, 4785-4796.

Lough, J.M., 2001: Climate variability and change on the Great Barrier Reef. In: Wolanski E (Ed). *Oceanographic processes of coral reefs: physical and biological links in the Great Barrier Reef*, CRC Press, Bocan Raton, Florida, pp 269-300.

Lough, J., R. Berkelmans, M. van Oppen, S. Wooldridge, and C. Steinberg, 2006: The Great Barrier Reef and Climate Change. *Bulletin Australian Meteorological and Oceanographic Society*, **19**, 53-58.

Lucas, C., K. Hennessy, G. Mills and J. Bathols, 2007: *Bushfire Weather in Southeast Australia: Recent Trends and Projected Climate Change Impacts*. Consultancy report by the Bushfire CRC, Australian Bureau of Meteorology and CSIRO Marine and Atmospheric Research for The Climate Institute, 50 pp, submitted.

Luo, Q., R.N. Jones, M. Williams, B. Bryan, and W. Bellotti, 2005: Probabilistic distributions of regional climate change and their application in the risk analysis of wheat production. *Climate Research*, **29**, 41-52.

Macphail, M.K., 1979: Vegetation and climates in southern Tasmania since the last glaciation. *Quaternary Research*, **11**, 306–41.

Mann, M.E., M.A. Cane, S.E. Zebiak and A.C. Clement, 2005: Volcanic and solar forcing of El Nino over the past 1000 years. *Journal of Climate*, **18**, 447-456.

Manning, M.R., 2003: The difficulty of communicating uncertainty. *Climatic Change*, **61**, 9-16.

Marshall, G.J., 2003: Trends in the Southern Annular Mode from observations and reanalyses. *Journal of Climate*, **16**, 4134.

Mastrandrea, M.D., and S.H. Schneider, 2004: Probabilistic integrated assessment of "dangerous" climate change. *Science*, **304**, 571-575.

McBride, J., J. Kepert, J. Chan, J. Heming, G. Holland, K. Emanuel, T, Knutson, H. Willoughby, and C. Landsea, 2006: Statement on tropical cyclones and climate change. WMO/CAS Tropical Meteorology Research Program, by participants of the 6th WMO International Workshop on Tropical Cyclones (IWTC-VI), Costa Rica, Nov. 2006.

McGregor, H.V., and M.K. Gagan, 2004: Western Pacific coral delta-18O records of anomalous Holocene variability in the El Nino-Southern Oscillation, *Geophysical Research Letters*, 31, L11204.

McInnes, K.L., L.M. Leslie, and J.L McBride, 1992: Numerical simulation of cut-off lows on the Australian east coast: Sensitivity to sea-surface temperature. *International Journal of Climatology*, **12**, 1-13.

McInnes, K.L., K.J.E. Walsh, G.D. Hubbert, and T. Beer, 2003: Impact of sea-level rise and storm surges on a coastal community. *Natural Hazards*, **30**, 187-207.

McInnes, K.L., D.J. Abbs, and, J.A. Bathols, 2005a: *Climate Change in Eastern Victoria. Stage 1 Report: The effect of climate change on coastal wind and weather patterns*. Report to Gippsland Coastal Board. 26 pp.

McInnes, K.L., I. Macadam, G.D. Hubbert, D.J. Abbs, and J.A. Bathols, 2005b: *Climate Change in Eastern Victoria. Stage 2 Report: The effect of climate change on storm surges*. Report to Gippsland Coastal Board. June 2005, 37 pp.

McInnes, K. L., I. Macadam, and G. D., Hubbert, 2006: Climate Change in Eastern Victoria. Stage 3 Report: The effect of climate change on extreme sea levels in Corner Inlet and the Gippsland Lakes. Report to Gippsland Coastal Board. July 2006, 40 pp.

McInnes K.L., J.L. McBride, and J.J. Katzfey, 2006: Winter storm tracks in a global climate model simulation, *Climate Change*, submitted.

McInnes, K.L., D.J. Abbs, S.P. O'Farrell, I. Macadam, and J. O'Grady, in preparation: Coastal zone climate change impact event definition: A project undertaken for the NSW Department of Natural Resources.

McKenzie, G.M., and J.R. Busby, 1992: A quantitative estimate of Holocene climate using a bioclimatic profile of *Nothofagus cunninghamii* (Hook.) Oerst., *Journal of Biogeography*, **19**, 531–540.

McMichael, A., R. Woodruff, P. Whetton, K. Hennessy, N. Nicholls, S. Hales, A. Woodward, and T Kjellstrom, 2002: *Human Health and Climate Change in Oceania: A Risk Assessment*, Commonwealth of Australia, Canberra, ACT, 128 pp.

McNeil, B.I., R.J. Matear, R.M. Key, J.L. Bullister and J.L. Sarmiento, 2003: Anthropogenic CO2 Uptake by the Ocean Based on the Global Chlorofluorocarbon Data Set. *Science*, **299**, 235-239.

Meehl, G.A., T.F. Stocker, W.D. Collins, P. Friedlingstein, A.T. Gaye, J.M. Gregory, A. Kitoh, R. Knutti, J.M. Murphy, A. Noda, S.C.B. Raper, I.G. Watterson, A.J. Weaver, and Z.-C. Zhao, 2007: Global climate projections. In: Solomon, S., D. Qin, M. Manning, Z. Chen, M. Marquis, K.B. Averyt, M. Tignor, and H.L. Miller (eds.). *Climate Change 2007: The Physical Science Basis. Contribution of Working Group I to the Fourth Assessment Report of the Intergovernmental Panel on Climate Change*. Cambridge University Press, Cambridge, pp 747-846.

Meinke, H., P. deVoil, G.L. Hammer, S. Power, R. Allan, R.C. Stone, C. Folland, and Potgieter, A. 2005: Rainfall variability at decadal and longer time scales: Signal or noise? *Journal of Climate*, **18**, 89-96.

Meneghini B, I. Simmonds, and I.N. Smith 2007: Association between Australian rainfall and the Southern Annular Mode. *International Journal of Climatology*, **27**(1), 109.

Meyers, G., P. McIntosh, L. Pigot, and M. Pook, 2007: The years of El Niño, La Niña and interactions with the Tropical Indian Ocean, *Journal of Climate*, **20**, 2872-2880.

Miller, R.L., G.A. Schmidt, and D.T. Shindell, 2006: Forced annular variations in the 20th century of IPCC FAR models. *Journal of Geophysical Research*, **111**, D18101.

Mills, G.A., 2004: Verification of operational cool-season tornado threat-area forecasts from mesoscale NWP and a probabilistic forecast product. *Australian Meteorology Magazine*, **53**, 269-277.

Mitchell, T.D., 2003: Pattern Scaling, *Climatic Change*, **60**, 217-242.

Moise A.F., and D.A. Hudson, 2007: Probabilistic Predictions of Climate Change using the Reliability Ensemble Average (REA) of IPCC AR4 Model, Simulations, Part 1: Australia, *Journal of Geophysical Research*, submitted.

Morgan, M.G., and M. Henrion, 1990: *Uncertainty: A Guide to Dealing with Uncertainty in Quantitative Risk and Policy Analysis*. Cambridge University Press, New York, 344 pp.

Morton, F.I.,1983: Operational estimates of areal evapotranspiration and their significance to the science and practice of hydrology. *Journal of Hydrology*, **66**, 1-76.

Moser, S.C., and L. Dilling, 2004: Making climate hot: communicating the urgency and challenge of global climate change. *Environment*, **46**(10), 32-46.

Mpelasoka, F., K.J. Hennessy, R. Jones and J. Bathols, 2007: Future drought events over Australia under global warming. *International Journal of Climatology*, accepted.

Murphy B., and B. Timbal, 2007: A review of recent climate variability and climate change in south eastern Australia. *International Journal of Climatology*, accepted.

NAST (National Assessment Synthesis Team), 2000: *Climate Change Impacts on the United States: The Potential Consequences of Climate Variability and Change*, National Assessment Synthesis Team, U.S. Global Change Research Program, Cambridge University Press, New York, NY, USA.

Nelson R., and P. Kokic, 2004: *Forecasting the regional impact of climate variability on Australian crop farm incomes*. ABARE eReport 04.23. Grains Research and Development Corporation, Canberra.

Nelson, R., P. Kokic, L. Elliston and J. King, 2005: Structural adjustment: a vulnerability index for Australian broadacre agriculture. *Australian Commodities*, **12**(1), 171-179.

Niall, S., and K. Walsh, 2005: The impact of climate change on hailstorms in southeastern Australia. *International Journal of Climatology*, **25**, 1933-1952.

Nicholls, N. 1979: Possible method for predicting seasonal tropical cyclone activity in the Australian region. *Monthly Weather Review*, **107**, 1221-1224.

Nicholls, N. 1984: The Southern Oscillation, sea surface temperature, and interannual fluctuations in Australian tropical cyclone activity. *Journal of Climatology*, **4**, 661-670.

Nicholls N. 1985: Predictability of interannual variations of Australian seasonal tropical cyclone activity. *Monthly Weather Review*, **113**, 1144-1149.

Nicholls, N., 2003: Continued anomalous warming in Australia. *Geophysical Research Letters*, **30**, 1370.

Nicholls, N. 2004: The changing nature of Australian droughts. *Climatic Change*, **63**, 323-336.

Nicholls, N. 2005: Climate variability, climate change, and the Australian snow season. *Australian Meteorological Magazine*, **54**, 177-185.

Nicholls, N., 2006: Detecting and attributing Australian climate change: a review. *Australian Meteorological Magazine*, **55**, 199-211.

Nicholls, N., B. Lavery, C. Frederiksen, W. Drosdowsky, and S. Torok, 1996: Recent apparent changes in relationships between the El Niño-Southern Oscillation and Australian rainfall and temperature. *Geophysical Research Letters*, **23**, 3357-3360.

Nicholls, N., C. Landsea, and J. Gill, 1998: Recent trends in Australian region tropical cyclone activity. *Meteorological Atmospheric Physics*, **65**, 197–205.

Nicholls, N., and D. Collins, 2006: Observed climate change in Australia over the past century. Energy & Environment, **17**, 1-12.

Nott, J., 2003: Intensity of prehistoric tropical cyclones. *Journal of Geophysical Research*, **108**(D7):4212-23.

Nott, J., and M. Hayne, 2001: High frequency of "super-cyclones" along the Great Barrier Reef over the past 5,000 years. *Nature*, **413**, 508-512.

Ohe, M., and S. Ikeda, 2005: Global warming: risk perception and risk-mitigating behaviour in Japan. *Mitigation and Adaptation Strategies for Global Change*, **10**, 221-236.

Oouchi, K., J. Yoshimura, H. Yoshimura, R. Mizuta, S. Kusunoki, and A. Noda, 2006: Tropical cyclone climatology in a global-warming climate as simulated in a 20 km-mesh global atmospheric model: Frequency and wind intensity changes. *Journal of the Meteorological Society Japan*, **84**, 259.

Patt, A., and S. Dessai, 2005: Communicating uncertainty: Lessons learned and suggestions for climate change assessment. *Comptes Rendus Geoscience*, **337**, 425-441.

Patt, A.G., and D.P. Schrag, 2003: Using specific language to describe risk and probability. *Climatic Change*, **61**, 17-30.

Patt, A., R.J.T. Klein, and A. de la Vega-Leinert, 2005: Taking the uncertainty in climate-change vulnerability assessment seriously. *Comptes Rendus Geoscience*, **337**, 411-424.

PB Associates, 2007: *Assessment of the Vulnerability of Australia's Energy Infrastructure to the Impacts of Climate Change*. Prepared for the Australian Greenhouse Office, Department of Environment and Heritage, Canberra, Australia.

Philip, S.Y., and G.J. Van Oldenborgh, 2006: Shifts in ENSO couplings under global warming. *Geophysical Research Abstracts*, **8**, 03594.

PIA (Planning Institute of Australia), 2004: *Sustainable Regional and Urban Communities Adapting to Climate Change: Issues Paper*. Planning Institute of Australia, Queensland Division, Brisbane, 88 pp.

Pickering, C.M., R. Good, and K. Green, 2004: *Potential Effects of Global Warming on the Biota of the Australian Alps*. A report for the Australia Greenhouse Office.

Pitman A.J., G.T. Narisma, R.A. Pielke, and N.J. Holbrook, 2004: The impact of land cover change on the climate of south west Western Australia. *Journal of Geophysical Research*, **109**, D18109.

Pittock, A.B., 1988: Actual and anticipated changes in Australia's climate. In: *Greenhouse. Planning for climate change*. CSIRO, 35-51, 752 pp.

Poloczanska, E.S., R.C. Babcock, A. Butler, A.J. Hobday, O. Hoegh-Guldberg, T.J. Kunz, R. Matear, D. Milton, T.A. Okey and A.J. Richardson, 2007: Climate change and Australian marine life. In: *Oceanography and Marine Biology: An Annual Review, Volume 45*. R.N. Gibson, R.J.A. Atkinson and J.D.M. Gordon (Eds.). CRC Press, Cleveland, 544 pp.

Pook, M., S. Lisson, J. Risbey, P. McIntosh, C. Ummenhofer, and M. Rebbeck, 2006: Autumn breaks in southeastern Australia; characteristics, trends and synoptic climatology. In: Abstracts, 17th Australian New Zealand Climate Forum, Canberra, 5-7 September 2006.

Power, S.B., F. Tseitkin, M. Dix, R. Kleeman, R. Colman, and D. Holland, 1995: Stochastic variability at the air-sea interface on decadal time-scales. *Geophysical Research Letters*, **22**, 2593-2596.

Power, S.B., F. Tseitkin, S. Torok, B. Lavery, R. Dahni, and B. McAvaney, 1998a: Australian temperature, Australian rainfall and the Southern Oscillation, 1910-1992: coherent variability and recent changes. *Australian Meteorological Magazine*, **47**, 85-101.

Power, S.B., F. Tseitkin, R.A. Colman, and A. Sulaiman, 1998b: *A coupled general circulation model for seasonal prediction and climate change research*. BMRC Research Report No. 66, Bureau of Meteorology, Australia, 52 pp.

Power, S.B., T. Casey, C. Folland, A. Colman, and V. Mehta, 1999: Interdecadal modulation of the impact of ENSO on Australia. *Climate Dynamics*, **15**, 319-234.

Power, S.B., M.H. Haylock, R. Colman, and X. Wang, 2006: The predictability of inter-decadal changes in ENSO activity and ENSO teleconnections. *Journal of Climate*, **19**, 4755-4771.

Power, S.B., and R. Colman, 2006: Multi-year predictability in a coupled general circulation model. *Climate Dynamics*, **26**, 247-272.

Power, S.B., and N. Nicholls, 2007: Temperature variability in a changing climate. *Australian Meteorological Magazine,* accepted.

Preston, B.L. and R.N. Jones, 2006: *Climate change impacts on Australia and the benefits of early action to reduce global greenhouse gas emissions*. A consultancy report for the Australian Business Roundtable on Climate Change. CSIRO, Melbourne, 41 pp.

Rahmstorf, S., A. Cazenave, J.A. Church, J.E. Hansen, R.F. Keeling, D.E. Parker, and R.C.J. Somerville, 2007: Recent climate observations compared to projections. Science, **316**, 709-710.

Randall, D.A., R.A. Wood, S. Bony, R. Colman, T. Fichefet, J. Fyfe, V. Kattsov, Pitman, A., J. Shukla, J. Srinivasan, R.J. Stouffer, A. Sumi, and K.E. Taylor, 2007: Climate Models and Their Evaluation. In: Solomon, S., D. Qin, M. Manning, Z. Chen, M. Marquis, K.B. Averyt, M. Tignor, and H.L. Miller, (eds). *Climate Change 2007: The Physical Science Basis. Contribution of Working Group I to the Fourth Assessment Report of the Intergovernmental Panel on Climate Change*. Cambridge University Press, Cambridge, United Kingdom and New York, NY, USA.

Raphael, M.N., and M.M. Holland, 2006: Twentieth century simulation of the Southern Hemisphere climate in coupled models. Part 1: Large scale circulation variability. *Climate Dynamics*, **26**, 217-228.

Raven, J., K. Caldeira, H. Elderfield, O. Hoegh-Guldberg, P. Liss, U. Riebesell, J. Shepherd, C. Turley, and A. Watson, 2005: *Ocean acidification due to increasing atmospheric carbon dioxide*. The Royal Society, London.

Rayner, D.P., 2007: Wind run changes are the dominant factor affecting pan evaporation trends in Australia. *Journal of Climate*, **20**, 3379-3394.

Rayner, N.A., E.B. Horton, D.E. Parker, and C.K. Folland, 1996: *Version 2.2 of the Global sea-Ice and Sea Surface Temperature dataset, 1903-1994*. Climate Research Technical Note, CRTN74, 28 pp., Hadley Centre, Meteorological Office, Bracknell, UK.

Roderick, M.L., and G.D. Farquhar, 2002: The cause of decreased pan evaporation over the past 50 years. *Science*, **298**, 1410-1411.

Rogers, J.C., and H. van Loon, 1982: Spatial variability of sea level pressure and 500mb height anomalies over the Southern Hemisphere. *Monthly Weather Review*, **110**, 1375–1392.

Rotstayn, L.D., W.Cai, M.R. Dix, G.D. Farquhar, Y. Feng, P.Ginoux, M. Herzog, A. Ito, J.E. Penner, M.L. Roderick, and M. Wang, 2007: Have Australian rainfall and cloudiness increased due to the remote effects of Asian anthropogenic aerosols? *Journal of Geophysical Research*, **112**, D09202.

Ryan, B., and P. Hope, 2005: *Indian Ocean Climate Initiative Stage 2: Report of Phase 1 Activity: July 2003-Dec 2004*. IOCI, Perth, Australia, 40 pp.

Ryan, B., and P. Hope, 2006: *Indian Ocean Climate Initiative Stage 2: Report of Phase 2 Activity: January 2005-June 2006*. IOCI, Perth, Australia, 46 pp.

Sabine, C.L., R.A. Feely, N. Gruber, R.M. Key, K. Lee, J.L. Bullister, R. Wanninkhof, C.S. Wong, D.W.R. Wallace, B. Tilbrook, F.J. Millero, T-H. Peng, A. Kozyr, T. Ono and A.F. Rios, 2004: The Oceanic Sink for Anthropogenic CO_2. *Science*, **305**, 367-371.

Sarewitz, D., R. Pilke, Jr., and M. Keykhah, 2003: Vulnerability and risk: Some thoughts from a political and policy perspective. *Risk Analysis*, **23**, 805-810.

Sarmiento, J.L., C. Lequere, and S.W. Pacala 1995: Limiting Future Atmospheric Carbon-Dioxide, *Global Biogeochemical Cycles*, **9**, 121-137.

Schneider, S.H., S. Semenov, A. Patwardhan, I. Burton, C.H.D. Magadza, M. Oppenheimer, A.B. Pittock, A. Rahman, J.B. Smith, A. Suarez and F. Yamin, 2007: Assessing key vulnerabilities and the risk from climate change. *Climate Change 2007: Impacts, Adaptation and Vulnerability. Contribution of Working Group II to the Fourth Assessment Report of the Intergovernmental Panel on Climate Change.* M.L. Parry, O.F. Canziani, J.P. Palutikof, P.J. van der Linden and C.E. Hanson (Eds.). Cambridge University Press, Cambridge, UK, 779-810.

Schuster, S.S., R.J. Blong, and R. Leigh, 2005: Characteristics of the 14th April 1999 Sydney hailstorm based on ground observations, weather radar, insurance data and emergency calls. *Natural Hazards Earth System Sciences*, **5**, 613-620.

Shindell, D.T., and G.A. Schmidt, 2004: Southern Hemisphere climate response to ozone changes and greenhouse gas increases. *Geophysical Research Letters*, **31**, L18209.

Shulmeister, J., and B.G. Lees, 1995: Pollen evidence from tropical Australia for the onset of and ENSO-dominated climate at c. 4000 BP. *The Holocene*, **5**, 10-18.

Shulmeister, J., I. Goodwin, J. Renwick, K. Harle, L. Armand, M. S. McGlone, E. Cook, J. Dodson, P. Hesse, P. Mayewski, and M. Curran, 2004: The Southern Hemisphere westerlies in the Australasian sector over the last glacial cycle: a synthesis. *Quaternary International*, **118-119**, 23–53.

Simmonds, I., K. Keay, and E.-P. Lim, 2002: Synoptic activity in the seas around Antarctica. *Monthly Weather Review*, **131**, 272–288.

Skelly, W.C., and A. Henderson-Sellers, 1996: Grid box or grid point: what type of data do GCMs deliver to climate impact researchers? *International Journal of Climatology*, **16**, 1079-1086.

Smith, I.N., 2004: An assessment of recent trends in Australian rainfall. *Australian Meteorological Magazine*, **53**, 163-173.

Smith, I.N., M. Dix, and R.J. Allan, 1997: The effect of greenhouse SSTs on ENSO simulations with an AGCM. *Journal of Climate*, **10**, 342-352.

Soden, B.J., and I.M. Held, 2006: An assessment of climate feedbacks in coupled ocean-atmosphere models. *Journal of Climate*, **19**, 3354–3360.

Sterman, J.D., and L.B. Sweeney, 2002: Cloudy skies: assessing public understanding of global warming. *System Dynamics Review*, **18**, 207-240.

Stern, N., S. Peters, V. Bakhshi, A. Bowen, C. Cameron, S. Catovsky, D. Crane, S. Cruickshank, S. Dietz, N. Edmondson, S. Garbett, L. Hamid, G. Hoffman, D. Ingram, B. Jones, N. Patmore, H. Radcliffe, R. Sathiyarajah, M. Stock, C. Taylor, T. Vernon, H. Wanjie, and D. Zenghelis, 2007: *Stern Review on the Economics of Climate Change*. Cambridge University Press, in press.

Suppiah, R., and K.J. Hennessy, 1996: Trends in the intensity and frequency of heavy rainfall in tropical Australia and links with the Southern Oscillation. *Australian Meteorological Magazine*, **45**, 1-17.

Suppiah, R., and K.J. Hennessy, 1998: Trends in total rainfall, heavy rain events and number of dry days in Australia, 1910-1990. *International Journal of Climatology*, **18**(10): 1141–1164.

Suppiah R., K.J. Hennessy, P.H. Whetton, K. McInnes, I. Macadam, J. Bathols and J. Ricketts, 2007: Australian Climate Change Scenarios Derived from AR4 GCM Experiments. *Australian Meteorological Magazine*, accepted

Tebaldi, C., R.W. Smith, D. Nychka, and L.O. Mearns, 2005: Quantifying uncertainty in projections of regional climate change: A Bayesian approach to the analysis of multi-model ensembles. *Journal of Climate*, **18**, 1524-1540.

Tebaldi, C., K. Hayhoe, J.M. Arblaster, and G.A. Meehl, 2006: Going to the extremes: An intercomparison of model-simulated historical and future changes in extreme events. *Climatic Change*, **79**, 185-211.

Tebaldi, C., K. Hayhoe, J.M. Arblaster and G.A. Meehl, 2007: Going to the extremes: An intercomparison of model-simulated historical and future changes in extreme events (erratum). *Climatic Change*, **82**, 233-234.

Thompson, D.W.J., and J.M. Wallace, 2000: Annular modes in the extratropical circulation. Part I: Month-to-month variability. *Journal of Climate*, **13**, 1000-1016.

Thompson, D.W.J., and S. Solomon, 2002: Interpretation of recent Southern Hemisphere climate change. *Science*, **296**, 895–899.

Timbal, B., 2004: South West Australia past and future rainfall trends. *Climate Research*, **26**(3), 233-249.

Timbal, B., and B.J. McAvaney, 2001: An Analogue based method to downscale surface air temperature: Application for Australia, *Climate Dynamics*, **17**, 947-963.

Timbal, B., Dufour A., and McAvaney. B.J., 2003: An estimate of climate change for Western France using a statistical downscaling technique, *Climate Dynamics*, **20**, 807-823.

Timbal B., J.M. Arblaster and S.P. Power, 2006: Attribution of the late 20th century rainfall decline in southwest Australia. *Journal of Climate*, **19**, 2046-2062.

Timbal, B., and J. M. Arblaster, 2006: Land cover change as an additional forcing to explain the rainfall decline in the southwest of Australia. *Geophysical Research Letters*, **33**, LO7717.

Timbal, B., and D. Jones, 2007: Future projections of winter rainfall in Southeast Australia using a statistical downscaling technique. *Climatic Change*, in press.

Tudhope A.W., C.P. Chilcott, M.T. McCulloch, E.R. Cook, J. Chappell, R.M. Ellam, D.W. Lea, J.M. Lough, and G.B. Shimmield, 2001: Variability in the El Niño- Southern Oscillation through a glacial-interglacial cycle. *Science*, **291**, 1511–1517.

Van Oldenborgh, G.J., and G. Burgers, 2005: Searching for decadal variations in ENSO precipitation teleconnections. *Geophysical Research Letters*, **32**, L15701.

Van Oldenborgh, G.J., S.Y. Philip, and M. Collins, 2005: El Niño in a changing climate: a multi-model study. *Ocean Science*, **1**, 81–95.

Victorian Government, 2007: I*nfrastructure and climate change risk assessment for Victoria*. Report to the Victorian Government by CSIRO, Maunsell Australia Pty Ltd, and Phillips Fox. Melbourne, Victoria, Australia, 173 pp.

Walsh, K.J.E. and B.F. Ryan, 2000. Tropical cyclone intensity increase near Australia as a result of climate change. *Journal of Climate*, **13**, 3029-3036.

Walsh, K., K. Hennessy, R. Jones, K. McInnes, C. Page, B. Pittock, R. Suppiah and P. Whetton, 2000: *Climate change in Queensland under enhanced greenhouse conditions. Third annual report 1999-2000*. CSIRO Atmospheric Research, Aspendale, Victoria, Australia. 108 pp.

Walsh, K.J.E., K.C. Nguyen, and J.L. McGregor, 2004: Finer-resolution regional climate model simulations of the impact of climate change on tropical cyclones near Australia. *Climate Dynamics*, **22**, 47-56.

Wardle, R., and I. Smith, 2004: Modeled response of the Australian monsoon to changes in land surface temperatures, *Geophysical Research Letters*, **31**, L16205,

Watterson, I.G., 1996: Non-dimensional measures of climate model performance. *International Journal of Climatology*, **16**, 379-391.

Watterson, I.G., 2007: Calculation of probability density functions of temperature and precipitation change under global warming. *Journal of Geophysical Research*, submitted

Watterson, I.G., and M.R. Dix, 2003: Simulated changes due to global warming in daily precipitation means and extremes and their interpretation using the gamma distribution. *Journal of Geophysical Research – Atmospheres*, **108**(D13), 4379.

Webb, L.B., 2006: *The Impact of Projected Greenhouse Gas-Induced Climate Change on the Australian Wine Industry*. PhD Thesis. University of Melbourne, Melbourne, Australia.

Webster P.J., G.J. Holland, J.A. Curry, and H-R. Chang, 2005: Changes in tropical cyclone number, duration, and intensity in a warming environment. *Science*, **309**, 1844-1846.

Whetton P.H., K.L. McInnes, R.N. Jones, K.J. Hennessy, R. Suppiah, C.M. Page, J. Bathols, and P.J. Durack, 2005: *Australian Climate Change Projections for Impact Assessment and Policy Application: A Review*. Climate Impact Group, CSIRO Marine and Atmospheric Research, Aspendale, Victoria, Australia.

Whetton, P., I. Macadam, J. Bathols and J. O'Grady, 2007: Assessment of the use of current climate patterns to evaluate regional enhanced greenhouse response patterns of climate models. *Geophysical Research Letters*, **34**, L14701.

Williams, S.E., E.E. Bolitho, S. Fox, 2003: Climate change in Australian tropical rainforests: an impending environmental catastrophe. *Proceedings of the Royal Society of London Series B-Biological Sciences*, **270**, 1887-1892.

Woodruff, R., S. Hales, C. Butler, and A. McMichael, 2005: *Climate Change Health Impacts in Australia: Effect of Dramatic CO_2 Emissions Reductions*. Report for the Australian Conservation Foundation and the Australian Medical Association, 44 pp.

Xie, P., and P.A. Arkin, 1997: Global precipitation: A 17-year monthly analysis based on gauge observations, satellite estimates, and numerical model outputs. *Bulletin of the American Meteorological Society*, **78**, 2539-2558.

Yamaguchi, K., and A. Noda, 2006: Global warming patterns over the North Pacific: ENSO versus AO. *Journal of the Meteorological Society Japan*, **84**, 221-241.

Yin, J.H., 2005: A consistent poleward shift of the storm tracks in simulations of 21st century climate. *Geophysical Research Letters*, **32**, L18701.

Zelle, H., G.J. van Oldenborgh, G. Burgers, and H. Dijkstra, 2005: El Niño and Greenhouse Warming: Results from Ensemble Simulations with the NCAR CCSM. *Journal of Climate*, **18**, 4669–4683.

Zhang, K., B.C. Douglas, and S.P. Leatherman, 2004: Global warming and coastal erosion. *Climatic Change*, **64**, 41-58.

Australian Government

Department of the Environment and Water Resources
Australian Greenhouse Office

Bureau of Meteorology

www.climatechangeinaustralia.gov.au